THE ETHOLOGY OF HONEYBEES (*APIS MELLIFERA*) STUDIED USING ACCELEROMETER TECHNOLOGY.

Michael-Thomas Ramsey

A thesis submitted in partial fulfilment of the requirements of Nottingham Trent University for the degree of Doctor of Philosophy

JULY 17, 2018

NOTTINGHAM TRENT UNIVERSITY

Copyright statement

Resulting publications

Ramsey M, Bencsik M, Newton MI (2017) Long-term trends in the honeybee 'whooping signal' revealed by automated detection. *PLoS ONE*, 12(2): e0171162

Ramsey, M., Bencsik, M. and Newton, M. (under review). Vibrational quantitation and long-term automated monitoring of honeybee (Apis mellifera) dorsoventral abdominal shaking signal. *Scientific Reports*.

Digital information

Supplied on the data disk associated with this thesis are all videos and audio that have been used to support the findings of this work across all chapters.

Abstract

While the significance of vibrational communication across insect taxa has been fairly well studied, the substrate-borne vibrations of honeybees remains largely unexplored. Within this thesis I have monitored honeybees with a new method, that of logging their short pulsed vibrations on the long-term, and I have started the longstanding endeavour of underpinning the applications of it. The use of advanced spectral analysis and machine learning techniques as part of this new method has revealed exciting statistics that challenges previous expert's interpretations.

This work is comprised of three results chapters with the aim of determining (1) what can the in-situ monitoring of specific honeybee pulsed vibrations tell us about the status of a colony? (2) What long-term statistics be can identified to help to disentangle the function of two specific pulses of vibrations? (3) How effective is honeycomb-embedded accelerometer technology at assessing the ethology of honeybee colonies?

In the first results chapter, I explore the contributions of developing pupae and larvae to accelerometer datasets by monitoring brood frames isolated from the colony with embedded accelerometers. From this, I show that very little vibrational information is obtainable from capped brood using accelerometer. However, I am able to showcase the quantitation of specific vibrational waveforms that are indicative of brood emergence from the honeycomb.

In the second results chapter, the automated detection of honeybee whooping signals was achieved with an 83% accuracy, revealing never-before-seen long-term statistics of vibration, once thought to be an inhibitory or food request signal. Statistics show that this pulse is very common, highly repeatable, occurs mainly at night with a distinct decrease towards midday, is correlated with the brood cycle, and can be elicited en masse as a startle response by bees following the gentle knocking of the hive.

Through synchronisation of high-definition video and accelerometer data, the honeybee dorso-ventral abdominal shaking (DVA) signal has been physically quantitated, for the first time, giving a one-to-one association between behaviour and intra-comb vibrations. From this, a novel method for the continuous in-situ non-invasive automated detection was developed for a honeybee signal previously thought to have no vibratory component. I show that the signal is detected with high frequency and repeatability, occurring mostly at night with a minimum towards mid-afternoon; inverse to that of the signal's amplitude over an average day. An unprecedented increase in the cumulative amplitude of DVA signals occurs in the hours preceding and following a primary swarm. These statistics suggests that the DVA signal may have additional functions other than as a foraging activation signal, and that the amplitude of the signal might be indicative of the switching of its dual, and potentially multiple functions.

This work has pioneered the use of accelerometer technology for the long-term monitoring of honeybee pulsed vibrations, making significant contributions to the emerging field of biotremology. The applications of this work, however, go far beyond the realms of the honeybee. The methods developed throughout this thesis could easily be adapted for the automated in-situ monitoring of biologically relevant vibroacoustics of multiple wild taxonomic groups, including wasps, termites, elephants and bats, as well as for replacing the need for visually compiled ethograms within lab-based manipulative experiments.

Table of Contents

Chapter 1: Introduction

In the current chapter, I review the current literature surrounding this thesis. The chapter is segregated by relevant subheadings to guide the reader through the wealth of information. First, the chapter explores the current ecological status of honeybees and their importance as an ecological service to both humanity and nature. From there, the biology of the honeybee is explained as well as a review of the communication pathways that orchestrates their complex social structure, focusing on two particular signals: the whooping and DVA signal. The novelties of this research is then explored before a general thesis overview that provides the core questions for the research.

Figures and supplementary videos for this chapter are categorised using the letter 'I': "*Figure I1…*" for example. Images obtained from other sources have been obtained with permission and the copyrights are cited in the figure captions.

1.1.0. The biology of the honeybee

1.1.1. Current ecological status of honeybees

Honeybees are arguably one of the most successful organisms across the globe, occupying most areas of the world alongside humans. They are what is known as a "keystone species" providing an extensive ecosystem service in the way of pollination of crops and wild flora as they fly between plants foraging resources to take back to the hive. Honeybees, alongside other pollinating fauna, are crucial for maintaining biodiversity because they have evolved alongside numerous plant species that require an obligatory pollinator for fertilisation (Allen-Wardell, 1998). Economically, the value of insect pollination services to arable agriculture was estimated at £400 million in the UK (Breeze, et al., 2011; Carreck and Williams, 1998) and £165 billion worldwide (Gallai, et al., 2009). In 2007, it was reported that insects alone contributed 34% of the total world pollination service demands, with 80% of it solely coming from honeybees (POST, 2010).

The global number of managed honeybee colonies have increased by around 45% since mid-last century driven mostly by a few countries and in particular China and Argentina (Aizen and Harder, 2009). However, statistics from across central Europe and in North America are reporting declines by around 25% (Aizen and Harder, 2009) and 57% (National Research Council, 2007) respectively. This has worrying implications regarding the stability of honeybee pollination services (Potts, et al., 2010a; Seitz, et al., 2015; van Engelsdorp, et al., 2010a). Pollinator declines and/or failure of pollinator populations to increase in line with the rate of pollinator-dependent crop expansion could have serious effects on world food security, just as the recent increased demand for corn for ethanol production has had significant effects on food prices (Elobeid, et al., 2007). While it is impossible to identify a single causal factor that accounts for all national and global colony losses, several biological and environmental factors acting alone or in combination have been identified as having the potential to cause premature colony mortality. These include Colony Collapse Disorder (van Engelsdorp, et al., 2009), diseases and parasites, including *Varroa destructor* (Rosenkranz, et al., 2010), deformed wing

virus (de Miranda and Genersch, 2010a), acute bee paralysis virus (de Miranda and Genersch, 2010b), American (Hansen and Brødsgaard, 2015) and European foul brood (Forsgren, 2010), and agricultural practices such as monoculture and pesticide use. Since 1988, three comprehensive reports of the condition of honeybee populations around the world have been published, with the most recent published in 2015 (Ellis and Munn, 2015). Within this document there is a long list of honeybee diseases, be it parasitic or microbial, and the data they reviewed showed the alarming rate at which all honeybee diseases are spreading across the globe (Ellis and Munn, 2015). In the UK, the National Audit Office put together a comprehensive study into honeybee health in England and Wales (Mumford and Knight, 2008) showing that whilst some diseases (such as American and European foul brood) are being kept reasonably under control, there is growing concern about the ever-increasing resistance of the multiple disease-carrying Varroa to chemical treatment.

As a result, honeybee colonies in the USA have declined from the 5.9 million managed in 1947 to 2.3 million reported in 2008 (Potts, et al., 2010a; van Engelsdorp, et al., 2010a). Since then, US colonies have seen annual winter losses of around 33% (BIP, 2017), 18% higher than the “acceptable” value of 15% (Bee Informed Partnership, 2017) with a similar trend in the UK and other northern European countries (EPILOBEE, 2015). To decrease and possibly reverse the rate of the decline of honeybee colonies, the National Audit Office, as well as other International bodies, have stressed that beekeepers must increase the proportion of their apiaries that are monitored each year (Mumford and Knight, 2008). Therefore, development of non-invasive *in-situ* techniques to monitor honeybee hives will provide beekeepers with a powerful tool to make assessments into the health status of their hives.

1.1.2. The Honeybee Hive

1.1.2.i. Members of the colony.

Honeybee (*Apis mellifera*) colonies are highly social and organised communities. They usually exhibit population sizes exceeding 40,000 individuals depending on the season. During the spring/summer active season, there is a higher volume of workers assigned to gathering resources, such as pollen and nectar, to sustain them over the inactive winter months when the population size reduces (Winston, 1987). Colonies are comprised of a single queen, a few hundred male drones and thousands of female worker bees, as well as developing eggs, larvae and pupae (collectively known as brood) within the honeycomb (Winston, 1987; Bodenheier, 1937).

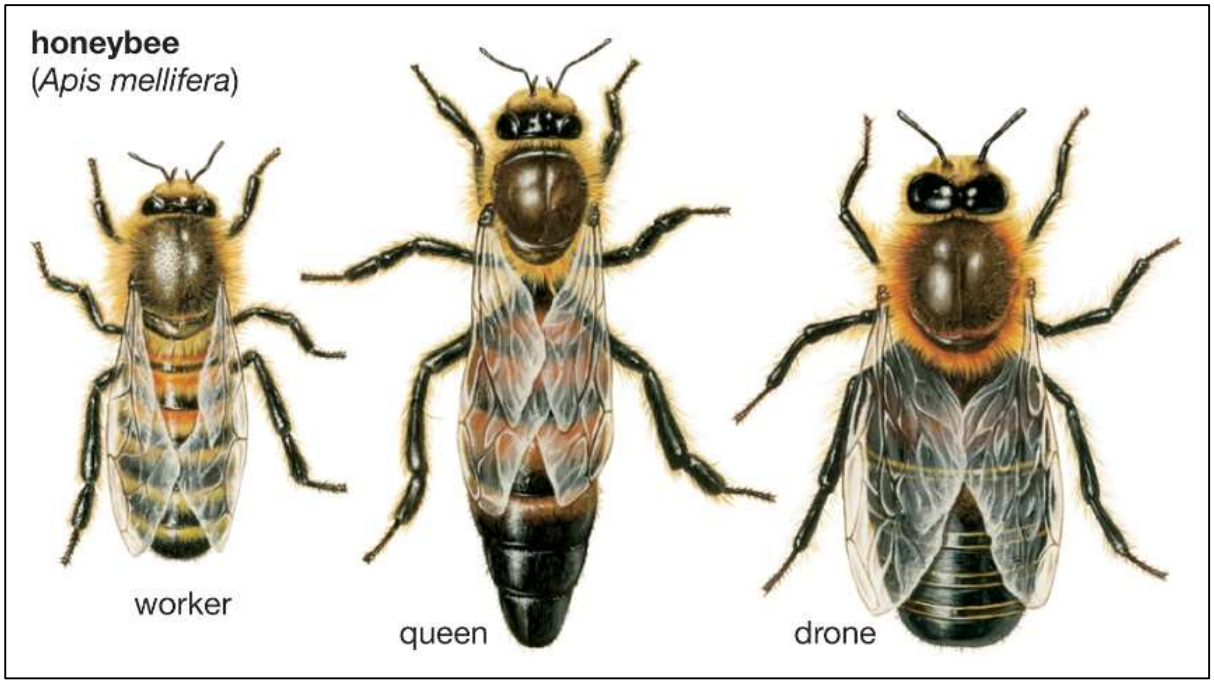

Figure I1. Pictorial representation of a worker honeybee (left) a queen honeybee (centre) and a male (or drone) honeybee (right). By courtesy of Encyclopaedia Britannica, Inc., copyright 2006; used with permission.

The honeybee queen (Figure 1, centre) is the sole reproductive female of the colony (Winston, 1987; Moore, et al., 2015). The queen's quality is often associated with its ability to reproduce as a poor

laying queen can have detrimental effects on honey production, disease prevalence, and the ability to survive the winter (Amiri, et al., 2017). The failure of “poor queens” is consistently listed as the primary problem for beekeepers, ranking as potentially the top reason for colony failure (Amiri, et al., 2017; van Engelsdorp, et al., 2010a). The genetic makeup of a queen honeybee is the same as that of any other female worker; the difference comes in how they are reared. When the colony deems it appropriate, a few selected eggs are transferred into specialised ‘queen cells’ that resemble monkey nuts. From this point onwards, queens are fed a diet comprising entirely of royal jelly (a secretion from the workers mandibular glands), while workers are provided with a combination of glandular secretions, pollen, and nectar, which come together to form worker jelly. The different diet administered to the developing queens allows them to mature in 16 days as opposed to 21 (see section 1.1.3.) and become 50% larger than the worker population, and with fully developed ovaries. Five to six days after emerging, the newly emerged queen will leave the hive on her mating flight to find a drone congregation area (Winston, 1987; Tarpy, et al., 2004). After successful mating, a queen will commonly lay 1,500 eggs in a single day. It takes around 2-4 years to exhaust the supply of sperm and for the queen to start producing un-fertilized eggs, at which point the colony will supersede her (Winston, 1987)

The drones (Figure 1, right) are the male reproductive individuals of the colony and are usually haploid (having only one set of chromosomes) and the product of an unfertilised egg. They are around 50% longer than and twice as wide as the individuals of the worker population with specialised ovipositors instead of stings. Their eyes are twice the size of a worker, which probably assists them as they mate with queens in flight (Winston, 1987). The drones are thought to be tolerated by the colony solely for reproduction and probably serve no use to their parent colony, as queens will not mate with their own drones because under single locus complementary sex determination (sl-CSD), infertile diploid males will be produced from any fertilized eggs that are homozygous at the sex-determining locus (Adams, et al., 1977). Only a few hundred drones are produced during the swarming season and any remaining are expelled in the autumn (Winston, 1987).

The worker bee (Figure 1, left) population makes up 99% of the colony. All worker bees are diploid females and undertake every job that is required outside of reproduction. These include, for example, honey preservation, nursing drones, building honeycomb, pollen and nectar collection and storage, removal of the dead, carrying water, thermoregulation and guarding the hive against invaders (Seeley, 1982; Winston, 1987; Ratnieks and Anderson, 1999). Worker bees also make the majority of colony decisions such as when and where to relocate the colony in a swarm. At around 1.5 cm long, they are the smallest individuals of the colony (Winston, 1987).

1.1.2.ii. The honeybee hive.

Figure I2. A British National Standard hive. This particular hive is based at the NTU apiary situated on the Brackenhurst campus of the university.

A typical British Standard honeybee hive consists at least of a floor, one 460x460x225mm brood box, a queen excluder, usually two additional 460x460x150mm honey supers, a crown board (residing immediately underneath the roof, not visible in Figure 2), and finally a roof, all together forming 'a set'. Within the three boxes is a series of ten to twelve wooden frames that are most often initially provided with a sheet of bees wax, known as foundation comb, which is thinly pressed to around 2mm

with hexagonal indentation upon which the bees will build the honeycomb (Figure 3). These frames are placed next to each other vertically in each box with brood box frames being larger than the ones of the honey supers, to allow the beekeepers to collect the honey crop in boxes that are of a manageable weight.

The function of the floor is to prevent direct contact between the brood box and the ground and to provide an easily exchangeable entrance, particularly useful for cleaning and sterilisation purposes, in which the honeybees can traffic in and out of the hive. Floors are most often made of mesh to provide draught free ventilation in the hive and allow debris to fall out of the hive. There is usually a brightly coloured inspection board suspended between the mesh floor and the ground that can be removed to assess the fallout from the colony within. The fallout from a colony is mostly made up of forage items such as pollen that is dropped by the bees and wax shavings from work within the cells of the honeycomb. Within the debris there will also be mites and moths present that will give the beekeeper an idea as to the level of parasitisation and health issues that the colony is experiencing.

Immediately above the floor is the brood box. The queen is restricted to reside within the brood box by the means of a queen excluder, which has a grid with gaps only just big enough for the workers to pass. The brood box therefore contains the developing larvae of the colony as well as pollen and honey. By restricting the queen to the brood box, the beekeeper ensures that the supers are solely used by the colony as honey (and sometimes pollen) storage. The crown board sits to segregate the top honey super from the roof. This allows a 2-inch gap for any feeding and / or treatment to be administered to the colony.

Figure I3. A British National Standard brood box frame. This is a two-sided frame with fresh foundation wax, a manufactured thin (around 2mm) sheet of pressed wax with a uniform series of shallow hexagonal depressions.

1.1.2.ii. The honeycomb.

When looking into a thriving honeybee hive, it is easy to see how they have elicited such fascination from scientists for so long. The uniform comb made entirely of wax (as opposed to the paper material observed in social wasp nests) that forms the infrastructure of the nest is fashioned entirely by the worker population in to a repeating series of perfect hexagonal cells (Winston, 1987). The honeycomb is used for nearly the entirety of honeybee activity. It is a communication highway for intra-colony interactions, it is the storage unit for colony resources and it is the rearing capacity for honeybee brood. It therefore provides a sophisticated platform on which to observe the activities being undertaken at the heart of honeybee society.

The hexagonal cells that make up the honeycomb can be broken into four functional categories. The first are the honeybee worker cells at 21-24mm wide (Seeley and Morse, 1976). These are the most common cells found within the honeycomb and contain developing brood through their uncapped larval and capped pupa stages until they emerge as adults. Outside of the rearing of honeybee brood,

these cells are hold a second function as the capped and uncapped resource storage cells (Seeley and Morse, 1976). These contain the deposits of wet nectar with a moisture content of above 18.6% (must be equal to or lower than to be honey) or tightly packed pollen. The honey cells are intentionally left open to promote the evaporation of this moisture until the bees are satisfied that it meets the requirements of honey. They then cap the cells with a thin layer of beeswax that is flush with the edge of the cells to stop the evaporation process and to keep it sealed from predators. Bees do not tend to cap pollen cells and often only half fill them (Winston, 1987).

Drone cells are slightly bigger than the majority of cells at 25-29mm wide, to accommodate the larger size of the male individuals (Seeley and Morse, 1976), and are usually found clustered at the outer edges of the frame (Taber and Owens, 1970). This cluster of drone cells is most often referred to as "drone comb" (Winston, 1987). They are easily distinguished from the worker cells by their protruding cupped wax capping.

Queen cells are constructed to develop new queens for three major reasons: (1) the colony is intending to swarm with the old queen, (2) the colony intends to supersede their poor functioning queen, and (3) the old queen has died and they need to produce a new one (Winston, 1987). When completed, queen cells look very different to the rest of the cells of the comb. They resemble a peanut shell that hang vertically off the frames, being rough textured, elongated and around 2.5 cm long (Winston, 1987). The difference between a swarming queen cell and a supersedure queen cell is location. Swarm cells tend to be located at the outer limits of the frame (usually the bottom) but the supersedure cells tend to be in the centre of the frame. This is because in the case of an emergency or supersedure, the worker bees will have to construct the cell around an already placed egg in the honeycomb (Winston, 1987).

The physical properties honeycomb have been shown to impact on the propagation of vibrational waves. Sandeman, et al. (1996) tested the vibrational properties of frames, partially detached and open honeycomb using laser vibrometry measurements. Comparison between the framed and

unframed honeycomb that was tested as part of their experiment revealed that only open unframed comb provided a relatively unimpeded path for signals at frequencies around 250 Hz. Interestingly, unframed combs were actually found to amplify the signals transmitted across areas not restricted by the support of the wood frame. Honeycomb bound by frame around all four sides were shown to carry a low frequency signal (about 15 Hz), however higher frequency vibrations were heavily attenuated.

A common phenomenon is for honeybees to detach the outer edges of the frames found closest to the entrance of the hives, and it is in these areas that honeybee dances are most likely to take place (Sandeman et al., 1996). Additionally, Tautz (1996) showed that forager honeybees waggle-dancing on open, empty combs recruit up to three times more of their in-hive conspecifics to feeding sites than those that dance on capped brood combs. In this free area of the comb, Sandeman et al. (1996) showed a particular amplification of low frequency (10 to 500 Hz) vibrations. Conversely, in an attached area of the same comb, these low frequency vibrations were transmitted with significant attenuation. This work showed that honeybees are able to identify the physical properties of honeycomb best suited for signal transmission, and will adapt the honeycomb for this purpose.

1.1.3. Annual cycle

One of the features that is unique to a honeybee colony's life cycle in relation to other bee species, is that honeybee colonies will over-winter instead of nest disbanding and queen hibernation. During the colder winter months, the honeybee queen's egg laying is limited and the colony size reduces. The bees within the overwintering nest will form what is known as a winter cluster, pooling the metabolic heat generated by microvibrations of the wing muscles (Lemke and Lamprecht, 1990; Heinrich, 1993; Watmough and Camazine, 1995; Stabentheiner, et al., 2003). This cluster will maintain a core temperature of 30°C (Heinrich, 1993; Watmough and Camazine, 1995). During the winter months, honeybee colony size reduces to a few thousand individuals and they survive by consuming the honey

stores they collected the previous summer. The transition of winter into spring causes the core temperature of the cluster to rise to around 34°C, triggering the colony to begin to rear brood (Seeley, 1985). By late spring, the colonies are back to nearly full capacity at over 30,000 individuals (Seeley, 1985).

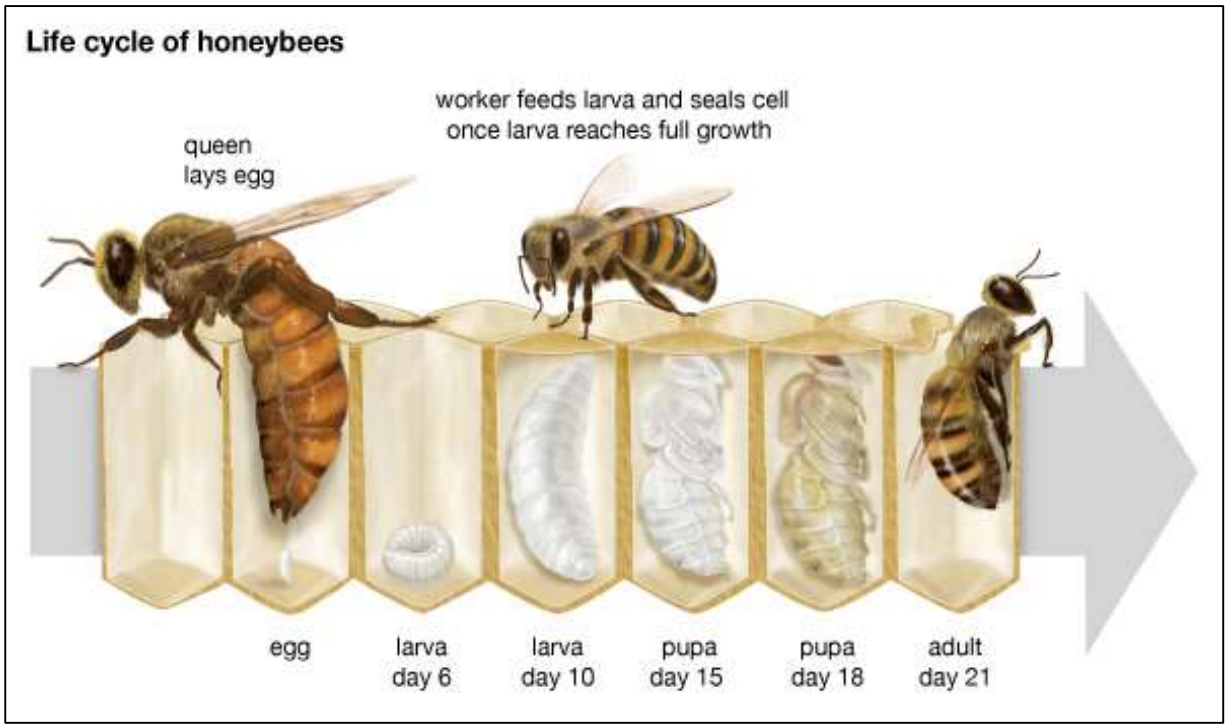

Figure I4. The life cycle of the honeybee. By courtesy of Encyclopaedia Britannica, Inc., copyright 2013; used with permission.

The individual worker bee life cycle starts with the queen laying a fertilised egg into a cell. She does this by placing her abdomen into the the cell and sticking the egg to the base. A healthy queen is capable of laying up to 2000 eggs a day (Winston, 1987) and she does this by using an organised pattern. Moving from cell to cell and starting at the centre of a frame with fully drawn out honeycomb, a queen will spiral outwards leaving the outer edges for the workers to store honey, royal jelly and other foods for the developing larvae (Winston, 1987) (see Figure 5 for a photographic example of a frame with fully capped brood). The next six days is the period of most intensive care from the workers

to the brood. After around nine days, the cells containing the larva and a little bit of food (made up of honey pollen and mandibular secretions known as bee milk) are then capped by the workers (see Figure 5) and the inhabitants each begin to make a cocoon. The last eight to nine days of development see the honeybee in a pupal stage before emerging on day 21 (see Winston (1987)). Owing to the fact that after the ninth day, the larva are capped and only receive care in the form of thermo-regulation by the worker population, experiments into temperature effects on brood development (see Tautz, et al., 2003; Czekońska et al., 2015) have had great success with rearing capped brood using laboratory based incubators without the presence of nurse bees.

Figure I5. A frame exhibiting fully capped worker brood in its centre, somewhat revealing the laying patterns of honeybee queens. The empty cells of this frame exhibit a zigzag pattern from left to right. This is caused by the queen's reluctance to lay eggs on the metal wire that is present within that acts to strengthen the comb. Capped honey is also present at the top left of the frame.

1.1.4. Social structure

Honeybee bee society (as well as around 15300 other Hymenopteran species of ants, bees and wasps) is maintained by a complex organisation known as eusociality; defined as the cooperative care of offspring born from reproductive individuals but reared by non-reproductive individuals with overlapping generations within a colony (Nowak et al., 2010; Yan, et al., 2014). Eusociality, in which some individuals see their own lifetime reproductive potential reduced, in order to raise the offspring of others, is believed to have evolved from inclusive fitness. Inclusive fitness theory suggests that an organism's own fitness can be increased by increasing the reproductive output of other individuals that share their genes, especially their close relatives (Nowak et al., 2010; Yan, et al., 2014). This is believed to have evolved especially in honeybees owing to their haplo-diploid genetic makeup, leading to a female being more related to full-sisters (0.75) than they would be to their daughters (0.5) (Hamilton, 1964).

Honeybees make a captivating model for the study of eusociality because their ecological success relies heavily on division of labour into specialised behavioural groups (known as castes) (Johnson, 2010) that interact, forming a superorganism (Seeley, 1989b; Moritz and Fuchs, 1998). For example, upon returning to the hive, foragers deliver the nectar collected in the field to nectar receivers for processing and storage (Seeley 1992, 1995). Nectar receiving is one task of the middle-aged caste whilst nectar retrieval is one of the forager caste, made up of the most mature individuals (Seeley, 1982; Page and Robinson, 1991; Pankiw, 2004; Johnson 2008, 2008b). Honeybees will often switch between the tasks within their "task repertoire" (Seeley 1982; Johnson 2008, 2009) depending on specific conditions within the hive (e.g. a sudden influx of nectar).

Comparison between different eusocial animal groups reveals large variations in the overall social organisation. In "diplo-diploid" eusocial termites, there is both a queen and a king who solely undertake reproductive tasks within the colony producing offspring that are fifty percent male and fifty percent female (Roisin, 2000), compared to a single queen or foundress as with haplo-diploid ants,

bees and social wasps. Like honeybees, termites have a caste system. However, as termites live within their food (wood), the non-reproductive castes are comprised of two groups: soldiers who defend the nest (Adams 1987) and workers who build the nest and care for offspring (Ladley & Bullock 2005). Whilst honeybees utilise age-dependent caste-determination (see Figure 6), it is still largely unknown what mechanisms determine an individual's caste within termite colonies. Most ant colonies follow a flexible task-allocation system that is considered more robust than the age-dependant task determination of honeybees (Robinson, et al., 2009).

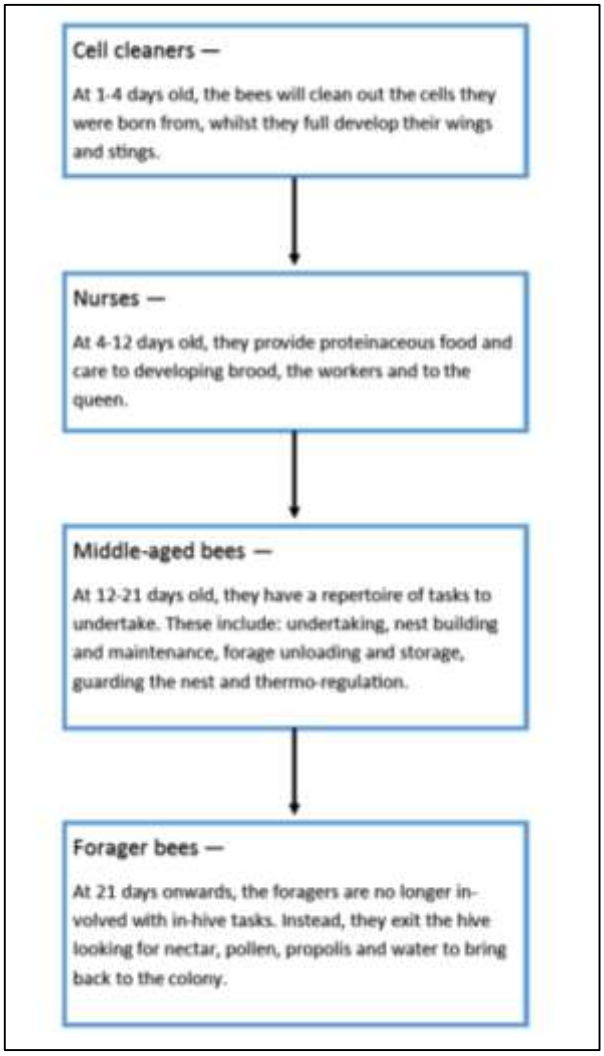

Figure I6: Age-dependent task partitioning in honeybee hives (Seeley, 1982).

It is apparent that the social structure of a honeybee colony (as well as all other eusocial communities) is a complex network of interlinking activities being undertaken by tens of thousands of individuals simultaneously. Eusocial insects must therefore implement an equally sophisticated communication network in order to orchestrate their activities. Coordination is therefore, mediated through many cues and signals produced by individuals of the colony (Seeley 1995, 1998; Pankiw 2004).

1.1.5. Types of Communication pathways

Communication in the animal kingdom is extensive in its diversity and its complexity. A communication signal, under Darwinian evolution, will only develop and persist within populations if the receiver can decode it and respond in a way that increases the fitness of the sender.

1.1.5.i. Visual

Visual cues are not commonly used as the direct communication in many social insects (Billen, 2006). Honeybees have incredibly good eyesight, clearly seeing objects that are as small as 1.9 degree with the smallest perceivable object being 0.6 degree (Rigosi, et al., 2017) (human eyesight has an angular resolution of 0.0128 degree). However, honeybees will only use visual cues outside of the nest for activities such as orientation (Towne et al., 2017). Even though bees can see parts of the light spectrum that human beings cannot (Peitsch, et al., 1992), they still need access to some form of external light to rely on their eyes for sensory information. Honeybees will naturally seek out dark areas to build their nests, such as tree cavities (Seeley and Morse, 1976) and within the dark confines of a honeybee hive and as a result, there is little visual information that a honeybee can decipher. Instead, they will communicate using a mixture of tactile (touch), chemical (pheromone) and, most importantly to this study, vibrational signals.

1.1.5.ii. Chemical

Pheromones are chemical substances secreted by an animal's exocrine glands that elicit a behavioural or physiological response by other individuals of the same species (Karlson and Lüscher, 1959).

In honeybees, there are two types of pheromones: primer pheromones and releaser pheromones (Bortolotti and Costa, 2014). The former act at a physiological level, initiating complex longstanding responses generating both developmental and behavioural changes in the recipient (Bortolotti and Costa, 2014). Honeybee queens are known to emit a primer pheromone known as "queen signal". This signal has a major effect on the physiology of the worker population, inhibiting their ovarian development (Camiletti, et al., 2013). Releaser pheromones act to alter the behaviour of the recipient (Bortolotti and Costa, 2014). An example of this can be found in the honeybee alarm pheromone. This pheromone is made up of a complex of chemicals that are released by the stinging apparatus when stuck in a victim. Detection of this chemical by other members of the colony causes the exposed individuals to become aggressive and to engage the victim with further stinging behaviour (Bortolotti and Costa, 2014).

Honeybee workers have five glands that can produce different pheromones: the mandibular gland in the mandibles, pretarsal glands in the feet and the tergal, venom gland and Nasanov's glands in the abdomen. Pheromone production has been most intensively studied in relation to honeybee queens. A queen will produce a multitude of different pheromones eliciting different responses from the members of her colony. For example, the queen mandibular pheromone contains active compounds that attracts drones for mating (Gary and Marsden, 1971), elicits retinue behaviour in nurse bees (the group of bees that surround and attend to the needs of the queen; Free, 1987), attracts workers during a swarm (Winston et al., 1989) and finally, may have some influence on worker activity partitioning (Pankiw et al., 1998). For a full review, see Bortolotti and Costa (2014).

Recent advances in honeybee brood-worker communication has focused on the use of pheromone cues produced by developing brood and its causal effects on worker bee behaviour. This pheromone,

known as Brood Pheromone (BP), is a blend of ten fatty acid esters (see Le Conte, et al. 1995; 2001). These fatty acid esters are present at different concentrations during larval development allowing nurses to gauge the various requirements of the brood at any specific time, including when to cap the cells (Le Conte, et al. 1994).

The most recognized worker-exclusive pheromone in honeybees is a secretion of Nasanov pheromone from the Nasonov gland, and is composed of seven volatile compounds (Pickett, et al. 1980) which are fanned by the honeybee wings to orientate members of the colony back to the hive or swarm cluster.

The alarm pheromone is secreted from the sting apparatus (Blum, et al. 1976) and the mandible gland (Shearer and Boch, 1985). These pheromones elicit a defensive and aggressive response to danger by the members of the colony. They can be released by bees without stinging, during stinging, and from stings left in the victim. When another honeybee detects this signal, the individual will become activated to a defensive behaviour in attack against the source of danger (Millor, et al. 1999).

1.1.5.iii. Mechanical (vibrational)

Sound and vibration, whilst often confused, are who distinct phenomena. Sound can be defined as a sequence of waves of pressure that propagates through compressible media such as air or water. Vibration, on the other hand, is the local displacement propagating through a solid medium. For many years, it was thought that honeybees were deaf to airborne sound (Goodman 2003). However, it has been shown that honeybees can detect air-particle movements (Towne and Kirchner 1989), with a chordotonal organ in the antennae (Dreller and Kirchner 1993a) that converts mechanical vibrations into nerve impulses relayed to the brain (McNeil 2015). This sensory system is sensitive to sounds with frequencies up 500 Hz. It is well suited to detect the 200-300 Hz sounds produced by dancing bees (Kirchner et al. 1991; Kirchner 1994), and this is the only natural context, other than its possible use in the control of flight (Heran 1959 in Towne 1994), in which this particular sensory system is known to be used (Dreller and Kirchner 1993b).

Vibrations are propagating waves distinct from sounds because they are transmitted through a solid medium rather than through the air. The quantity that propagates is a local displacement rather than local pressure. They can be substrate-borne or delivered during direct physical contact between other individuals of the nest. They also can be induced by sound reaching the solid substrate, and a vibrating solid substrate will usually induce a sound that propagates in the air around it. Vibrational signals are known to play a role in communication between honeybee workers, between queens and workers, between virgin queens and between workers and drones but their function is often debated among scientists (Nieh, 1993). There are eight identified signals with at least some (intentional or otherwise) vibratory component coming from within the hive. These include the dorsoventral abdominal shaking signal (Neih, 1998), the whooping signal (Ramsey, et al. 2017), queen tooting and quacking (Michelsen, et al., 1986a), worker piping (Thom, et al., 2003), grooming requests (Land and Seeley, 2004) and the waggle and tremble dances (Kirchner et al. 1991; Kirchner 1994).

For the transmission of information through the sound, individuals have to be relatively large in relation to the wavelength of the sound they emit (Markl 1983, Bennet-Clark 1998). Sending vibrations through the substrate rather than airborne sound is therefore advantageous in that these are probably less costly and more far-reaching signals for communication. Propagation of vibrational signals is also more localised to intended recipient and the signal is confined within the substrate, making the source of the message easier to locate by conspecifics and less likely to attract the attention of most predators (Bennet-Clark 1998) who usually rely on sound for prey location. The most common way for a honeybee to generate a vibration is by pressing its abdomen against the receiver or the honeycomb and activating the flight muscles (Seeley and Tautz, 2001). Alternatively, the pulse can be transmitted into the receiver or the honeycomb through the legs of the sender (Kilpinen and Storm, 1997).

It is hypothesised that honeybees detect substrate-borne vibrations through the subgenual organ (SGO), which is located in the tibia of each leg, just distal to the femur-tibia joint in each of their six legs (Kilpinen and Storm, 1997). It is an exceptionally sensitive vibration receptor in honeybees and is

found across many other insect taxa (Autrum and Schneider 1948). Much like the structures within the bee's antennae (Figure I7a), the SGO (Figure I7b) is a chordotonal organ suspended in a haemolymph channel between the cuticle of the leg and two tracheae (Kilpinen and Storm, 1997). Substrate vibrations received via the legs are sensed by the subgenual organs where they are translated into nerve impulses that are transmitted to the central nervous system. Schnorbus (1971) compared the SGO to an accelerometer, i.e. a mass suspended from a spring and oscillating in a damping medium. Kilpinen and Storm (1997) determined using electrophysiology that sensory cells respond to displacements of the organ relative to the leg.

The extensive research that has been undertaken into study of vibrational communication has led to the emergence of the field of biotremology.

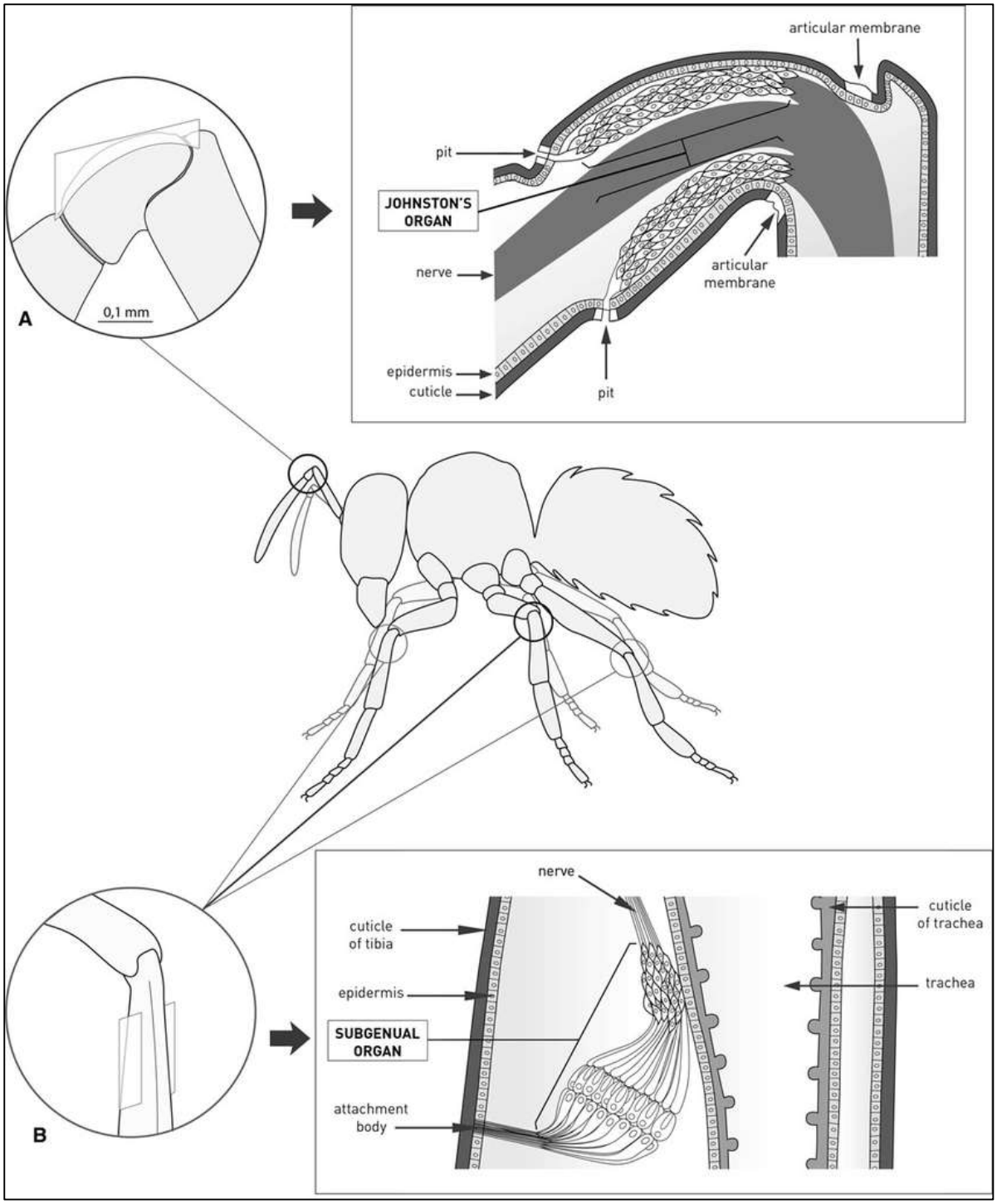

Figure I7. The Johnston's organ (a) and subgenual organ (b) are the primary receptors for vibro-acoustic signals (Hunt and Richard, 2013). By courtesy of Springer Nature, copyright 2013; used with permission.

1.2. Novel methods for the study of honeybee behaviour – Biotremology

1.2.1. What is Biotremology?

Biotremology explores the production, dispersion and reception of mechanical vibrations by animals, and the subsequent effect this has on the behaviour of the recipient. Swedish entomologist Frej Ossiannilsen was one of the first to suggest in 1949 that substrate-borne vibrations were used to transfer information between conspecifics, rather than air particle movement (Hill, 2016). Biotremology became the accepted term in 2007 and the first international symposium occurred in 2016. It is quickly becoming a recognised stand-alone field is demonstrated collated works in Cocroft et al. (2014). Biotremologists are interested in both vibrational information that is produced incidentally or purposefully as part of a communication strategy (Lehmann, et al., 2014). Biotremology studies over the last 40 years have made extraordinary progress in a relatively short time and have mostly been occupied with signal production, signal analysis, substrate properties, networks, playback experiments and discovering new and fascinating information about how the world works (Hill and Wessel, 2016).

1.2.2. How can studying the biotremology in honeybees contribute to their conservation?

As mentioned in an earlier chapter of this thesis, the National Audit Office as well as other international bodies have stressed that beekeepers need to increase the proportion of apiaries that are monitored each year (Mumford and Knight, 2008) and vibrational information from the heart of honeybee hives could be an important key to non-invasively monitor the status of honeybee colonies. Most sounds emanating from a beehive are by-products of bee activity and not thought to be a direct form of bee communication. However, as previously highlighted, there are vibrational signals widely used for honeybee communication that provide a rich source of information about the status of the colony.

The main obstacle of studying the ethology of honeybees within the hive is that they live in almost complete darkness and will propolise any foreign entity, such as microphones and video equipment that a scientist places inside the nest in order to observe their behaviour. Additionally the size of the equipment that is needed also poses potential issues. Honeybees live in narrow interstices between two parallel frames that is usually only just wide enough to allow bee trafficking, and this makes their monitoring with video equipment even more difficult. Alternative methods of monitoring the behaviour of honeybees must therefore be developed. Vibrational signals are seemingly a very important communication pathway for honeybees, and methods that allow us to obtain transferred information between conspecifics will provide us with insight into the current situation within the hive.

Pulsed vibrational waveforms that are generated as a consequence of honeybee activity can be just as important as intentional communicational signals themselves. Bencsik et al. (2015) presented a study whereby the brood cycle of the honeybee colony under investigation could be monitored using the mean overall vibrations occurring between midnight and 4am, when all of the colony were residing within the hive. In 2011, Bencsik et al. also demonstrated that by placing a vibrational sensor on the outside of a wooden hive, a unique set of vibrational features could be easily identified prior to swarming, giving an accurate method for identifying an impending swarm several days before it happened.

Studying the vibrations of honeybees has the potential to shed light on other physiological processes in honeybees, and can be applied to better understand the health issues recently encountered by pollinators. The collection of work contained within this thesis has pioneered the study of long-term trends in honeybee pulsed vibrational signals. The sensors used can reside within the colony for longer durations than that of the colonies life, with modern hard disks allowing the recording of years of continuous data from the heart of the colonies.

Within this thesis, after initial experimentation aiming to decipher signals coming from within the honeycomb from those coming from the emerged population upon it, I will focus on investigating two

worker bee signals: the DVA signal and the whooping signal. These were chosen due to the wealth of research that has been conducted on them over the last century. The whooping signal is a well-documented highly distinctive vibrational pulse exhibiting an excellent signal to noise ratio on my accelerometer logs, making it a favourable starting point for the development of novel techniques for in-situ monitoring of pulsed vibrations (see section 1.3.0. for a full review). The DVA signal was chosen due its suggested role, in extensive literary sources, as a modulatory signal that is highly meaningful, most often associated with queen-rearing, drone-maturation, swarming and foraging (see section 1.4.0. for a full review). The explicit function of both of these signals has proven difficult to identify with manipulative studies.

1.3. Whooping signals

1.3.1. Known physical properties from existing literature

The second chapter of my study focuses on the long term monitoring and the resulting statistics of a type of honeybee vibrational pulse most recently named in the literature as the 'stop signal', which is one of three established types of worker piping (Nieh, 1993). Regardless of the type, worker piping is thought to be generated by a bee that contracts her thoracic muscles (Figure I8) whilst in contact with the honeycomb. The signal is believed to be transmitted through the sender striking its head into a recipient whilst pressing her thorax against the honeycomb (Nieh, 1993) and producing a relatively brief vibrational pulse (Kirchner, 1993) with her wing muscles. This signal has been observed at frequencies between 200 and 400Hz for a duration of 0.05 to 0.2 seconds (Kirchner, 1993; Lau and Nieh, 2010; Pastor and Seeley, 2005). Having a mean duration of 0.14 seconds and negligible inherent frequency sweep (Lau and Nieh, 2010), it differs significantly from the other, much longer, forms of worker piping (Esch, 1964; Michelsen, et al., 1986a; Thom, et al., 2003). Wings-together and wings-apart piping are known to last much longer with a duration of 0.5 to 2 seconds (Kirchner, 1993; Pratt, et al.,1996; Qhtani and Kamada, 1980; Seeley and Tautz, 2001) with the former exhibiting a frequency sweep upwards from 100-200Hz (Seeley and Tautz, 2001). Seeley and Tautz (2001) identified wings together piping by nest scouts as acting to stimulate other bees to warm up their wing muscles prior to lift-off during preparation for swarming. Wings apart piping, however, can be found under many other circumstances within the hive (Kirchner, 1993; Pratt, et al., 1996; Qhtani and Kamada, 1980; Seeley and Tautz, 2001).

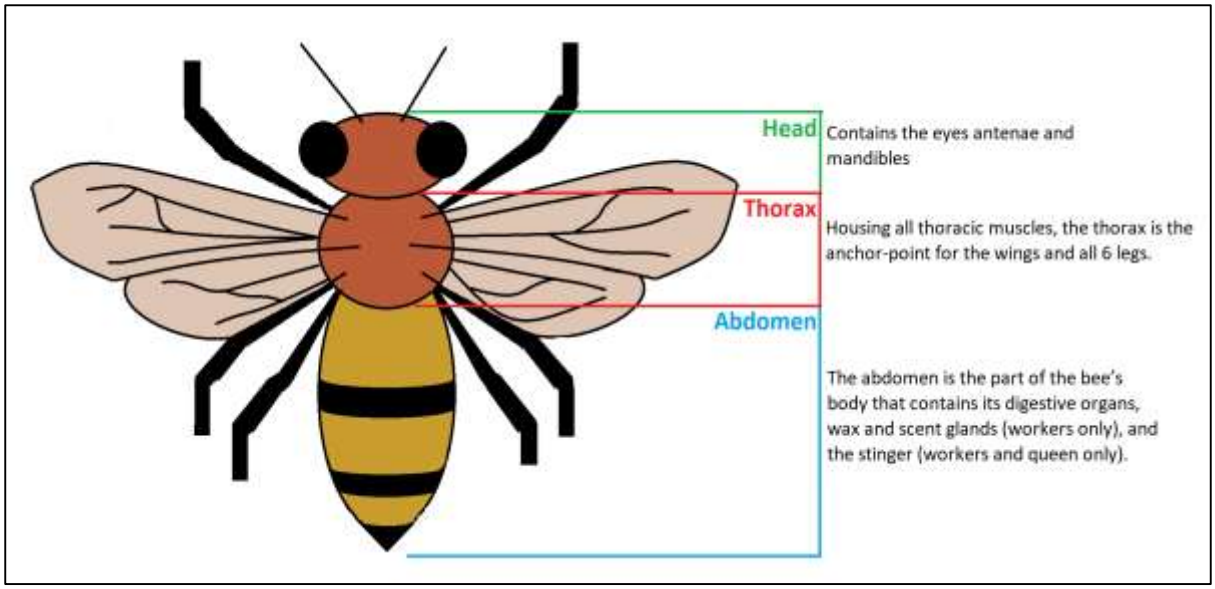

Figure I8. Depiction of the location of honeybee body segments.

1.3.2. History and Controversy

1.3.2.i. The begging signal

There is some controversy in the literature over the function of the brief vibrational pulse of main interest to section 1.3. It was first described by Esch (1964) as a begging call for trophallaxis by a dance follower to a waggle dancer advertising a nectar source. According to this hypothesis, the piping bee is requesting a sample of the nectar brought home by the dancer. This 'begging call' hypothesis also features in an earlier study by Von Frisch (1946; 1967) in which he examined how the bees following a dancer gain knowledge of the scent of the flowers that the dancer is advertising. "The signal may cause the dancer to interrupt, allowing the follower to approach the dancer for food" (Von Frisch, 1946). Esch (1964) replayed sounds recorded on tape into the hive and observed that all the bees became motionless if the sound was of very high intensity or was transmitted through the substrate. The phenomenon of immobilising honeybees using various types of strong vibrations has also been explored later on by several groups (Frings and Little, 1957; Spangler, 1969).

1.3.2.ii. The stop signal

The begging signal hypothesis features prominently throughout Michelsen, et al.'s (1986a, 1986b, 2014) studies. This definition was generally accepted until many years later when Nieh (1993) presented an alternative hypothesis for the function of this pulse: it serves as a stop signal to prevent foraging at overexploited food sources by inhibiting recruitment by waggle dancing bees. This hypothesis arose from Nieh's (1993) observation (later supported by Thom et al., 2003) that the primary senders of these pulses are nectar foragers that are engaged in performing tremble dances. Kirchner (1993) stated that there are vibrational signals emitted by tremble dancers, supporting the hypothesis that there is a vibratory channel of communication employed within tremble dances and that these are indistinguishable from those produced by the dance followers recorded by Michelsen et al. (1986b). Allowing a large number of foragers to build up at a feeder was seen to have several effects such as increasing forager wait time and colony nectar intake. Lau and Nieh (2005) recorded an increase of 100% in the number of these pulses coming from bees returning from a crowded feeder as compared to a feeder at which they did not need to wait.

Kirchner (1993) demonstrated that waggle dancers that received a stop signal had shorter dance durations and were more likely to leave the dancefloor but also that dancers did not show a strong, freezing response to a stop-signal (Nieh, 1993; Pastor and Seeley, 2005; Seeley, 1995), nor did they then offer nectar to their pipers. This is characteristic of modulatory signals, which are produced in a variety of contexts and are characterized by slightly shifting the probability of receiver behaviours, depending upon receiver response thresholds (Nieh, 1993; Thom, et al., 2003). Producing a modulatory signal makes functional sense under the condition of a colony experiencing an excessive surge in its nectar influx, so that the colony needs to supress the recruitment of additional nectar foragers and facilitate the recruitment of additional nectar receivers (Nieh, 1993; Thom, et al., 2003). Inhibiting waggle dancers can also have a secondary effect in that more nectar receivers can be recruited (reviewed in Keitzman and Visscher [23]). Consequently, it is not surprising to see that

tremble dancers act to inhibit waggle dancers, as reported by Lau and Nieh (2005), Nieh (1993) and Thom, et al. (2003).

The brief vibrational pulse investigated in our present study has also been identified as having another function: a signal for the warning of danger (Srinivasan, 2010). Nieh (2010) suggested that a bee may produce this signal upon return to the hive in response to a traumatic experience she received at a food source. This is hypothesised to be a method of preventing a particular location being advertised to prevent other bees from suffering a similar fate. In the study, Nieh (2010) pinched the leg of a bee at the food source to replicate an insect bite and recorded these signals upon return. Interestingly, the study showed that those bees who came under attack and won or came back unharmed from the battle did not signal danger upon returning to the hive as opposed to those who were injured by the predator. A recent study by Tan et al. (2016) using tethered hornets also showed a great increase in these signals on waggle dancers who were advertising food sources where the presence of a predator had been detected. Interestingly it was shown that the larger the hornet, the greater the number of these pulses that were recorded (Tan et al., 2016). They also showed that a honeybee would identify the dangerous location that is being advertised based on the smell of the dancer (Tan et al., 2016).

Aside from its function within the context of foraging, Seeley et al. (2012) presented an excellent study showing that this pulse played an integral role within the democracy of choosing a nest site during swarming via a process called “cross-inhibition”. Waggle dancers advertised the locations of their preferred nest sites and scout bees used ‘stop signals’, identified visually through a head-butt twinned with microphone recordings, to inhibit the dancers from advertising the locations that they deemed less favourable (Seeley, et al, 2012).

Nieh (1993) also suggested that, although these pulses may act to influence other bees, such as food-storers or nurse bees, waggle dancers do appear to be the primary focus. Through playbacks of the signal via a vibration probe, waggle dancers significantly reduced the amount of time that they danced for (Nieh, 1993). It was also shown that most of the foragers did not stop immediately during or after

receiving a 150ms vibration, so this inhibitory effect on waggle dancers cannot be explained by a general freezing response to vibrations (Nieh, 1993).

1.3.2.iii. The whooping signal

For clarity purposes, for the remainder of this thesis I will refer to this pulse as the honeybee "whooping" signal as this expression is onomatopoeic of the produced vibration. Alternative terminology such as "begging signal" emphasises a possible singular function of the signal made by dance followers, which seems questionable after the recent work of Nieh (1993). The term 'stop signal' emphasises a function as an inhibitory signal produced mainly to stop waggle dancers from advertising potential nest sites and food sources under a variety of different contexts.

1.3.3. Summary

The honeybee whooping signal is a brief vibrational pulse that has been observed under many differing situations. For this reason, the most accepted name for the pulse has changed several times over the years. Additionally, this signal has never been monitored on the long term or outside of the realms of manipulative behavioural experiments. All published work that has utilised handheld microphones and laser vibrometers have never definitively discriminated between the sender and receiver of the signal or been able to show the exact mechanism for its production. As there is ambiguity around the function of this signal, I have therefore renamed the pulse 'the whooping signal' in order to avoid the suggestion of any specific function.

1.4.0. DVA signals

1.4.1. History and controversy

The DVA shaking signal was first described by Haydak (1929) and since has been referred to under many different names: ''jerking dance'' (von Frisch, 1967), ''vibration signal'', ''vibration dance'' (Schneider, et al. 1986a), ''shaking signal'' (Allen, 1956), ''DVA-V signal'' (Milum, 1955). For the purpose of this paper, however, the signal will retain the name honeybee dorsal ventral abdominal shaking signal (or DVA signal) as it unambiguously points to the signal that I am focussing on. For the full list of alternative names, see Schneider and Lewis (2004).

As with the choice of name, the function of the DVA signal also causes debate amongst scientists. However, it is generally recognised as having a modulatory function (Markl, 1985; Hölldobler and Wilson, 1990). Distinctive behavioural responses are hard to establish in modulatory signals making them difficult to associate with any explicit function (Nieh, 1998). Owing to their non-specificity, modulatory signals can act upon many different individuals; acting to increase the performance of numerous different contemporaneous activities (see Schneider and Lewis, 2004).

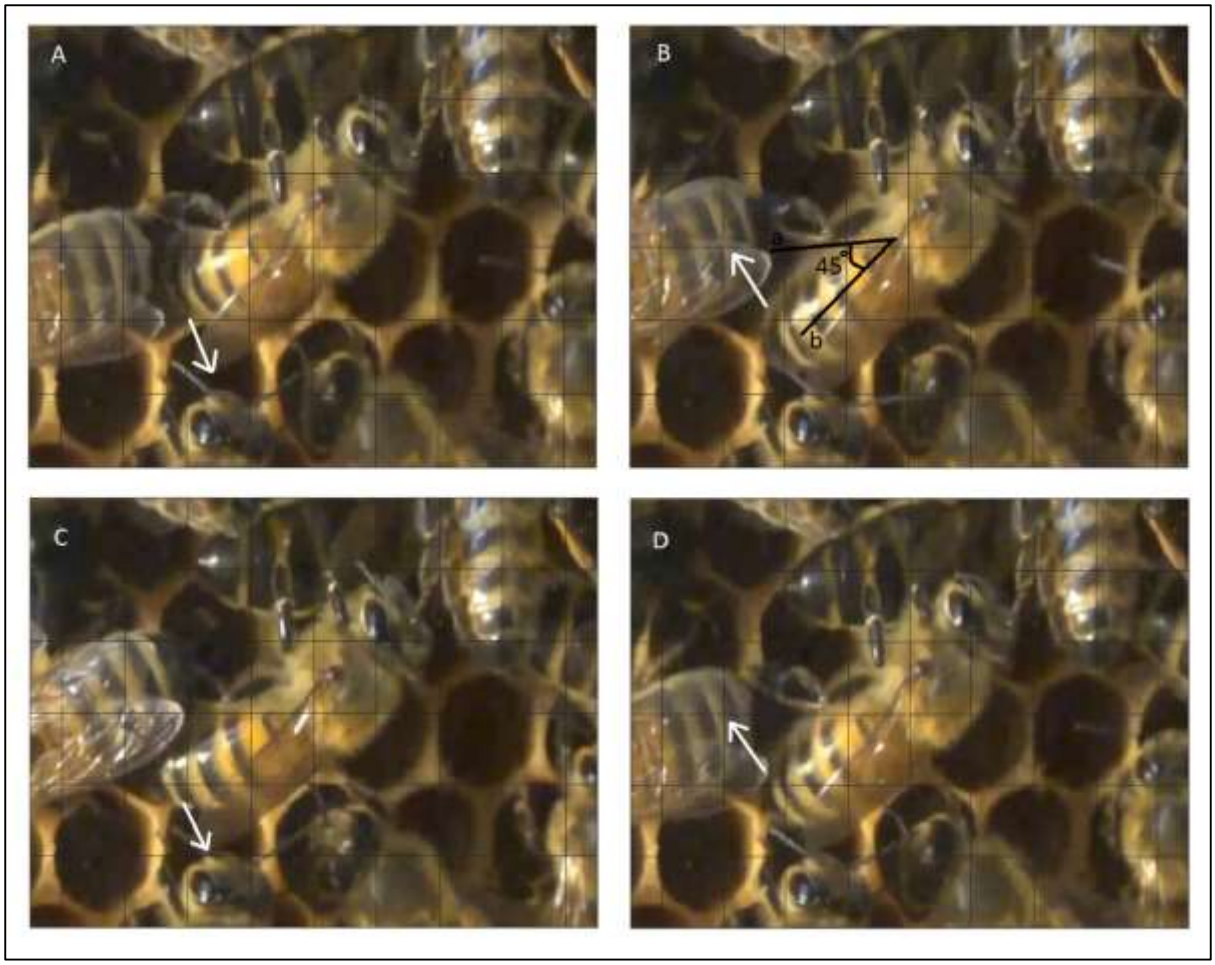

Figure I9. A honeybee performing a DVA signal. In four frames of video, it can be seen that (A) the honeybee starts with her body close to the recipient (a) gripping hold with its prothoracic and mesothoracic legs. The bee then thrusts its abdomen outwards 45° away from the honeycomb (b). The signaller then retracts this movement and pulls her abdomen back towards the receiver (B). This action is then repeated (C and D) up to 25 times a second.

1.4.3 Signal transmission

1.4.3.i. Known Characteristics of the signal

When a honeybee performs a DVA signal on another bee, it does this by gripping the comb with its metathoracic legs, the receiver with its prothoracic and mesothoracic legs (Figure I9 and I10), and then vigorously and rhythmically shaking its abdomen (Figure I8 and I9) in a direction normal to the plane of the honeycomb (see, Nieh, 1998; and Seeley, 1998) for 0.9 to 1.5 seconds, producing vibrations at 10 to 22 Hz (Gahl, 1975, Seeley, 1998b). During the shaking, the recipient of the signal appears compliant, remains fixed in one spot upon the comb, only motioning in response to the shaking body of the signaller (Nieh, 1998). It has been demonstrated in numerous studies that (i) honeybees will produce this signal on multiple individuals concurrently, and (ii) a bee will also often deliver DVA signals directly onto the honeycomb. In addition, honeybees producing DVA signals often do so as part of "shaking runs" (see Video I1), in which they roam over large areas of the hive, producing a series of these signals (up to 20 or more per min) that can last from several minutes to over an hour (Schneider, 1986; Nieh, 1998b; Seeley, 1998; Lewis et al., 2002; Schneider and Lewis, 2003).

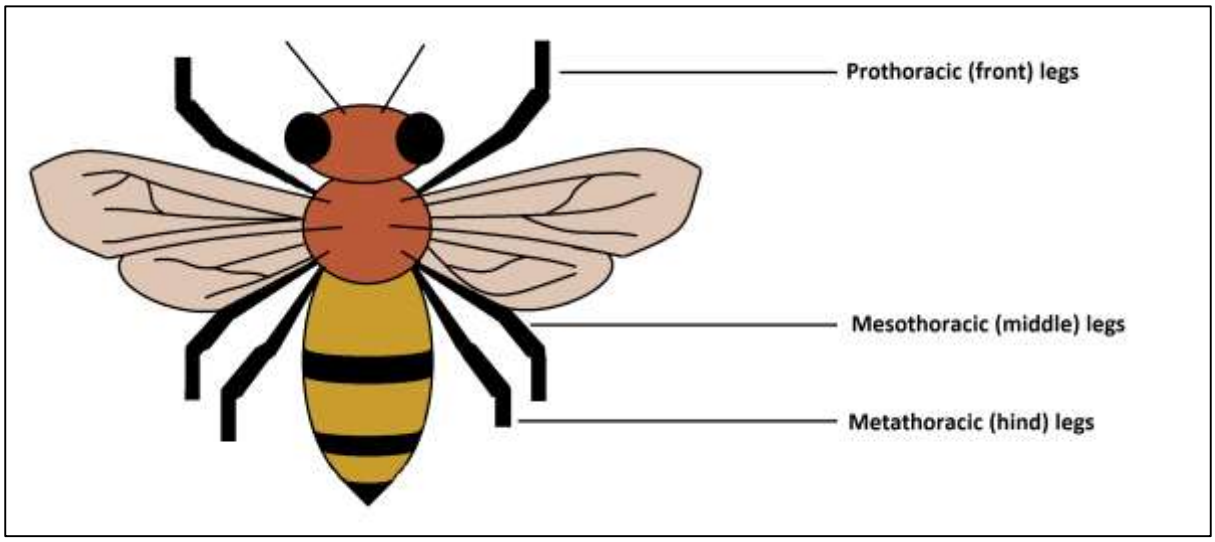

Figure I10. Depiction of the location of honeybee legs.

1.4.3.ii. Worker population

Even though only around 13% of workers ever perform DVA signals during their lifetimes (Painter-Kurt and Schneider, 1998a, b), it has been suggested that the DVA signal can be observed hundreds of times per hour regulating two distinct colony activities: foraging and swarming (Winston ,1987). The signallers tend to be restricted to the older workers within the foraging caste (Gahl, 1975; PainterKurt and Schneider, 1998a, b). However, it has been shown that two-day-old worker bees can perform DVA signals on fellow workers, as well as on queens and on queen cells (Allen, 1959a; Gahl, 1975; Painter-Kurt and Schneider, 1998a, b). It has also been demonstrated that the DVA signal primarily affects individuals of the middle-aged and foraging caste (Allen, 1959b). Upon receiving a DVA signal, the recipient has been demonstrated to increase their speed of movement within the hive, particularly towards the location of waggle dancers, and increase the overall rate of any hive-based activity they are engaged in (Schneider et al. 1986a; Schneider and McNally 1991). After a few days of successful foraging, it has also been suggested that there is an increase in the number of DVAs acting within a colony in the early morning before foraging begins and in the late afternoon after foraging has ceased (Nieh, 1998). Seasonal peaks in DVA signal occurrences associated with peak foraging times are also thought to occur. Seeley, et. al. (2010) showed that individuals returning from their first few trips to a newly found resource patch would only produce DVA signals within the hive. Further successive trips to the new forage patch resulted in signallers gradually transitioning from DVA signalling to waggle dancing until only waggle dances were seen.

1.4.3.iii. Drones and queens

The individuals of the worker population are not the only intended recipients of DVA signals. Queens have also been observed receiving DVA signals from worker bees. Allen (1956, 1958, 1959a) and Hammann (1957) noted that honeybees tended to DVA signal their queens before she was about to leave the hive, taking flight either with a swarm or to mate. Fletcher (1975; 1978a; b) suggested that

the rate of which a mated queen receives DVA signals rises rapidly once queen rearing begins and drops off a few hours prior to swarming. Similarly, Peirce et al. (2007) also observed that DVA signal production increases in the 2 to 3 days preceding swarming. This evidence all supports the message of “prepare for flight or greater activity” reported by Schneider (1991). Additionally, drones also have been observed to be DVA signals recipients (Boucher and Schneider, 2009). It is believed that the DVA signal has an active role in drone maturation and maintenance by making them more active within the hive and thus more likely to receive the care (grooming and trophallaxis) required for sexual development (see: Boucher and Schneider, 2009).

1.4.4. Summary

The vast majority of studies on this signal focus on its occurrences within worker-worker interactions, as these are the most common recipients. Early studies suggested it had a function within the foraging domain (Allen, 1959b; Gahl, 1975) but convincing evidence was lacking. The extensive work of Schneider and various colleagues, (Schneider, 1986; 1987; 1989a; and Schneider et al., 1986a and b) later confirmed by Neih (1998) and Seeley et al. (2010), provided evidence that it is a signal that conveyed the message “prepare for increased activity levels”. This means that the colony is ready to make best use of an imminent energetically expensive opportunity, such as a high-level forage influx. Additionally, this signal has never been monitored on the long term, outside of the realms of manipulative behavioural experiments. Regardless of the explicit function of this signal, however, it is clear that this signal acts within many different situations and intra-hive processes. For this reason, it must carry a versatile and meaningful message to honeybees that it is hoped will provide a powerful tool to monitor the colony status.

1.5.0. Novelties of the Research

This section of the introduction focusses on the major novelties of the research undertaken as part of this thesis.

1.5.1. Accelerometer technology

1.5.1.i. Accelerometer sensors

An accelerometer is an electromechanical device that measures acceleration. Acceleration may be static, like the one due to the constant force of gravity, or they can be dynamic, caused by the motion or vibration of the accelerometer. In this thesis, I will be using piezoelectric accelerometer systems to measure the intra-substrate vibrations that occur within the honeycomb of honeybee hives.

The piezo-electric material inside an accelerometer can be manmade or naturally occurring crystals that produce a charge when they are compressed, flexed or subjected to shear forces (Bruel, 1980). The word piezo stems from the Greek word for squeeze. In a piezoelectric accelerometer, a suspended mass is attached to a piezo-electric crystal, which is in turn mounted to the inner housing of the accelerometer (Bruel, 1980). When acceleration is applied to the body of the accelerometer, by such means as a vibration, the mass that is mounted on the piezoelectric crystal compresses and stretches the crystal (Bruel, 1980). This causes a measureable voltage to be generated on the crystal. The piezoelectric accelerometer obeys Newton's second law, Force = mass * acceleration, in that the force acting on the measuring element is directly proportional to the acceleration produced.

The Bruel and Kjaer 1000 mV/g (g = 9.81 m/s^2) piezoelectric accelerometers (Bruel, 1980) that I use can be placed into the hive and can be subjected to enormous stress. They are intended for welding against the side of buildings or equipment to monitor, for example, the vibrations of heavy machinery as well as for various applications within the automotive industry (Bruel, 1980). The accelerometer is small (1cm x 1cm x 1cm) and has an external protective housing made of solid stainless steel. They therefore will have no issue withstanding any possible stress administered by the members of the colony and remain fully functional even under propolisation and other activities.

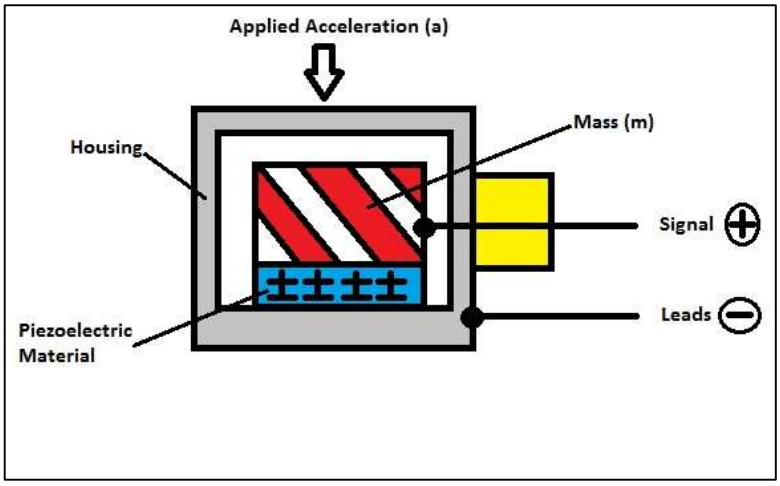

Figure I11. A Piezoelectric accelerometer

Other than the work of Bencsik, et al. (2011; 2015), no other research group is known to use high-specification accelerometer technology to monitor colonies of honeybees and there is no published work detailing the study of individual vibratory (or other) signals over long-term continuous recordings. In addition, accelerometers are very rarely used in biotremology. One short-term study on the abdominal wagging behaviour of Polistes dominulus is available, where the authors combined video footage with accelerometer data to identify vibrational components of the wagging behaviour (Brennan, 2007).

1.5.1.ii. In-situ and non-invasive continuous vibrational monitoring of honeybee hives

The use of accelerometer technology to observe honeybee behaviour is a novel feature of this thesis. Compared to the wealth of studies that employ traditional behaviourist methods of observing animal behaviour for short periods of time under well controlled experimental conditions, the use of the accelerometer technology in this thesis is non-invasive and non-manipulative, allowing honeybee hives to be monitored 24 hours a day under natural conditions for longer than the life-span of the colony itself.

The work of this thesis is amongst the first to feature the use of accelerometers to observe honeybee communication and activity from within the heart of the hive. Previously published work to study

honeybees has mainly involved the use of microphone measurements. The use of microphones, while they have proven effective, are restricted to relatively short observation durations, because they cannot be left inside the hive (see patented materials: Bromenshenk, et al., 2007; Etter, et al., 2007; Bromenshenk, et al., 2009), and are usually restricted to single bee measurements (Michelsen, et al, 1987). In studies by Nieh (1993), Thom (2003b) and Lau and Nieh (2009), marked foragers were continuously tracked with a microphone (with a Tephlon attachment to help localise any recorded sound to the focal bee, in the case of Nieh (1993)) held 1cm above the focal bee. It was stated that the microphone was most sensitive to the region immediately around the subject, but whooping (stop) signals produced in other areas of the dance floor were also audible. This method requires the frame to be extracted, is rather invasive and lends itself to much human error in that the microphone can vary in distance from the focal bee as the observer tries to track it across the honeycomb by hand. With an accelerometer, the measurement is unbiased, or the bias is standardised, as it is fixed to a set location on the honeycomb and there is no need to lift the frame or maintain the sensor against propalisation.

Vibrational data has also been measured by video analysis from transparent observation hives (Schneider and Lewis, 2004; Brennan, 2007). This method, again, is very invasive, as such a measurement requires a specialised transparent system with at least some light source as it cannot easily be undertaken in the natural darkness to which honeybees are accustomed. Another method to measure the substrate-borne vibrations is with laser doppler vibrometry (Nieh and Tautz, 2000; Tautz, et al., 2001; Seeley, 2005), which is sensitive to the solid boundary displacement. This procedure is particularly sensitive to the smallest relative displacement between the observed specimen and the vibrometer. No literature was found that detailed the application of laser doppler vibrometry to long-term in-situ measurements of fauna. Compared to accelerometer technology outlined in this thesis, laser doppler vibrometry is sensitive to temperature changes, causing slow drifts in measurement, and from any optical interference such as dirt particles that

obstruct the light path. Reader and Duce (2009) proposed a less expensive methodology that can be applied to the study of vibrations in individual insects through the use of the stylus of a ceramic cartridge that is placed in contact with a substrate, such as a honeycomb. This technique, however, relies on the measurement of displacement of the substrate. In comparison to an accelerometer system, this tool is less sensitive, has a lower signal-to-noise ratio and samples less of the honeycomb.

1.5.1.iii. Brood-isolated recordings

Using our embedded accelerometer technology within frames temporarily isolated (for up to 5 hours at a time) from the mobile emerged members of the colony, I am able to (i) monitor extensively the vibrational signatures exclusive to that of developing / emerging brood as well as (ii) quantitate the level of electrical noise from the equipment and (iii) the amount of noise from irrelevant contributions from outside the hive, such as birds and passing vehicles. In other words, I am able to present for the first time, the exact vibrational information relevant to un-emerged brood developing within the cells of a honeybee hive frame.

1.5.2. Detection software

1.5.2.i. Existing software

One previous study used spectrograms as a tool to identify the occurrences of Right Whale calls within a long-term dataset (Gillespie, 2004). This study did not use any automated techniques in its detection process. Instead, researchers built spectrograms of the recorded audio from their deep-sea hydrophones and visually inspected them for the signal of interest. Although the technique frees the user from the burden of having to listen to hundreds of hours of recordings, it is still very time consuming, requires a well-trained eye to pick them out and inherently leads to substantial error and subjective bias. The most extensive Right Wale call recording period that was examined was 6-months in duration (Gillespie, 2004), requiring a team of multiple individuals to manually examine this data.

A commercial product that exists and aims at the automated detection of animal vocalisations within prerecorded datasets is the Sound ID software (Boucher, et al., 2012). This has been used as a method for the detection of acoustic signals in bats, whales, humans (Jinnai, et al., 2012) and birds (Boucher, et al., 2012). The software analyses the geometric distance between instantaneous spectra of a template and systematic points along a sample of data. This software was specifically developed using acoustic signals of animals, which are, by nature, purposely conspicuous against the background information (e.g. mating calls). I worked closely with the company director and creator of the software, Neil Boucher, over a series of weeks and was unsuccessful with achieving any meaningful output from the software, most probably due to the low SNR of the honeybee pulsed vibrational cues found in my recordings. The main feature that sets the whooping signal detection software developed as part of this thesis from the Sound ID software is that it utilises spectrograms (see below) instead of spectra, and compares a template spectrogram to systematic points along the spectrogram of a sample using the ratio of the cross correlation product / Euclidian distance for the matching of images rather than the geometric distance used by Sound ID. The software also utilises a machine learning (discriminant function analysis on principal component scores) algorithm and is able to discriminate between whooping signals, worker/queen piping and clicks. The detection of DVA signals required a different strategy to both Sound ID and the whooping signal detection software. The 2-dementional Fourier transform (see below) was computed over one second long windows, instead of a spectrogram, and fed directly into a machine learning algorithm specifically trained for the discrimination between DVA signals, worker pipes and clicks.

1.5.2.ii. Use of spectrograms

The Fast Fourier Transform (FFT) is the numerical tool that allows us to deconstruct a waveform into its individual sinusoidal components with ultra-high speed. This can then be plotted as a spectrum of the frequency components showing the power (amplitude) of each frequency over a given time-

course. A spectrogram is a 3-dimansional image built from a sequence of spectra that are stacked side by side along the time axis and whereby the amplitude of each frequency is displayed as pixel intensity. The final plot displays time along the horizontal axis, frequency along the vertical axis, and the amplitude of the signal at any given time and amplitude is displayed by the colour scale. The duration over which each spectrum is computed along a waveform is known as its temporal resolution. The lesser the duration over which each spectrum is calculated (and subsequently stacked horizontally), the higher the horizontal resolution of the image. Such higher resolution will show a more detailed evolution of the frequency of a signal over time. The spectrogram is used multiple times throughout this thesis, as it is a highly effective method of highlighting features within a waveform. Visually, it allows for a quick and effective inspection of data that spans over long periods of time (e.g. 1 hour) but also is a powerful method to characterise brief signals that occur within my datasets. The spectrogram of the whooping signal is computed in this thesis and shown in comparison to other forms of piping signals common within the datasets.

1.5.2.iii. Two-dimensional Fourier transform

A two-dimensional Fourier transform (2D-FT) is computed numerically, in two stages that are both involving 'standard', one-dimensional Fourier transforms. The first FFT is carried out on the waveform in the same way as described for the spectrogram. In the 2D-FT, the FFT is then carried out again on the horizontal lines of the spectrogram calculated in the first stage. The result shows each spectral component's repetition frequency within the time-course of the waveform. In this thesis the 2D-FT is used in the spectral analysis and automated detection of the DVA signal and is the first known instance of this analysis being applied to a honeybee vibrational pulse. It is most suited to this kind of honeybee pulsed vibration due to it being composed of 13-27 consecutive repeating knocks. The 2D-FT does not reveal much information regarding the honeybee whooping signal, for example, as it is a short pulse that does not comprise of a repeated spectrum.

1.5.2.iv. Fully automated detections

The detection software that were developed as part of this thesis are fully automated. This is an improvement on the visual inspection of spectrograms previously used, for example, to track the occurrence of Right Whale calls (Gillespie, 2004). Whilst techniques assisted by man can be more sensitive, automated techniques are more objective. They can be used to process enormous quantities of data, which is essential in the analysis of long-term continuous datasets such as those presented this thesis, where thousands of hours of recorded vibrations need to be processed and can be done so in less than a week (e.g. 730 hours of data takes 24 hours to scan for whooping signals). Automated methods can also analyse multiple channels simultaneously. This allows concurrent monitoring of several different locations, or of the information gathered from the same source received at several different sensors. This can act to alleviate the user from recording the large raw data and reduce the need for large storage capacities. Sounds and vibrations above or below the frequency range of human hearing can be also be processed with the same methods without the need for extra analysis.

The low signal to noise ratio of the particular vibratory signals discussed this thesis pose additional challenges for their detection. All known studies involving the automated detection of animal signals have been focussed on high signal to noise ratio (SNR) acoustic signals within marine environments (Clark et al., 1987; Chabot, 1988; Fristrup and Watkins, 1994), for example. No known study has attempted to automatically monitor the low SNR and highly localised vibrations that are characteristic of social insects.

1.5.2.v. Detection and classification of ultra-low SNR signals using DFA on PCA scores

Principal Component Analysis (PCA) is a common tool in many scientific fields of interest including the field of chemometrics as a multivariate technique used to emphasise variation and identify significant patterns in a dataset for the purpose of reduction and unsupervised classification (Ringnér, 2008). Data reduction is achieved by identifying directions, called principal components, which explain most

of the variation within a dataset. By using just a few of these components, the original database can be more efficiently represented by relatively few numbers that are transformed into coordinates known as PCA scores. As the principal components are uncorrelated, they may represent different aspects of the samples (Ringnér, 2008). These PCA scores can then be plotted within an imaginary axis known as the PCA space, making it possible to visually assess the similarities and differences between them and determine whether they can be grouped on the basis of these differences. PCA deciphers these features based solely on the variance within the data in an exercise known as "unsupervised clustering". To identify the subtle differences that exist between predetermined groups, a "supervised clustering" algorithm is required. Discriminant Functional Analysis (DFA), for example, can be applied to the features identified by the PCA to find linear combinations of PCA scores, known as DF scores, which best discriminate between the predetermined groups (Dunteman, 1984). This combination of algorithms to achieve reduction and classification of structures within a database creates an effective machine-learning exercise.

Bisele, et al., (2017) discussed how previous studies have not considered how the quality of the data used to train the computer to discriminate between predetermined populations (a.k.a. the training database) can severely affect the outcome of the machine learning exercise. At the computer training stage, it is common practice to supply a training database with as many examples of each representative group as possible causing features of interest to reside within numerous different PCA scores. This has a blurring effect and reduces the DFAs ability to identify discriminating features. As Bisele et al., (2017) have shown, it is more important to supply the algorithm with an optimised training database that has been carefully selected to reveal the best, highly generic, discriminating features that are representative of the entire group. They showed that it is possible to optimise the dataset used to train the computer through an iterative process where the individual samples contributing to the training stage are systematically permuted (Bisele et al., 2017).

Through implementation of such analysis, I am able to create PCA scores and DF curves to effectively train the computer to discriminate between groups of signals within my long-term datasets, based on the spectrograms of similar, yet mutually exclusive, honeybee and non-honeybee signals (queen/worker pipes, whooping signals, rain drops and the sporadic high amplitude broadband spikes referred to as clicks) to reveal exciting statistics in the long-term trends of the honeybee whooping signal, a honeybee pulsed vibration that has never been monitored for more than just a few hours, consecutively.

Using DFA on optimised (using the permutation exercise presented in Bisele, et al., (2007)) PCA scores created using multiple 2D-FT images representing four categories of 1-second long signals, which contain high amplitude spikes, I also propose a method for the long-term tracking of a honeybee signal otherwise thought to have no auditory/vibrational component within vibrational datasets: the DVA signal. Using this machine learning exercise, I present a study that is the first ever to quantitate the vibrational properties of the honeybee DVA signal and automatically monitor it continuously for time durations longer than one year.

1.5.3. The Observation Hive

For a full breakdown of the construction and design of the observation hive extensively used throughout the chapters of this thesis see Appendix 1.

Several types of observation hive are commercially available and here I provide an overview of a few of them that are most commonly used by people wanting to showcase honeybees and that are most widely available across multiple manufacturers. The first is the “National Mobile Nucleus Hive” (Figure I12). This hive is a small (around five frames) brood box, known as a nucleus hive) with a sixth frame permanently fixed and suspended above the rest behind two glass panels. These mobile observation are very effective in fulfilling their purpose of short-term colony showcasing, for example, at events.

However, due to the inability of the colony to thermo-regulate efficiently in the observation stage, the bees will soon abandon the suspended frame. In addition, due to them being purposely constructed to be small to allow the ease of mobility, colonies have no room to expand further than the five or six frames. As demonstrated by Simpson and Riedel (1963), restricting the space available for the adult bees often leads to colony swarming. It is for these reasons that this hive was not fit for the long-term monitoring purposes.

Figure I12. The National Mobile Nucleus Hive. By courtesy of Thorne LTD, copyright 2007a, used with permission.

The second type of observation hive presented in this theses, is known as the Bespoke Observation hive. These hives consist of three to six frames that are stacked vertically behind observation glass in a box that is permanently fixed in its location. Often they are hinged so that both sides can be viewed easily. With ongoing maintenance, these hives can be sustained for longer than the life of a colony and can provide a wealth of visual information to hobbyists that showcases the activities of the inhabitants. However, it is known that honeybee colonies struggle in and often abscond from hives that are space restricted with lack of room for expansion (Simpson and Riedel, 1963) and, similarly to the observation stage seen in the previous design (Figure I12), impedes colony's inability to thermoregulate effectively. These hives, are very different to that of a British National beehive or a nest that a honeybee would construct naturally, having comb that is positioned vertically rather than horizontally. Therefore the Bespoke Observation hive was not appropriate for the long-term monitoring of honeybees studied in this thesis, as the colony was required to be kept in as natural conditions as possible, as would be provided by a commercial beekeeper.

Figure I13. The Bespoke Observation Hive. By courtesy of Thorne LTD, copyright 2007b, used with permission.

The third type of observation hive that I have decided to present is manufactured by a company called Peak-Hives, UK (Figure I14). The Observation National hive is essentially a British National Standard hive with observation windows around the outside of the brood and honey super boxes that make up the set. These hives are designed for hobbyist and novice beekeepers to observe and learn about the movements of the colony within. This design is advantageous in that it provides a honeybee colony with the exact conditions of a normal British National Standard hive, as would be given by a commercial beekeeper. The drawback to this design is that the windows only provide a view of the outside face of the peripheral frames of the colony.

Figure I14. The National Observation Hive. By courtesy of Peak-Hives LTD, copyright 2018, used with permission.

A major novelty of this project is the use of a specially designed observation hive I developed as part of this PhD research that has successfully addressed many shortcomings of commercially available products for the effective research into the heart of honeybee colonies (Figure I15). The frequent extraction and repositioning of a core or central frame into an observation unit was an essential requirement, as, in addition to the narrow corridors between frames making filming in the vicinity of the accelerometer virtually impossible, any video recording hardware placed into the centre of the hive would be propolised by the bees in a very short space of time.

The hive consists of one or two British National Standard brood boxes with 10 frames in each that are divided by a splitter. The floor is adapted to provide a modified entrance whereby the bees can enter and exit through a tube that extends through the wall of the research lab facility and to the outside. The observation unit was fixed on top of the top brood box and is made of double-glazed acrylic with ventilation holes. On top of the unit is a motor that drives two threaded rods, which when activated, gently extracts the observation frame into the observation unit.

Accelerometers were embedded into the honeycomb and can be plugged directly into the microphone jack of two video cameras positioned to face each side of the observation frame, allowing synchronous recording of visual and accelerometer data. When filming is completed, the frame is steadily placed back into the hive. This system allows the visual and vibrational recording of data from the heart of the colony and allows them to otherwise experience natural conditions when not under observation. During times of observation the bees appear unfazed by the by the lifting of the frame, probably due to the smooth transition of the frame into the observation chamber that is provided by the use of a motorised extractor, with vibrational information being observed at a similar rate as to before the frame was lifted.

In order to reduce heat loss and condensation, a thermal blackout curtain was purchased and is placed over the hive at all times when not under observation. Occasionally, considerable condensation can still cover the inside of the Perspex unit. A fan heater can then be used to warm up the cavity prior to

extraction of the observation frame. After less than 5 minutes, the condensation is completely removed. The blackout curtain also has the advantage of extensively reducing the amount of light that penetrates into the observation unit. This is important because honeybees are phototactic (Menzel and Greggers, 1985) and attracting them up into to the observation unit is likely to result in them building honeycomb within in. In addition to the blackout curtain, giving the colony ample space to expand into a second brood box placed at the bottom of the set has prevented them from building in the observation unit.

Figure I15. The finished design of the observation hive designed and built as part of this study.

1.5.4. Non-manipulative ethological study

This thesis focuses on two particular signals: the self-coined whooping signal and the Dorso-Ventral Abdominal shaking signal (DVA signal). Both of these have attracted much attention from scientists throughout the years and as a result, they benefit from substantial past peer-reviewed publications. However, unlike von Frisch's waggle dance (von Frisch, 1967) the explicit function of these signals still elicits some dispute amongst scientists and since communication is a behaviour, manipulative behaviourist experiments are often employed to study it.

Behavioural experiments often involve a hypothesis, which is investigated by means of an animal's response to a stimulus (Manning and Dawkins, 2012). This experimental approach models the basic features of behavioural processes under well-controlled, manipulative test conditions that yield meaningful responses in less time than would be observed naturally in the field (Cohn and MacPhail, 1996). The controlled environments of these experiments also increases our confidence in the model, allowing predictions to be made as to the effects of a stimulus that may occur under natural exposure. This approach, however, has several drawbacks. First, the results of the manipulations can be invalid within a wider ecological context. Individuals have previously been shown to behave differently when subjected to alien environments (Mench, 1998), thus analysis of animal behaviour within laboratory situations can provide biased information regarding their behavioural activities under natural circumstances (Cuthil, 1991). Second, behaviourism investigations often over-exaggerate the stimulus in order to elicit a response within a specific context, an approach that often removes these behaviours from the realistic context that gives them their significance (Toates, 1998). For example, based on manipulative behavioural experiments, it was concluded that the honeybee was colour-blind because its affinity to certain wavelengths was in line with that of colour-blind humans (von Hess, 1913). However, von Frisch showed that in the captive, laboratory context the colour of lights was not relevant to the bees (von Frisch, 1914). However, within a foraging situation observed under natural conditions outside in the field, honeybees were able to distinguish colours to gain access to the forage

(von Frisch, 1914). An improvement to the manipulative behavioural experiment could be to design experimental situations that mimic the natural conditions, but simplified so as not to distort the phenomena. Unfortunately, not enough information is often known to the extent of which these environmental parameters act upon the observed individuals.

An alternative approach to the study of communication can be found in ethology, which recognizes that the behaviour of an organism is intimately coupled with its environment (Tinbergen, 1963). Subjecting an organism to an over-exaggerated stimulus can destroy the context for its resulting behaviour. Ethology therefore promotes the studying of organisms under natural conditions (Lehner, 1998). Animals are very sensitive to environmental factors and it is difficult to control the many variables that will modulate it in the field. Therefore, ethologists must understand all the environmental factors potentially driving the observed behaviour (Lehner, 1998), something that is not always possible. There is also a drawback to studying animals under natural conditions, in that instances of observed behaviour can often be saturated by the large amount of time it can take for the behaviours to appear. However, in a study (such as the one presented in this thesis) where the desired outcome is to make assessments into a behaviour in relation to natural phenomena and towards the status of the study organism, ethological studies provide much richer outcomes than behavioural studies.

One of the key components of ethological studies is that the focal organism must be observed without influencing its natural behaviour (Tinbergen, 1963). Honeybees pose an interesting challenge in that any previously used recording devices, such as microphone probes (Neih, 1993; Thom, 2003b; Lau and Neih, 2009), are short-term methods that require removal of the bees from the hive. One of the greatest novelties of this thesis is that I am able to show how honeybee activities can be monitored on the long term using in-situ and non-invasive accelerometer technology. Our methods give an interesting alternative perspective providing a wealth of information that will contribute to the further

understanding of two important honeybee signals (DVA and Whooping signals) especially in relation to colony status.

1.6.0 Thesis overview and core questions

1.6.1. Thesis overview

The overall goal of the work in this thesis was to explore the physical properties and long-term statistics of honeybee pulsed vibrations accessed by accelerometer technology placed into the centre of honeybee hives. This work pioneers the use of ultra-sensitive accelerometers to non-invasively obtain continuous long-term vibrational information from the heart of honeybee hives. Software has been developed that scans for and collects the timings of various vibrational pulses of interest that reside within the complex vibrational database. This dataset has enabled me to identify any long-term trends in the occurrences and also the vibrational characteristics of those detected pulses. My observation hive has been extensively used in conjunction with accelerometer data to gain synchronous video and vibrational information to help validate and give meaning to my findings.

This thesis is divided into three main results chapters. The first is focussed on larval vibrations within the colony. In this chapter, I experimentally remove accelerometer- equipped frames from the colony that have capped brood residing in them. After removing the workers by gentle shaking, I then place these frames in an insulated, heat-regulated holding box for the duration of the data collection. Over a series of brood-isolated recordings, lasting up to 5-hours each time, I examine the extent to which the un-emerged population contribute to the overall vibrational dataset obtained using the accelerometer technology.

In the second results chapter, I explore the short honeybee vibrational pulse previously named ‘begging signal’ or ‘stop signal’. The study demonstrates long term (over 9 months) automated in-situ non-invasive monitoring of this honeybee vibrational pulse using ultra-sensitive accelerometers embedded in the honeycomb located at the heart of honeybee colonies. In this chapter, I show that

the signal is very common and highly repeatable; occurring mainly at night with a distinct decrease in instances towards midday. I have also shown that it can be elicited en masse from bees following the gentle shaking or knocking of their hive with distinct evidence of habituation. The results of this study suggest that this vibrational pulse is generated under many different circumstances, thereby unifying previous publication's definitions, and I demonstrate that this pulse can be generated in response to a surprise stimulus. I therefore propose the new term "honeybee whooping signal" as it is onomatopoeic of the generated pulse rather than giving it an explicit function.

The third and final results chapter of this thesis is focussed on the honeybee Dorso-Ventral Abdominal Shaking signal. As with the whooping signal, the honeybee DVA signal has some controversy over its name and function amongst authors in the literature. For the first time, this signal has been quantitated vibrationally and analysed spectrally using 2-dimensional Fourier transforms. I show that this pulse, previously thought to have no vibrational component, can be detected within long-term vibrational datasets. The statistics are in line with the 21- day life cycle of the honeybee, they also show a lull at lunchtime, a decrease as the colony prepares for winter and an increase during swarming preparation, suggesting that this signal is produced by members of the foraging caste.

At the end of this thesis, I also discuss the findings, significance and future directions of this work.

1.6.2. Core questions

This thesis can be broken down into three central questions that the body of work aims to answer:

1) What can the in-situ monitoring of specific honeybee pulsed vibrations tell us about the status of the colony?
2) Can long-term statistics be identified to help to disentangle the function of specific pulsed vibrations?
3) How effective is accelerometer technology at assessing the ethology of honeybee colonies?

Chapter 2: Exploration of honeybee brood-specific vibratory information detected by accelerometer technology.

In the current chapter, I begin the experimental portion of this thesis with an exploration into some of the activities that make up the complex vibrational waveforms obtained using ultra-sensitive accelerometer technology placed within the honeycomb of honeybee hives. In particular, I focus on the contribution of the developing larvae and pupae within the cells of the honeycomb towards the overall vibrational measurement, looking for unique vibrational signatures that have the potential to non-invasively allow assessments into the presence of brood.

This chapter consists of a brief introduction explaining the motivation behind the study and its overall aims. The methods used are presented in detail along with the results, which are discussed at the end of this chapter. Figures and supplementary videos for this chapter are categorised using the letter 'B': "*Figure B1…*" for example.

2.0.1. Abstract

Whilst pheromones appear to be the major communication pathway in worker-brood interactions, there is evidence amongst honeybees and other taxa (wasp, ants and spiders) for the use of vibrational cues and signals. Recent research has focused on the use of vibrations as a communication pathway in honeybees (Bencsik, et al., 2011; Bencsik, et al., 2015; Ramsey et al., 2017). However, until now, no one has assessed the efficacy of vibrational monitoring for this purpose. If this study reveals vibrational information specific to honeybee brood, it would provide a starting point for a non-invasive strategy to assess the health status of honeybee bee brood without any disturbance to the hive. This chapter of the thesis is therefore centred on the vibrations associated with developing honeybee brood and aims to establish the vibratory contribution of the un-emerged population and how it compares to other signals found within complex vibrational datasets that can be obtained using the accelerometer technology.

Here I show that very little vibratory information pertains to the brood within a honeybee hive that can be detected using ultra-sensitive accelerometers, suggesting that communication with the emerged worker population must rely on other methods. One vibratory cue was found, however, that has the potential to indicate the presence of emerging bees. Honeybees emerging from the cells of the honeycomb use their mandibles to cut the wax capping covering the entrance. This is shown to produce high amplitude clicks on the accelerometer recording that are similar in sound and magnitude to those clicks that were discovered to originate from an emerged adult worker bee operating upon the cells, however, with a distinctly different waveform. Further long-term statistics on the occurrence of the emerging bee clicks within long-term continuous accelerometer datasets reveal its power in determining the presence of emerging brood and, therefore, as a tool for monitoring the honeybee brood cycle.

2.1.0. Introduction

Parental care of offspring is widespread in insects, but the role of communication in parent-offspring interactions remains largely unknown. In the sub-social treehopper *Umbonia crassicoris*, aggregated nymphal offspring produce substrate-borne, vibrational signals in synchronized bursts that elicit the mother's anti-predatory behaviour (Cockroft, 1999). Brach (1976) showed that the mother-offspring communication of funnel-web wolf spiders *Sosippus floridanus* occurs primarily through intra-web vibrations. In social wasps, vibrational signals are associated with adult-brood communication (Savoyard et al. 1998, Cummings et al. 1999) and with worker-queen communication that intensify the activities within the nest (Ishay et al. 1974). Contextual evidence and results of sampling larval saliva indicate that lateral vibrations by foundresses signal larvae to withhold or reduce their secretion of saliva in preparation for receiving a liquid meal from an adult female wasps (Cummings et al. 1999). Vibrational communication by developing larvae has also been observed within the symbiotic relationship between ants and caterpillars. DeVries (1990) observed 19 species of nodinids and 30 species of lycaenids caterpillars that possessed the ability to produce low-amplitude, substrate-borne calls. It was further demonstrated that those caterpillars restricted from the production of calls attracted fewer ants (DeVries, 1990).

As previously discussed in section 1.3.3, honeybees are eusocial animals. The intimate relationship between communication and sociality is well illustrated by eusocial taxa, in which complex systems of communication among colony members allow cooperative, colony-level responses to changes in the environment (Wilson, 1985a; Holldobler and Wilson, 1990; Seeley, 1995; Judd and Sherman, 1996) as well as competitive interactions among individuals (West-Eberhard, 1983; 1984; Keller and Nonacs, 1993). Recent advances in honeybee brood-worker communication has centred on the use of pheromone cues produced by developing brood and its causal effects on worker bee behaviour. This pheromone, known as Brood Pheromone (BP), is a blend of ten fatty acid esters (see Le Conte, et al. 1995; 2001). These fatty acid esters are present at different concentrations during larval development

allowing nurses to gauge the various requirements of the brood at that time, including when to cap the brood cells (Le Conte, et al. 1994).

Worker bee rearing of virgin queens gives evidence that chemical communication is not the only pathway of interaction between developing larva and the emerged population. Piping from within the capped cells may function to inform the worker population and the emerged queen that there are virgin queens present in order to prevent a queenless colony after swarming (Winston, 1987). During the period following the primary swarm, workers will produce DVA signals on the queen cells with increasing intensity until the exit of an afterswarm (Schneider et al., 2001). Queen cells that received the most DVA signals produce queens that have greater fitness and overall success (Schneider et al., 2001). The queens of the cells that received little or no DVA signals tended to have lower success or undergo execution by the workers (Schneider et al., 2001). This suggests, particularly in this instance, that vibrational communication is utilised by honeybees to control queen rearing and emergence.

A vast number of diseases and infections can affect the population of a honeybee colony with a vast number of them specifically targeting the developing brood. The most notable of these diseases are foul brood (American and European), chalk brood, and sacbrood (Baily et al., 1964), all of which act to kill the defenceless individuals developing within the cells of the honeycomb. If this study reveals vibrational information specific to honeybee brood, it would provide a starting point for a non-invasive strategy to assess the health status of honeybee bee brood without any disturbance to the hive.

Many long-term honeybee monitoring methods have been explored (see Meikle and Holst, 2015) with some companies (e.g. Arnia, UK) claiming that their devices that observe brood temperature are an effective, non-invasive method of assessing the presence of brood. Recent research has focused on the use of vibrations as a communication pathway in honeybees (Bencsik, et al., 2011; Bencsik, et al., 2015; Ramsey et al., 2017). However, until now, no one has assessed the efficacy of vibrational monitoring for this purpose. Honeybee brood vibrations might not have direct communication

purposes but the developmental activities (thoroughly studied within the literature) may have a vibrational by-product that can be used to monitor intra-cellular activities.

Previous experiments by Bencsik, et al. (2015) and Ramsey et al. (2017) have shown that the brood cycle can be monitored extensively by analysis of long-term term trends in overall night-time vibrational signal production. However, this requires weeks of data to be analysed retrospectively. As a result, his study investigates the extent of the contribution towards the overall vibrational information detected by our accelerometer technology within the honeycomb that is a direct result of honeybee brood residing within the cells. Exploration of this data will reveal any trends that can be exploited as an effective method for monitoring the status of honeybee brood and whether this contribution is significant enough to allow us to detect its presence non-invasively at any given time.

2.1.1. Aims

The aim of this work is to explore the vibrational information recorded by the accelerometer technology within honeybee frames temporarily (for a few hours) inhabited only by the un-emerged worker population in order to (1) identify any brood-specific contributions to the overall dataset, and (2) identify signals specific to emerging brood. The methods also allow a unique opportunity to make in-depth assessments into the accelerometer technology, breaking down the complex waveforms emanating from the hive into the individual signals that contribute to the overall vibrational datasets.

2.2.0. Methods

2.2.1. Equipment

2.2.1.i. The frames

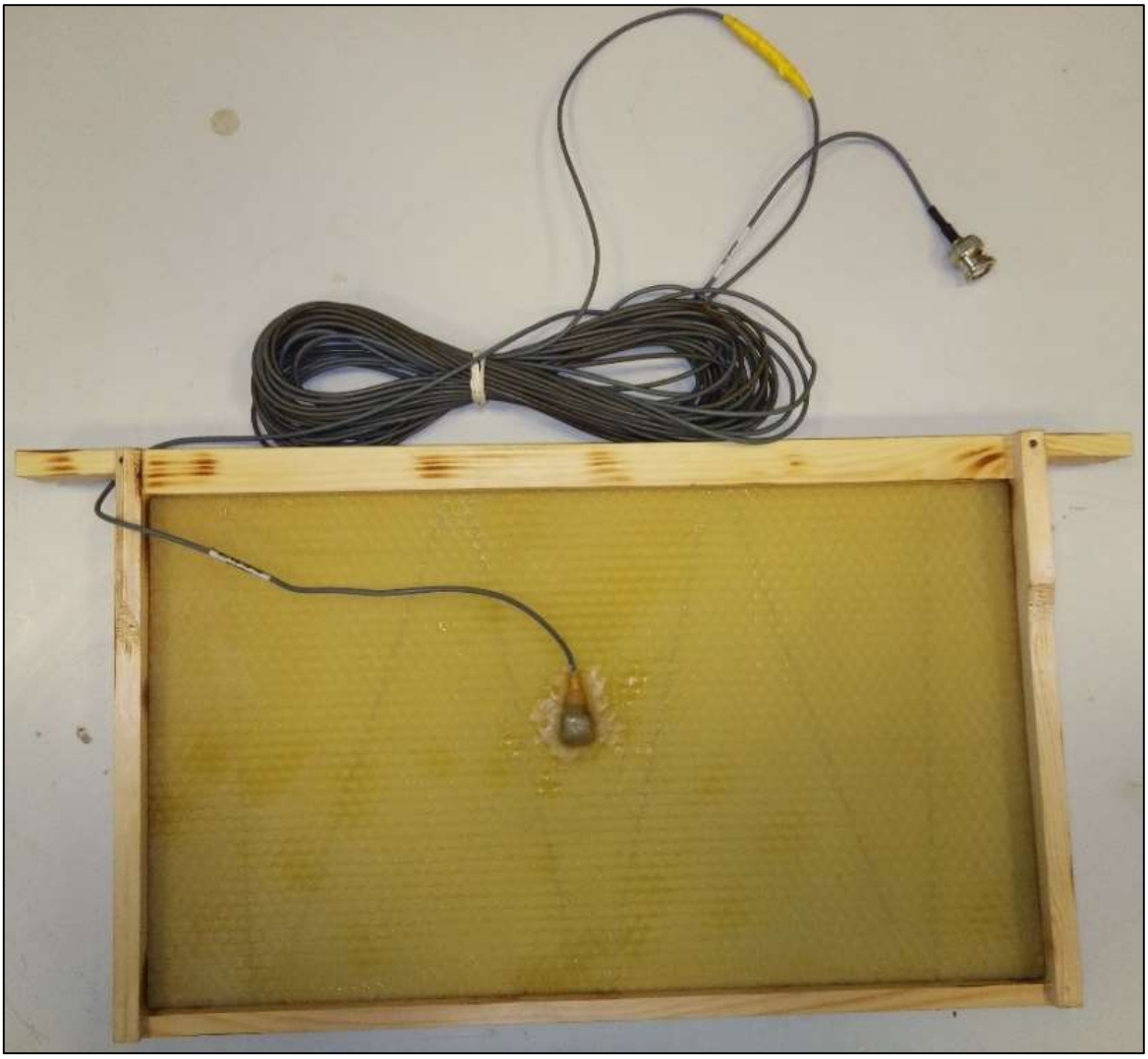

Figure B1. A British National Standard honeybee brood frame equipped with foundation comb and an accelerometer secured in place using molten honeybees wax.

Two new brood box frames were constructed and sanitised by using a blowtorch to lightly scorch the entirety of the woodwork to remove any fungus or bacteria. A new sheet of foundation comb was placed in the centre of each of the wooden frames and were heat-treated with a hot air gun to remove residing bacteria. An accelerometer (Brüel and Kjær, 1000 mV/g) was placed directly at the centre of

each frame's foundation comb and secured by dripping hot molten wax directly onto it and the surrounding area (Figure B1). The frames were then placed into the centre of an established beehive containing a seemingly strong and healthy colony of Italian strain honeybees (Figure B2) for the individuals to draw out the foundation wax into fully built honeycomb around the accelerometer. This was achieved by the removal of the two outer-most frames of the colony, which had very little honey stored in them. The remaining frames were shifted outwards in each direction from the centre so that the middle two slots of the brood box were vacant and the colony's existing brood was split either side of the experimental frames in order to encourage the colony to work on them.

The accelerometers were polarised with individual ENDEVCO 4416B conditioners (MEGGITT, U.S.A.), the output of which was plugged into an i02 sound card (ALESIS, U.S.A.) for digitisation at 22kHz sampling rate. The accelerometers in this study were calibrated in m/s^2 using an Aim-TTi TG5011A 50MHz Function Generator to drive a 50mV signal directly onto the accelerometer. Vibrational datasets were continuous and made up of one-hour long audio files, stored on an external SAMSUNG 4TB storage station via a home-built bash code on a Linux O.S. based computer that was set to reboot itself every 100 hours. To monitor the progress of comb building, GNU Octave software was developed in Linux that automatically computed a spectrogram of the previous day's vibrational data and then sent this figure to ourselves via email every day at 2am.

Figure B2. The hive pertaining to the focal colony. The set consisted of a 10-frame brood box, a queen excluder, two honey supers, a crown board, floor and a roof. The blue item at the bottom is an ARNIA beehive scale that records the mass and temperature of the hive.

2.2.1.ii. The incubation box

Brood rearing temperature is one of the most precisely controlled physiological parameters in a honeybee colony. Adult workers keep the central brood area between 34 and 36°C (Heinrich and Esch, 1994; Himmer, 1927; Tautz, et al., 2003; Czekońska et al., 2013). Although natural temperature fluctuations experienced by developing brood exist (from 32 to 36°C, Tautz, et al. 2003), it has been shown that a difference in rearing temperature by as little as 1°C has significant influence on the behavioural and cognitive performance of the individuals (Tautz et al., 2003) as well as on their susceptibility to pesticide poisoning (Medrzycki, et al., 2010). In order to monitor the brood in natural conditions but without mobile bees residing on it, it was therefore imperative that the temperature was controlled with the same precision in laboratory experiments as would be in the hive.

Previous studies into the effects of rearing temperature on brood development (see Tautz, et al., 2003; and Czekońska et al., 2013) have had great success with rearing capped brood using laboratory-based incubators without the presence of nurse bees. Therefore, in this study, a specialised incubation box was purchased (warming cabinet with thermostat; Thorne, UK) to house focal frames (Fig B3) when they contained brood. This is a 735x395x563cm wooden box with 2cm thick polyisocyanurate rigid foam insulation core, with a thermal conductivity of 0.022W/mK and low emissivity, aluminium foil facings on both sides (Figure B3). A 125W trace heating cable, which is regulated by a thermometer probe and thermostat set to 35°C, provides the heat for the incubation of the developing brood during the time spent (1 - 5 hours) isolated from the colony. Prior to experimentation, the box was set up in the laboratory and the temperature was monitored hourly throughout three consecutive days using a Lutron TM-920C thermocouple. This resulted in an average temperature of 35±1.8°C, well within the boundaries of natural, hive temperature variations (Seeley and Heinrich, 1981; Tautz, et al. 2003). The lid of the box also contained a sheet of rigid polyisocyanurate foam to aid in the insulation during experimental periods. The lid was secured in place via four stainless steel hook catches (Fig B3) that fit tightly to reduce heat loss. Within the box, two wooden bars were fixed in place, perpendicular to the length of the box, 46cm apart (slightly wider than the width of the body of a frame) for the frames to be hung during experimental data collection.

The heating system that was installed by the manufacturer (Thorne, UK) of the box used for incubation often provided relatively high amplitude spurious vibrations than can be described as ‘humming’ and ‘whistling’. As the focus of this study is on the detection of ultra-low amplitude vibrations, this issue was remediated by replacing the heating system with Aquapet, UK, 80W vivarium heat cables in line with an electronic thermostat. The result is a completely silent system, except for a single click when the thermostat turns the heater on.

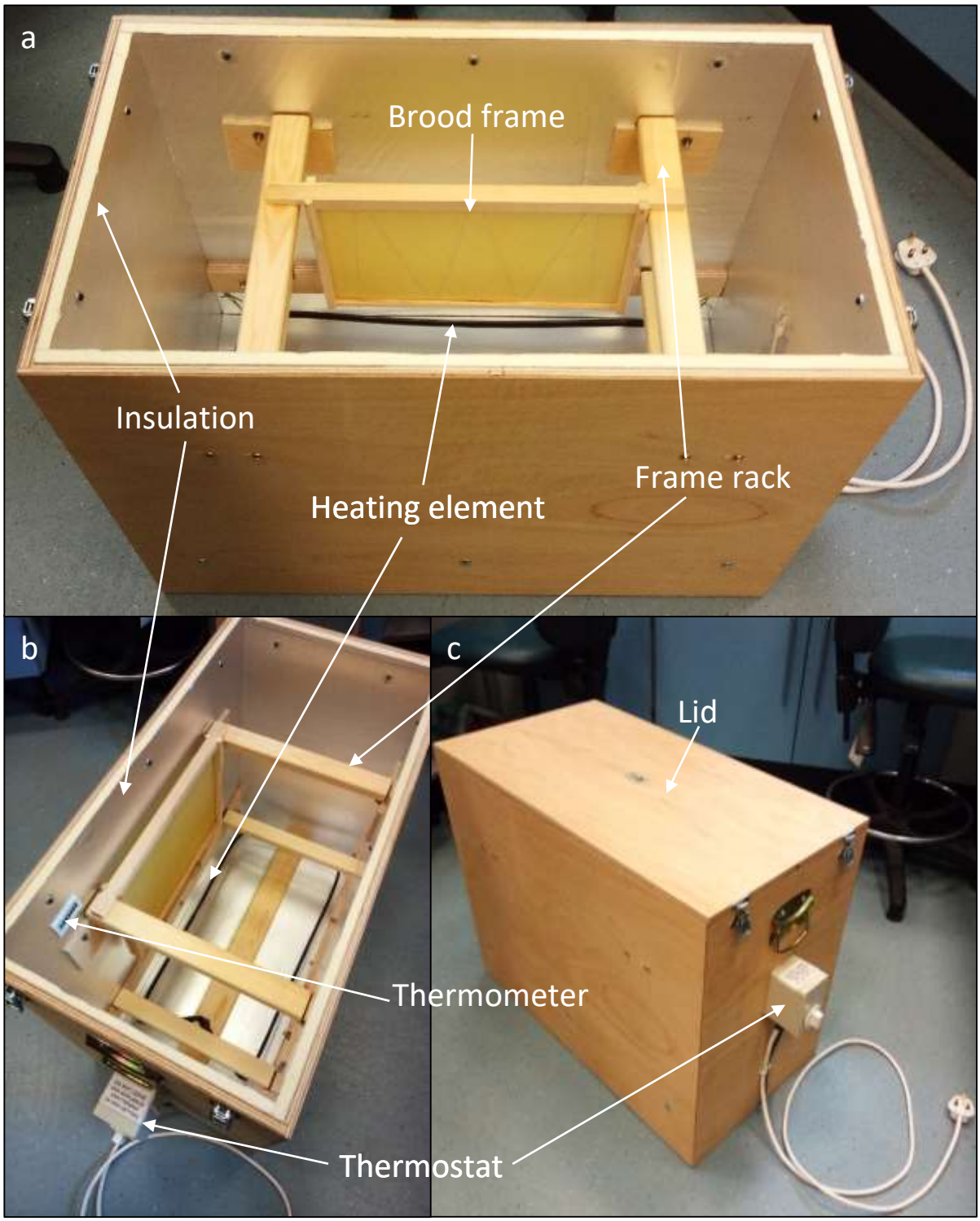

Figure B3. The incubation box. (a) An angle view into the open box showing the insulation, the frame rack supporting a frame with foundation comb and the black heating element; (b) A birds-eye view into the box further revealing the heating element, thermostat, frame rack, thermometer and insulation; (c) The box with its secured lid. Consisting of a double-armed rack, the box contained ample space to enclose two frames with accelerometers. Once placed in, the frames were spaced towards opposite ends to reduce the chances of vibrations from one frame being detected by the accelerometer on the other. The original purpose of this box is that of a honey warmer to liquidise crystallised honey in large quantities.

2.2.2. Data collection

Figure B4. The incubation box set up in the field and frames laden with fully capped brood containing single accelerometers placed at the centre. (a) The field based set up. The beehive in the background contains the colony from which the frames were extracted for measurements in the isolation box that was powered by 50m extension to mains electricity. (b) An extracted focal frame containing honeycomb predominantly filled with capped honeybee brood a double inverted V pattern of empty occurs as the queen avoids the metal wire of the foundation comb. (c) An accelerometer completely embedded by the bees into the honeycomb of a focal frame. These images was taken after the first experiment before the incubation box was placed into an additional acoustic isolation chamber during recordings.

Once the focal frame's honeycomb had been fully drawn and laden with capped brood (Fig B4b), relevant data collection could commence. The incubator was taken near to the hive containing the focal frames and plugged into a mains supply via a 50m extension cord (Figure B4a). Once the internal temperature of the incubator had reached 35°C and remained stable for 5 minutes, the focal frames containing an accelerometer each were extracted from the hive. The emerged population of honeybees were removed from the frames by smoking and gentle shaking over the hive. The focal frames were then placed on the rack inside the incubation box with a gap of 20cm between each other and the wall of the box to reduce any potential inter-frame detections. The lid was then secured in place, after having ensured that no flying bees had been mistakenly trapped in the box. At no point during the process was the recording interrupted. The focal frames were retained within the box for up to 5 hours at a time (the shortest duration of residence in the box was experiment 1 that lasted 90-mins), being examined after the first 90 minutes to check for any issues. A preliminary run of data collection was conducted on the 28th July 2017 and lasted 90 minutes. In this recording the box was left outside next to the hive from which the frames were extracted. As emerging brood was observed on the 28th July 2017, the next recording, which lasted 5 hours, was delayed until 10th August 2017 to allow the rest of the workers to emerge, the queen to lay more eggs and the majority of cells to be capped. The next two sampling dates were on the 15th and 18th August 2017, which each lasted for 5 hours. The next 5-hour recording was delayed again until the 1st September as emerging bees were observed on Frame 1 on the 18th August 2017. To help standardise the experiment, all recordings were taken between 10am and 3pm on sunny days. From the 10th August 2017 onwards, the box was placed in a field based acoustic isolation chamber (boot of a car) to further reduce the amount of vibrations induced by outside noise and for comparison to the signals recorded by the accelerometer when the incubator was placed directly in the field. For a full list of quantitative information pertaining to each experiment, see Table 1 below.

After each session of brood-isolated data collection, the lid was removed from the incubation box, each frame was extracted and then placed back into the hive with the exact positioning and

orientation found before it was extracted. The hive was then left without any intervention, with the accelerometer data still continuously recording, until the next set of data collection took place. In total, 21 hours of data specific to honeybee brood at varying developmental stages, covering two brood cycles, was obtained.

2.2.2.i. Individual experiments

Exp. No.	Date	Start time	End time	Dur.	Weather	Box location	% brood coverage Frame 1	% brood coverage Frame 2	No. that emerged
1	28th July 2017	13:30	15:00	90 mins	Sunny 20°C	Field	30 Capped	50 Capped	11
2	10th Aug 2017	10:00	15:00	5 hours	Sunny 20°C	Car	66 Capped	66 Capped 2 Uncapped	0
3	15th Aug 2017	10:00	15:00	5 hours	Sunny 21°C	Car	66 Capped	66 Capped	0
4	18th Aug 2017	10:00	15:00	5 hours	Cloudy 18°C	Car	50 Capped	70 Capped	32
5	1st Sep 2017	10:00	15:00	5 hours	Sunny 19°C	Car	70 Capped	30 Capped 30 Uncapped	0

Table B1. Quantitative information pertaining to each experiment. "% brood coverage" is an estimate of the total number of honeycomb cells containing capped or uncapped honeybee brood. "Number that emerged" refers to the number of honeybees counted that were residing on Frame 1 after experimentation. Frame 1 is only shown as no bees were counted on Frame 2 throughout the experiments.

From Table B1 it is possible to suggest a discrepancy of around four days between the brood cycles of Frame 1 and Frame 2. On the 28th July and the 18th August 2017, brood were observed emerging from Frame 1. As the honeybee has a twenty-one day brood cycle (Figure I4), this suggests that on the 10th August the brood in Frame 1 would be 13 days old. Frame 2 had two remaining uncapped cells containing larvae on this date, suggesting that the other cells had just been capped; this provides an estimate that brood in Frame 2 was around 9 days old at this point (Figure I4), four days younger than those in Frame 1.

This discrepancy of 4 days between the brood cycles of each of the two focal frames explains why capped brood was not observed on Frame 2 on the 18th August and around half of the brood were uncapped on the 1st September 2017.

2.2.3. Data Analysis

2.2.3.i. Spectral analysis of complex waveforms

The data files that corresponded to the hours of brood-isolated recordings were obtained from the database of continuous vibrational recording, in addition to one hour of in-hive recordings pre-extraction and post-replacement. The recordings were initially examined via the critical listening of the raw accelerometer audio files and visual assessments of the corresponding signal waveform, displayed as the time course of the acceleration. Next, the fast Fourier transform was used to break the complex waveform into its individual sinusoidal components and then log-scaled spectrogram images of the data were constructed in the MATLAB® core that allowed visual analysis of the power of each frequency present within the time domain. The spectrograms were built with a temporal resolution of 0.1s, as to account for the duration of the shortest pulsed vibration of interest to this thesis, the honeybee whooping signal. Sample images over a duration of 30-minutes are provided that are best representative of each of the days recordings. The logarithmic scale highlights ultra-low amplitude vibrations that occur within the accelerometer data.

2.2.1.ii. Analysis of the signal to noise ratio

Collection of data that was isolated from the emerged worker population gave a unique opportunity to make assessments into the contribution of different sources that make up the complex waveforms of the honeybee vibrational recordings.

The level of electrical noise (or "thermal noise") within the dataset was deciphered by selecting the quietest section of recording over a 10 second duration from the 1st September 2017 dataset. This dataset was chosen because it was identified as having the least vibrational information recorded by the accelerometers as there was no emerging brood during the recording and the box was placed in the isolation chamber. The spectrogram was calculated for a temporal resolution of 0.1-seconds and then averaged over the full range of frequencies (44 kHz) over the entire 10 second sample. The amplitudes within this averaged spectrum were then sorted in order of increasing magnitude. The lowest 10% of signal amplitudes were then averaged to give an amplitude value representative of the electrical noise.

Next, the mean amplitude of high quality examples of waveforms stemming from (i) a passing tractor on the road about 15m away, (ii) high amplitude clicking sounds (clicks) that probably result from a honeybee working on the wax of the honeycomb (Video B1), (iii) the 125Hz buzzing of the bees, (iv) a purring signal (a common 200 to 400 Hz accelerometer trace that lasts for up to 3 seconds and sounds like a cat purring), (v) a DVA signal (see section 1.4), (vi) a whooping signal (see section 1.3), (vii) worker pipe (see section 1.3 and Nieh, 1993) and a (viii) queen pipe (Wenner, 1962) were all computed for comparison to each other and the noise. The buzzing of the bees was subdivided into two categories: "Winter Buzzing" and "Summer Buzzing". These were both extracted from calibrated datasets recorded within the lab-based observation hive at 11am on the 11th November 2017 and the 16th July 2017, respectively. An audio file has been created that compiles examples of all of the signals that have been analysed as part of the creation of Figure B12 and this has been provided in Audio L.A1, with a full description provided in Appendix 2.

For the high amplitude clicks, a collection of 10 individual high amplitude spikes was collected from the 18th August 2017 data, aligned and averaged. The acceleration could then be read from the time course of the acceleration. For the DVA signal, a waveform was extracted from a signal delivered directly onto the calibrated accelerometers of the lab-based observation hive during the 2017 season.

The individual knocks that make up the signal were aligned and averaged to give a representative amplitude of the signal as a whole (see section 4.3.1. on DVA signals for further information), which could be read from the peak of the time course of the acceleration.

All other signals were extracted from various datasets presented within this thesis that had been calibrated prior to data collection. The time course of each extracted waveform was cropped tightly around its respective boundaries and the power spectrum was computed using the fast Fourier transform for a temporal resolution of 0.1s. The computed spectra were then averaged and the mean spectrum was plotted. The magnitude of the power spectrum over the bandwidth of frequencies associated with the signal of interest was identified. These were then plotted alongside one another to show their individual contributions to the overall vibrational dataset in m/s^2. These signals represent examples of high quality pulsed vibrations that occurred in the immediate vicinity of the accelerometer.

2.2.1.iii. The emerging population

In datasets recorded throughout in which a number of bees had emerged, the evolution of the density of high-amplitude clicks, which probably results from emerging bees cutting the wax capping of their cells with their mandibles, was explored. A home-built MATLAB function was created to count the number of clicks that occurred over a five-minute period of data that was moved in increments of one minute along the time axis throughout each of the brood-isolated recordings. The eminent spikes that occurred around once every 30mins and lasted around 0.1ms in the accelerometer waveform of each dataset, that resulted from the heater turning on and off, were easily identified by critical listening and the fact that they were present on the both frames at identical time-points. These were removed from the data using Audacity® software for this analysis only.

The software uploads five-minute long samples of the focal dataset and computes its spectrogram, cropped to frequencies above 2,000 Hz. This frequency range is used in this analysis because the clicks

have a broadband spectrum of frequencies (Figure B5) and honeybee 'non-click' signals all take place below 2000 Hz. The mean acceleration is computed across all frequencies above 2000 Hz on the spectrogram and the gradient of the gradient is computed along this curve to identify the sharp inflection point, a feature prevalent amongst clicks, allowing the filtering out of irrelevant noise and a curve that produces a negative spike in the presence of a click. A threshold value was determined for each dataset, below which the software identifies the presence of a click. The number of detected clicks are then tallied by the software. The threshold value was optimised for each dataset by uploading two minutes of data, computing its spectrogram, manually counting the number of sharp vertical broad bands above 2000 Hz, and lowering the threshold until all genuine clicks were counted. Once optimisation was complete, software scanned the entire length of each dataset.

2.2.1.iv. Quantitation of emerging honeybee clicks

To explore further the properties of the clicks, a selection of their waveforms were compared to those that probably emanate from a honeybee working in a cell as seen in Video B1. The "individual clicks from an emerging bee" presented in Figure B15 were taken from the beginning of the 18th August 2017 dataset at a time when there was no emerged bee on top of the frame. These clicks are therefore most probably originating from individuals emerging from the honeycomb.

In Video B1, a honeybee was captured on film, in full HD resolution at 50fps, working at the bottom of a cell within the honeycomb that is directly behind the embedded accelerometer. The video also contains the synchronous accelerometer data, made available in its soundtrack. In the film, the honeybee's residence in the cell appears correlated with the clicks in the audio, stopping and continuing as the individual leaves and re-enters the cell. These clicks were further extracted from the corresponding raw accelerometer file for comparison to the emergence clicks from the 18th August 2017 dataset.

2.3.0. Results

2.3.1. Spectral analysis of brood isolated accelerometer recordings.

The sections of each audio recording that was used in the creation of the spectrograms for each sampling date below have been provided in Audio B2 to B6.

2.3.1.i. Experiment 1, emerging brood

Throughout the duration of the brood-isolated recordings on the 28th July 2017, 11 individuals successfully emerged from the cells of the honeycomb and were found to reside on their prenatal frame upon opening the incubation box. Visual inspection suggested that mandibular cutting of the wax capping of the cells, from which the inhabitant was emerging, were possibly the cause of the high amplitude "clicks" that were audible within the corresponding vibrational dataset, as they appeared to occur in synchrony. This wax cutting behaviour caused high amplitude spikes over a broad band of frequencies, exceeding 4000 Hz, and these are especially visible and higher in quantity on Frame 1 compared to Frame 2, potentially due to the delay in laying times by the queen (as suggested by the timings of capped / uncapped brood throughout Table 1) or a difference in mass-density of the honeycomb between the two frames as a result of the increased number of empty cells in Frame 1. There appears to be a strong trace at 115 Hz and another at 300 Hz that are constant through the recording and can be attributed to the general buzzing of the bees around the box (Bencsik et al., 2015; Ramsey et al., 2017). The strong trace at 125Hz at the beginning of the recording originates from buzzing of a bee trapped inside the incubation box with the focal frames, identified through critical listening. This 125Hz buzzing then returns 20 minutes later as gradually individuals successfully hatched from their cells. The narrower band spectral clouds (0 to 800Hz) seen at 9, 15 and 19 minutes with peaks around 150 Hz with harmonics at 300, 450 and 600 Hz can be attributed to outside noise of passing vehicles and ground work identified on site and by critical listening to the audio track. Other than the wax cutting, no other honeybee-associated signal was heard within the accelerometer data.

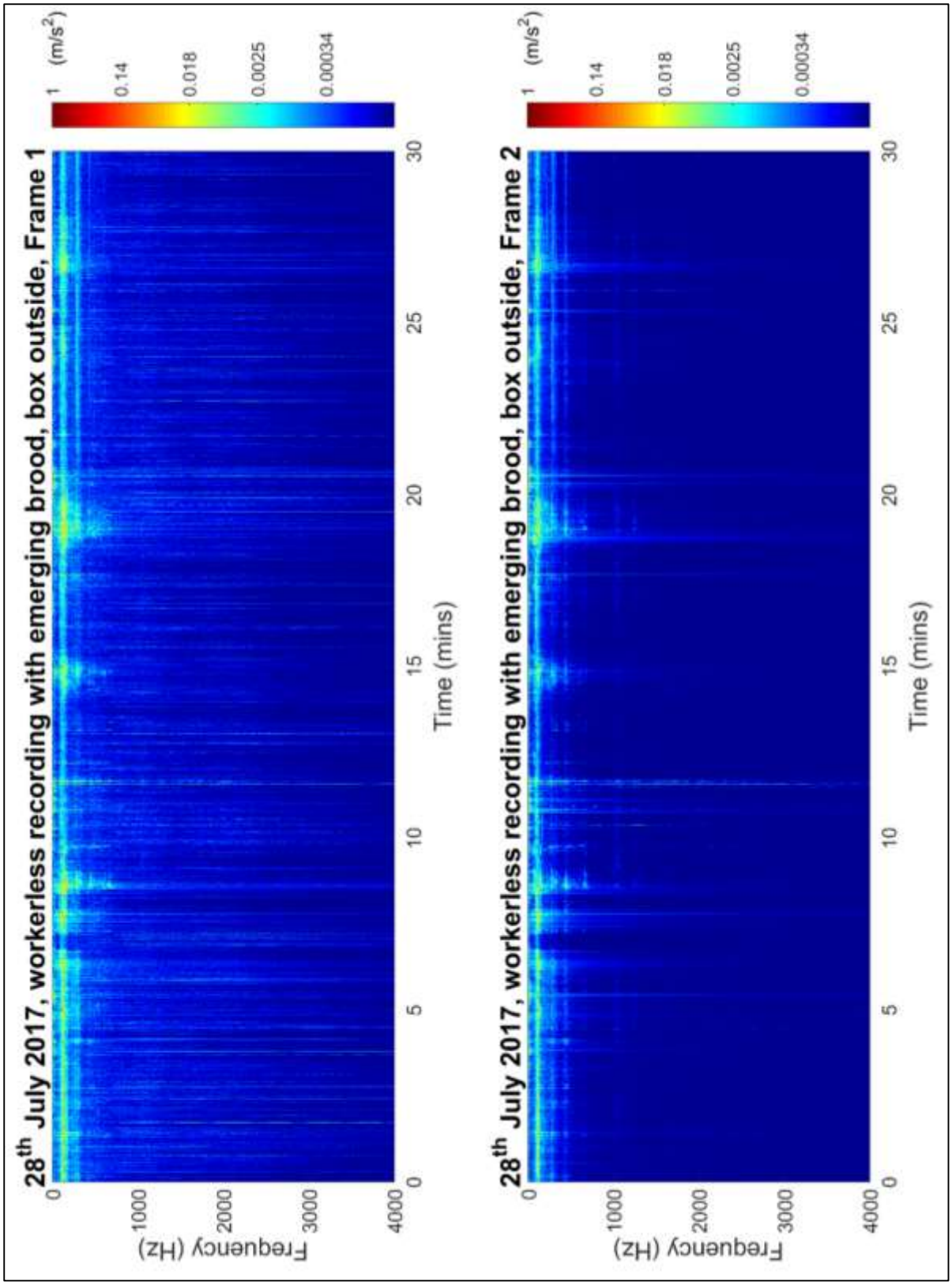

Figure B5. The spectrogram of a 30-minute excerpt of data from a brood-isolated recording from 28th July 2017 when the incubation box was kept outside in the field during experimentation.

The figure shows the spectrum of frequencies from 0 to 4000Hz for both frames that were placed in isolation. Pixel intensity is in logarithmic scale denoting the acceleration in m/s^2.

2.3.1.ii. Experiments 2, 3 and 5, no emerging brood

Experiments 2 and 3 were conducted on the 10th and 15th August 2015, respectively; Experiment 5 was conducted on the 1st September 2017. These experiments have been grouped together in this section as they show mirroring results. Below in Figure B6, the results of experiment 5 are shown. The results for Experiments 2 and 3 can be found in Supplementary Figures 1 and 2 of Appendix 3, respectively.

The further insolation of the incubation box from outside noise by placing it in an acoustic isolation chamber (boot of car) reduced the contribution of outside noise, evident by the reduction in the magnitude of the broadband clouds and the 300 Hz band from around 0.0025m/s^2 to around 0.0008m/s^2, as seen in Figure B6 and in Supplementary Figures 1 and 2 of Appendix 3 (Experiments 2 and 3). The frames under observation (for which data is showcased in Figure B6) contained mostly fully capped brood (Table 1) with some uncapped larvae, honey and pollen. No individual emerged from the cells of either frame during the entire recording of this data. On the spectrogram in in Supplementary Figure 1 of Appendix 3 (Experiment 2), we can see a high-amplitude broadband spike at seven minutes that is due to the thermostat turning on the heating system. Faint broadband clouds from zero to 500Hz that are apparent on both frames in Supplementary Figure 1 of Appendix 3 (Experiment 2) at 16, 22, 27 and 29 minutes are the result of passing vehicles and nearby roadwork. The 115Hz continuous trace apparent in the 27th July recording remains in this dataset; however, the 300Hz trace has disappeared from the data obtained in the isolation chamber (Figure B6 and Supplementary Figures 1 and 2 of Appendix 3). The traces than can be seen on both datasets are slightly more apparent on Frame 2 than on Frame 1 potentially due to a difference in load between the two honeycombs. As honeybees cap their brood after around 9 days (Figure I4), it is suggested in Table 1 that in Frame 2, the brood cycle may be up to 4 days behind that of Frame 1 (on the 10th August 2017 there were two cells remaining to be capped, suggesting the brood was around 9 days old). As suggested by Bencsik et al., (2015), the mass density of the honeycomb increases with

development of the brood potentially causing of the increased magnitude of signal observed on Frame 2.

Compared with Figure B5, there are no broadband spikes on either frames' spectrogram exceeding 2000 Hz in Figure B6. In addition, no clicks could be heard on the recording or identified within the raw data file. During this experiment, no individuals were witnessed emerging from the honeycomb and all wax caps were intact following each of Experiments 2, 3 and 5, giving further confidence that clicks detected in Figure B5 are pertaining to emerging honeybees.

The lower frequencies present in the spectrogram were explored by zooming in on the 0 to 200 Hz spectral band to identify any information specific to the brood residing within each frame, e.g. well-developed pupae moving within their cells. As demonstrated by the 30 minute sample of the 15th August 2017 dataset provided in Figure B7, all information below 200 Hz could be observed on both channels, such as the electrical noise at 50 and 100 Hz and the faint continuous trace at 125Hz that could be attributed to the bees buzzing outside of the isolation chamber (Bencsik, et al., 2015; Ramsey, et al., 2017). This particular dataset was chosen for this further analysis because it is known that, based on the information in Table B1, both frames' brood were capped and the brood in Frame 1 were only two to three days away from hatching.

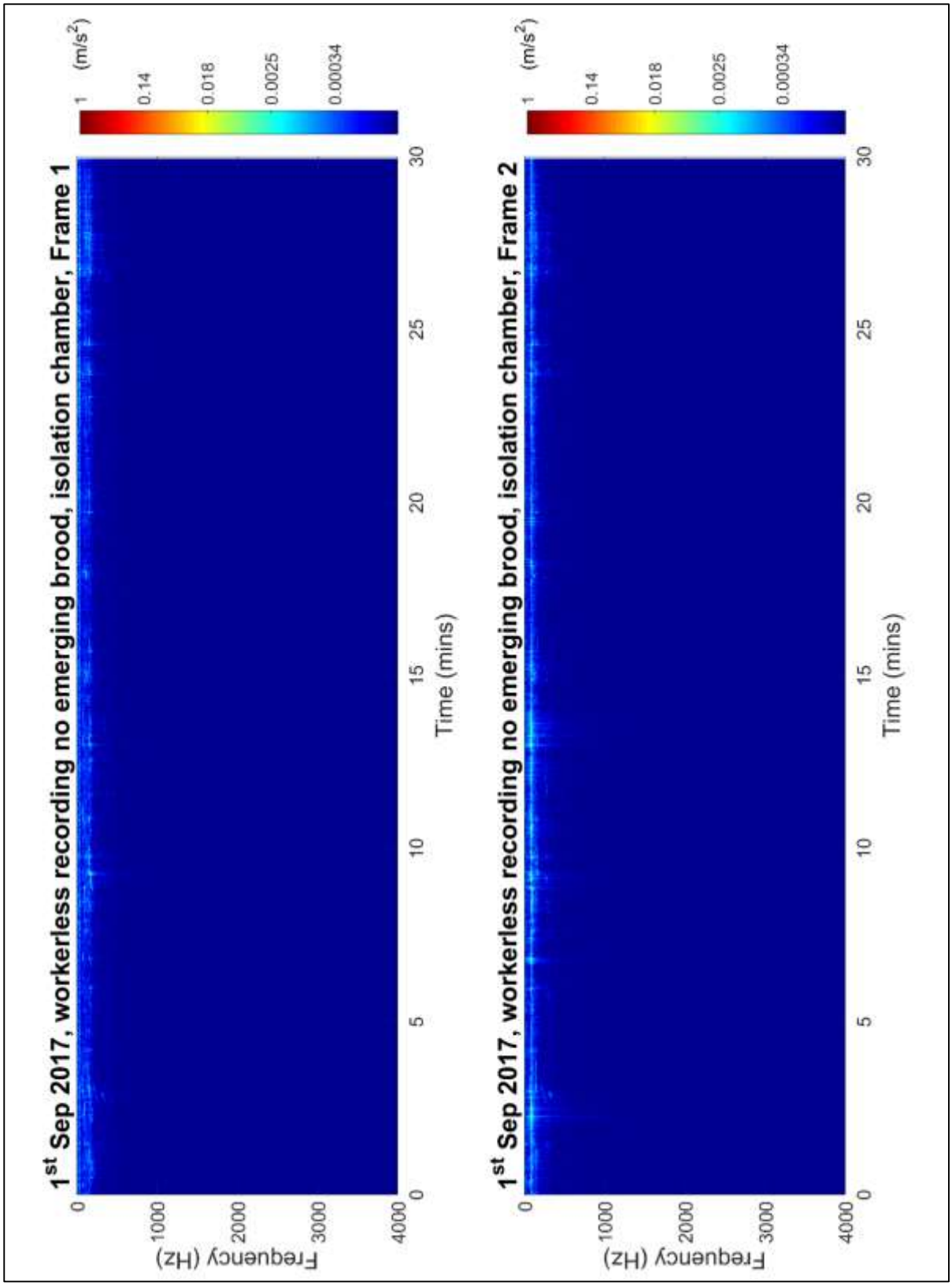

Figure B6. The spectrogram of a 30-minute excerpt of data from a brood-isolated recording from 1st September 2017.

The figure shows the spectrum of frequencies from 0 to 4000Hz for both frames that were placed in isolation.

Pixel intensity is in logarithmic scale denoting the acceleration in m/s^2.

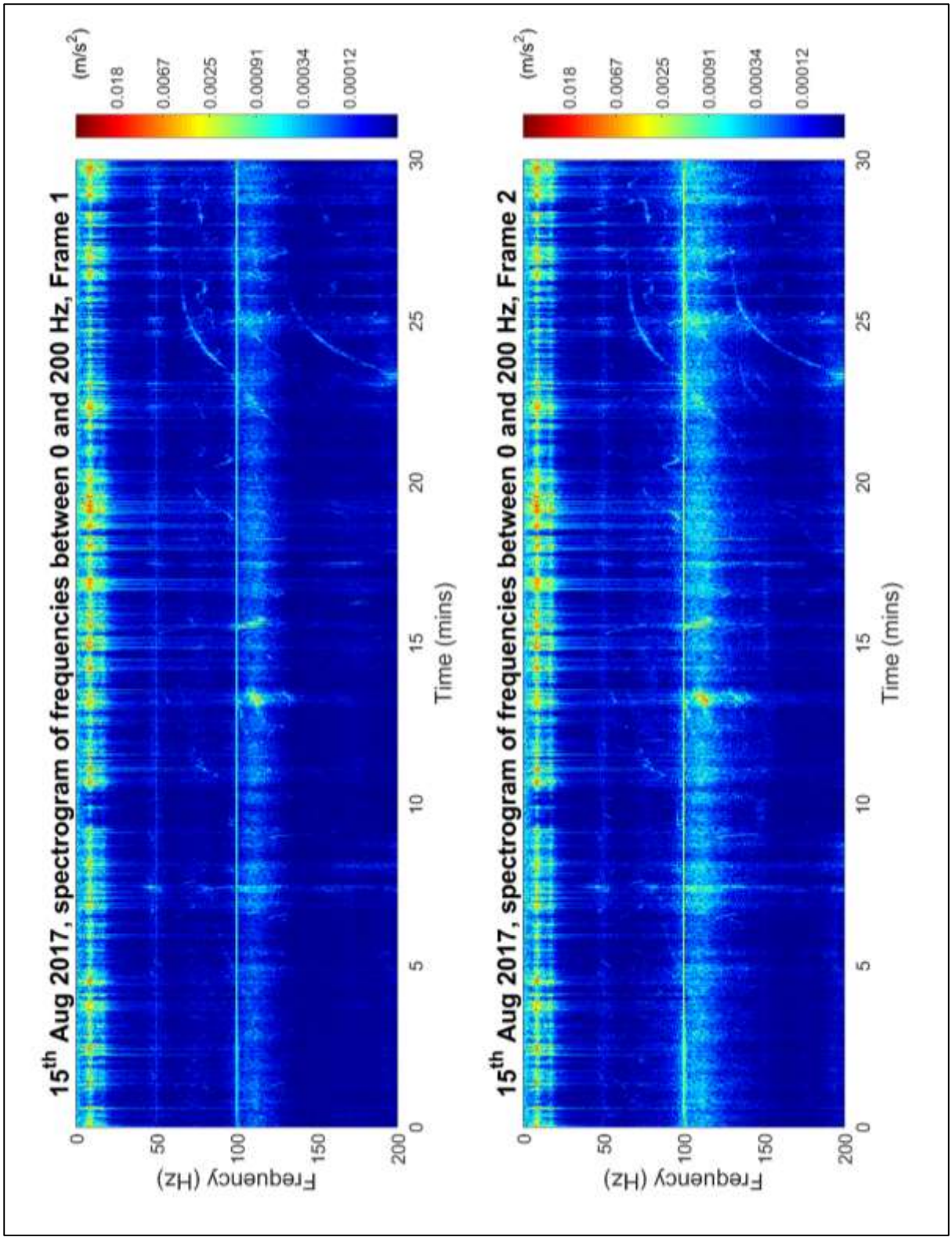

Figure B7. The spectrogram of a 30-minute excerpt of data from a brood-isolated recording from 15th August 2017 cropped between 0 and 200 Hz. The figure details are the same as provided for Figure B6.

2.3.1.iii. Experiment 4 - 18th August 2017, emerging brood

During the course of the recordings on the 18th August 2017, 35 individuals emerged from the cells of the honeycomb on Frame 1. However, interestingly no individual honeybee had emerged before the scheduled 90 minute examination. There was around 70% of the honeycomb with capped brood cells counted on Frame 2. Whilst there is evidence of some low amplitude wax cutting on the accelerometer dataset during this recording, after inspection of the wax capping of the cells following experimentation it was concluded that, as they all appeared intact, no bees had emerged from this frame during the 5 hours of recording. Owing to the reduction in the amplitude of the broadband spectral clouds seen in Figure B5, it would appear that there is less contribution of outside noise to this dataset when compared to that of 28th July 2017 due to the placement of the box in the acoustic isolation chamber. We again see the high-amplitude broadband spikes on the top spectrogram consistent with the wax chewing of emerging brood also seen on the dataset form 21st July 2017. The constant trace at 8Hz is still apparent; however, the trace previously seen at 115Hz resides at 95Hz in this data set. There is also a faint trace seen at 300Hz, which was also observed in the 27th July dataset with brood emergence. Four ultra-high amplitude spikes appear on both datasets at 3, 4, 9 and 10-minutes which is the thermostat switching on and off the in-built heater. Other traces of around 150Hz observed on both frames throughout the data set can be linked to the contribution of noise from the surrounding outside environment.

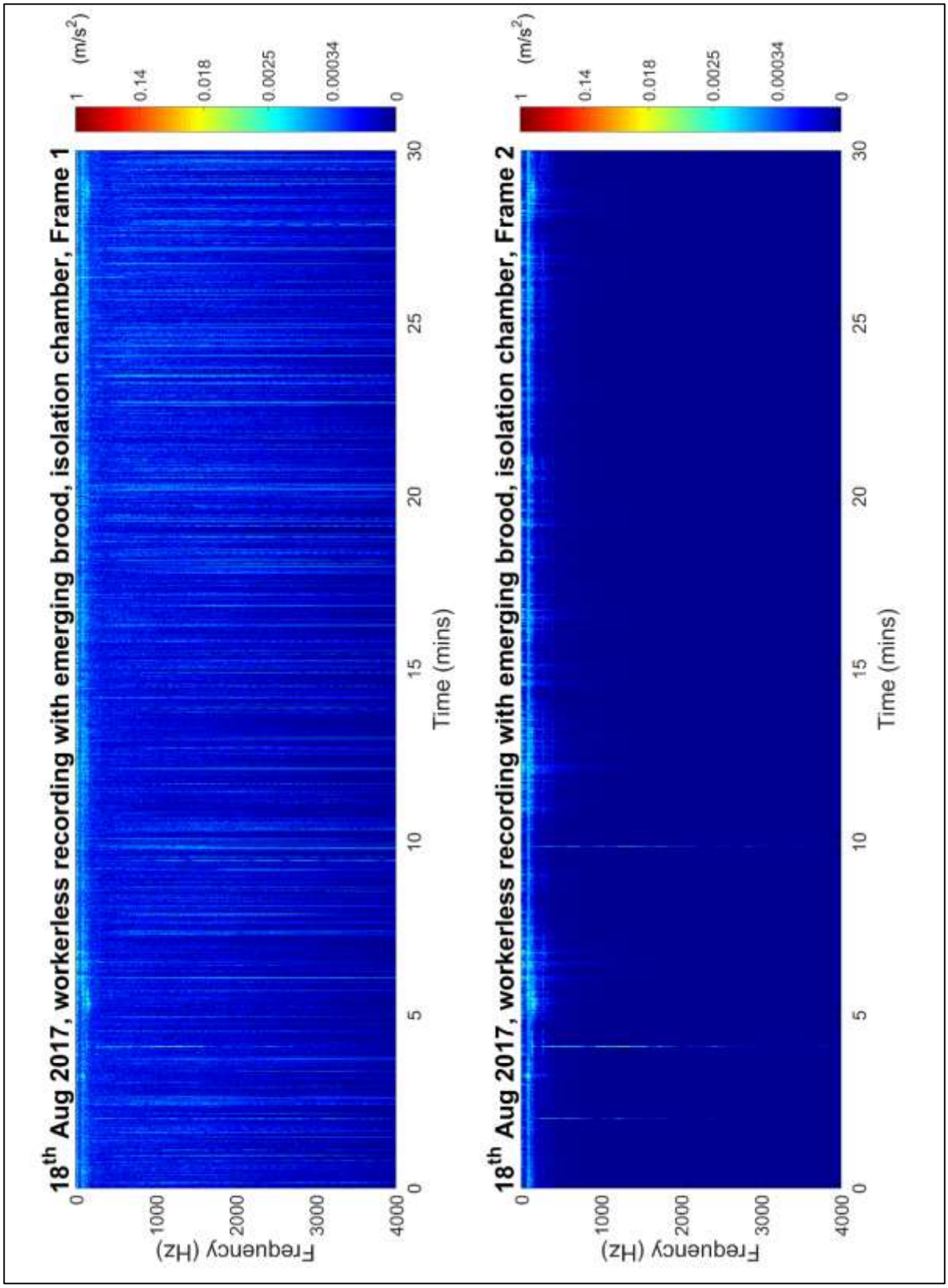

Figure B8. The spectrogram of a 30-minute excerpt of data from a brood-isolated recording from 18th August 2017. The figure details are the same as provided for Figure B5. This figure displays the high density of ultra-short high magnitude broadband clicks on Frame 1 related to the emerging individuals.

2.3.2. Analysis of the intensity of wax cutting behaviour

As no bees emerged from the honeycomb during the 10th and 15th August and the 1st September experiments, no clicks were observed on the spectrograms of, or by critical listening to, the corresponding raw audio files. As a result for this analysis, only results from the 28th July and the 18th August 2017 experiments are shown below.

2.3.2.i. Experiment 1 - 28th July 2017

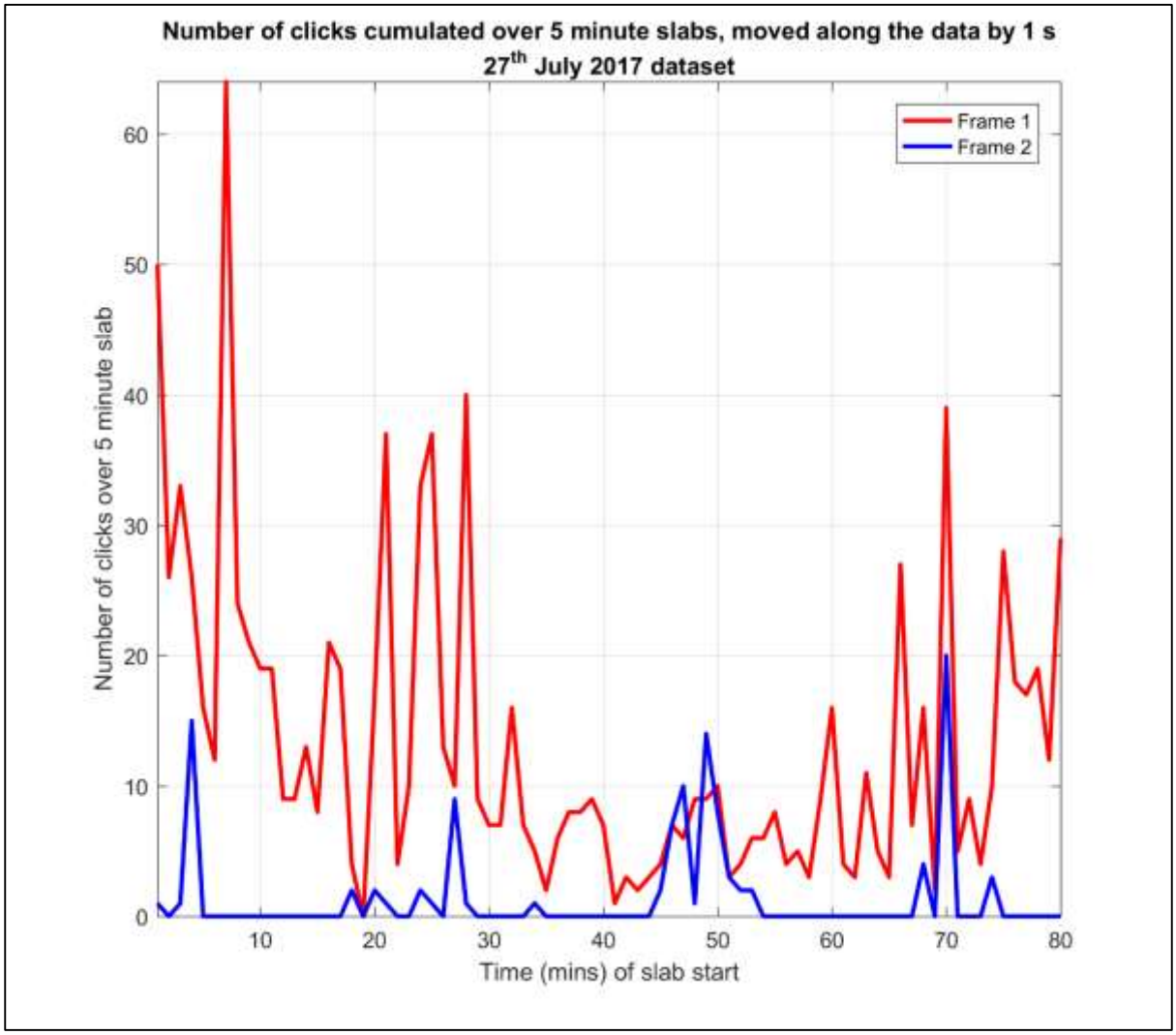

Figure B9. The evolution of the density of emerging clicks as identified by the cumulating the number of clicks over five minute windows moved in increments of one minute along the time axis of the colony-isolated recording obtained on the 28th July 2017. Each line corresponds to a different frame as seen in Figure B5.

As seen in Fig B9, the density of emerging clicks detected by the accelerometer technology situated in Frame 1 appears to gradually fall by 98% from the initial count of 50 in the first instance, reaching a minimum of one at 42 minutes. Spikes in occurrence at 9 minutes, and between 20 and 30 minutes, matches well with the corresponding increases in click density seen in Figure B5. It is from this frame that 11 individuals were found to have emerged upon termination of the day's recording. Frame 2 also contained capped brood but no individuals were found to have successfully emerged at the end of the recording and thus little variation in signal can be seen above 2000 Hz, and the mean signal is much lower at any point in time. Upon removal of Frame 1 from the incubation box at the end of this experiment, it could be seen that a large number of wax caps (around 30% of the total brood) were being removed by more emerging individuals so the eleven that had already emerged would only contribute marginally, if at all, to the overall clicks detected by the accelerometer.

2.3.2.ii. Experiment 4 - 18th August 2017

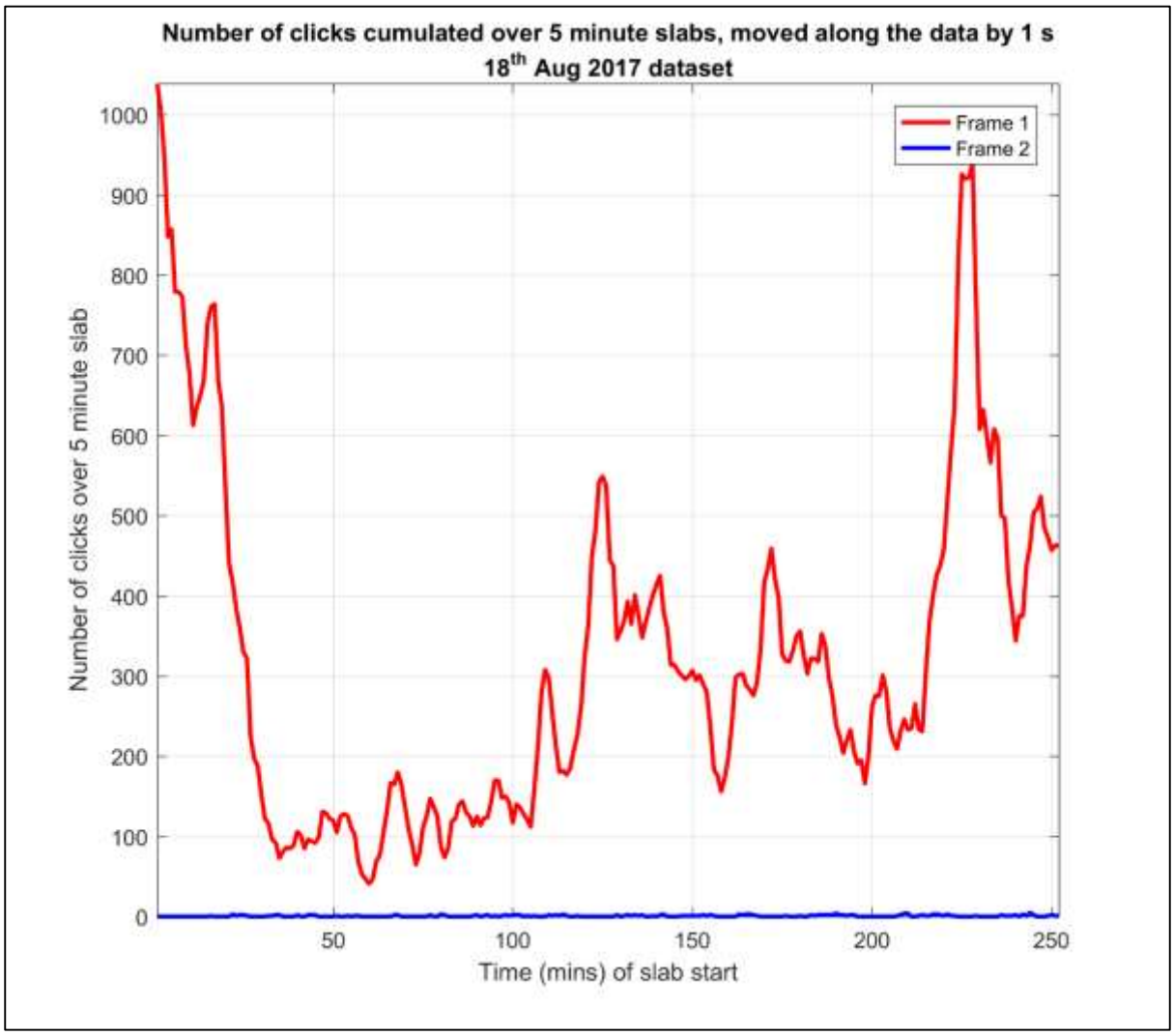

Figure B10. The evolution of the density of emerging clicks as identified by the cumulating the number of clicks over five minute windows moved in increments of one minute along the time axis of the colony-isolated recording obtained on the 18th August 2017. Each line corresponds to a different frame as seen in Figure B8.

With none of the capped brood emerging throughout the recording of Frame 2 and only the occasional faint click being observed on the full spectrogram and audio for the 18th August 2017 experiment, the detected number of clicks for this frame remained close to zero. Thirty-two individuals emerged from Frame 1 throughout this experiment but none within the first 90 minutes. Through critical listening and visual inspection of spectrogram images (e.g. Figure B6), an increased density of high-amplitude

clicks can be observed that persist throughout the entirety of the recording of Frame 1. As seen in Figure B10, there is another instance of a reduction in the density of clicks over the first 40 minutes, decreasing by 95%. This signal then gradually increases throughout the dataset. No signal reduction can be seen for the accelerometer data corresponding to Frame 2.

2.3.3. The time course of individual clicks

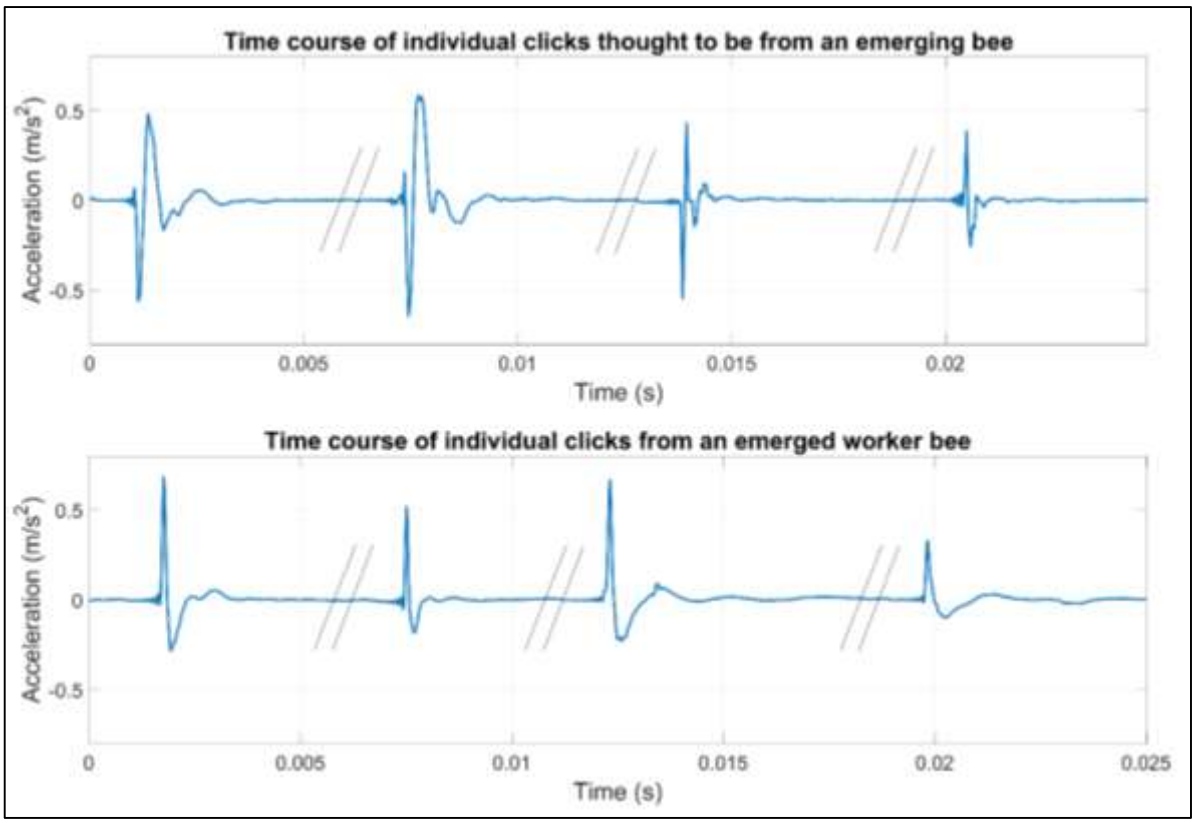

Figure B11. (**a**, top) The time course (s) of acceleration (m/s^2) of four individual high-amplitude clicks of similar magnitude that were extracted and concatenated from the start of the 18th August 2017 brood-isolated dataset as the first individuals were emerging; (**b**, bottom) The time course (s) of acceleration (m/s^2) of four individual high-amplitude clicks of similar magnitude that were extracted and concatenated from the calibrated accelerometer data associated with footage of an emerged bee working in a cell (see Video B1). // indicates the point the each click was concatenated in the file.

The “individual clicks thought to be from an emerging bee” in Figure B11 were extracted and concatenated from the beginning of the 18th August 2017 dataset, at a time when there was no emerged bee on the surface of Frame 1. These clicks therefore can confidently be linked to the individuals emerging from the honeycomb, however further video analysis is required to prove this. An oscillation is present at the start of each waveform that is of low amplitude and high frequency. The first deep negative/positive lobe is of similar magnitude to the positive/negative lobe immediately afterwards, although sharper. This phenomenon may occur in instances where a stimulus is not delivered normally to the surface of the honeycomb, which is the case in this instance of a bee picking at the wax during hatching. When the higher amplitude emerging bee clicks of this study are compared to that of an instance where a honeybee was captured working within a cell directly on the accelerometer (seen in Video B1 and graphically displayed in Figure B11), it can be seen, particularly in this instance, that the amplitude of an emerged bee click is of similar magnitude to that of an emerging bee for the first positive/negative lobe. However, the second negative/ positive lobe of an emerged bee click is of a magnitude that is 30% of that of the first, not equal like as seen in this example of the emerging bee clicks.

2.3.4. Signal to noise ratio of vibrational signals within the hive

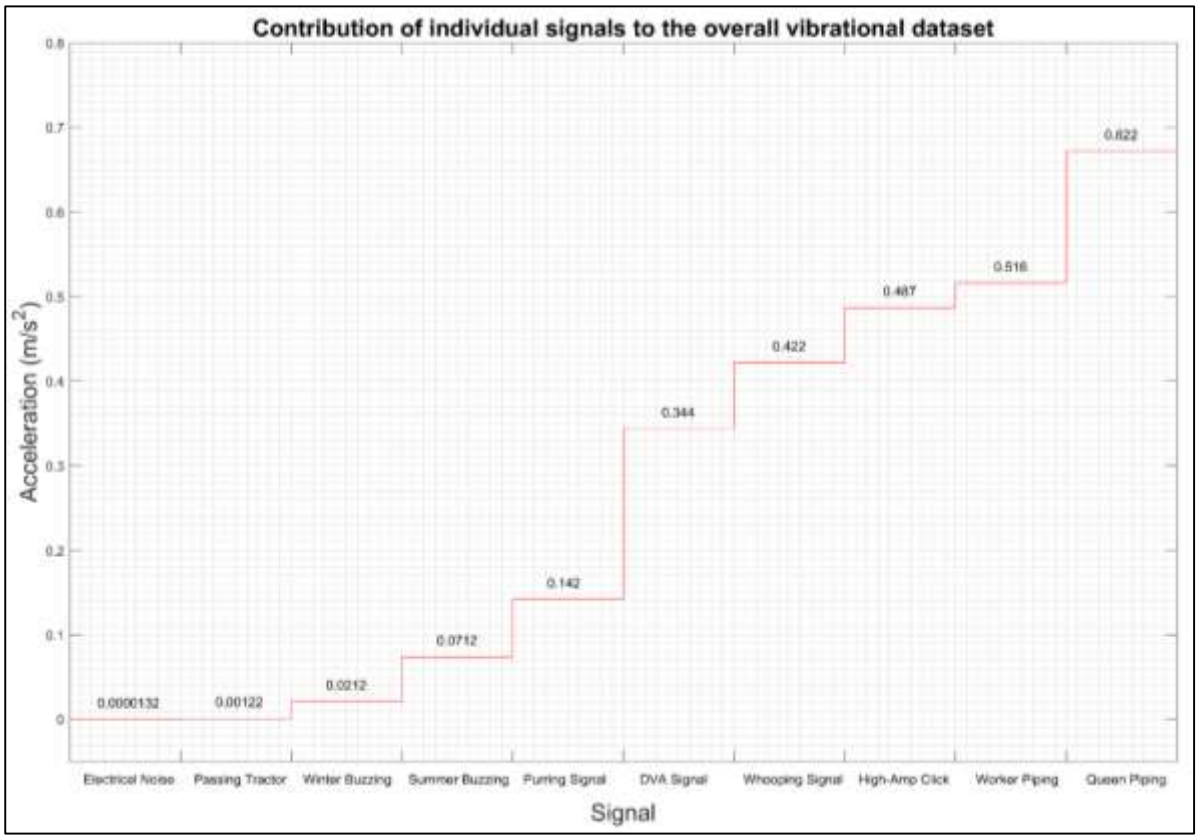

Figure B12. The individual contributions of a select group of signals that feature throughout this thesis.

Each signal is a representative example extracted from vibrational datasets obtained using calibrated accelerometer technology and their amplitudes are given in m/s^2.

The magnitude of any given signal category in Figure B12 represents the highest amplitude example that could be found within the extensive calibrated accelerometer datasets utilised within this thesis. It must be stressed that the amplitude of any given signal will substantially vary with the load/density of the honeycomb in which the accelerometer resides.

As seen in Figure B12, the electrical noise of these high sensitivity accelerometers is of negligible contribution to the signal coming from a honeybee hive. It results in acceleration that is 100 times smaller than the acceleration induced by a nearby passing tractor road about 15m away and 1606 times smaller than the acceleration induced by the 125Hz background buzzing emanating from the

wings of the bees in the wintertime. Figure B12 also shows that the 125Hz buzzing vibration of the bees is up to 3.4 times higher in amplitude during the summer than in the winter. As can be seen in Figure B11, the acceleration that stems from clicks by emerged and emerging bees are of similar magnitude and thus they have been grouped as “High-Amp Click” in Figure B12. They are of particularly high amplitude compared to other signals that are found in the hive due to the high-energy vibration caused by the abrupt physical pulling of the honeycomb. With an amplitude of 0.622 m/s^2, queen piping appears to be the highest amplitude signal that was explored as part of this study. Worker piping at 0.516 m/s^2, which is a similar phenomenon to queen piping, produced instead by worker bees, has the second highest amplitude. Whooping and DVA signals are of particular importance to this thesis. Although they do not possess the highest SNR, the respective amplitudes of 0.422 m/s^2 and 0.344 m/s^2 that they exhibit means they can be deciphered against the background noise of the hive, although DVA signals are generally weaker and necessitate delivery in the immediate vicinity of the accelerometer.

2.4.0. Discussion

2.4.1. Unique vibrational signatures.

In this chapter, I set out to explore the contribution of the un-emerged population to the overall vibrational dataset obtained by placing ultra-sensitive accelerometer technology in the centre of the honeycomb. Critical listening of the datasets recorded for each of the five experimental days revealed very little audible information associated with developing brood. Further visual analysis of these colony-isolated vibrational datasets through careful inspection of spectrogram images also revealed very little brood-specific information. This suggests that there are no particular pulsed vibrations used by developing larvae or pupae as intentional communicatory signals detectable by the accelerometer technology detailed throughout this thesis, although the most relevant dataset would have been obtained if one frame contained brood and the other did not. Such opportunity did not arise during the five experiments. It must be noted that newly emerged honeybees did not produce any detectable pulsed vibrations (such as DVA signals and whooping signals) either, when residing upon the honeycomb. However, it was discovered that a relatively high amplitude "clicking" could be observed during instances of emerging brood, probably caused by the individuals cutting out the wax capping of their cells using their mandibles, producing a waveform that can be distinguished from other sources of high amplitude clicking vibrations stemming from emerged worker bees.

Noticeable within all instances of individual clicks, produced either by emerged or emerging honeybees, is a low amplitude, high frequency tremor that is present at the start of each waveform. It is possible that the initial gripping of the honeycomb by the bee using its mandibles causes this. However, further accelerometer-linked video evidence is required to support this claim. It can be seen in Figure B11 that the high amplitude clicks that emanate from an emerged adult worker bee working upon the honeycomb and those clicks originating from an emerging bee removing the wax cap over its cell produce two different traces within the accelerometer waveform. Whilst both are of similar duration and magnitude, in the case of the emerging bee click, the first deep negative/positive lobe is

of similar magnitude to the positive/negative lobe immediately afterwards. This phenomenon seems occur if the stimulus is not delivered normally to the surface of the honeycomb, which is the case in the instance of a bee emerging from its cell. This provides an interesting avenue for further investigation utilising a larger, more statistically relevant group size to test the extent of the repeatability of these phenomena and examine whether these present and unique signature for use to non-invasively detect the presence of emerging brood.

2.4.2. Brood click density.

In the two experiments that took place on the 27th July and the 18th August 2017, individuals had emerged from their cells within the honeycomb of Frame 1 and were found residing on their prenatal frame. No bees emerged from the Frame 2 during data collection but distant occasional clicks can be observed during the recording on 27th July 2017. This is most probably due to the difference between the two focal frames in egg laying times by the queen.

A phenomenon that occurred in both instances of emerging bees is that the density of clicks quickly diminished reaching a minimum after around the first 40 minutes within acoustic isolation. The density of clicks then gradually increased over the remaining hours of recording. It is unlikely that the reduction in the number of clicks is a result of individuals successfully emerging from their cells, as only a minority of individuals emerged from the frame, 11 on the 27th July 2017 and 32 on the 18th August 2017. In addition, upon inspection after 90-minutes of recording on the 18th August 2017, no individuals had successfully emerged from the cells of the frame. For this trend to be linked with the bees emerging and thus terminating wax cutting behaviour, bees would have to have left their cells almost immediately after being placed in isolation from the colony.

It is possible that the bees within the capped cells of the honeycomb are somewhat aware of the abrupt change in the external environment. The disturbance of transferring each focal frame from within the hive into the incubator following the removal of the emerged adult worker population may

well have caused the still-unemerged honeybees to become stressed and perhaps even reluctant to surface from the safety of their capped enclosures until the potential threat has passed. From this point onwards, the gradual increase in clicks is them returning to normal activities, with a few individuals emerging within isolation. It is therefore possible that more individuals would have emerged within the observation time, should the colony been left undisturbed .In support of this, throughout my own observations during this thesis, I have seen first-hand the effect that a disturbance can have on a colony. Agitation of the members of a hive during winter clustering can be observed taking over 24-hours following the event to gradually return to normality (Supplementary Figures 1 and 2 of Appendix 4). However, this is perhaps an extreme example. With this in mind, it is also possible that had the frame been left undisturbed, many more individuals will have emerged in the time that the frame was under observation.

The difference in amplitude between the two frames at times when brood did not emerge is small but apparent upon analysis of the intensity of wax cutting behaviour. This minor difference may be due to the slight variation in density between the honeycombs of the two focal frames. There may have been an increase in the amount of honey or brood within the comb for Frame 1 that caused an increased dampening effect and thus the observed difference in overall amplitude. Additionally, as seen in Figure B4, honeybees cap their brood after around 9 days. It is suggested in Table 1 that, based on the dates of (i) brood emergence observed for Frame 1 and (ii) the presence of uncapped larvae on Frame 2, the brood cycle of Frame 2 may be three to four days behind that of Frame 1. As suggested by Bencsik, et al., (2015), the mass density of the honeycomb increases with development of the brood and this may have been a contributing factor towards the difference in the magnitude of signal observed between the frames.

2.4.3. Analysis of individual signal contributions

The examples used in the creation of Figure B12 are representative of high quality examples of honeybee vibrational pulses that occurred on or within the immediate vicinity of the accelerometer. In reality, these signals can be detected at varying amplitudes depending on the energy exerted by the individual, the frame load of the honeycomb and their distance from the accelerometer.

Whilst not all signals that are present within the complex waveforms emanating from the honeycomb of honeybee hives could be extracted and analysed, what has been shown are the signals that harbour particular significance within this thesis. Analysis of the relative amplitude contributions shows that meaningful vibrations do have to have a high signal to noise ratio but the amplitude of the signal is not necessarily indicative of its relative importance as a direct communication between honeybees. For example, clicks have a very high amplitude relative to other known direct communication signals, such as DVA signals, yet they most probably are a vibrational cue that is the result of honeybee activity such as wax cutting. Meaningful vibrations perhaps have an amplitude that is tailored to the number of individuals intended to receive the message, with DVA and whooping signals being relatively localised whilst queen and worker piping are probably of colony-wide significance.

By placing the focal frames within an isolation box (that has the same wall thickness as a British Standard beehive) and then situating it outside, this study has also highlighted the minimal contribution of signal coming from outside noise from the surrounding environment towards the overall vibrational data set obtained by this method of placing an ultra-sensitive accelerometer into the centre of the honeycomb. It has also showcased the exceptionally high quality and sensitivity possessed by the technology that collected the data within this thesis, with the thermal, electrical noise from the equipment being over 2000 times smaller than the accelerometer trace due to 125Hz background buzzing of the bees.

2.4.4. Conclusions and future work

A major outcome of this study is in the analysis of the high-amplitude clicks that originate from the wax cutting of emerging honeybees. I have been able to show that the clicks of emerging bees potentially have a unique signature compared to the clicks of emerged worker bee activity providing a prospective identifier for the presence of emerging brood. To study this phenomenon further, the experiment could be repeated, e.g. with the addition of time-lapse infrared photography controlled by field-based Raspberry PI computers and USB cameras within the incubation box to capture the exact moment honeybee brood emerges. This information would allow in depth exploration into any changes within the time course or density of the honeybee emergence clicks in association with each hatching event. It would also enable me to show a one-to-one relationship between an emerging bee behaviour and the resulting accelerometer waveform. This vibrational information would then need to be explored within long-term studies such as in Bencsik, et al. (2015) and Ramsey, et al. (2017) to see if the occurrence of these particular clicks coincide with the brood cycle of the colony.

A repeat of this study for two (or more) frames in which only one contained capped brood and the other was either empty or used for honey storage would allow for assessments between the two frames where any differences would most certainly originate from the presence of the brood. If in this instance no difference could be detected, it would support findings of this study that we cannot detect any measureable vibrations specifically emanating from developing honeybee brood using this accelerometer technology.

Whilst this work poses an interesting starting point for further study, it has been effective in achieving its objectives. In the aims, I set out to explore the brood-specific vibrations of honeybees. In doing so, I have shown that developing / newly emerged honeybee brood provide very little contribution to the overall vibrational dataset recorded using this accelerometer technology with the majority of information coming from the emerged adult honeybee worker population upon the honeycomb. I

have shown a negligible contribution from outside and electrical noise, showcasing the outstanding signal to noise ratio and sensitivity of the accelerometer technology used throughout this thesis.

Chapter 3: Long-Term Trends in the Honeybee 'Whooping signal' Revealed by Automated Detection

In this chapter, I explore the physical characteristics and long-term statistics of the shortest identified pulsed vibration associated with the European honeybee: the whooping signal. Using evidence obtained from long-term trends with additional supporting video analysis from my unique observation hive, I subsequently proceed to challenge the accepted function of this pulse as an inhibitory signal.

This chapter consists of a brief introduction explaining the motivation and aims for this study, followed by the methods by means of which data was acquired and processed, the results of the long-term trends for the two hives under observation and a final discussion about these. Associated with this chapter are a number of accompanying videos and audio excerpts that can be found on the supplied DVD.

Figures and supporting videos corresponding to this chapter are categorised with the letter "W". "*Figure W1…*" for example.

3.0.1. Abstract

The present chapter demonstrates long term (over 9 months) automated in-situ non-invasive monitoring of a honeybee vibrational pulse, “the whooping signal”, with the same characteristics that have previously been described as a stop/begging signal using ultra-sensitive accelerometers embedded in the honeycomb located at the heart of honeybee colonies. It is shown that the signal is very common and highly repeatable, occurring mainly at night with a distinct decrease in instances towards midday, and that it can be elicited en masse from bees following the gentle shaking or knocking of their hive with distinct evidence of habituation. The results of this work suggest that this vibrational pulse is generated under many different circumstances, thereby unifying previous publication’s conflicting definitions, and it is demonstrated that this pulse can be generated in response to a surprise stimulus. This work suggests that, using an artificial stimulus and monitoring the changes in the features of this signal could provide a sensitive tool to assess colony status.

3.1.0. Introduction

In spite of the current literature explored in section 1.3, my own observations (see Videos W1 and W2 for examples) suggests that this pulse is not restricted to its current definition of 'stop signal'. In fact, (probably accidental) collisions between bees can often result in the detection of a pulse indistinguishable to what has been described as a honeybee stop signal, even though there is no waggle dance or trophallaxis involved (Video W3). Numerous other videos produced as part of this research show that it is very rare to find any visual evidence of the production of this pulse even though they can be heard very frequently, over thirty times over the course of one minute (Videos W4 and W5) on both accelerometers. In addition to this, it is easy to demonstrate that upon gentle shaking of a hive (or even if you were to knock it gently) this pulse is generated en masse by the bees residing within it (see Video W6). In this study, software is created and optimised that can accurately explore months of continuous vibrational data recorded non-invasively from the heart of honeybee colonies, collecting the timings of specific honeybee pulses of interest. Discussion of the resulting statistics for these pulses helps in suggesting that what has recently been systematically described in the literature as a honeybee stop signal is actually a remarkably common signal, being produced under many different circumstances, including that of a startle response to an unexpected stimulus.

3.1.1. Aims

The outcomes of this study will allow me to 1) discuss the results in terms of any evidence of long-term trends; 2) discuss the results in the context of the colony status; 3) compare the results of stop signals measured from within two different locations of the same frame; 4) discuss the results measured from a colony in the UK and another one in France and ; 5) explore the possible correlations between the focal signal's occurrences and weather trends, as these will strongly modulate some colony responses, in particular in terms of foraging and thermo-regulating activities. It is expected, for example, that weather patterns that would inhibit foraging would cause a decrease in waggle dances thus reduce the need for the associated 'stop signals'.

3.2.0. Methodology

No ethical approval was required as this study exclusively focussed on the *in-situ*, non-invasive acquisition of data from colonies of invertebrates.

3.2.1. Vibrational measurements

The recordings of vibrational data were taken from two hives, one located at the Clifton campus of the Nottingham Trent University (NTU), UK and the other at an apiary in Jarnioux, France after being granted specific permission from NTU Estates and Mr Joseph Bencsik respectively.

The UK Hive was monitored for around 4 months commencing on the 29/07/2014 until termination on the 11/11/2014, allowing me to monitor a colony as it prepares for winter. The French hive was continuously monitored from 16/04/2015 until 24/12/2015, disclosing the evolution of a colony across the entire active season. The data were analysed separately for each hive to allow a comparison of data taken from two different climates.

The recording of vibrational data was achieved using two ultra-high performance accelerometers (Brüel and Kjær with a sensitivity of 1000 mV/g) placed in the middle of the previously established honeycomb along a vertical line, one in the centre, and the other 7cm lower down (Figure W1). Exactly as in the previous chapter, small amounts of molten wax were dripped onto the accelerometers to secure them onto the frames and avoid the direct exposure of metal components. The frame was then placed back into the centre of the brood box. Unlike the previous chapter, the accelerometers here were installed into the fully built honeycomb of previously established frames within the colonies. The accelerometers were polarised with individual ENDEVCO 4416B conditioners (MEGGITT, U.S.A.), the output of which was plugged into an i02 sound card (ALESIS, U.S.A.) for digitisation at 22kHz sampling rate. Vibrational data sets were continuous and made up of one hour long audio files, stored on an external 4TB storage station via a home-built bash code on a Linux O.S. based computer that was set

to reboot itself every 100 hours, with recordings resuming automatically upon rebooting or power loss and auto-recovery.

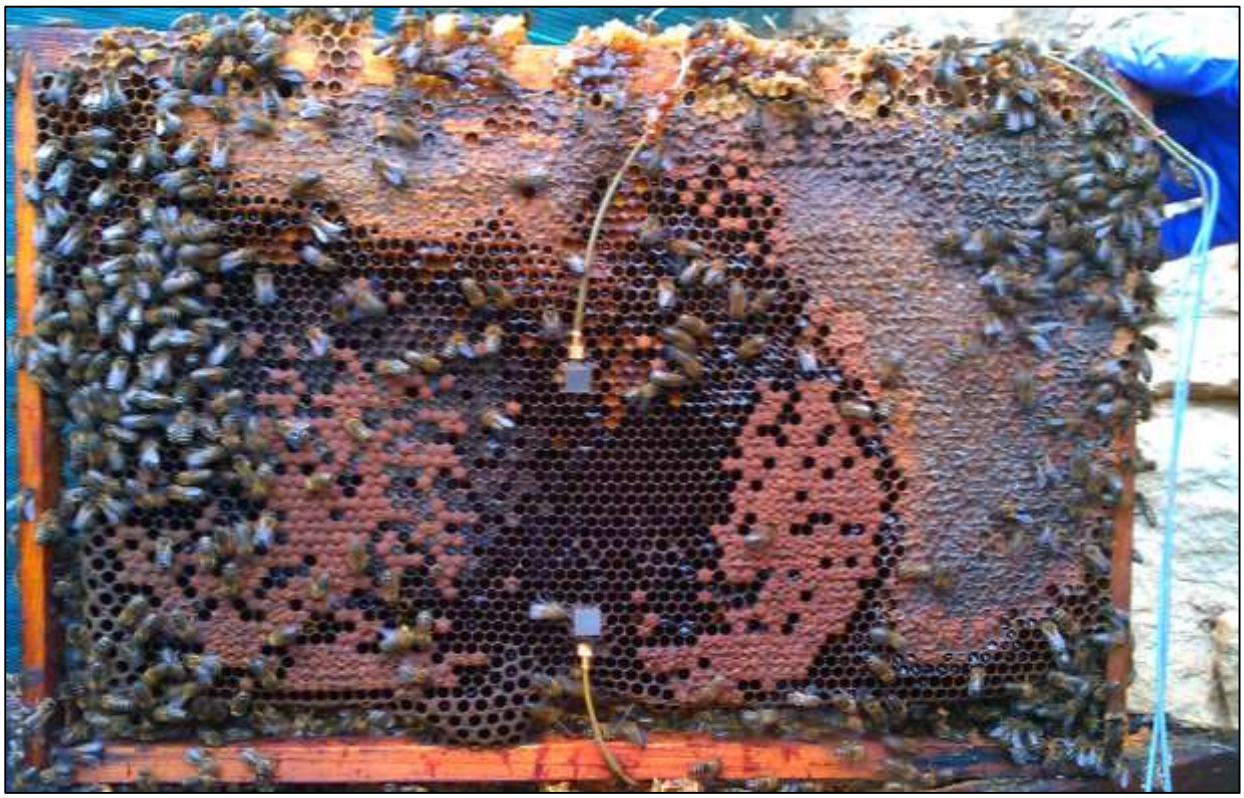

Figure W1. Accelerometer configuration. A brood frame equipped with accelerometers in the centre and at the periphery, located in the centre of a hive. This photo was taken one year after installation, with accelerometers surrounded by honeycomb cells in near perfect condition. The photo shows the French set-up, which is identical to that of the UK.

3.2.2. The detection software

Software was written in MATLAB® (The Mathworks, USA) and algorithms were optimised to detect and record the exact times at which whooping signals occurred within the vibrational data sets. The whooping signal detection is a two-step process. First, a spectrogram of a template pulse signal is matched to a spectrogram of the continuous recording by the ratio of the cross correlation product

and the Euclidean distance (See Figure W2 and W3). In this way, whooping signals and other pulses are detected. Second, the detected pulses are discriminated into ‘whooping signals’ and 'non-whooping signals’ by simple discriminant function analysis on PCA scores. When data sets consisting of the exact timings of the genuine honeybee whooping signals that occurred within each vibrational data set were identified, these were used to show the quantitative statistics of their occurrences over the entirety of both the UK and the French data sets.

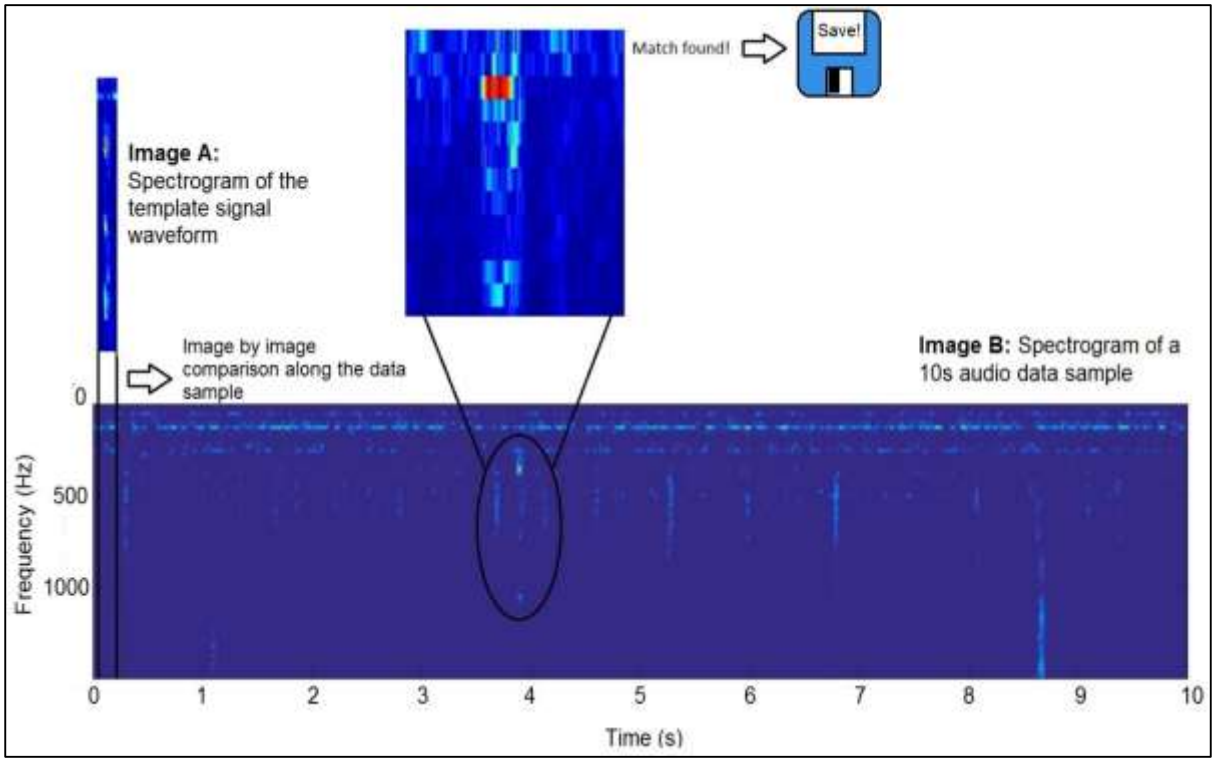

Figure W2. Pictorial representation of the algorithm (first pass) behind my whooping signal detection software. Rather than matching spectra (as most commonly used in detection of bird song (e.g. Boucher et al., 2012; Jancovic and Kokuer, 2011)), spectrograms are compared, providing a more specific criterion for detection, suitable for the highly repeatable features of the whooping signal.

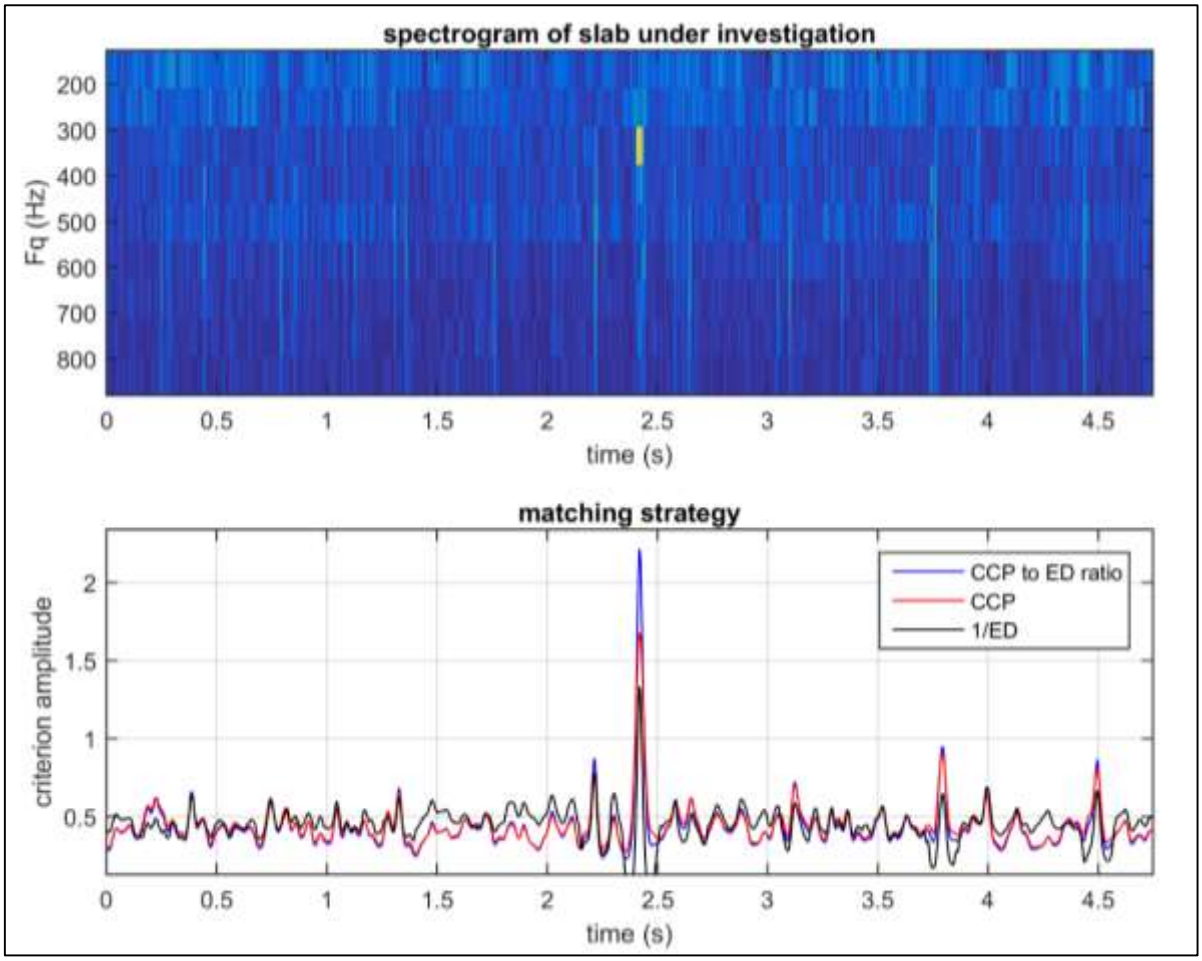

Figure W3. Comparison of the three matching strategies for the detection software. The reciprocal of the Euclidean distance (black line) gives similar importance to the spectrogram high and low signal intensity. The cross correlation product (red line) promotes the information found in the high intensities of the spectrogram (peaks). The ratio of the red to black (blue curve) gives the best outcome, when all curves are normalised to make noise levels (low criterion amplitude areas outside the central peak) identical.

3.2.2.i. Principal Component Analysis and Discriminant Function Analysis to discriminate between true and spurious whooping signals

Data was extensively examined by critical listening to ensure that the software was displaying true whooping signals. Once a histogram of hourly whooping signal occurrences had been generated, hotspots and potential anomalies were identified for further examination in both the UK and French data sets. The calendar timings of these were converted into epoch time (or UNIX time), which is the time elapsed in milliseconds since 1/1/1970. This is very useful to computer systems for tracking and sorting dated information in dynamic and distributed applications because it is a single number that can represent all time zones at once. A separate software was then used to upload the signals at these specific times from within the data set. The signal excerpts were then stacked in an audio file allowing a 1 second gap in between the detected pulses, to allow enough time for critical listening.

Following the methods of Bencsik et al. (2011), any signal or artefact that was falsely detected as a whooping signal was fed into the PCA/DFA software to train the computer to discriminate between them. For example, during occasional days throughout October and November of the UK data set, there were up to 1000 instances of automated detection events. The signals from these times of exceedingly high detection rates were extracted from the dataset, concatenated and analysed by critical listening. A vibration that is suspected to have resulted from a collection of water droplets falling on to the hive's roof after a bout of heavy rain, were found to be the cause of one of the detection hotspots. This was confirmed through analysis of the precipitation data from an onsite weather station. The high level of similarity between the spectrograms of a honeybee whooping signal and that of the vibrational pulse caused by a drop of rain falling onto the hive is demonstrated in Figure W4.

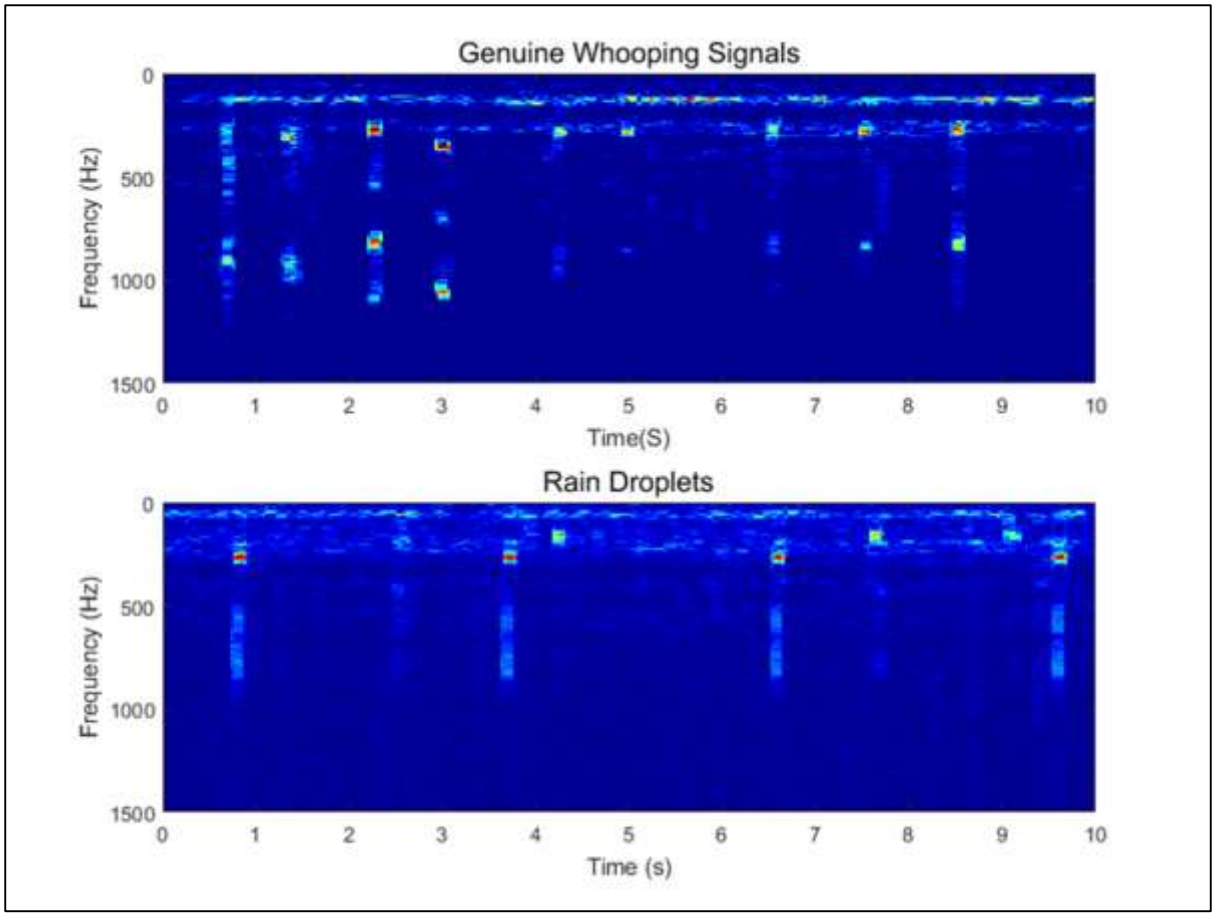

Figure W4. Comparison of genuine stacked whooping signals spectrograms (top) to that of the falsely detected rain droplets (bottom). Although critical listening allows easy discrimination, visual investigation of the spectrograms reveals high similarities, causing the algorithm to undertake spurious detections, in its "first pass".

Using the DFA algorithm implemented in the Matlab® core, further code was therefore developed that runs a second step discrimination analysis. A collection of 300 droplet timings were selected for comparison to a collection of 150 true whooping signals that were extracted from numerous points across the entire dataset. These pulses were then used to build a 'training database' for discrimination by supervised clustering. Each pulse was uploaded into the software allowing a 0.5s buffer either side of the recorded pulse time to ensure that the entire pulse waveform was captured. A spectrogram of the pulse was generated and then centred to an artificially generated reference pulse using the cross correlation product. This allowed careful phasing of all detected pulses. The frequencies were then cropped to between 65 and 3000Hz, as this frequency band contains the majority of the information

pertaining to the honeybee whooping signal (see Figure W7). The spectrogram was also coarsened by a factor two along the frequency axis, in order to make the spectrum less specific to a particular fundamental frequency value and improve the performance of the software. The pulse amplitude was then normalised by dividing it by its maximum in order to detect faint whooping signals equally as well as loud ones, and finally saved in the training database. This exercise was then repeated for all other selected pulses that were used for discrimination.

The whooping signals and rain droplets were carefully labelled within the training database and their PCA scores were calculated. By using a pair of cross correlation products with two discriminant functions identified by the DFA algorithm, the discriminant function coordinates, or 'DF scores', could then be calculated and plotted (See Figure W5). The number of PCA scores (i.e. features of the signals) used in the discrimination was explored until the best discrimination was achieved, identified through the calculation of the percentage error based on how many points from each cluster overlapped in the DF space. The upper and lower limit of the signal bandwidth were automatically changed and the percentage error was further recorded for optimisation. The parameters that yielded the lowest error in discrimination were used. The coordinates of the centroids of each of the clusters were calculated and software was developed to provide a threshold for determining whether a whooping signal was genuine or not though calculating its distance to the centroid of each cluster.

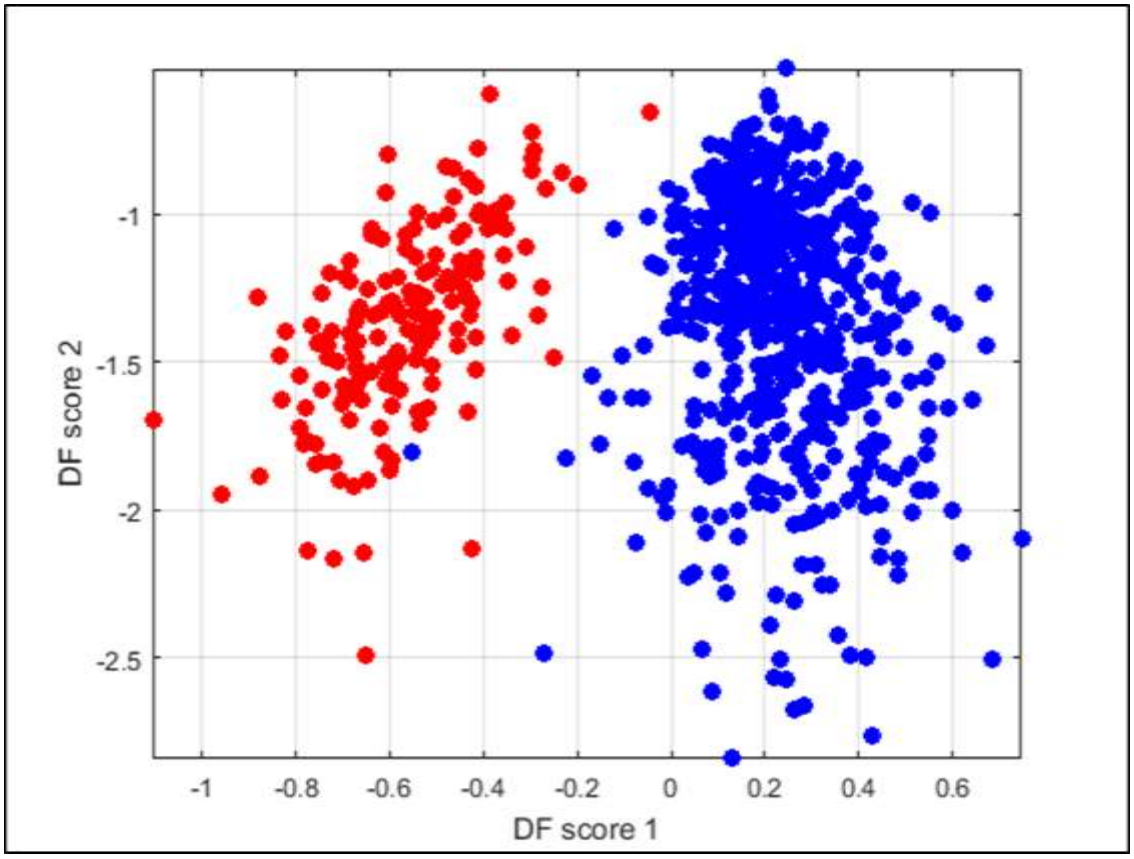

Figure W5. Outcome of the supervised clustering of whooping signals (red cloud) and rain droplets (blue cloud) for discrimination, shown in DF space. The overlap is negligible and well below 1 %.

The entire data set of whooping signal timings was then subjected to this procedure. Each pulse was uploaded in turn, its spectrogram was formed, centred, cropped, normalised and coarsened along the frequency axis. Next, the DF coordinates for each of the selected pulses were calculated by using the pair of cross correlation products and then its distance from each centroid in the DF space was established. The ratio of the two distances was tested to determine the cluster to which it belonged. The pulses were then saved as either rain droplets or true whooping signals.

The same discrimination procedure was also carried out on the French hive data set after it was revealed, in the "first pass" of the detection process, that queen pipes, worker pipes and high amplitude "clicks" had been wrongly detected as whooping signals owing to their spectral similarities. The same procedure of supervised clustering was used, this time with three clusters (Figure W6), and it allowed me to create separate data sets of whooping signals, piping, and click occurrences (Supplementary Figure 1 of Appendix 5 and 6).

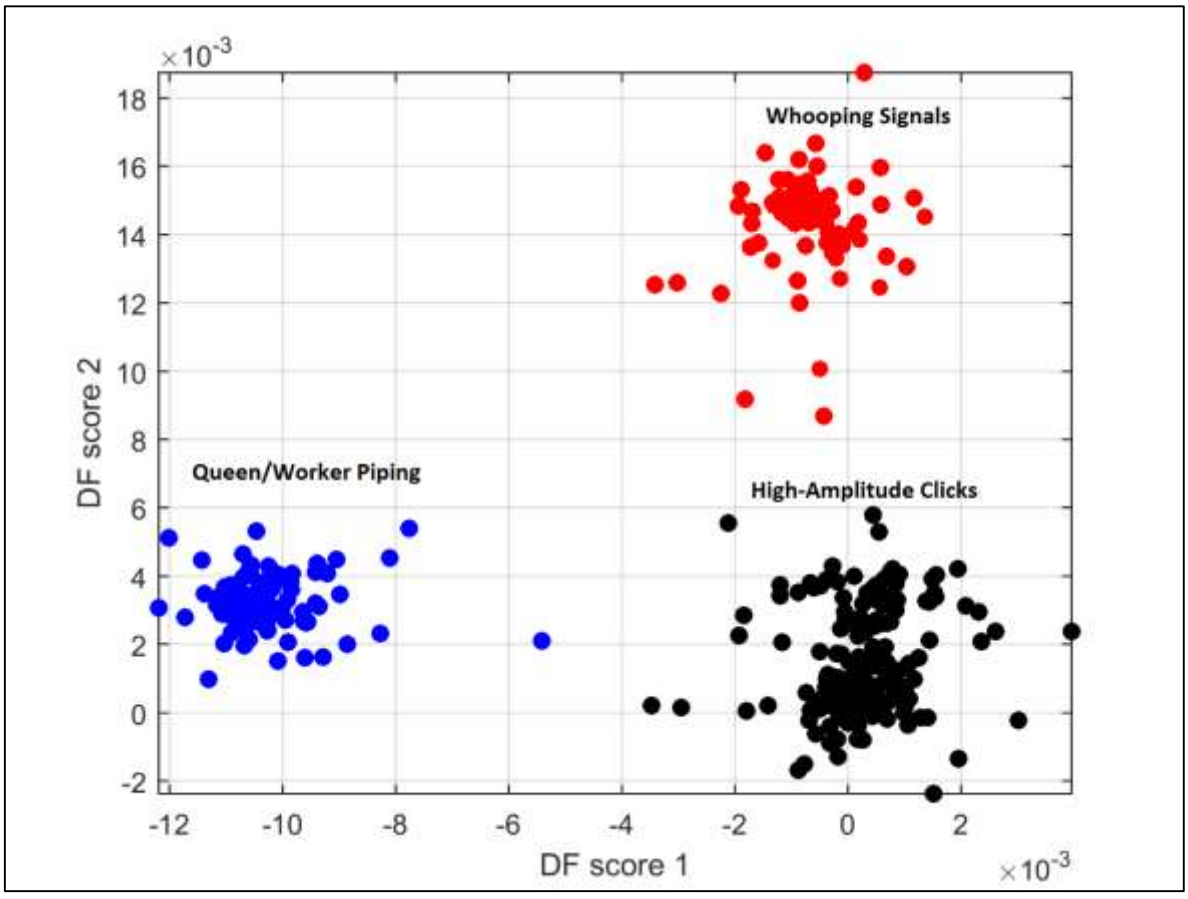

Figure W6. Outcome of the supervised clustering of whooping signals (red cloud) and queen/worker piping (blue cloud) and high-amplitude clicks (black cloud) for discrimination, shown in DF space.

As seen, there was an excellent discrimination with zero overlap.

The fact that only whooping signals remain after discrimination was checked by the critical listening of hundreds of signals taking place at random times of the year. Specific one-hour long sections of data where a large number of signals were detected in close proximity were also extensively listened to, and indeed revealed highly frequent whooping signals, as demonstrated in Audio W1. A movie of stacked spectrograms of whooping signals extracted by the software with their corresponding audio is also supplied in Video W7, which further validates the discrimination exercise.

3.2.3. Whooping signal parameter analysis

All data analysis, statistical and graphical, was undertaken in the MATLAB® core with occasional use of the statistics toolbox. All data was tested for normality using the Kolmogorov-Smirnov test and in some instances, normalisation is undertaken using Log_{10} transformation. When normal distribution could not be achieved, the non-parametric equivalent test was used. A Generalised Linear Model was used for the analysis of time on both the frequency and amplitude of whooping signals, and the Spearman's rank Correlation was used to test the relationship between frequency and amplitude of whooping signals.

3.2.4. The daily average occurrences and honeybee brood cycle

To see how the occurrences of whooping signals varied throughout the course of an average day, the number of whooping signals that occurred at each hour of the day was averaged across the entirety of the focal dataset and is shown with standard error for both the French and UK datasets. To examine the effect of the brood cycle, which causes cyclical density changes within the honeycomb as the progeny developed and ultimately hatch out, on the occurrences of whooping, the daily modal night-time amplitude of the overall vibrations (see Bencsik, et al., 2015) is also explored.

3.2.5. The Effect of weather on the occurrences of whooping signals

Local UK weather data was obtained via an onsite TechnoLine WS-2350 weather station. The French weather data was supplied free of charge by Météo France (www.metofrance.com) for the site and dates that I required. Hourly outside temperature, outside humidity and rainfall were analysed in relation to the occurrence of honeybee whooping signals, with the addition of atmospheric pressure for the UK dataset.

3.2.6. Analysis of duplications

Duplications occur when the same whooping signal is detected by both accelerometers. These need to be examined most importantly for the analysis of accelerometer locations for the detection of whooping signals. Duplications need to be removed otherwise the statistics of whooping signals will be misleading. To detect duplications, the raw data of whooping signal timings is first uploaded for both accelerometers on one frame. For any whooping signal found on the first accelerometer, the nearest whooping signal, in time, is found on the second accelerometer and the difference inspected. If its absolute value is smaller than 10ms, then the pulse with the lowest amplitude is labelled as a duplicate. From this, the percentage of duplications can be calculated by dividing the number of 'duplicates' by the total number of whooping signals, for example over one hour. The brood cycle daily modal values were then superimposed over the percentage of duplications to help visualise the effect of honeycomb mass-density on signal duplications.

3.2.7. Video recordings and observation hive design

Two accelerometers were also secured on the central frame of a separate colony kept in the laboratory, in Nottingham, UK, in a standard brood box. A transparent Perspex cavity was placed on the top of the hive, allowing this frame to be occasionally extracted and observed with video analysis on both sides, with the soundtrack provided by the accelerometer signals, for no longer than 20

minutes every day, up to twice a week, whilst being replaced in the brood box for the majority of the time. This allowed this colony and this frame to develop naturally without the major disturbances usually associated with permanent observation hives, where bees are forced to live in a planar geometry. For a full breakdown of the construction of this hive, see Appendix 1. Ten excerpts of these videos have been included for reference within this chapter and labelled have been “Video W1 – 10” to show examples of the situations in which whooping signals can occur within the hive and aid in the discussion of the statistics of these signals generated as part of this study.

3.3.0. Results

3.3.1. The physical characterisation of the ‘whooping signal’.

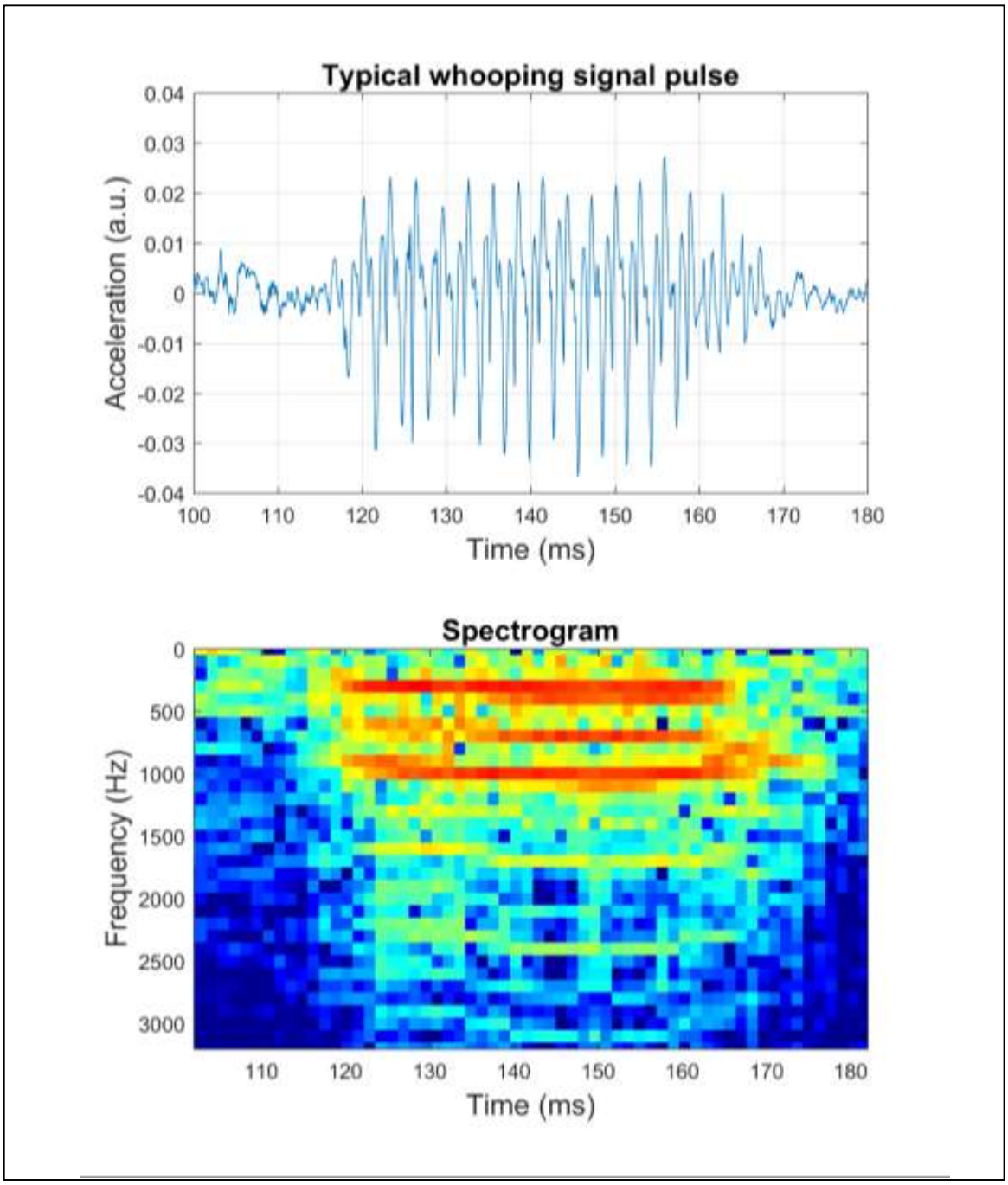

Figure W7. The time course and corresponding spectrogram of a typical honeybee whooping signal. The colour intensity of the spectrogram denotes the logarithmic amplitude of the measured acceleration with red being the highest acceleration and dark blue being the lowest.

The time course of the acceleration and the frequency components for a typical honeybee whooping signal, measured with an accelerometer, is shown in Figure W7. To create a spectrogram of such a brief vibrational pulse with such a high resolution without compromising the lower frequencies, an overlapping procedure was utilised whereby the Fourier transform was computed over 100ms of data. This widow is then shifted by 25 ms along the time axis of the pulse. This gives a high resolution moving average that can be displayed as in the spectrogram in Figure W7. Using a temporal resolution of 100ms, does mean that information at frequencies below 10Hz may be misleading, however as the pulse of interest has a fundamental frequency upwards of 200Hz, this is deemed not to be an issue. This particular signal has a fundamental frequency of 355Hz for a duration of 60ms. A common feature of this signal is to have two well-pronounced upper harmonics at twice and three times the value of the fundamental frequency. Numerous harmonics at even higher frequencies can also here be seen up to 3000Hz, with negligible but measurable amplitudes. Another common component of the signal, which can be seen on both the time-course and the spectrogram, is the ultra-short increase and decrease in the oscillation's frequency respectively at the start and the end of the pulse. The oscillations present in the waveform of whooping signals also appear unbalanced, with a clear minimum being of greater magnitude than the positive maximum, a feature not seen in the waveform caused by acoustic noise. Airborne sound can effectively pull the honeycomb due to the low pressure and push it due to the high pressure causing the honeycomb to oscillate around its equilibrium. On the other hand, a single honeybee producing a vibration hanging on a single face of the frame, is only able to push the honeycomb, providing more energy in a single direction. This causes an oscillating waveform that is asymmetrical.

To compare the signal I am detecting with the one recognised as a "begging signal" by previous authors, a MATLAB® extraction of the begging signal published in Michelsen et al.'s (1986b) study was undertaken (Figure W8). After transforming the velocity measurement into acceleration through calculation of the numerical gradient between each consecutive digital point, the spectrogram (Figure W9) shows a fundamental frequency of 345Hz with upper harmonics at twice, three times and four

times that of the first with the second harmonic being the next-most prominent peak. There is a step change in overall signal amplitude across all frequencies immediately prior to and throughout the honeybee pulse that is not seen on our own traces. As this is a MATLAB® extraction of Michelsen et al.'s (1986b) published pulse, it is difficult to suggest an origin for this feature. With a time duration of 50ms, the time course and spectrogram of the pulsed vibration that Michelsen et al. (1986b) described as a begging signal both match remarkably well with the tens of thousands of these signals that were detected and analysed with my software. It is interesting that the velocity measurement provided by Michelsen et al. (1986b) appears reasonably centred around zero. The acceleration, however, produces a clearly unbalanced pulse, just like the majority of the measurements from my own measurements.

In Video W7, the raw accelerometer data, along with the graphical representation of the waveform, spectrum and spectrogram of hundreds of randomly chosen whooping signals is showcased. Although I cannot show the entire collection of pulses that have been detected, my limited tests strongly support the fact that the vast majority of pulses that I have analysed are exclusively those pulses previously understood by experts as being stop / begging signals.

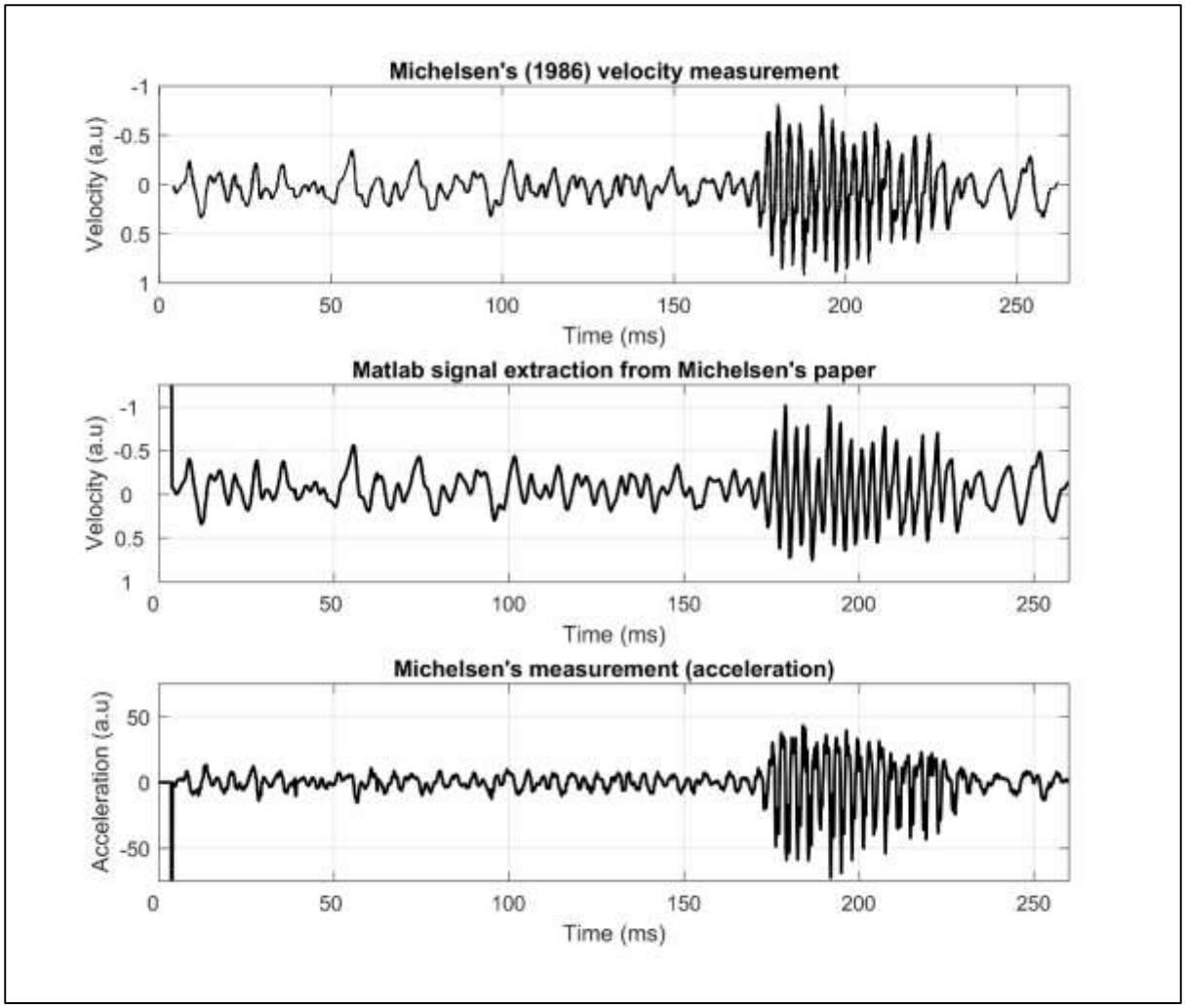

Figure W8. Matlab® extraction of Michelsen's begging signal published in 1986. a) The original waveform from the publication. **b**) The waveform extracted with home built MATLAB® code. **c)** The time differential of the previously extracted waveform, providing acceleration as a function of time.

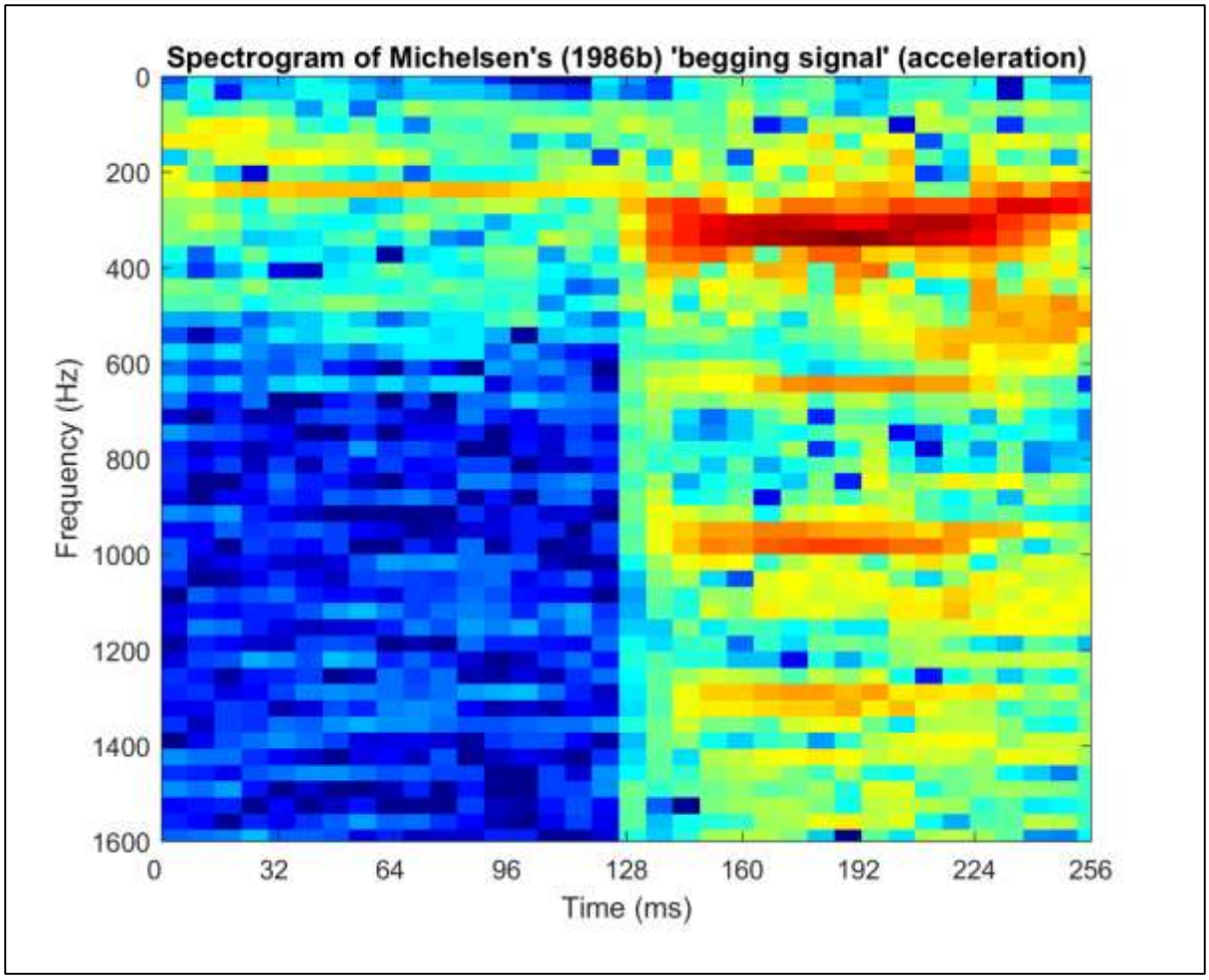

Figure W9. Spectrogram of Michelsen's (1986b) begging signal, after the processing displayed in Figure W8 to represent the pulse as acceleration. This signal draws striking resemblance to the whooping signal displayed in Figure W7, as well as the extensive collection provided in Video W7.

3.3.2. Long-term statistics in the occurrence of whooping signals

3.3.2.i. French hive

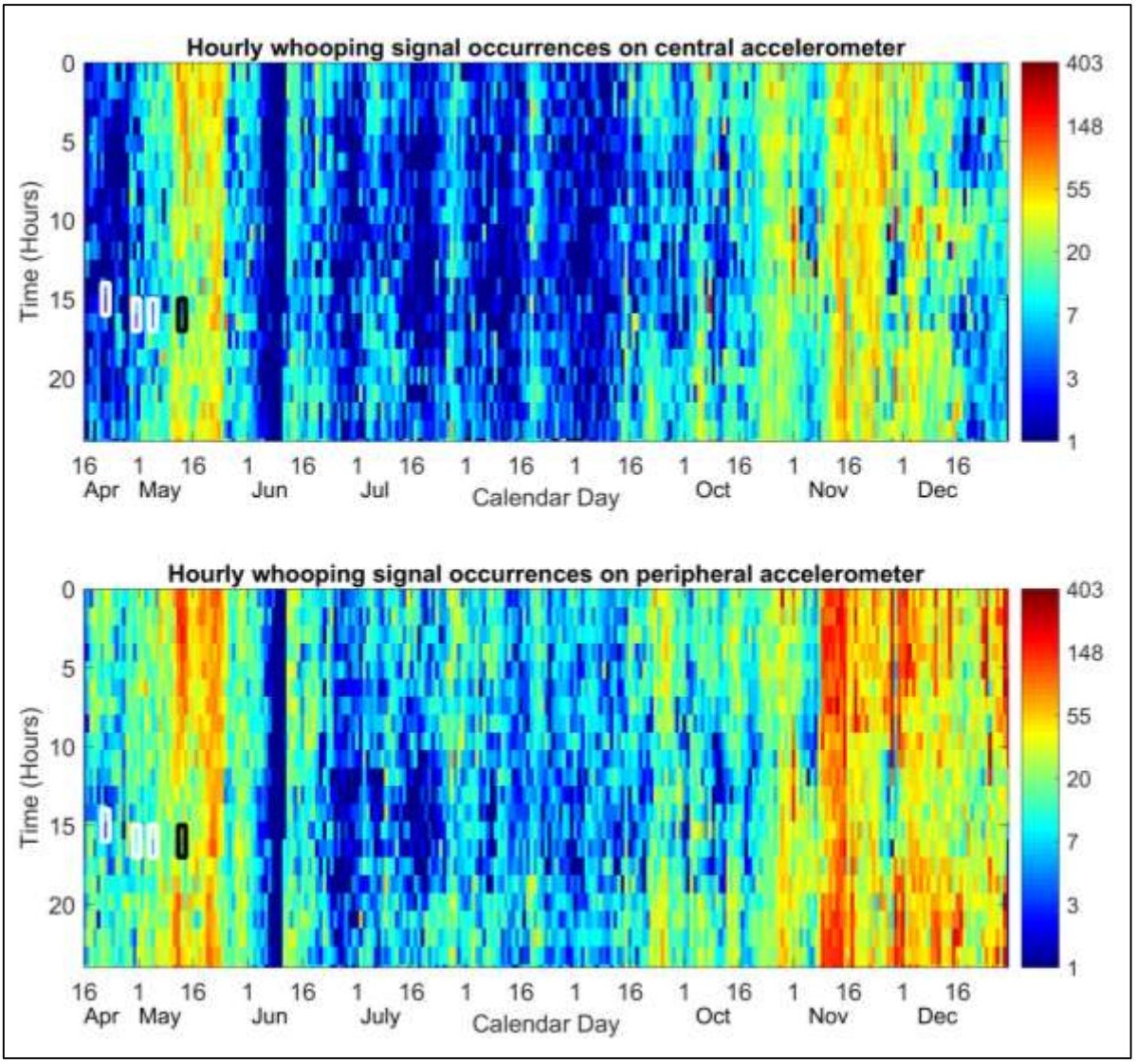

Figure W10. Whooping signal hourly occurrences. Central (top) and peripheral (bottom) accelerometer logs of the French hive (2015 season). The colour codes the number of hourly occurrences from dark blue (≤1) to dark red (403 signals) on a logarithmic scale. White rectangles highlight the occurrences of the three swarms that occurred from this hive, with the first one being the primary swarm. The Black rectangles show where the final queen pipe occurs within this recording.

The hourly occurrences of whooping signals shown in Figure W10 clearly demonstrates that (i) the signal occurs very frequently (up to 6 to 7 times per minute), and that (ii) there is a pronounced and

consistent midday decrease in the occurrences of this signal. This phenomenon is further evident upon averaging the hourly whooping signal occurrences for all 261 days on the central (Figure W11a) and peripheral (Figure W11b) accelerometers. It is seen that there is a large increase in occurrences after the last swarm and during the winter months. It is also seen that detections are somewhat modulated by the brood cycle with peaks every 21 - 24 days. Similar trends can be seen in the UK data, albeit on a shorter time scale (See Figures W12 and W13). Audio W1, recorded between midnight and 1 am on 12th May 2015, corresponds to a hotspot on Figure W10. Amongst other signals, including queen tooting, (that were successfully dismissed by the software), it is easy to check by critical listening the genuine commonness of whooping signals occurring during this time and how different they are compared to the various other signals. For comparison, in Audio W2, I have provided a sample of the "wings together" and "wings apart" pipes (Kirchner, 1993; Pratt et a., 1996; Qhtani and Kamada, 1980; Seeley and Tautz, 2001) that were filtered out by the software at the "second pass" of the detection process.

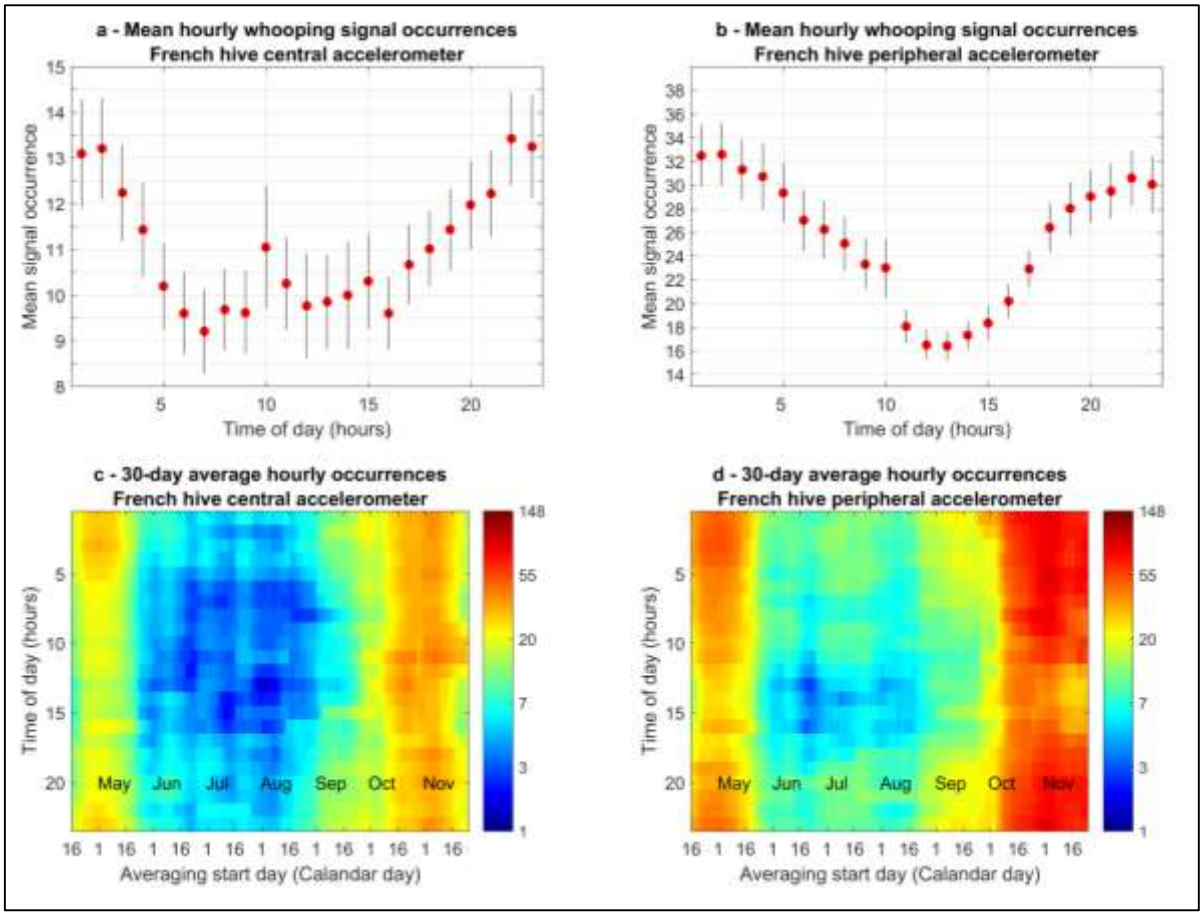

Figure W11. Average number of whooping signal occurrences observed for each hour of the day. This graph is obtained over the vibrational dataset shown in the previous figure. **a)** The overall mean hourly whooping signal occurrences for the central accelerometer and, **b)** for the peripheral accelerometer. The vertical bars indicate +/-1 SE. **c)** The moving hourly whooping signal occurrences computed over 30 days and shifted one day along the dataset for the central accelerometer and, **d)** for the peripheral accelerometer.

Figures W11.a and W11.b show that there is a percentage decrease of 64% between the average number of whooping signals recorded between midnight and 1am (33 pulses per hour), and those recorded between 12 and 1pm (16 pulses per hour). It can be seen that the curve is smooth with a sharp decrease in the number of whooping signals after 11am. There is also a much more gradual increase after 2pm with larger steps between 5 and 7 pm. Upon averaging the hourly occurrences over a 30-day period along the time axis, Figure W11.d shows that this trend holds stable across the entirety

of the recording. As a whole, Figure W11 also further highlights the increase in the number of detection from the peripheral accelerometer (Figure W11.b) compared the central one (Figure W11.a).

3.3.2.ii. UK hive

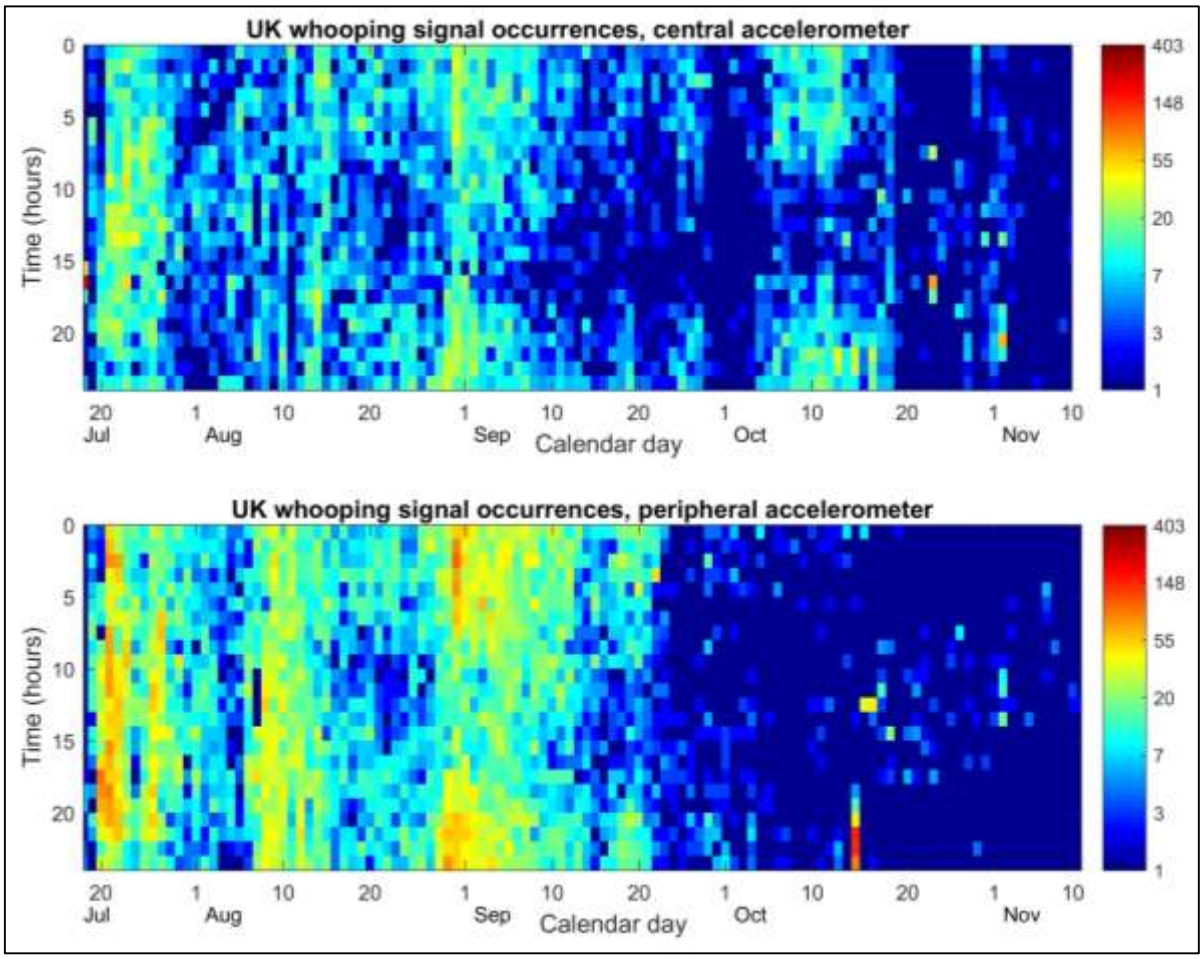

Figure W12. Hourly occurrences of whooping signals detected on the central and peripheral accelerometers of the UK hive (2014 season). The colour codes the number of occurrences on a logarithmic scale.

Figure W12 illustrates the hourly number of whooping signals that were detected throughout the four months of continuous vibrational recording from the heart of my UK hive located at the Clifton campus of NTU. The overall number of detections per hour is reduced in comparison to the French dataset in Figure W10 (maximum of 2 to 3 per minute compared to the 6 to 7 of the French hive). However, it is still apparent that whooping signals occur very frequently within the detectable range of the

accelerometers. Similar to what is observed within the French dataset, there appears to be roughly half the number of whooping signals detected on the central accelerometer compared to that of the peripheral accelerometer. In line with the French dataset again, the signal detection appears to be modulated by the brood cycle with peaks every 21 to 24 days (see Bencsik *et al.* 2015).

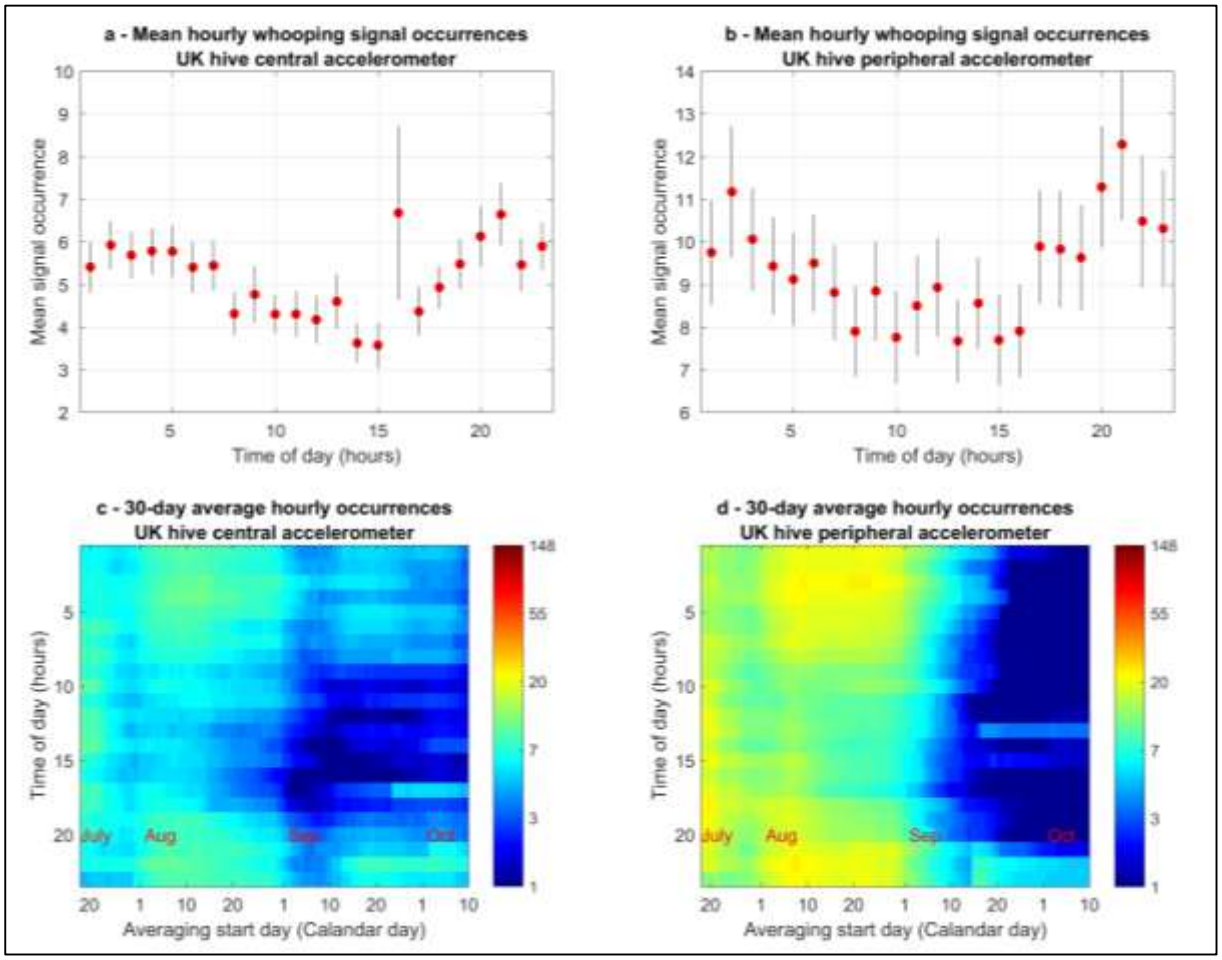

Figure W13. Average number of whooping signal occurrences observed for each hour of the day over the vibrational dataset shown in the previous figure. The data shown for the UK hive has been processed identically as in Figure W11.

In line with that of Figure W11 for the French dataset, a reduction by around 55% in the number of signals occurring between 11am and 4pm can be seen throughout the UK dataset, being made more apparent in Figure W13.a and W13.b, where the hourly whooping signals have been averaged for each

hour over all recorded days. As seen in Figure W13.c and W13.b, where the average hourly occurrence is computed over 30 days from the start date, this daily trend is not seen as apparently for whooping signals recorded at the end of July, perhaps due to the rainy summer experienced in 2014. The increase in whooping signals that were detected at the periphery of frame, as shown in Figure W12, can also be seen in this figure. The total number of whooping signal occurrences tails off towards the end of September on both accelerometers but returns at the centre towards the end of October.

3.3.3. Whooping signal occurrences under varying weather conditions

3.3.3.i. French hive

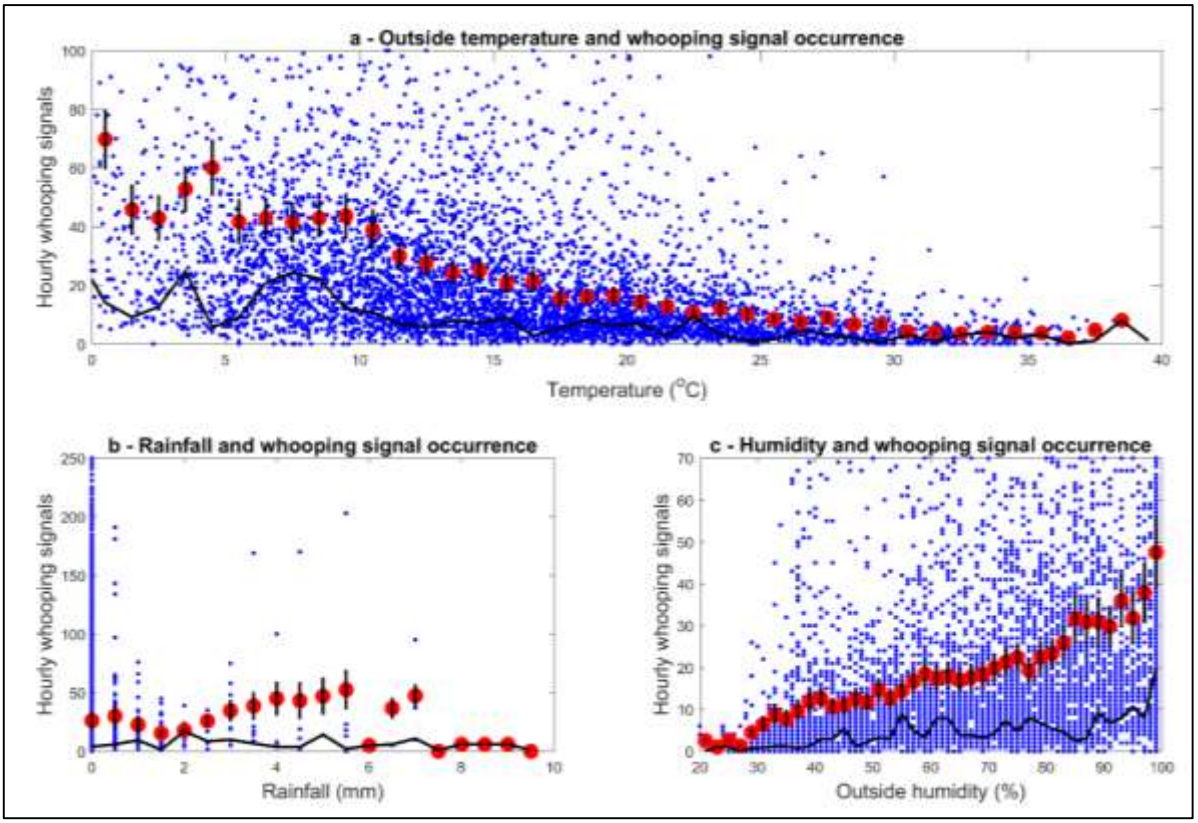

Figure W14. Hourly number of whooping signals with weather. French dataset with corresponding: **a)** average outside temperature; **b)** cumulative rainfall, and **c)** average outside humidity. Red dots indicate the average number of whooping signals with black bars displaying ± 1 SE. The black curve on each graph shows the modal hourly whooping signals.

It can be seen in Figure W14.a that there is a weak but significant negative effect of outside temperature *(R^2 = 0.16, p <0001)* on whooping signal occurrences with the greatest number of whooping signals being recorded at temperatures around 0°C. This can be seen by both the modal and mean number of whooping signals. There also appears (Figure W14.c) to be a gradual increase in the mean and modal number of whooping signal occurrences with increased outside humidity *(R^2 = 0.286, p < 0.001)*. There is no overall effect of rainfall on the number of whooping signals *(R^2 = 0.032, p = 0.249)* but it can also be seen that the majority of days saw very little precipitation (Figure W15).

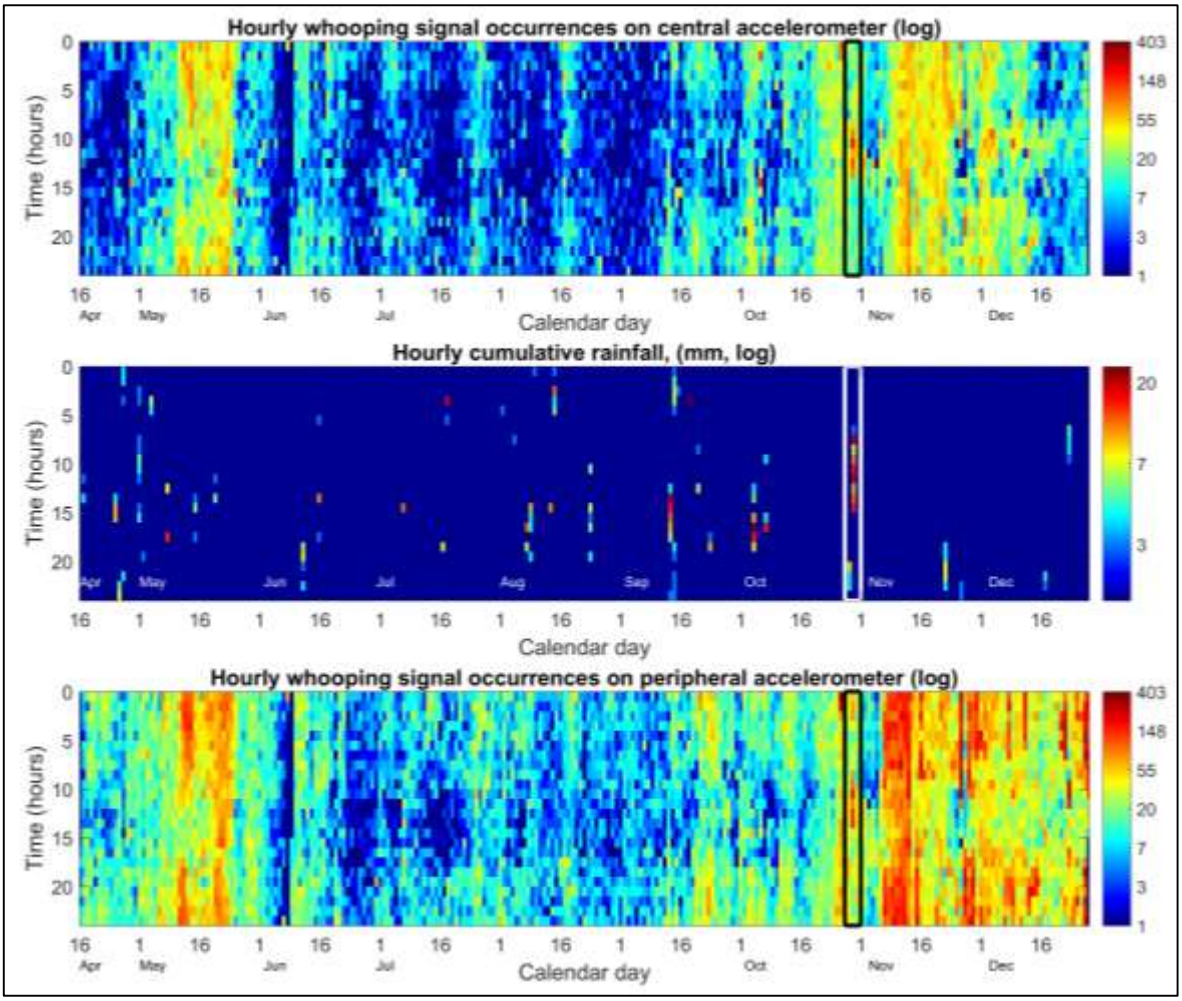

Figure W15. Hourly whooping signal occurrences with continuous rain. Central (top) and peripheral (bottom) accelerometers. Hourly rain is displayed in the central chart. Highlighted on all three plots is the 28th October 2015. Black / white rectangles highlight a particular bout of heavy rain that occurred throughout the middle of the day.

Figure W15 highlights how rare rainy days have been throughout the duration that the colony has been monitored. The rectangles in black and white draw attention to the data around the 28th October 2015. This is the only example where it heavily rained throughout most of the day, and it can be seen that there is a reversal in the usual daily trend of whooping signal occurrences, resulting in a pronounced lunchtime increase in whooping signal occurrences. A similar phenomenon takes place on the rainy days of the 11th September and 3rd October, where whooping signals appear continuously throughout the day, exhibiting no reduction at lunchtime.

3.3.3.ii. UK hive

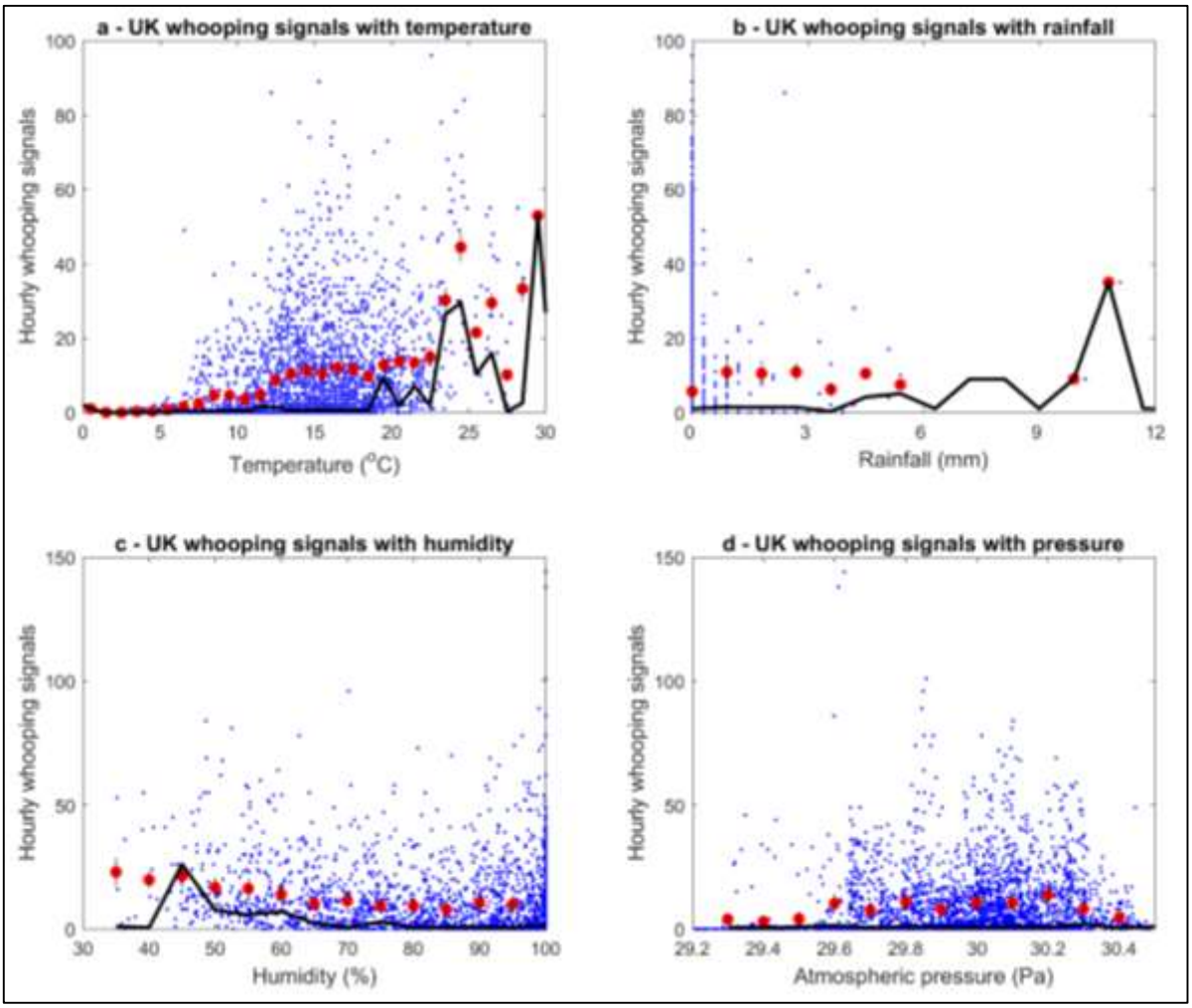

Figure W16. Hourly number of whooping signals with corresponding: a) average outside temperature; **b)** average outside humidity; **c)** cumulative rainfall; and **d)** average atmospheric pressure. Red dots indicate the average number of whooping signals with black bars displaying ± 1 SE. The black curve also shows the modal number of whooping signals.

In spite of substantial scatter, it can be seen in Figure W16a that there is a faint positive trend of whooping signals with outside temperatures with more whooping signals being recorded when the outside temperature is higher, however there is great variance within the data ($R^2 = 0.104$, $p < 0.001$). This directly contradicts that of the French temperature analysis in Figure W14a. The majority of signals occurred between 7 and 23°C, whereas in France the outside temperature went much higher. There is no significant effect of outside humidity ($R^2 = 0.042$, $p = 0.119$), also contradicting the result

of the French analysis. Rainfall ($R^2 = 0.001$, $p = 0.853$), as well as atmospheric pressure ($R^2 = 0.0014$, $p = 0.132$), also had no effect on the occurrence of whooping signals, in line with the data presented for the French hive in Figure W14. It must be highlighted that the contradictions between the French and UK datasets concern data that is substantially scattered.

It can be seen in Figure W17 below that, just like the French dataset (Figure W15), periods of rainfall occurring during foraging hours can cause the disappearance of the midday lull in signal occurrence. I draw the reader's attention to particular days of the 10th August and 23rd October.

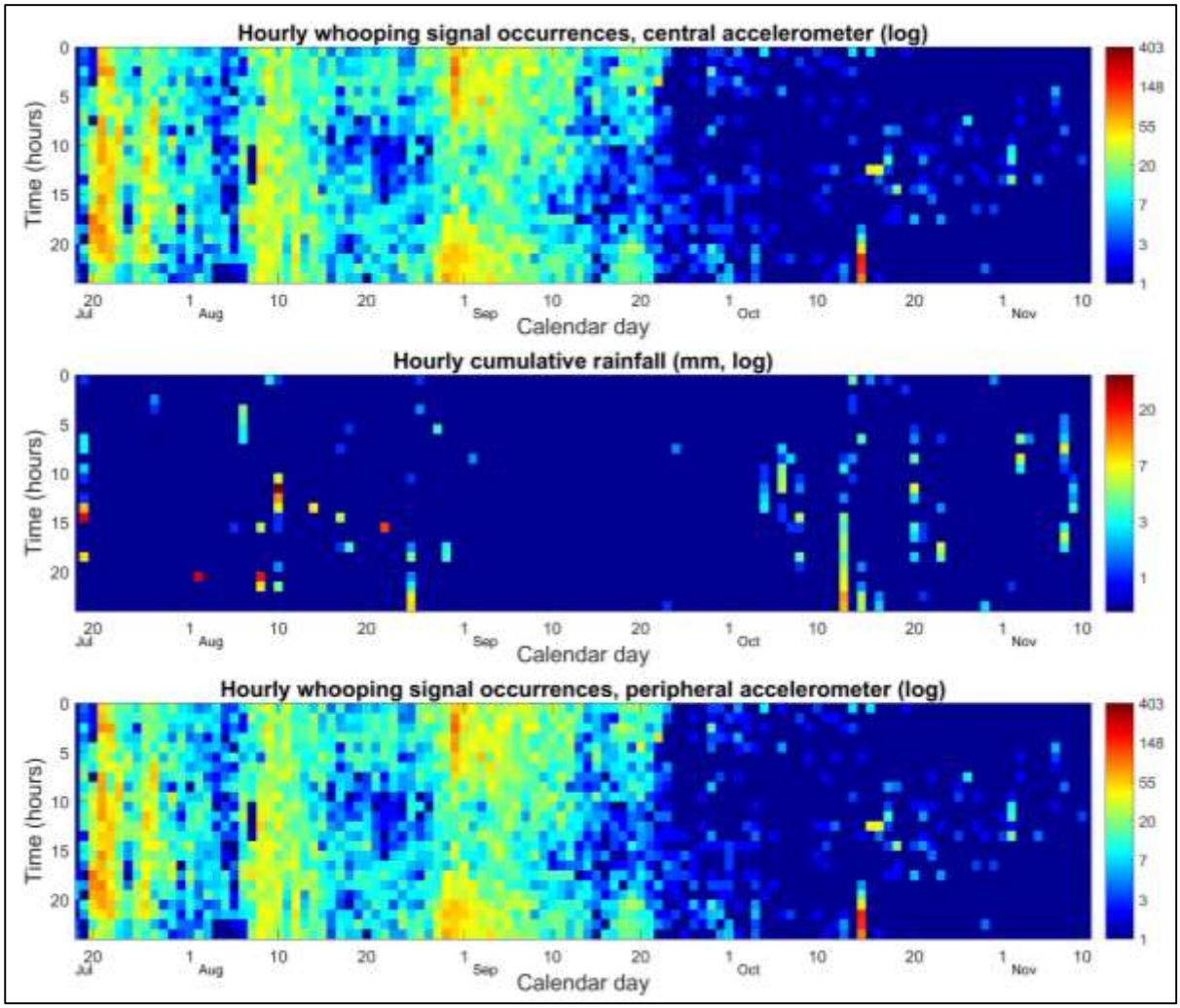

Figure W17. Hourly whooping signal occurrences with continuous rain for the UK hive.

Central (top) and peripheral (bottom) accelerometers. Hourly rain is displayed in the central chart with pixel intensity showing cumulative rainfall in mm.

3.3.4. Extensive characterisation of honeybee whooping signals

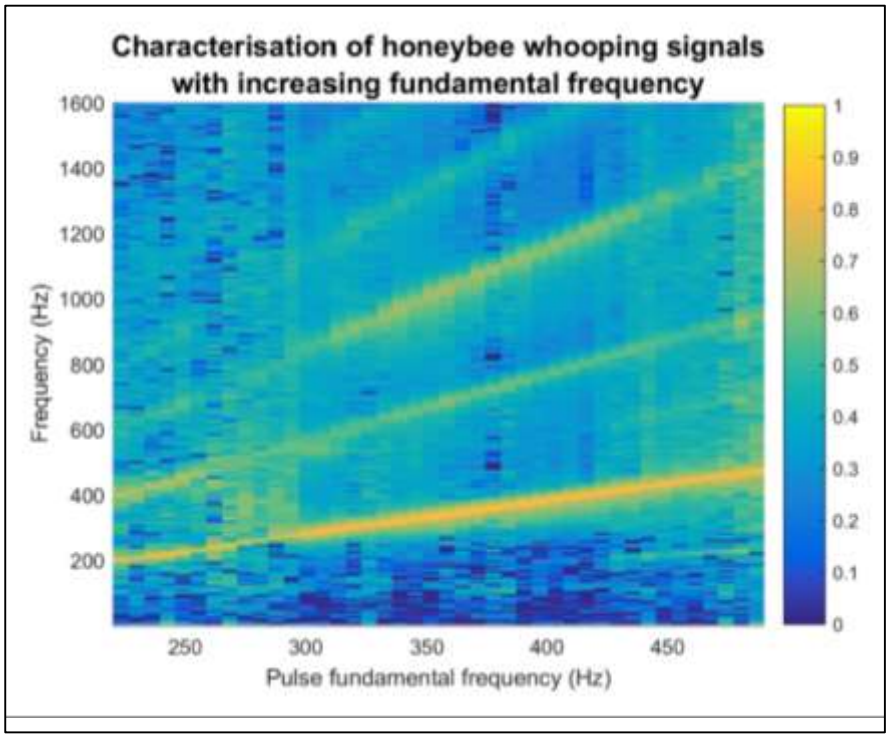

Figure W18. Extensive characterisation of honeybee whooping signals. Whooping signals spectra of similar fundamental frequencies were averaged, scaled to one by dividing by its maximum and stacked from left to right. The amplitude is displayed in a linear scale (yellow = high amplitude and dark blue = low amplitude).

In Figure W18, to achieve the extensive characterisation of honeybee whooping signals, the entire collection that was detected within the French dataset was used. As I have averaged together pulses of similar frequency, the plot displays very narrow spectral peaks. The signal to noise ratio does vary substantially along the horizontal axis of Figure W18, owing to the number of whooping signals that are found within a specific bandwidth will differ following the distribution shown later in Figure W20.a and W21.a. Nevertheless, the evolution of the fundamental frequency and its harmonics can be tracked extremely well over the entire range of frequencies spanning from 200 to 500Hz with harmonics seen up to four times the value of the fundamental. Interestingly, Figure W18 would suggest that whooping signals with a lower fundamental frequency (below 250Hz) exhibit an enhanced first harmonic, whereas those above 300Hz have an enhanced third.

3.3.5. Long-term evolution of whooping signal physical characteristics

3.3.5.i. French hive

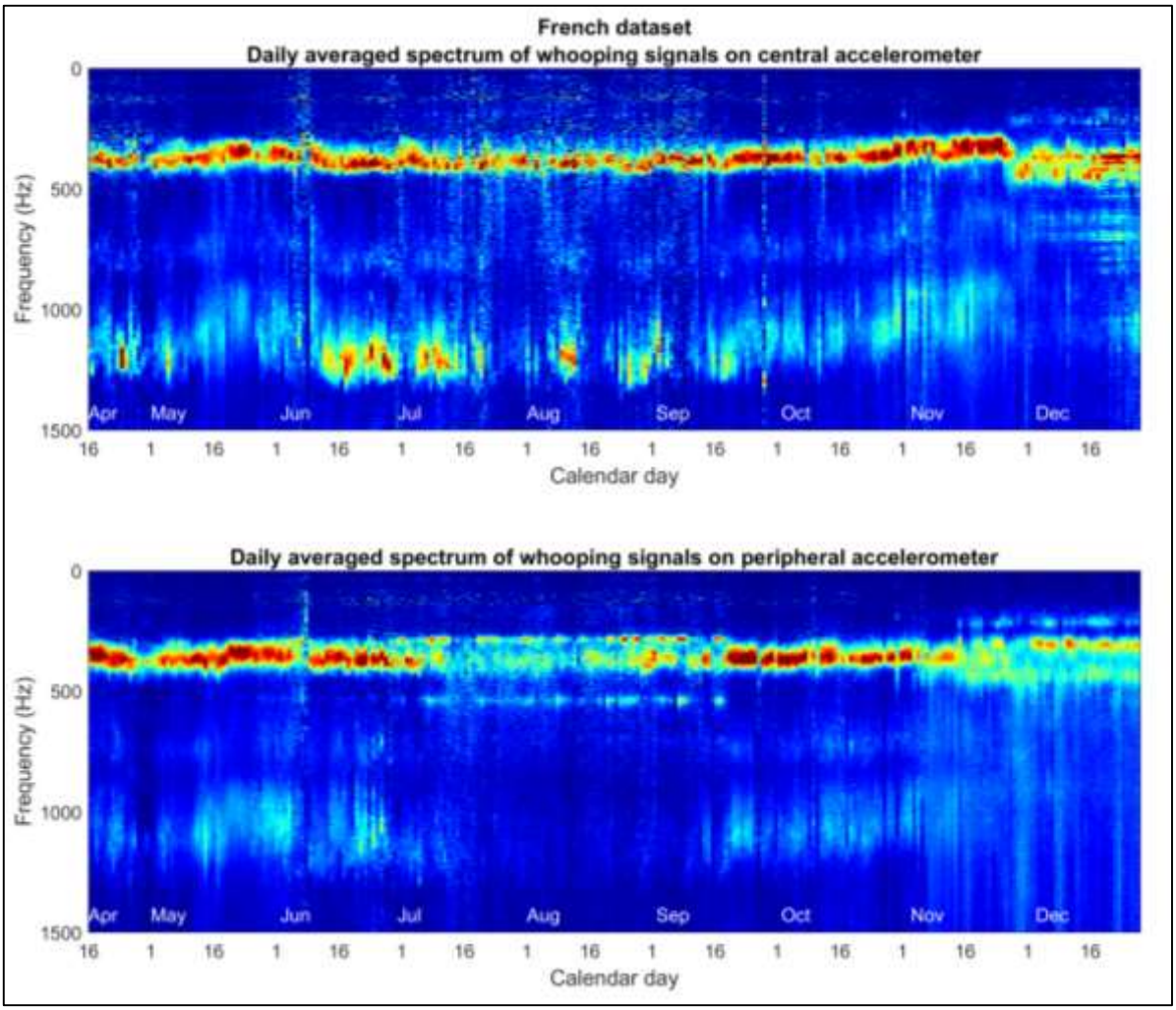

Figure W19. Long-term evolution of the daily averaged spectrum of whooping signals. Data from Apr 18th until Dec 25th 2015 is shown, obtained after the subtraction of the background signal, which would otherwise produce a pronounced peak at 125Hz coming from the bees' hum. Each individual spectrum was normalised to one by dividing it by its maximum to allow for a comparison between the peak frequency signals on a standard scale (between 0, blue, and 1, red).

It can be seen in Figure W19 that the whooping signal spectrum holds very stable with a fundamental frequency peak at 380 Hz across the whole data set. There is a slight reduction in frequency of around 15% in late May (seen more clearly in Figures W20.d and W21.d), which is most apparent through examination of the upper harmonics. However, the frequency returns to normality in mid-June until

mid-October when the average frequency begins to drop again by around 15%. The amplitude of the third harmonic at around 1200 Hz can be very high mostly on the central accelerometer for higher amplitude signals; revealing emitter bees in the close vicinity of the accelerometer (see Figure W20.c).

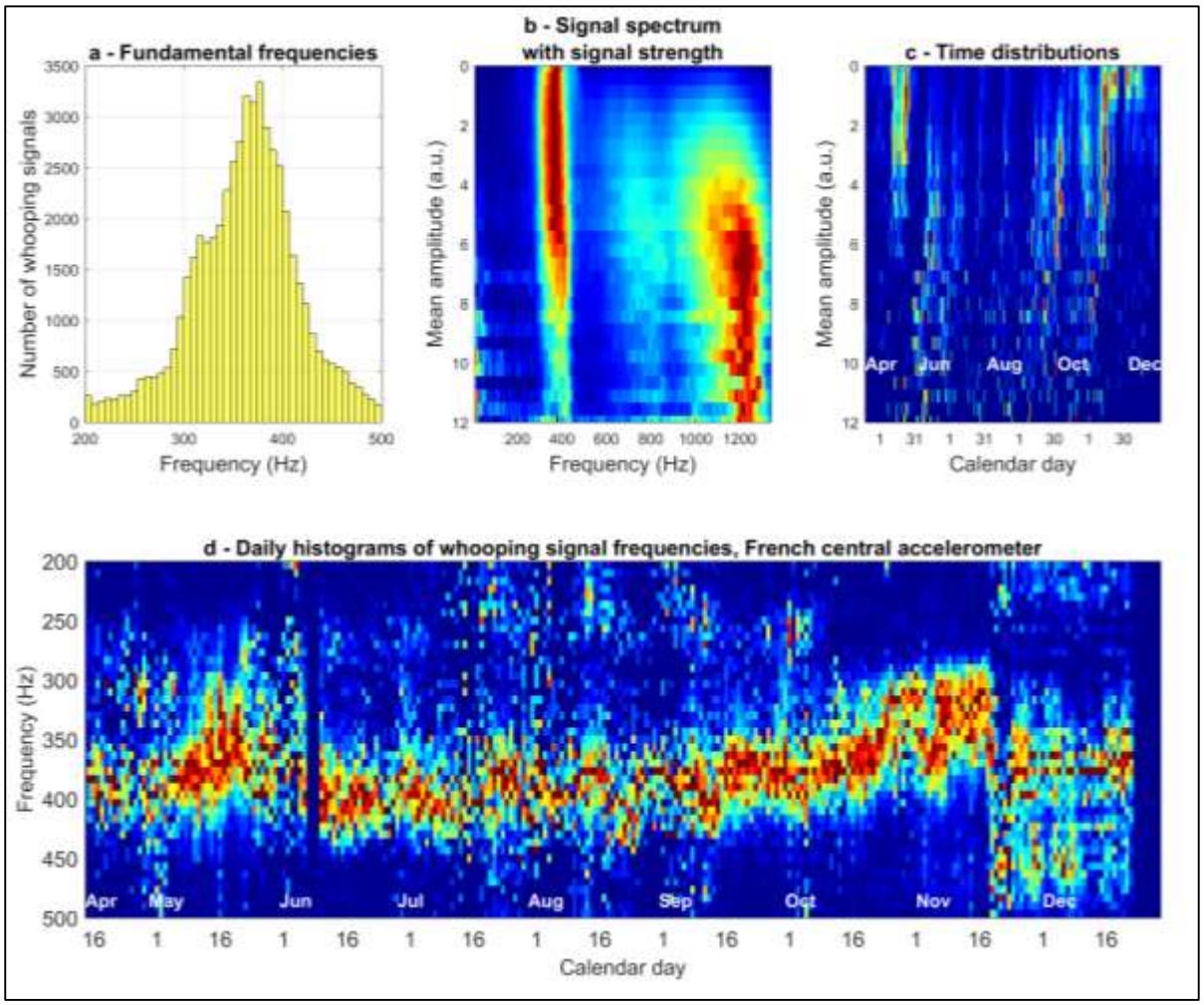

Figure W20. Distribution analysis for data coming from the central accelerometer. a) Fundamental frequency distribution;

b) The averaged spectrum of whooping signals with a specific amplitude displayed in descending order from highest (12 a.u.) to lowest (0 a.u.) amplitude with colour coding the measured amplitude in arbitrary units;

c) Temporal histograms of whooping signals of a specific amplitude. Colour codes the likelihood of occurrences;

d) Daily histogram of whooping signal fundamental frequencies.

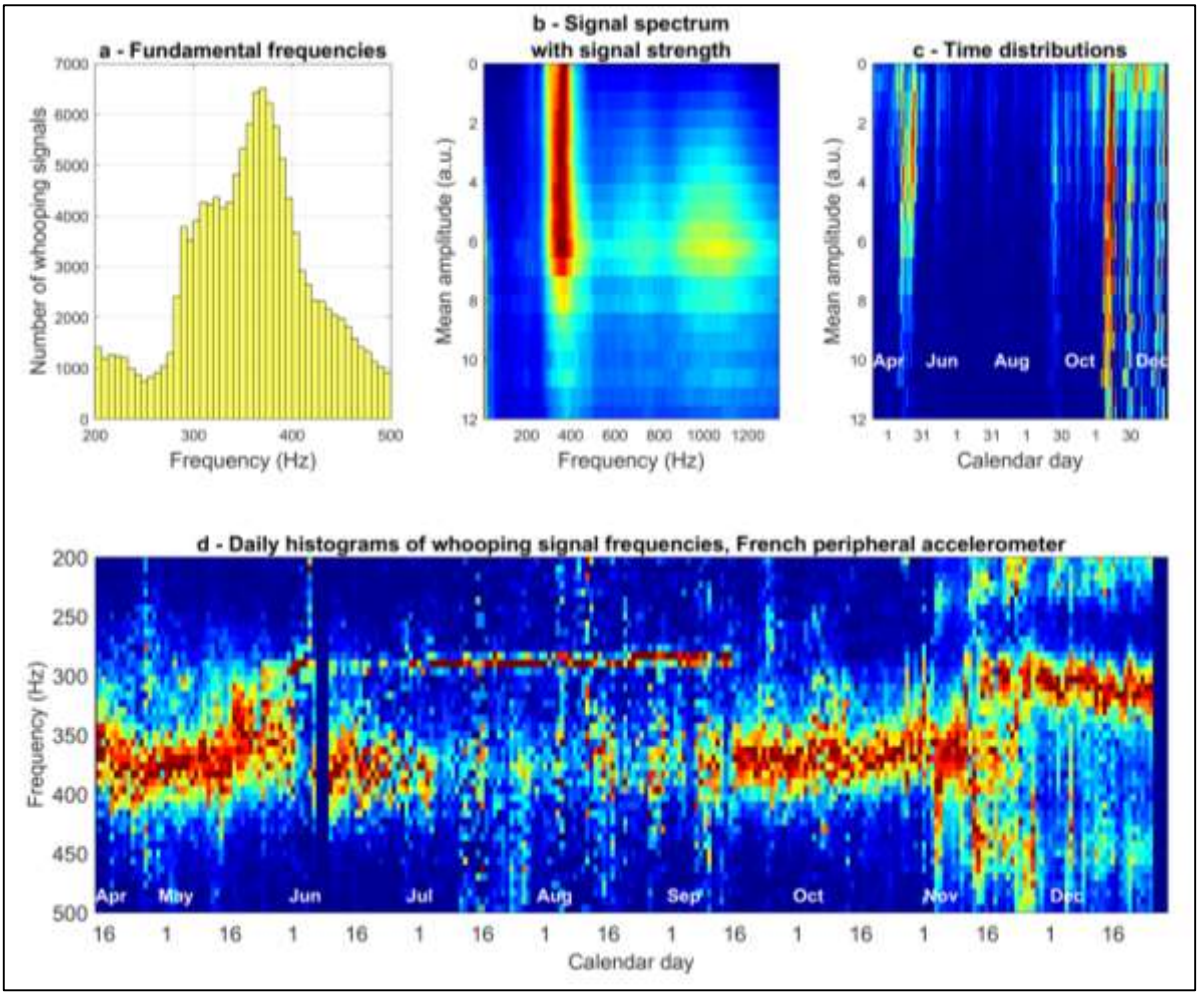

Figure W21. Distribution analysis for data coming from the peripheral accelerometer.

The data shown here for the peripheral accelerometer has been processed identically to that in Figure W14

Figure W20.a shows that on the central accelerometer the majority of whooping signals exhibit a fundamental frequency between 300 and 450Hz and this is mirrored for the data on the peripheral accelerometer (Figure W21.a). Relatively few signals occur at less than 250Hz or above 500Hz. This is confirmed in Figures W20.d and W21.d, showing that the majority of signals detected on a daily basis occur between 280 and 460Hz. There is negligible effect of time/season on peak frequency (Central*: R^2=0.001, p<0.001;* Peripheral*: R^2= 0.004, p<0.001*) across either channel (Figure W20.d and W21.d) providing further evidence that the signal spectrum holds stable throughout the active months. Note that there are slight oscillations apparent in the fundamental frequency of whooping signals,

particularly on the central accelerometer during the summer that appear to follow a 21-day cycle. To examine this further, the night time modal amplitude, shown by Bencsik et al. (2015) to correlate with the honeybee brood cycle due to the changes in honeycomb density caused by the growth and sudden hatching of honeybee brood, was computed for this dataset. Upon superimposition of this curve over the histograms of whooping signal fundamental frequencies in Figures W20.d and W21.d, this trend does appear well correlated with the brood cycle (Figure W22). Additionally, there is a tail-off in the fundamental frequency by around 20% towards the end of May and October, which is somewhat apparent in Figure W19. There appears to be a slight positive relationship between signal amplitude and frequency in the centre (Figure W20.c) and the periphery (Figure W21.c) (Central: *r= 0.1032, p <0.001;* Peripheral: *r = 0.06, N = 157521, p <0.001*) with the louder signals also exhibiting a more pronounced upper harmonic peak. A minority of low frequency signals also exhibit a stronger second harmonic as seen in Figure W18. The amplitude shows no daily trend in either the central (Figure W20.c) or the peripheral channel (Figure W21.c) (Central: R^2*=0.04, p=0.16;* Peripheral: R^2 *=0.043, p=0.12*), strongly suggesting that any amplitude (Figure W20.c and W21.c) can take place at any point in time, and is most probably a waveform spectral change due to the distance that the wave has propagated within the honeycomb, a phenomenon known as dispersion.

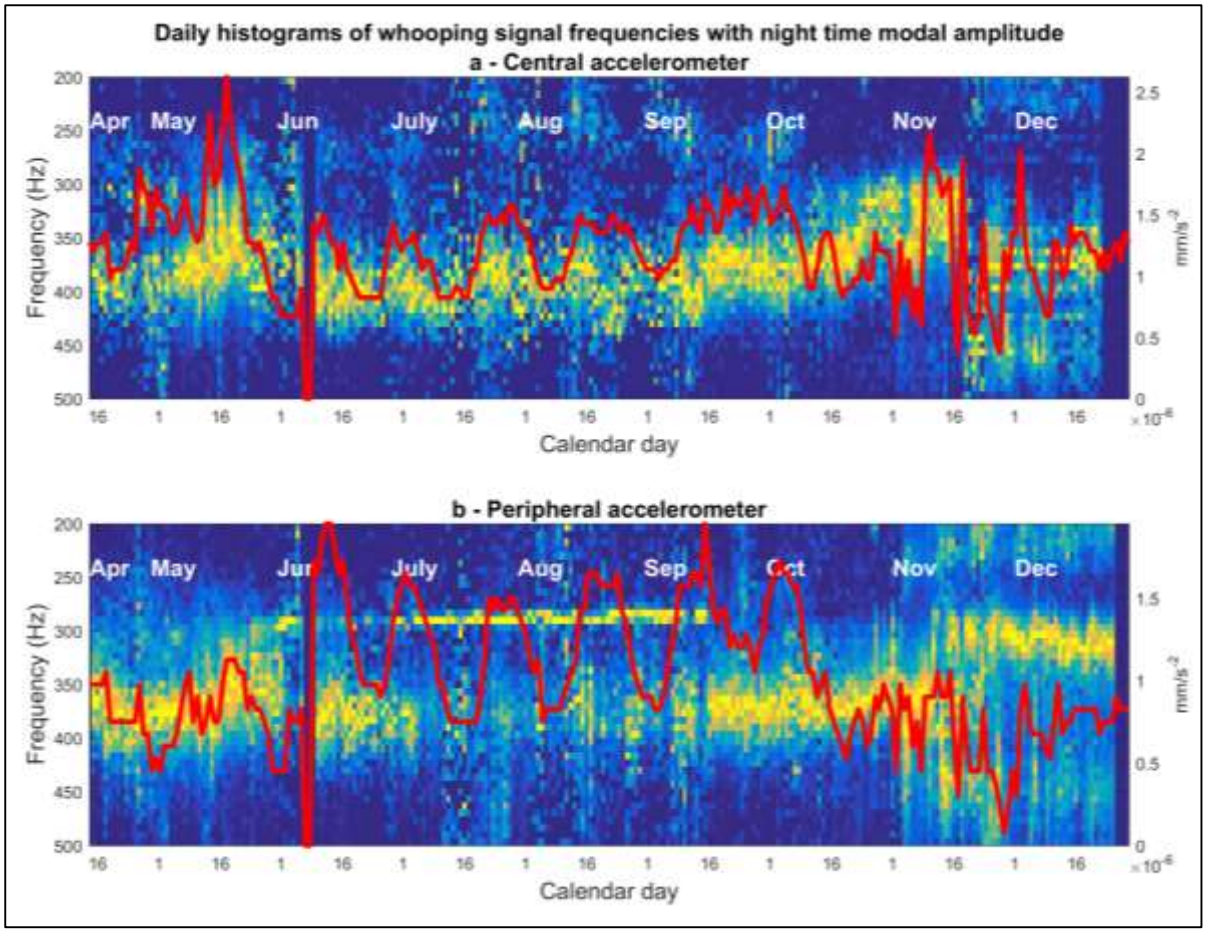

Figure (W22). The daily histograms of whooping signal fundamental frequencies derived from the centre (a) and periphery (b) of the honeycomb. The modal daily accelerometer signal amplitude distribution is superimposed with a red line and acceleration axis given on the right hand side in mm/s^2.

3.3.5.ii. UK hive

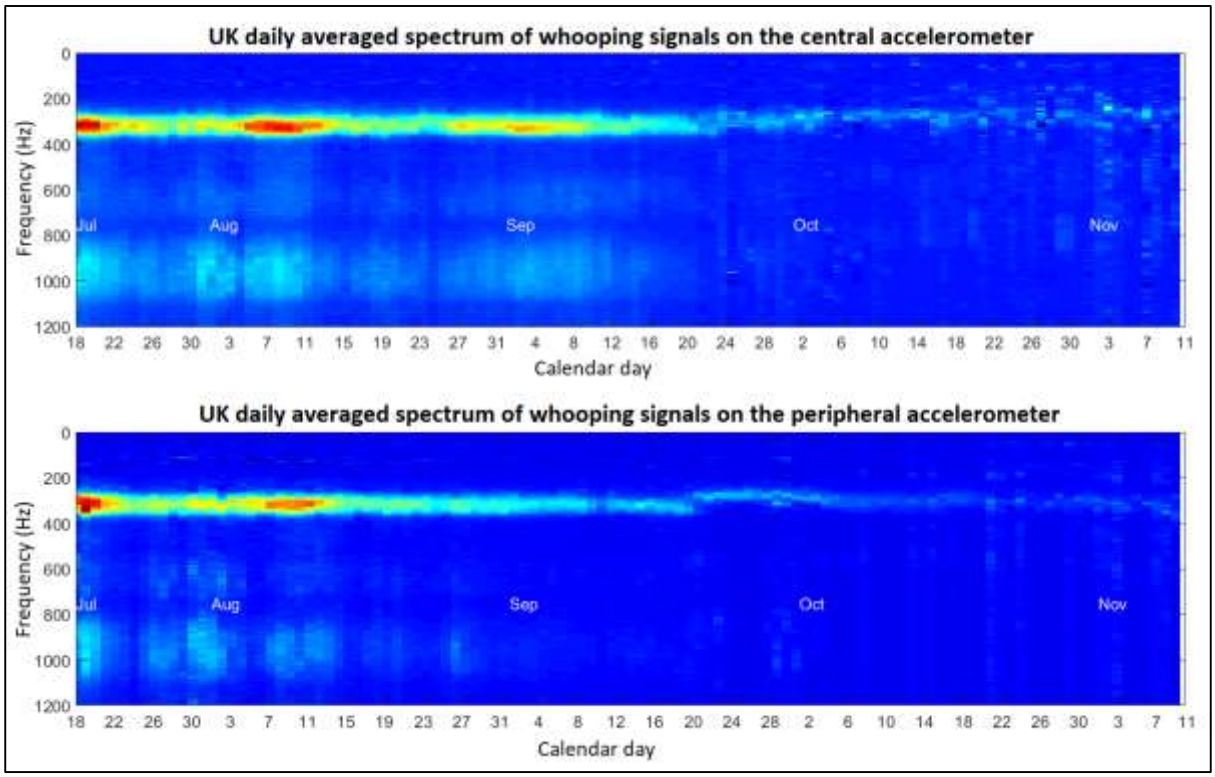

Figure W23. Long-term evolution of the daily averaged spectrum of whooping signals from Jul 18th until Nov 9th 2014 of the UK hive dataset. Data presented here was processed identically to that in Figure W12.

Figure W23, after removal of the background 125Hz 'wing buzz' and its 250Hz harmonic, is showing the long-term evolution of the daily averaged spectrum for every whooping signal detected by the software for the UK hive dataset. Unlike the daily average of French whooping signals, It is seen that the signal's average frequency from the UK hive holds very stable at 320Hz with clouds representing the upper harmonics, throughout the summer months until the end of September where it gradually decreases until the end of the recording in November. Peaks in occurrences take place every 21 days as seen on the French dataset. The average whooping signal frequency taken from all whooping signals in the UK data set was found to be 320 (± 30) Hz, approximately 17% lower than the average value of 380Hz obtained from the French data set.

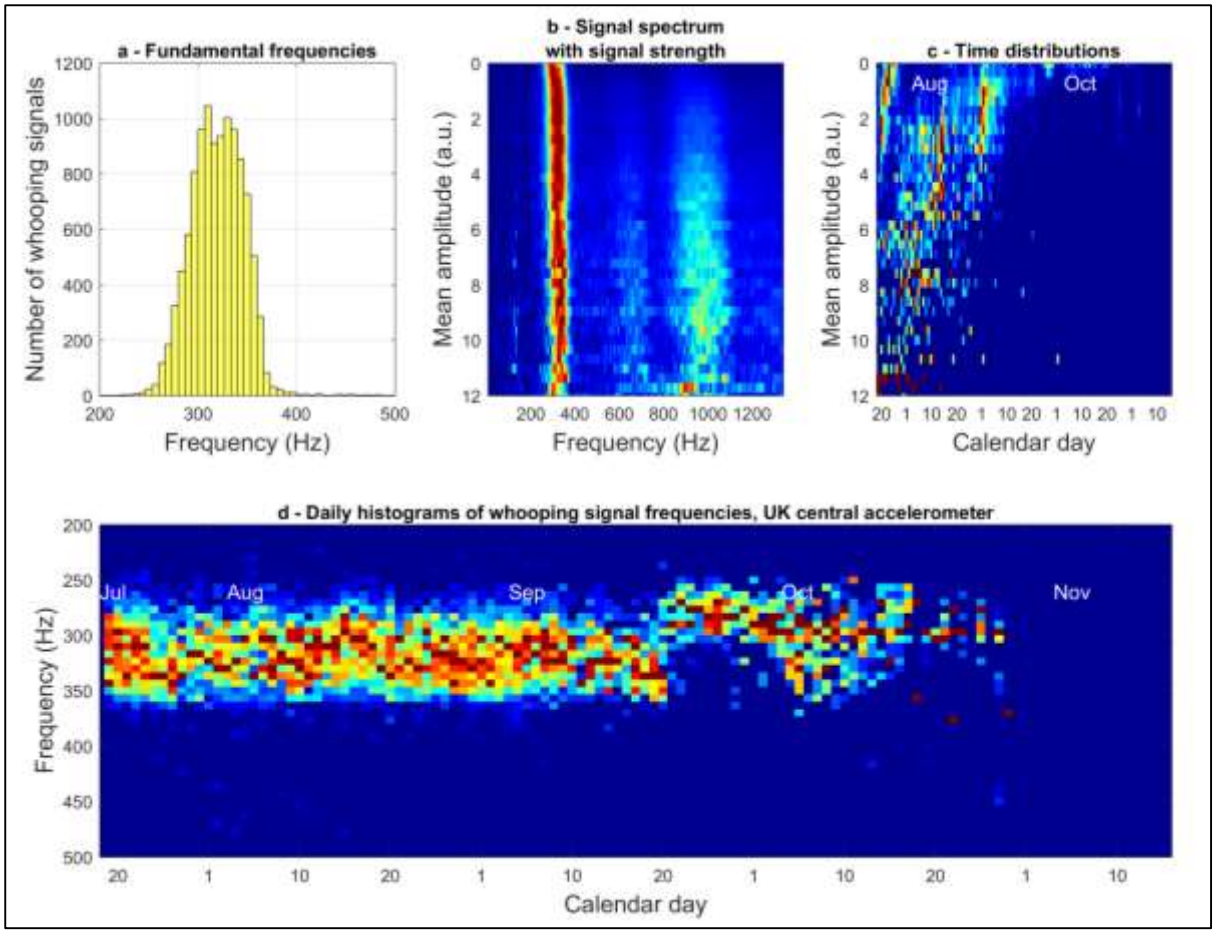

Figure W24. Statistics of whooping signals from the central accelerometer within the UK hive.

The data shown here for the UK hive's central accelerometer has been processed identically to that of the French hive's central accelerometer in Figure W13.

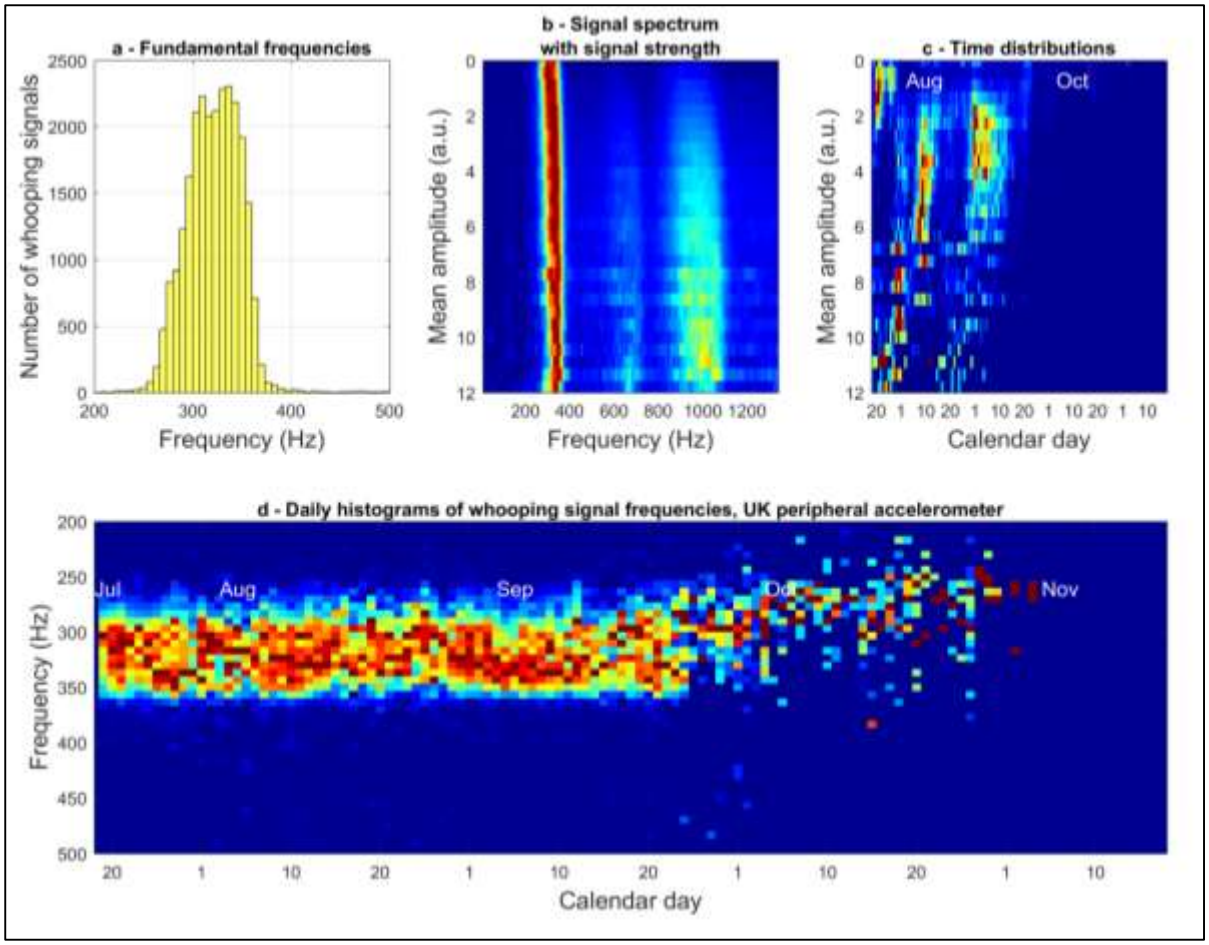

Figure W25. Statistics of whooping signals from the peripheral accelerometer within the UK hive.

The data shown here for the UK hive's peripheral accelerometer has been processed identically to that of the French hive's peripheral accelerometer in Figure W13.

Figure W24.a shows that on the central accelerometer, the distribution of fundamental frequencies is approximately Gaussian with the majority of signals occurring between 250 and 370Hz. Relatively few (less than 5%) signals occur at less than 250Hz, or above 380Hz as seen in the French dataset. This is confirmed in W24.d and W25.d, showing that the majority of signals occurring on a daily basis occurs between 280 and 360Hz. As seen in the analysis of French statistics, there is no effect of time/season on peak frequency (Central: R^2*=0.0000222, p<0.001;* Peripheral: R^2*= 0.00217, p<0.001)* across either channel (Figure W24.b and W25.b) providing further evidence that it holds stable throughout the active months. However, a pronounced drop of the frequency towards the end of September / early

October is present that is also apparent in Figure W24. Figure W24.c also shows evidence of the return of whooping signals in late October on the central accelerometer that is also apparent in Figure W21. As for the French data, there appears to be a slight positive relationship between signal amplitude and frequency in the centre (Figure W24.c) and the periphery (Figure W25.c) (Central: $r = 0.1404, p < 0.001$; Peripheral: $r = 0.1775, p < 0.001$) with the louder signals exhibiting more of the upper harmonic frequencies and the amplitude shows no daily trend in either the centre (Figure W24.d) or the periphery (Figure W25.d) (*Central:* $R^2 = 0.0002, p = 0.16$; *Peripheral:* $R^2 = 0.0033, p = 0.12$).

3.4.6. Duplicated pulse detections

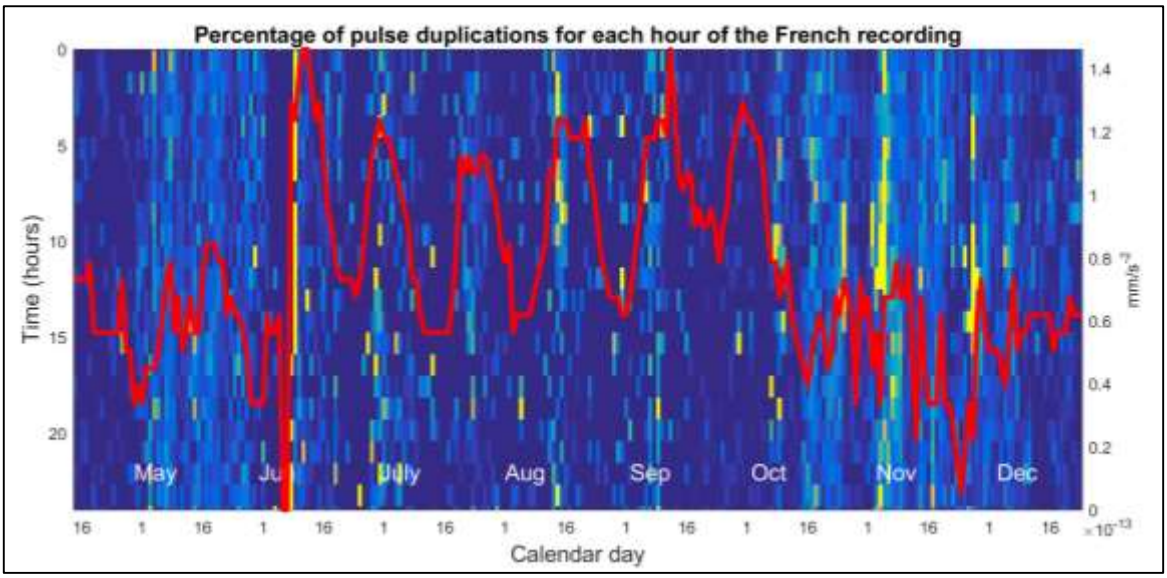

Figure W26. Time course of the percentage of duplicated pulse detections on both channels of the French dataset. Dark blue is 0% hourly duplications, yellow is 100% hourly duplications. The modal daily accelerometer signal amplitude distribution is superimposed over the top, with a black line and acceleration given on the right hand side in mm/s^2.

It was found that 6.5% of the entire collection of whooping signals that were detected on the peripheral accelerometer were also present within that of the central accelerometer. Figure W26 shows that the highest modal peak amplitude, known to follow the brood cycle in the summer season (Bencsik et al., 2015), coincides with the highest occurrences of duplications. This suggests that the boundary of each accelerometer's whooping signal detection range is right on the limit to each other, with a slight overlap at times when the honeycomb density is particularly light (e.g. after the hatching phase of the brood cycle). At 7cm apart, this would suggest a detection radius of approximately 3.5cm.

3.4.7. Channel-wise comparison of whooping signal amplitudes

Channel-wise analysis of non-duplicated pulses (Figure W27) revealed that the amplitude of whooping signals detected on the peripheral accelerometer of the French dataset *(median: 31.6 a.u; mean: 38.48 a.u; SE: +/- 0.35)* was greater than on the central accelerometer *(median: 17.8 a.u; mean: 22.5 a.u; SE: +/- 0.236)* and this was confirmed by the Wilcoxon's Signed Rank test *($Z = 48.937$, $p < 0.001$).*

Although not as pronounced as seen for the French hive in Figure W27, there is a slight increase in the amplitude of those signals detected at the periphery of the frame for the UK hive also *(median: 30.9 a.u; mean: 32.11 a.u; SE: ± 0.312)* compared to those detected at the centre *(median: 26.4 a.u; mean: 30.55 a.u; SE: ± 0.336)* and this was also confirmed by the Wilcoxon's Signed Rank test *($Z = 42.38$, $p = 0.029$).* Figures W27 and W28 both show that for both accelerometers, the whooping signals that have been detected exhibit a wide range of amplitudes from exceptionally quiet to very loud.

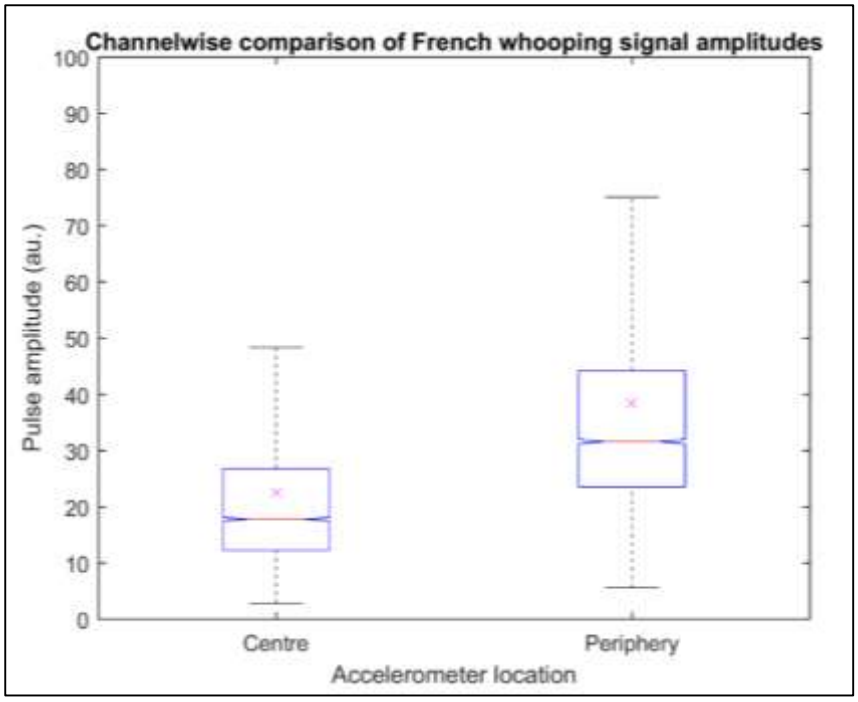

Figure W27. Comparison of the peak amplitude of all whooping signals recorded on the central and peripheral accelerometer of the French dataset. The red line denotes the median, x is the mean, and indents show the confidence intervals at 95%.

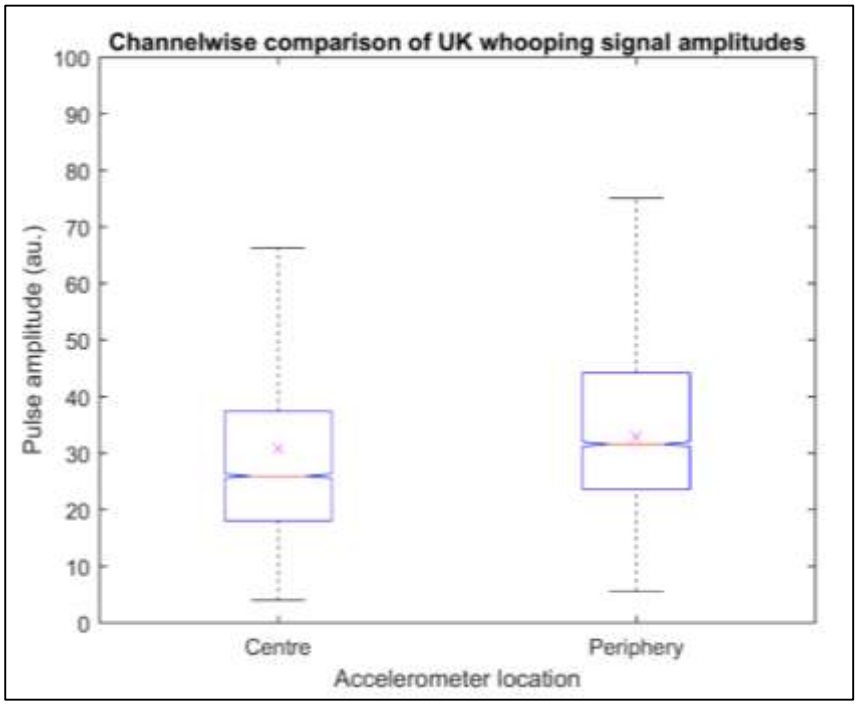

Figure W28. Comparison of the peak amplitude of all whooping signals recorded on the central and peripheral accelerometer of the UK dataset. Data is presented as in Figure W27.

3.4.7. Supporting video evidence

Video W1 and Video W2 provide evidence of bees producing whooping signals with no clear communicative motivation. Two accidental bee-to-bee collisions are shown in Video W3 and Video W10, with whooping signals elicited without measurable time lag. Video W4 and Video W5 are excerpts of recordings from both sides of a frame captured at precisely the same time; they demonstrate how often these signals can take place without any obvious matching visual phenomena (32 whooping signals in the first 30 seconds alone). A head-butting event leading to trophallaxis and a whooping signal is demonstrated in Video W8 and is slowed down in Video W9 of the Supplementary Material, with the sound track coming from an accelerometer embedded in the honeycomb under video analysis. It demonstrates a lag around 200ms between the head butting and the whooping signal.

An electromagnetic coil with a moving metal core (ZHO-1364S-36A13, ZenHen LTD., China) was secured to the brood-box of the observation hive to allow repeated mechanical knocks to be provided to the colony. The driving voltage pulse was set to nine volts and knocks were provided every second. Whooping signals are elicited en masse, with a distinct similar lag (200 ms) between stimulus and response, and habituation is clearly demonstrated with a substantial reduction of the bee response after the second stimulus, in Video W6.

3.5.0. Discussion

3.5.1. Whooping signal commonness and its implications

Never seen in any previous study, the most striking outcome of this work is the very high level of occurrences that these pulses exhibit within the detection range (approximately 3.5cm) of the accelerometers: up to 10 times per minute over both sensors (which monitor approximately $4r^2\pi$= 153cm^2, i.e. 1% of the hive's total honeycomb surface area, 2x10x35x21 cm^2), that can be extrapolated to a potential of 960 per minute over the whole colony, not counting bees in the super(s). This has strong implications that there is more to this pulse than *exclusively* being a waggle dance inhibitor. The results show that the majority of signals occur throughout the night, with a distinct decrease by 50% towards midday. During the night, no bee (and certainly no scout bee) ventures outside. Furthermore, it has been previously demonstrated that during the night, foragers enter a sleep-like state (Sauer et al., 2003; Klein et al., 2010). Therefore, it seems most implausible that at this time waggle dances would be taking place. In fact, Schneider et al. (1986a) measured the time-course of hourly waggle dance occurrences that almost shows the exact opposite trend to that shown in Figures W11 and W21. However, the observations of Schneider et al. (1986a) only took place throughout the daytime. This signal is also very frequent in the winter months when the colony is over-wintering. Again, it is most unlikely that waggle dances, or even foraging, would be taking place at this time. Furthermore, Seeley et al. (2012) suggested that this signal plays an integral role in the collective decision making during swarming. However, the figures display homogeneous results in terms of occurrence in the hours/days surrounding the primary and secondary swarms. The lack of signals throughout the day, except on days of heavy rain, also suggests that the majority of honeybee whooping signallers are older bees (i.e. foragers). In addition, I see a lack of overall correlation of hourly occurrences with rain on both datasets, but for this signal to be a waggle dance inhibitor, it is expected that I would see a negative effect of rainfall on whooping signals.

3.5.2. Whooping signal spatial distribution

The majority of trends and statistics are concordant across the two channels of the French and UK datasets, giving further confidence in the results. It suggests that activities associated with whooping signals do not alter based upon the bee's location on the comb. However, it was seen that around twice more whooping signals were observed at the periphery of the frame in both the French and UK data sets. On the UK data set, it is also seen that there is a return of whooping signals in October on the central accelerometer. It is unclear what caused this drop off in signals but the continuing of the whooping signals being recorded at the centre whilst they disappear from the periphery could be an effect of the bees gathering in a central area forming a "winter cluster" (Omholt, 1987). This phenomenon is not observed for the French dataset and this is likely due to the exceptionally mild winter season experienced in the south of France in 2015: with temperatures remarkably exceeding 20°C around Christmas, it is unlikely that a winter cluster would have formed.

3.5.3. Extensive characterisation of whooping signals

In the results of further physical characterisation of honeybee whooping signals (Figure W18), I show the average of whooping signals that occur at similar frequencies. This subsequently removes the broadening of the spectrum that occurs when a daily average is calculated (Figures W12 and W23) over whooping signals produced over the full range of possible fundamental frequencies, and showing that whooping signals exhibit very narrow Fourier peaks (coming from a perfect sinusoidal oscillation) and very well defined upper harmonics. The daily averaged spectrum of all whooping signals on the UK data set shows that throughout the more active months, the frequency of the whooping signal is very stable at around 320Hz, which is 16% lower than the 380Hz observed on the French dataset. However, both the values are fitting with Lau and Nieh (2010) who claimed that stop-signals had an average duration of 0.14s and an average fundamental frequency of 328.3 ± 58.8 Hz. Peak frequency

and daily histograms for both data sets show no other obvious trend than stated previously, further supporting the finding that the signal frequency holds stable throughout the year. Through calculation of the daily averaged spectrum, more evidence is provided showing that whooping signals decrease in terms of number and frequency from late September until the end of the data set in November. The reduction in occurrences on the UK can be attributed to the ever-declining population in the lead up to the colony failure. It is seen on the French data that whooping signals actually increase during the winter, but this may be an artefact of a decreased honeycomb mass density. This is a result of the honeycomb becoming much lighter and thus there is less attenuation of propagation waves. In this scenario, it would possibly be a result of the eating the honey stores or the cells remaining empty after the final hatching of the last brood cycle.

The apparent reduction in signal frequencies that are found during the winter months of both datasets and after the last swarm of the French data is highly robust. It appears to be occurring at times when the brood cycle is interrupted and thus the mean age of the worker population is temporarily increasing. It is therefore possible that whooping signal frequency can give an indication of the average overall age of the worker bees.

3.5.6. Modulation of measured whooping signals by honeycomb status

The frequency of the signal appears to correlate positively with its amplitude with louder signals also exhibiting more of the upper harmonics than quieter ones. Although, a minority of low frequency whooping signals also exhibit a stronger second harmonic as seen in Figure W18. The lack of trend in signal peak amplitudes over time seen over both datasets suggests that the detected amplitude of each pulse is a result of the distance between the accelerometer and the individual signalling bee. The relative amplitudes of Fourier peaks may therefore provide a means to estimate that distance.

Upon analysis of pulses detected on one channel only, it was found that the signal amplitude was significantly greater on the peripheral accelerometer. At the periphery, it has been shown that by detaching the honeycomb from the frame, honeybees are able to amplify their signals across areas not restricted by the support (Sandeman et al., 1996). In the centre of the comb, the frame load would also usually be much greater, with honey, pollen and brood being stored there (Michelsen et al., 1986b). Signals being sent in this region would therefore be more severely attenuated than those sent at the periphery (Michelsen et al., 1986b) and this is one likely explanation for the difference in the number of whooping signals detected between the two channels on both datasets. Duplicated results also give us an indication of the range of detection for each of the accelerometers. The sensors were placed 7cm apart with only 6.5% of all detected signals being duplicates. When the honeycomb is fully loaded, no duplications are found, suggesting a radius of sensitivity less than 3.5cm for each accelerometer. However, when the honeycomb is light, the low level of duplications suggests a radius of approximately 3.5cm. Whooping signals that are not delivered in-between the two accelerometers will not be duplicated, even in instances where this radius is around 3.5cm, resulting in this low duplication rate. The modal amplitude in Figure W26 is relatively stable on the central accelerometer throughout April and May. This suggests that the large increase in whooping signal detection seen between April and June is genuine and not the consequence of lower honeycomb mass density.

It is seen throughout the results that the honeycomb mass density does influence the number of detected pulses. From a daily perspective, however, over the course of 24hours, the change of the density is minimal, and so is the resulting change of the sensitivity of the accelerometer. The hourly trend in whooping signal occurrences as seen in Figure W11 for the French hive and W13 for the UK hive is therefore a genuine phenomenon and not an artefact of accelerometer sensitivity. In addition, the brood cycle has finished upon entering the winter months and thus the fluctuations in signal amplitude can be mostly attributed to the overall activity of the bees.

3.5.7. Whooping signals variations with weather

Within the French dataset, days of precipitation are actually quite rare, skewing the analysis. This could explain why, overall, rainfall had no effect on whooping signal occurrences. The decrease in whooping signals with temperature within the French data contradicts that of the UK dataset and what I was expecting: an increase in temperature would elicit an increase in activity and thus whooping signals. The days of temperatures below 5°C were uncommon over the period of data collection but the trend is not affected if this data is removed from the analysis, suggesting it is genuine. It could be suggested that there is a diurnal effect of temperature; the warmest parts of the day being when the foragers would be out of the nest and producing waggle dances, further suggesting that this signal is more than just an inhibitory signal. Humidity appeared to have a slight positive effect on the number of whooping signals in the French colony; however, no trend is seen for that of the UK. This contradiction of results between the French and UK colony may suggest that weather can affect colonies differently depending on other intrinsic or extrinsic factors. Daily and seasonal trends are in any case much more robust than trends correlating whooping signals to weather, perhaps due to the excellent ability of the honeybee to thermo-regulate within the colony.

A possibility is that the signal that I have analysed serves as a warming mechanism. This is somewhat suggested by the negative correlation between whooping signals and outside temperature in Figure W14 (however, this is disputed by the reversed trend in Figure W16 for the UK dataset), the enhanced occurrences in the winter in Figure W10 and the night time whooping signal maxima. However, closer inspection reveals that the coldest day in the year (3rd December) exhibits a decrease in occurrences, and that the high occurrences taking place in May correspond to an exceptionally mild spring (daily temperatures ranging from 15 to 28°C), whilst the coldest daily temperatures are known to usually take place at sunrise, where Figure W11 does not exhibit a maximum. This data, therefore, does not provide support for the idea that the whooping signal is also associated with warming.

The results that I am showing encompass long time durations, during which the colony status will change substantially, resulting in artefacts due to 'statistical non independence'. If data on numerous colonies simultaneously recorded was available, an interesting future study would be to do such correlation plots at specific times of the year, to somewhat remove the artefacts that presently lie within the data.

3.5.8. More than just an inhibitory signal

In the videos where whooping signals are seen because of a collision between two bees, there is no waggle dance or trophallaxis present on the frame under investigation. A measurable time lag around 200ms often separates the collision from the vibrational pulse although there are instances without any measurable lag.

Evidence of time-lag between a stimulus and a whooping signal features within my work, suggesting that whooping signals increase at times when honeybee density increases within the hive when members of the foraging caste would be considered to be in a state of rest, i.e. at night, in winter and at times of heavy rain. This would lead to a greater potential for surprise collisions to occur within the more crowded, less-sensitised hive. Additionally, it must be noted that a colony consists of upwards of 40,000 individuals hanging on a vertical plane, always at risk of falling, particularly if they are disturbed by a surprise stimulus, such as a knock or a collision with another bee.

In the majority of cases, numerous instances of whooping signals can be logged without any visual evidence of any specific phenomenon taking place on the honeycomb (see Videos W4 and W5). In other instances, all observations reveal whooping signals as a startle response or linked with trophallaxis, usually with a measurable reaction time around 200ms. Whooping signals elicited en masse as a startle response can sometimes also be demonstrated without any sophisticated equipment, when collecting a swarm into a cardboard box and leaving it undisturbed for

approximately 20 minutes. When lifting the box, beekeepers will be familiar with the distinct 'whoop' sound emanating from the box, acting as a speaker membrane.

This in combination with statistical trends, leads us to the proposition that this pulse cannot be *exclusively* be limited to the definition of 'stop signal' but can be detected under many different circumstances with the addition of being a startle response to an unexpected stimulus. Following this suggestion, signal occurrences may therefore reveal a mixture of bee density, overall colony agitation, and inhibitory or trophallaxis request head-butting events.

Further work would be to investigate this pulse when it is associated with a startle response. It will require accelerometer measurements where I artificially startle bees within the proximity of the sensor within an observation hive. I will be able to quantitate the extent to which a bee becomes habituated to the startle stimulus. When applied to the entire colony, e.g. at a random time of the day to avoid conditioning, it will be possible to assess the extent to which the response changes on the long term, providing an indicator of the status of the central nervous system of the average worker of a colony, similar to what is presently done in humans and mammals.

To conclude, the results of this study show that this pulse occurs within a variety of contexts, which in turn acts to unify all previous author's results. In future work, authors should therefore exercise caution in assigning specific interpretations.

3.6.0. Supporting Information

Video W1. The video shows one frame of the observation hive, with two accelerometers embedded in the honeycomb. The accelerometer closest to the event of interest (the left hand side one) output was fed into the video recorder, providing the mono sound track of the footage. The coaxial cable of the accelerometer can be seen. The window highlighted with a white rectangle is scaled up on the right of the image, below the spectrogram of the accelerometer track. The video shows a bee producing two successive rapid wing movements in perfect synchrony with detected whooping signal vibrations. No direct communication with another bee can be seen.

Video W2. The video (with the same set up as Video W1 for video and audio) shows a bee closing its wings in perfect synchrony with the detection of a whooping signal. No direct communication with another bee can be seen.

Video W3. The same set up as for Video W1 showing an accidental collision between a falling bee and another one on the frame, generating a whooping signal that is synchronous with the event. Note that a louder whooping signal can be heard immediately before the collision, coming from an event not identified on the frame under investigation.

Video W4. The video (with the same set up as Video W1 for video and audio) shows one side of the frame (I film both sides simultaneously) and is a demonstration of how often these whooping signals can naturally occur within the vicinity of the accelerometers without any corresponding visually evident bee activity/interaction. Throughout the first 30 seconds alone, 32 whooping signals are recorded without any corresponding visually matching evidence or phenomena that I can see. The audio is stereo with the left side accelerometer corresponding to left channel and the right side accelerometer to the right channel.

Video W5. The video is a simultaneous recording of the other side of the frame in Video W4. The audio has been inverted to match the channel to the corresponding side.

Video W6. The video shows the set up with the observation hive. The spectrograms of each uniaxial accelerometer output are shown. The broodbox is stimulated with an electromagnetic coil with a moving inner metal part, secured to the side of the broodbox as shown in Figure W28, with a 9 Volts pulse, once every second. The whooping signals elicited en masse are clearly heard and seen on the spectrograms, with decreasing response as the stimulus is repeated, and a distinct time lag around 200 ms between stimulus and honeybee response.

Figure W28. Electromagnetic coil secured laterally to the brood box of the observation hive.

Video W7. This video displays the accelerometer waveforms (blue/ orange for left/ right channel) that can also be heard in the audio. The corresponding spectrograms of a random selection of 245 whooping signals detected by the software are also shown (bottom).

Video W8. A video, with the same set up as Video W1 for video and audio, where a collision between two bees is clearly seen, followed by a whooping signal, followed by trophallaxis.

Video W9. The same video as Video W8 is provided, with a frame rate decreased from 50 to 15 frames per second.

Video W10. The video shows one frame of a different observation hive, in 2015, with a single tri-axial accelerometer that measures acceleration along its X (into the comb, perpendicular to the plane of the honeycomb face), Y (horizontally across the plane of the comb) and Z-axis (horizontally along the plane of the comb) that was embedded in the centre of the honeycomb. As the Z-axis data revealed little information, only the accelerometer x and y outputs were fed into the video recorder, providing the stereo sound track of the footage. The protruding accelerometer can be seen. The spectrograms x and y output are shown. An accidental collision is clearly seen, in near perfect synchrony with a whooping signal.

Audio W1. This is an hour-long accelerometer recording from the heart of the honeybee hive in Jarnioux, France. The track was recorded on the 12th May 2015 between midnight and 1am, and is a whooping signal hotspot as identified by Figure 3. This particular track was chosen because it allows the reader, by critical listening, to (1) appreciate how often this signal occurs naturally, (2) further demonstrate that the hotspots are genuine, and (3) hear how different whooping signals are compared to the other various signals that can be heard on the track, including queen toots.

Audio W2. Some of the worker pipes identified and displayed in Appendix 6. Some of the detected timings were used to extract a short excerpt of recording, and these were concatenated one after the other to produce this file.

Chapter 4: Extensive Vibrational Characterisation and Long-Term monitoring of honeybee Dorso-Ventral Abdominal Shaking signals

In this chapter, I explore the physical characteristics of the honeybee dorso-ventral abdominal shaking signal, a probably intentional signal the vibrational properties of which have never been explored. Using the information obtained from this characterisation, supported by additional supporting video analysis from my observation hive, novel methods are shown that allows for the automated detection of this signal and the subsequent analysis of long-term trends within continuous accelerometer datasets.

This chapter follows the same structure as the previous one on whooping signals; however, the results are shown and discussed for three hives. As with the previous chapter, there are a number of accompanying videos and audio excerpts that can be found on the supplied DVD.

Figures as well as supporting videos and audio corresponding to this chapter are categorised with the letter "D", as in "*Figure D1…*" for example.

4.0.1. Abstract

The dorso-ventral abdominal shaking (DVA) signal is a very common honeybee signal with the most widely accepted interpretation as having the modulatory function: “prepare for greater activity”. In this chapter, using ultra-sensitive accelerometer technology embedded in the honeycomb, I visually confirm the one-to-one relationship between a DVAV signal being produced and the resulting accelerometer waveform, allowing the measurement of DVAV signals without relying on any visual inspection. I then demonstrate a novel method for the continuous in-situ non-invasive automated monitoring of this honeybee signal, not previously known to induce any vibration into the honeycomb, and most often inaudible to human hearing. A total of three hives were monitored in the UK and France, showing that the signal is very common, highly repeatable and occurs more frequently at night, exhibiting a distinct decrease in instances and increase in amplitude towards mid-afternoon. I also show an unprecedented increase in the cumulative amplitude of DVAV signals occurring in the hours preceding and following a primary swarm. It is concluded that DVAV signals may have additional functions beyond solely being a foraging activation signal, and that the amplitude of the signal might be indicative of the switching of its purpose.

4.1.0. Introduction

Unlike the work in the previous chapter and that of Bencsik et al. (2011), which focussed on the long-term monitoring of potentially unintentional signals that occurred within a honeybee hive, I here provide a breakthrough in the long-term monitoring of a signal that is highly meaningful to honeybees (see Section 1.4 for more information), which may provide an indirect assessment of the status of the honeycomb, specific information on health disorders and may indicate the colony's intention to swarm.

4.1.1. Aims

As with the previous chapter, the outcomes of this extensive monitoring will allow the discussion of results (1) in terms of any evidence of long-term trends; (2) in the context of the colony status; (3) measured from multiple colonies in the UK and France, one of which features a primary swarm and two secondary swarms, one that failed in November and one that was measured at the periphery of a colony that superseded its queen. Should previous work be accurate in their findings, this analysis of daily and long-term statistics should reveal that (1) more signals are produced in the morning with a decrease towards the afternoon; (2) more signals are produced in the spring and summer as opposed to the winter; and (3) more signals are recorded at times when more foragers will be in the hive, at night and during times of heavy rain, for example.

4.2.0. Methods

No ethical approval was required as this study wholly focussed on the in-situ, non-invasive acquisition of data from colonies of invertebrates.

4.2.1. Continuous Recording of vibrational data

The configuration of the hardware involved for the continuous recording of the vibrational data set was identical to that used in the previous chapter for the detection of honeybee whooping signals (Section 3.2.0.). The accelerometers in this study were calibrated using an Aim-TTi TG5011A 50MHz Function Generator to drive 50mV directly into the sound card.

Three hives were monitored as part of this study. The first named the "French 2015 hive", is the same vibrational dataset as used for the "French hive" in Chapter 3. It was continuously monitored from 16th April 2015 until 26th December 2015 with two accelerometers vertically aligned, disclosing the evolution of a colony across the entire active season. This colony swarmed three times within the first month of the dataset on the 21st April, 1st May and 6th May 2015.

The second hive is named the "Clifton Observation hive" as it was located on the Clifton campus of Nottingham Trent University, UK. This hive was used to collect all of the video recordings as part of this study. It was continuously monitored (and is still monitored today) starting on the 24th May 2016 with two accelerometers aligned across a central horizontal line 11cm from each other and the surrounding wooden frame. This frame was at the periphery of the colony until it moved to its centre after April 2017. This colony was also found to have superseded their queen in June 2017.

Finally, the "French 2017 hive" was located at the same apiary in Jarnioux, France as the "French 2015 hive". It was monitored from 15th April 2017 until 28th November 2017. It was recorded using a single accelerometer placed at the centre of the middle frame of the colony. This colony did not swarm and died at the end of the 2017 active season.

4.2.2. Video recordings

For the collection of video data, the same observation hive was used as in the previous chapter and its contributing long-term dataset is referred to as the "Clifton Observation hive" throughout this chapter. The camera arrangement was identical to that of the previous chapter with both cameras recording in 1080p definition at 50fps. This framerate, at well above twice the frequency of a normal DVA signal, was a minimum requirement to be free from Nyquist ghosting (Lyons, 2004). To allow the bees to experience conditions as natural as possible, no more than two 10 to 20 minute recordings were conducted each week. During all other times, the bees experienced the same conditions that they would within a normal dark honeybee hive. This allowed this colony and the observation frame to develop naturally without the major disturbances usually associated with observation hives with static frames, where bees are forced to live in a planar geometry. Some excerpts of these videos have been included to support some of the claims and aid in the discussion of the statistics of these signals generated as part of this study as accelerometer traces usually provide very poor (if any) audible evidence of DVA signals (in great contrast to whooping signals). Video recordings were therefore essential to validate many of the claims of this chapter.

4.2.3. Vibrational quantitation of DVA signals

Within the extensive collection of video recordings gathered as part of this thesis, two honeybees were captured upon the focal frame of the Clifton Observation hive producing DVA signals with clearly audible traces, one directly onto the accelerometer and one on the other side of the frame. This was significant because due to the way the accelerometer is secured, it is not sandwiched exactly in the middle of the frame, rather it protrudes from one side. These are presented in Videos D1 and D2, respectively, and provide an interesting comparison between the properties of DVA signals delivered on opposite sides of the accelerometer. Using a home-built MATLAB® (The Mathworks, USA) program, the waveforms were extracted from the dataset. The acceleration waveform was calibrated into m/s^2

and the time course was cropped around the signals for careful further examination. The pulses were split into ultra-short windows of equal length, so that a single abdominal knock resided in each. These windows were horizontally stacked and shown as an image with the pixel intensity representing the acceleration. This is shown in synchrony with the DVA signal directly onto the accelerometer in Video D1 and on the other side of the frame in Video D2. The knocks were then further aligned in time relative to the position of their peak and then averaged to display the time course of the acceleration of an averaged abdominal knock.

Even when the honeybee delivers a DVA signal directly onto the accelerometer, the amplitude of the corresponding waveform is relatively low compared with the overall amplitude of the complex waveform resulting from the hundreds of other honeybees residing within the close vicinity of the sensor. Owing to this, the power spectrum of the acceleration of a DVA signal waveform reveals little or very poor quality information. Due to the regularity of the periodicity of the timings and the shape of the knocks, however, the 2-dimensional Fourier transform (2D-FT), which computes the frequency of repeating power spectra over a set time period (see Section 1.5.2.iii), is much more successful in highlighting very interesting features and is displayed as a colour plot (see Figure D4). 2D-FT analysis is also shown in synchrony with the DVA signal delivered directly onto the accelerometer in Video D1 and on the other side of the frame in Video D2.

A collection of 27 DVA signal waveforms was extracted from various vibrational datasets in the UK and France, and were each given an ID based upon the time and date at which they occurred. The waveforms were each analysed by the methods above, and they were carefully studied to highlight features unique and common to all DVA signals that can be later utilised within a supervised clustering algorithm to best distinguish DVAs from other pulsed signals in a long-term scan of a colony's vibrational log. The results of the physical quantitation of these pulses can be found in Video D3, displayed with their corresponding acceleration traces supplied as the soundtrack of the audio.

4.2.4. Visual detection

From visual and auditory inspection of the extensive collection of video recordings, it is apparent that the detection of an audible DVA signal trace is entirely restricted to those instances where a honeybee delivers it in the immediate vicinity of the accelerometer (up to 2 to 3 cm away from it), and directly onto the honeycomb rather than onto a fellow honeybee. Using the video data obtained from the observation hive across the 2016 and 2017 seasons, a grid was superimposed over the honeycomb within the footage (see Video D4) in order to facilitate the recording of the coordinates at which each DVA signal occurred. These were then plotted along with the mean and the median of the collection of coordinates to show the spatial distribution of DVA signals occurring over the honeycomb. All of the videos used in this analysis of spatial co-ordinates were recorded between 11am and 1pm.

4.2.5. Long-term automated scan

4.2.5.i. Detection software overview

Software was written in MATLAB® and algorithms were optimised to detect and record the times at which DVA signals occurred within the vibrational data sets. The optimised DVA signal detection is a two-stage discrimination process. In the first pass, the software uploads 2-minutes of data from the file, creates a one-second long window that moves along the data sample by one tenth of a second in each iteration. The waveform within the window is discriminated into ‘DVA signals’ and 'non-DVA signals’ by simple discriminant function analysis on the 2D-FT (2-dimensional Fourier transform) of the waveform under scrutiny. Analysis of the 2D-FT in combination with some critical listening to the pulses detected in this way revealed instances of single vibrational “knocks” unfortunately being occasionally erroneously identified as a DVA signal. In the second pass, the waveform detected as a DVA signal is further verified using a second test optimised to check the periodicity of the knocks in addition to the information provided for each pulse by calculating the gradient of its acceleration waveform. Once the end of the sample is reached, the software moves on to the next two minutes

until the entire dataset has been scanned. Such a scan of one month of recorded data typically requires around 12hours of computer processing. When datasets consisting of the timings that honeybee DVA signals occurred within each vibrational recording are constructed, quantitative statistics of their occurrences over the entire seasons be showcased.

4.2.5.ii. Principal Component and Discriminant Function Analysis to discriminate between true and falsely detected DVA signals

The first pass.

For the purposes of the vibrational pulse detections required in this study, individual one-second-long accelerometer waveforms were categorised as being a member of one of three distinct categories: "DVA signals", "Worker Pipes" and a third category called "Noise" that contained spurious high-amplitude sharp-peaked signals. A 'training database' for discrimination was constructed using 150 examples of signals, of varying SNR, extracted from the French 2015 dataset, that were deemed to be highly representative of each category. Each pulse waveform was separately uploaded into the software prior to being manually centred within the one-second long window through visual analysis of the position of each waveform. Each pulse underwent processing whereby the sampling rate was coarsened by a factor 3 in order to reduce the specificity of the individual pulses in the training database. The 2D-FT frequencies were cropped vertically and horizontally respectively to 1500 and 70 Hz, data ranges shown to contain the information that is most relevant to DVA signals. The overall amplitude of the resulting cropped 2D-FT was then normalised to one in order to try to detect weak DVA signals equally as well as strong ones. The data was then reshaped to create a linear array which could later be fed into the PCA/DFA algorithm (for further information see Bencsik, et al. 2015) to identify the features of the signal waveforms that are unique to each category.

The pulse categories were carefully labelled within the training database and their PCA scores calculated. By using a pair of cross correlation products with two discriminant functions identified by

the DFA algorithm, two discriminant function coordinates, or 'DF scores', could then be calculated for each pulse in the training database. The centroid coordinates for each group were further calculated. To determine whether a given pulse belonged to the DVA signal category, the ratio of distances between the individual pulse and the DVA signal centroid to the sum of the distances of the pulse to the centroids of the other groups was calculated. From this, a threshold value was determined for categorisation depending on how close the pulse resided to the centroid of the DVA signal group in the DF space. The optimum threshold was that which had the lowest percentage error based on how many points from each cluster overlapped with the DVA cluster. The best threshold gave an error rate smaller than 1.4%.

The maximum number of meaningful PCA scores used in the discrimination phase was carefully set by avoiding too much numerical noise being fed into the search (Bisele et al., 2017). This was monitored by displaying the amount of variance that each PCA score accounted for ranked from highest to lowest. To reduce the possibility of over-fitting, an iteration procedure similar to that of Bisele et al., (2017) was also implemented whereby every pulse combination was explored within the training database, removing all pulses except for the collection allowing for clustering with the lowest error. However, pulses removed from the training database that were not included within the computer training stage, were still involved within the clustering process to find their co-ordinates within the DF space (Figure D1).

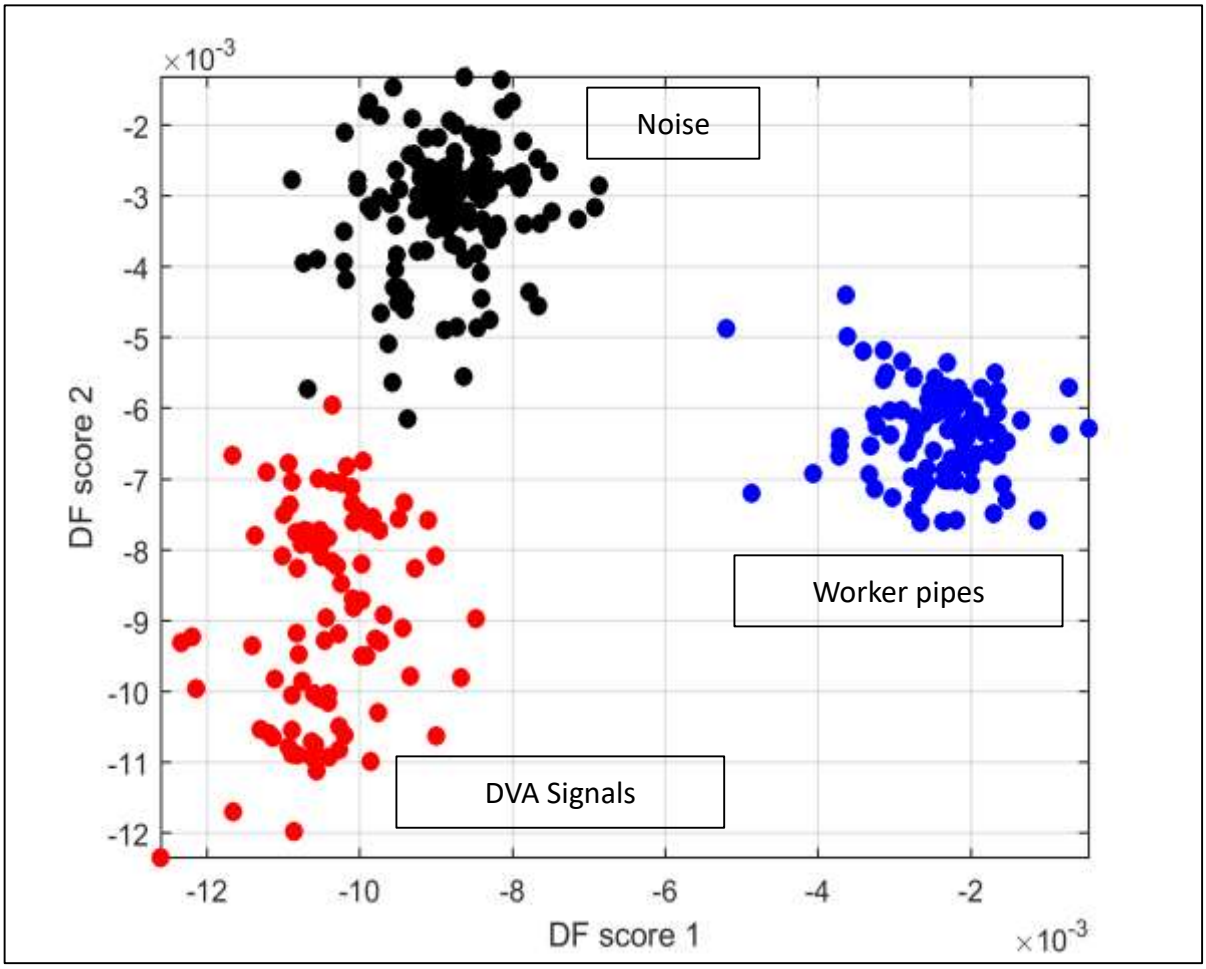

Figure D1. The outcome of the supervised clustering of the groups previously identified as "DVA signals" (red cloud), "worker piping" (blue clouds) and "noise" (black cloud) for discrimination, shown in two-dimensional DF space. The overlap is negligible and below 1.4 %.

The second pass.

To discriminate true DVA signals from those one-second-long accelerometer waveforms comprising of high-amplitude spurious sharp peaks, a protocol similar to the first pass algorithm was implemented with additional information to that used in the first pass. A common source of wrongly detected signals came from high-amplitude "clicking" within the dataset, originating from sources such as a honeybee "working" on the wax honeycomb (as seen in Video B1) probably by using its mandibles. When comparing the averaged DVA knock (as described below in Figure D5d) to the individual clicks in Figure D2 extracted from the raw accelerometer audio of Video B1, it is easy to see how the software misidentified these signals in the first pass. The honeycomb does appear to react in a very similar way

during honeybee wax cutting or when receiving a DVA signal, however a rapid oscillation, which was first identified in Chapter 2, is present at the start of each click waveform that is of low amplitude and high frequency. Highlighted in red in Figure D2, this is probably caused by the honeybee as it grips the honeycomb with its mandibles before pulling at the wax. This feature provides a rapid oscillation with sharp inflection points. Whilst the magnitude of this is relatively low, the slope of the individual spikes is relatively high. This additional information was exploited by computing the gradient of the acceleration to help the software to discriminate between DVA signals and clicks. In addition to the computation of the 2D-FT, as in the first pass, the spectrum of the gradient of the acceleration of the digital signal waveform that had been coarsened by a factor 3, cropped to 1500Hz, normalised to its mean amplitude and finally underwent log transformation was calculated. This information was then reshaped into a linear array and fed into the training database. Optimisation was then achieved by the same methods as for the first pass. The coordinates of the cluster's centroids was then computed which allowed identification of the best threshold for characterisation as a true DVA signal or a spurious signal (Figure D3). The threshold for pulse classification as a DVA signal was determined by establishing the maximum radius from the DVA signal centroid that allowed for the lowest overlap between clusters.

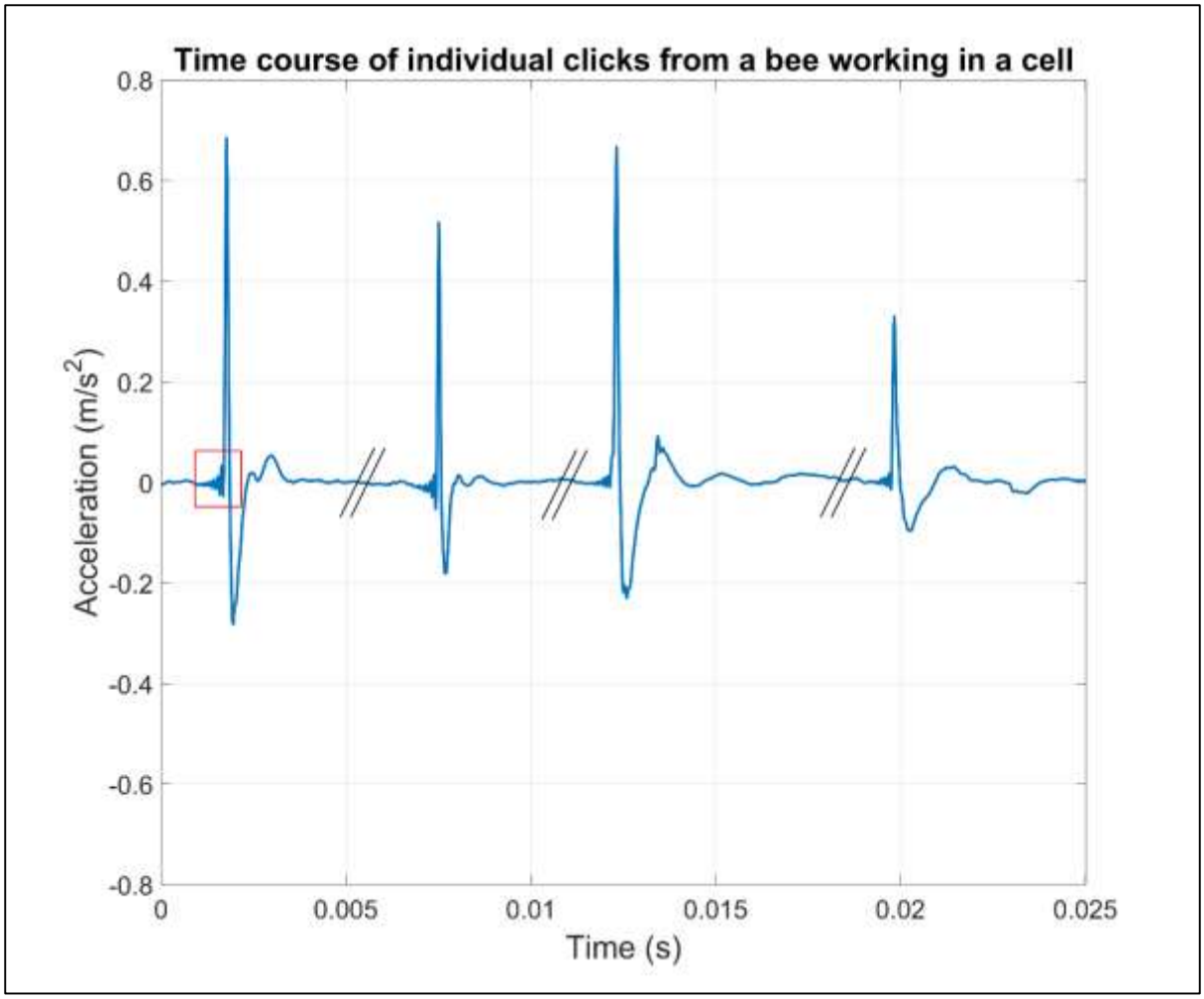

Figure D2. The time course (s) of acceleration (m/s^2) of four individual high-amplitude clicks of similar magnitude that were extracted and concatenated from the calibrated accelerometer data associated with footage of an emerged bee working in a cell (see Video B1). The symbol // shows the point at which the individual clicks were concatenated. The red box highlights a feature to this type of signal that potentially separates it from DVA signals.

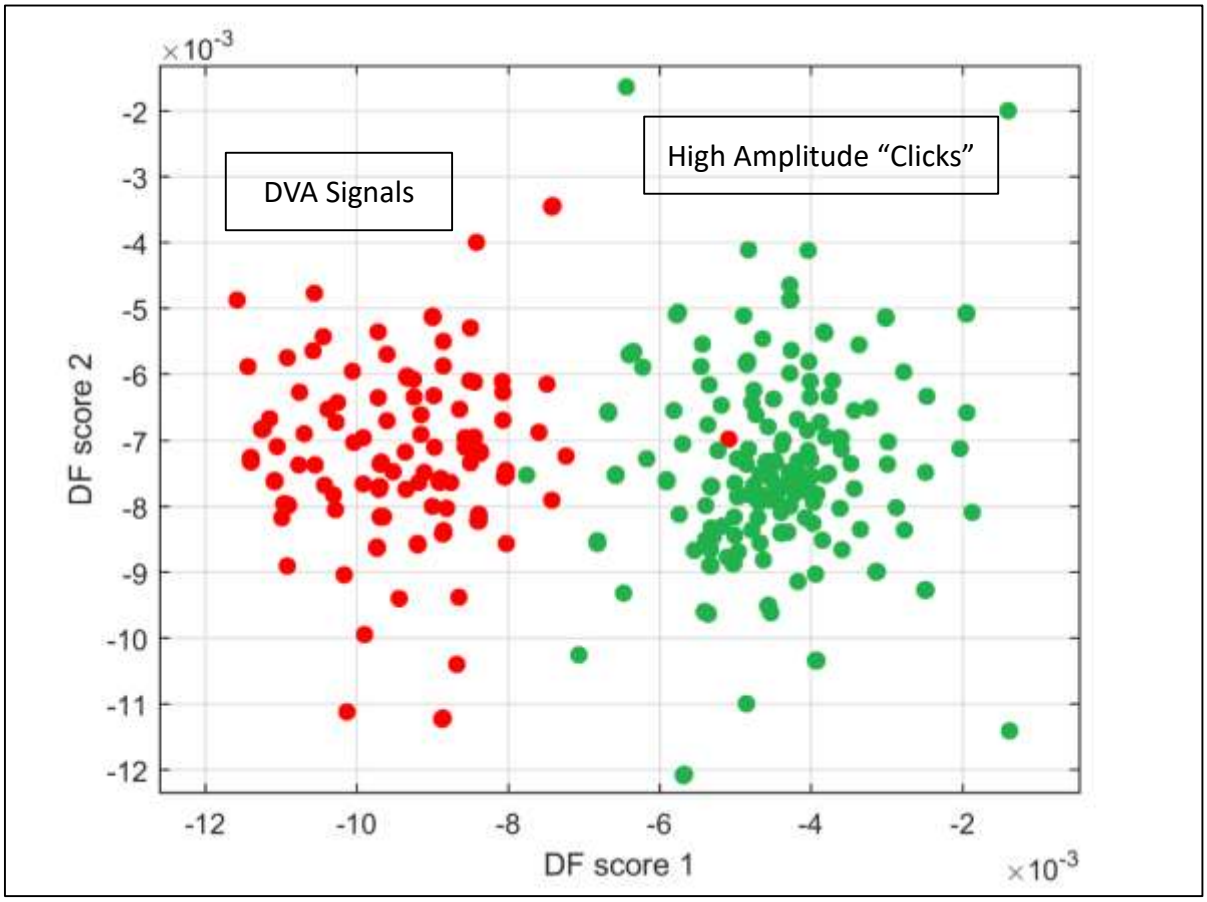

Figure D3. The outcome of the supervised clustering of the groups previously identified as “DVA signals” (red cloud), and “high amplitude clicks” (green cloud) for discrimination, shown in two-dimensional DF space.

The overlap is negligible at below 1 %.

4.2.5.iii. Validation of the detection software.

Extensive analysis of DVA signals captured on video that is synchronised with accelerometer audio showed that critical listening usually fails at identifying a clear audible DVA signals. The validity of the automated detections of DVA signals was therefore examined by applying the detection software to scan the raw vibrational accelerometer data associated with the entire collection of video footage, cumulating a total time duration of eight-hours. The list of detections were checked against the corresponding DVA signals that were visually detected within the footage and the results of this analysis is shown in Table 3. The percentage error of “false positives” (spurious pulses that were detected as DVA signals by the software) was around 17%, giving an overall true DVA detection rate

of 83%. The parameter values of the 2D-FT images used in the training database, such as signal bandwidth, pulse duration and spectral resolution, as well as the best threshold for pulse classification as a DVA signal, were optimised by an iterative process that explored the combination of different values for each until the maximum number and percentage of true positive DVA signal detections was achieved for the accelerometer data associated with each video footage. For results obtained with optimum parameter values see section 4.3.3. Following this, over 600 randomly selected DVA signals were extracted from the raw data and the 2D-FT was computed and displayed for each to ensure they produced vertical broad bands between 14 and 25 Hz. To further demonstrate the sensitivity the 2D-FT for the detection of DVA signals, the 2D-FT of a correctly detected DVA signal that produced no audible trace has been given in Video D5. Specific one-hour long sections of data where hot spots in the number of occurrences found were also critically listened to, in addition to the visual inspection of the pulses' 2D-FT, and indeed revealed highly frequent DVA signals, as demonstrated in Audio D1, which presents a large collection of DVA signals that were detected by the software in the half an hour preceding and following the primary swarm that took place at 2pm on the 21st April 2015, and concatenated into a three minute audio file.

Upon completion of the validation of the detection software, it was set to run over the duration of each of the three long-term datasets described in Section 4.2.1.i. Histograms showing the hourly number of DVA signals that occurred within the dataset was computed for each day and were displayed vertically, with the day under investigation appearing on the horizontal axis. The logarithm of the number of hourly occurrences is denoted by the pixel intensity of the colour plot.

4.2.6. Long-term signal parameter analysis

All data analysis, statistical and graphical, was undertaken in MATLAB® with occasional use of the statistics toolbox. All data was tested for normality using the Kolmogorov-Smirnov test and in some instances, normalisation is undertaken using Log10 transformation. When normal distribution could

not be achieved, the non-parametric equivalent test was used. The signals were checked for any duplications, as this would suggest that a local DVA had not been detected, rather something of much higher amplitude occurring on the honeycomb. No duplications were ever detected because of the close proximity essential for their detection.

4.2.7. The brood cycle and daily average

To see how the occurrences of DVA signals changed throughout the course of an average day, the number of DVA signals that occurred within each hour of the day was averaged and is shown, together with standard error in Figure D12 for the French 2015 hive data, in Figure D24 for the 2017 French hive in and Figure D30 for the Clifton Observation hive. To investigate the effect of the brood cycle, the daily modal amplitude of vibrations as a whole is explored for the French 2015 dataset. In addition, the daily average of DVA signals is also compared to the daily average of whooping signals assessed within the previous chapter.

4.2.8. Inter-signal 2DFT comparisons

To give a high quality characterisation of the average DVA signal, DVA signals that were detected by the software were ordered by decreasing amplitude and the first 150 were selected. The 2D-FT was then computed for the acceleration over the time course of signals. The mean over these signals was computed and then displayed as a colour plot with pixel intensity exhibiting the amplitude at each frequency. To showcase the unique features of the DVA signals that are emphasised by 2D-FT analysis, the averaged 2D-FT was also computed for a collection of other one-second long signals that were removed by the discrimination software. These signals included the mean of 150 worker pipes as well as 150 high-amplitude “scratches” and 150 “clicks”, having being given these names as an onomatopoeic description of their audible trace.

4.2.9. Hourly averaged 2DFT

To assess how the DVA signal parameters evolve throughout an average day, each DVA signal detected by the software across the dataset was placed into one of 24 groups depending on which hour of the day it occurred. The signals within each group were then extracted from the raw dataset, allowing a 2 second window centred on the pulse timing. Following this, the 2D-FT was calculated for each DVA signal and the background information was removed by subtracting the 2D-FT of the two seconds of data immediately following the end of the focal DVA signal. Once the hourly collections of DVA signals had been obtained, the average 2D-FT image of all pulses in each group was computed and displayed as a colour plot representing the typical DVA signal occurring for each hour of the day. To further this analysis, the average amplitude of the broad band occurring for a spectral repetition between 14 and 25Hz was averaged for frequencies between 400 and 1500Hz and placed in a scatter plot showing the average signal strength across each hour of the day with standard deviation for all datasets.

4.2.10. Daily averaged 2DFT

To assess any seasonal changes to the DVA signal parameters, all DVA signals detected by the software for each day were extracted from the raw dataset, allowing a 2 second window centred on the pulse timing. After this the 2D-FT was calculated for each DVA signal, the background information was removed by subtracting the 2D-FT of two seconds of data immediately following the end of the focal DVA signal, and then the average of all 2D-FT images was computed. This was repeated for all days within the dataset. The mean was then calculated to show the average signal at each value of the spectral repetition frequency of each day's mean 2D-FT, which was then plotted vertically in a colour plot with each day stacked horizontally in chronological order to show the evolution of the DVA signal spectral repetition across all days for all datasets.

4.2.11. The effect of weather on the occurrences of DVA signals

The French 2015 and 2017 weather data was kindly supplied free of charge by Météo France (www.metofrance.com) for the site and dates that were required. The relationship between outside temperature, outside humidity and rainfall, and the hourly occurrence of DVA signals recorded by the accelerometers was explored using a regression model. For the analysis with rainfall, linear regression was used to assess whether increased rainfall had an effect on the number of DVA signals.

The weather data is included in Supplementary Figure 1 in Appendix 7 for the 2015 season and Supplementary Figure 1 in Appendix 8 for the 2017 season. For ease of use, this figure has been formatted to match that of the hourly histogram computed from the long-term trends of DVA signal occurrences.

4.3.0. Results

4.3.1. Vibrational quantitation of DVA signals

4.3.1.i. The physical properties of a DVA signal

The physical properties of a specific DVA signal that was delivered directly onto one of the accelerometers (Video D1), where its abdomen motions parallel to the axis of the sensor in a positive direction (see Figure D7), can be found in Figure D4. For comparison between this DVA signal and one delivered on the other side of the frame (that is seen in Video D2), refer to Figure D6 and D7. The particular signal displayed in Figure D4 has a duration of 1.1 s, a fundamental frequency of 22.1 Hz and a mean peak acceleration of 0.162m/s^2 (Figure D4d). Figure D4b demonstrates the same DVA signal recording, which has been segregated into equal length windows called frames around each of the individual "knocks", revealing the characteristic "Π-shape", shown in synchrony with the pulse in Video D1, which is unique and common to all of these signals (see subplot b throughout Video D3). This graph highlights the initial increase and later decrease in the rate at which the honeybee delivers its abdominal knocks during signal production, with the longest part of the signal, in between, exhibiting a constant rate of delivery. These knocks are then aligned to each other in Figure D4c and averaged in Figure D4d to show how, following one abdominal knock, the honeycomb reacts and relaxes with typical time decays that are orders of magnitude longer than the duration of the actual bee to comb collision. There is an initial sharp burst of negative acceleration consistent with the downward movement of the honeybee's abdomen, which is followed by oscillations that gradually decrease in amplitude as the honeycomb returns to a state of equilibrium (Figure D4d). It is also apparent that the honeycomb fully reaches it equilibrium before the next abdominal knock commences (Figure D4c and d), within approximately 10ms. The bee abdominal collision in Figure D4d is well described by a Gaussian peak with amplitude 0.2 m/s^2, full width at half-maximum 0.56ms, and centred at 1.54ms. The oscillations taking place in the honeycomb immediately after the knock are well described by the sum of three exponentially decaying sinusoidal functions. The parameters of

these oscillations will change with the local honeycomb load. For this particular signal, the first component is a fast oscillation with an amplitude of 0.2 m/s^2, a frequency of 808Hz and a decay constant of 2ms (Figure D4d). The next is a mid-range oscillation with an amplitude of 0.0253 m/s^2, a frequency of 135Hz and a 2.8µs decay constant. Finally there is the third and slowest oscillation with an amplitude of 0.0266 m/s^2, a frequency of 60Hz and a 2ms decay constant. This relaxation curve gives a remarkable insight into the local natural vibrational modes of the honeycomb.

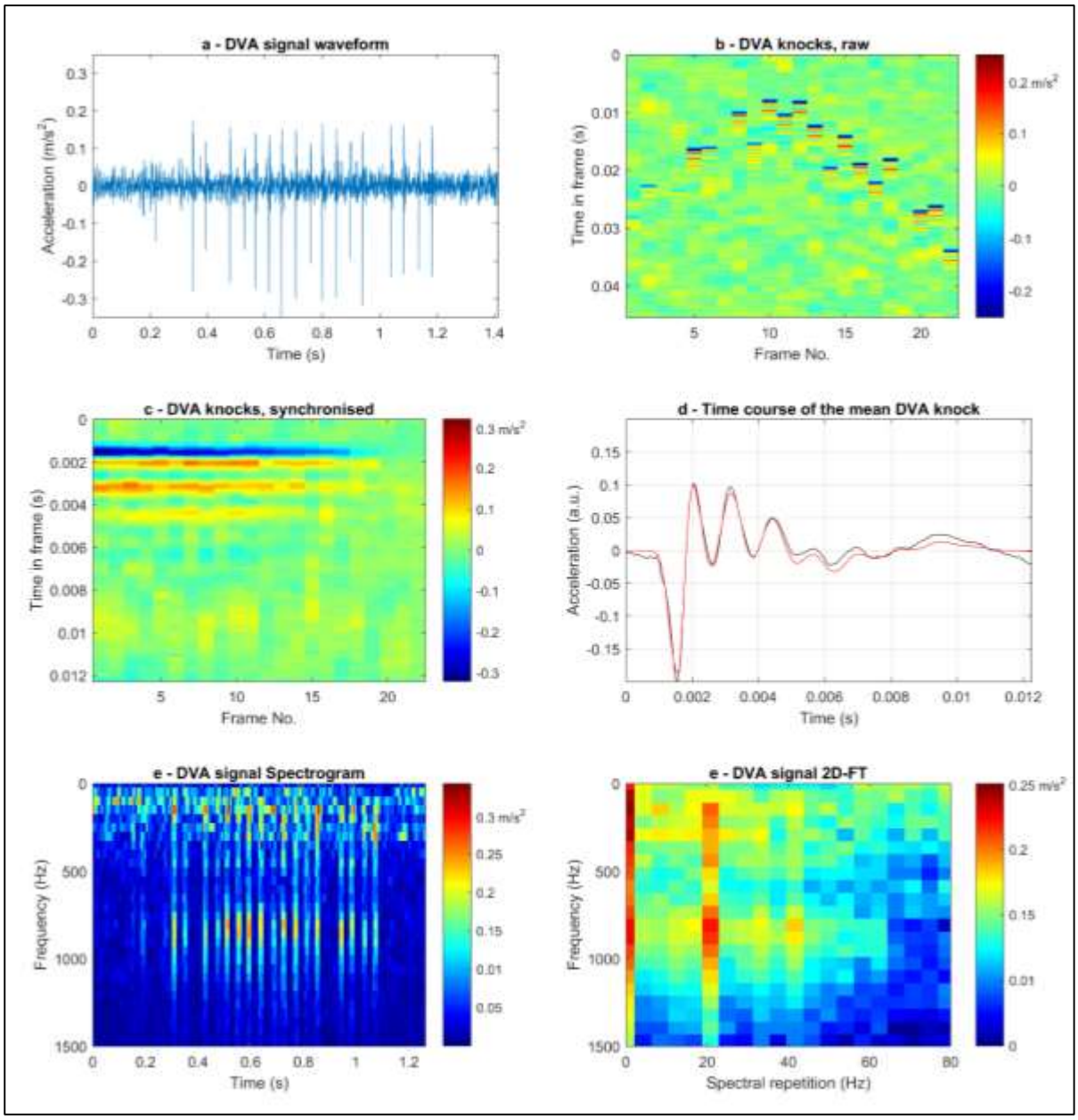

Figure D4. Vibrational properties of a DVA signal delivered onto an accelerometer. (a) Time course of honeycomb acceleration waveform during the delivery of a DVA signal; (b) The same waveform, shown in successive frames adjusted to the time gap residing between two individual abdominal-honeycomb collisions; (c) The DVA signal knocks, aligned to the first one; (d) The time course of the mean of the DVA signal knocks; (e) The spectrogram of the complex DVA waveform in (a); (f) The 2D-FT image of the complex DVA waveform in (a). The colour bar displays the linear scale amplitude in m/s^2.

In many instances, including this one, the honeycomb relaxation can be observed even on the individual knocks (Figure D4b and c), although it is much clearer on the averaged knock (Figure D4d). To see a large collection of analysed DVA signals with their corresponding audible accelerometer data, see Video D3 and the corresponding analysis in Table D1 that can be found in Section 4.3.3. (Extensive visual inspection). In Figure D5 below is the same analysis, undertaken on a commonly occurring honeybee signal from within the hive, which I call the “high-amplitude clicks” where spikes similar to those seen in DVA signals are observed. Video evidence (see Video B1) suggests that these particular clicks featured in Figure D5 are the result of a honeybee working at the bottom of an empty cell and have been extracted from the raw accelerometer data associated with Video B1 for comparison of their physical properties to the DVA signals. It can be seen in Figure D5a that the individual clicks produce high amplitude spikes of similar magnitude to the individual knocks of the DVA signal. However, as further highlighted in Figure D5b, they are sporadically distributed along the time axis and do not exhibit the characteristic Π–shape associated with DVA signals. The spectrogram in Figure D5c shows that, like a signal knock of a DVA signal, the individual clicks exhibit a broad band spectrum of frequencies. However, unlike the DVA signal where the majority of relevant information exists below 2500 Hz (Figure D4e), the broadband spectra of the clicks can extend up to 10 kHz. In addition, due to the irregularity in the distribution of the clicks within the time domain, the 2D-FT analysis (Figure D5f) shows no vertical bands at a specific spectral repetition even though in this particular example 13 clicks were recorded over 1 second (the duration of a typical DVA signal).

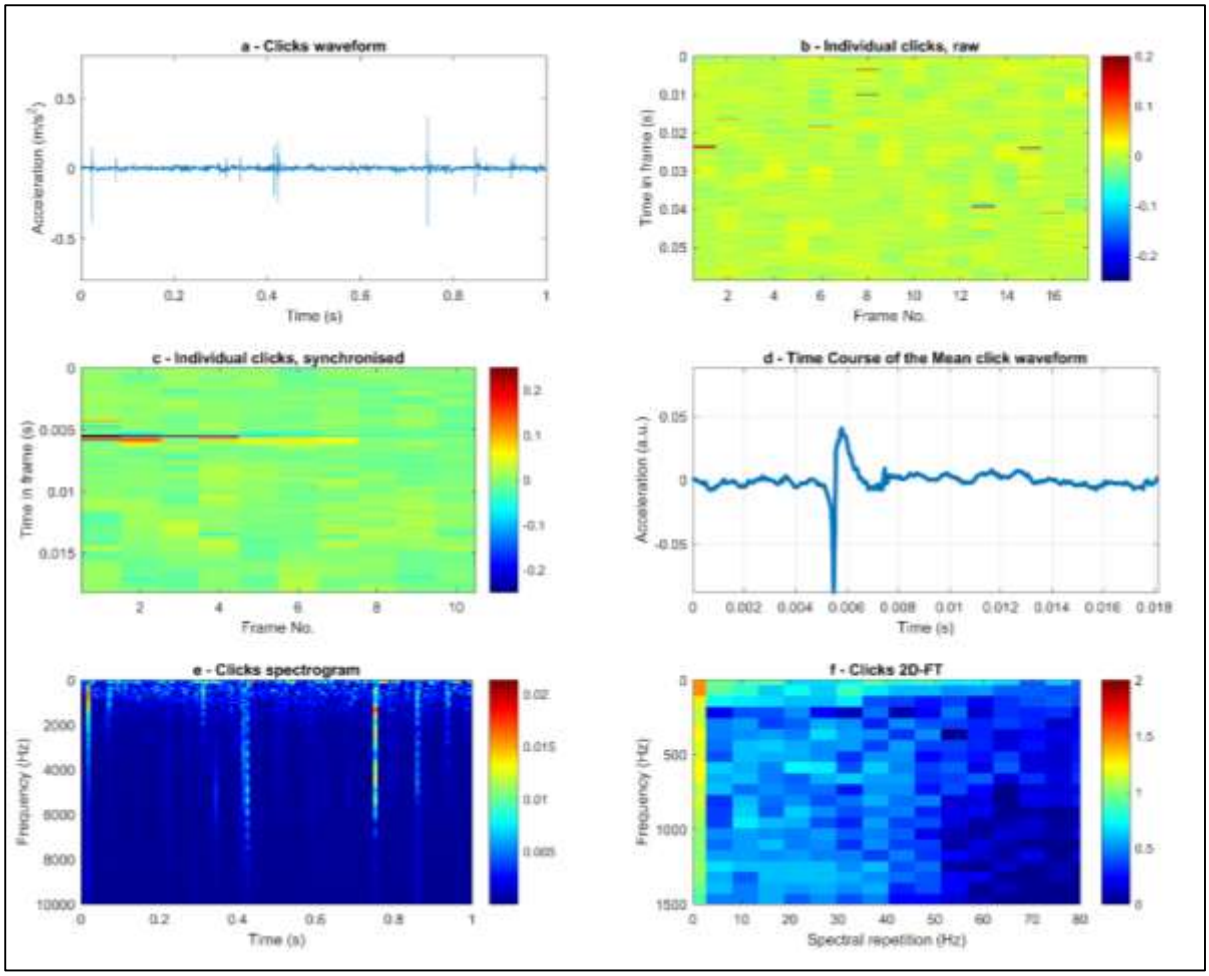

Figure D5. Vibrational properties of a series of high-amplitude clicks extracted from within the French 2015 dataset. (a) Time course of honeycomb acceleration waveform during the delivery of clicks; (b) The same waveform, shown in successive frames with the same time duration as an average DVA signal (0.06s); (c) The individual clicks, aligned to the first one; (d) The time course of the mean of the individual clicks; (e) The spectrogram of the complex waveform; (f) The 2D-FT image of the complex waveform. The colour bar displays the linear scale amplitude in m/s^2.

4.3.1.ii. DVA signal polarity

Here I show the full physical analysis of two DVA signals that were captured on video footage of the observation frame with each of them producing an audible accelerometer trace. The first (Figure D6) corresponds to D1 Video and occurred on the face of the frame with protruding accelerometers, whereby the direction that the honeybee hits the honeycomb during each knock of the signal is positive along the axis of the accelerometer. The next (Figure D8) corresponds to Video D2 and occurred on the opposite side without protruding accelerometers, being delivered whereby the abdomen of the honeybee hits the honeycomb in a negative direction along the axis of the accelerometer.

Due to the honeybee only being able to hit the honeycomb (it cannot pull on it effectively), for DVA signals that occur positively along the axis of the accelerometer (see Figure D7), the original sharp knocks are comprised of negative signal (Figure D6d) whilst the honeycomb relaxation wave is balanced around zero. However, if the signal was to occur negatively along the axis of the accelerometer, the original sharp knocks are comprised of positive signal. In both instances, again the honeycomb relaxation can be observed even on the individual knocks (Figure D6c and D8c), although it is much clearer on the averaged knock (Figure D6d and D8d). To see a large collection of analysed DVA signals with their corresponding audible accelerometer data, see Video D3. Because a honeybee is only able to push the honeycomb, it cannot effective pull it, this asymmetry within the oscillating waveform is typical of honeybee signals originally delivered as vibrations (as opposed to sounds) and is present in the waveform of most whooping signals (Ramsey, et al., 2017).

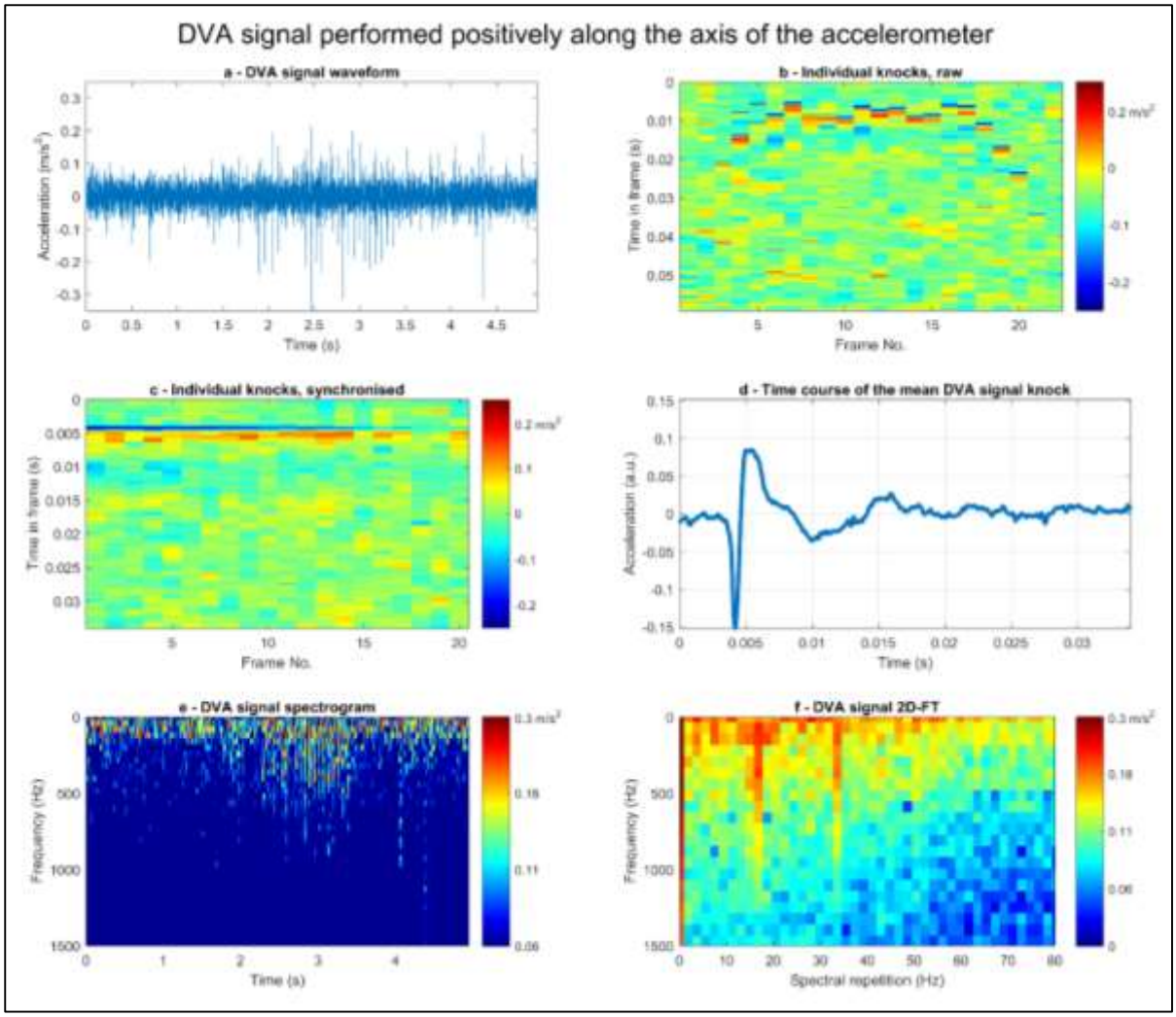

Figure D6. Vibrational properties of a DVA signal delivered onto the side of the frame with the accelerometers as seen in Video D1. (a) Time course of honeycomb acceleration waveform during the delivery of a DVA signal; (b) The same waveform, shown in successive frames adjusted to the time gap residing between two individual abdominal-honeycomb collisions; (c) The DVA signal knocks, aligned to the first one; (d) The time course of the mean of the DVA signal knocks; (e) The spectrogram of the complex DVA waveform in Figure D6a; (f) The 2D-FT image of the complex DVA waveform . The colour bar displays the linear scale amplitude in m/s^2.

In Figure D6a, I show the complex waveform of the DVA signal in Video D1 that occurred directly on top of the left accelerometer. The signal can be observed to last around one second and contains seventeen individual knocks (Figure D6b) that form the characteristic Π-shape when segregated into equal length frames around each of them. Upon averaging of the individual abdominal knocks, it can be seen that the sharp bursts of acceleration associated with DVA signals have a negative polarity as opposed to a positive polarity as in Figure D7 for the DVA signal that occurred on the other side of the

frame. Similar oscillations can be observed as in Figure D4 as the honeycomb relaxes but this is much weaker perhaps due to the increased lateral distance between the sensor and the signaller (see Figure D7). As seen for the spectrogram of the pulse in Figure D4e, Figure D6e reveals little useful information with regard to the DVA signal. In Figure D6f, however, we again see strong broadband peaks on the 2D-FT highlighting that this signal particular has a fundamental frequency of 16.9 Hz with upper harmonics at 34 and 52 Hz.

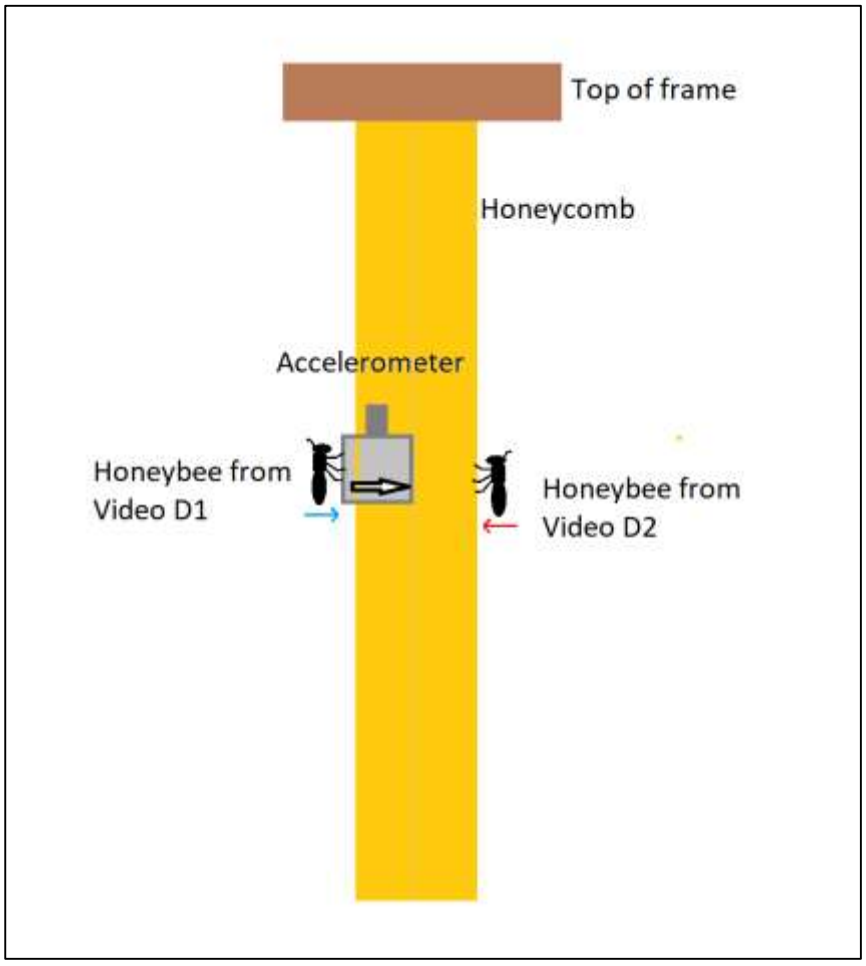

Figure D7. Cross-section of the honeycomb showing the lateral distances between the DVA signallers and the sensors in Videos D1 and D2, as well as the lateral position of the accelerometer within the comb. The blue and red arrows show the direction of the abdominal knocks delivered by the bees in Video D1 and D2, respectively. The white arrow inside the accelerometer shows the direction of the accelerometer axis. The faint grey line through the honeycomb shows the location of the wire mesh

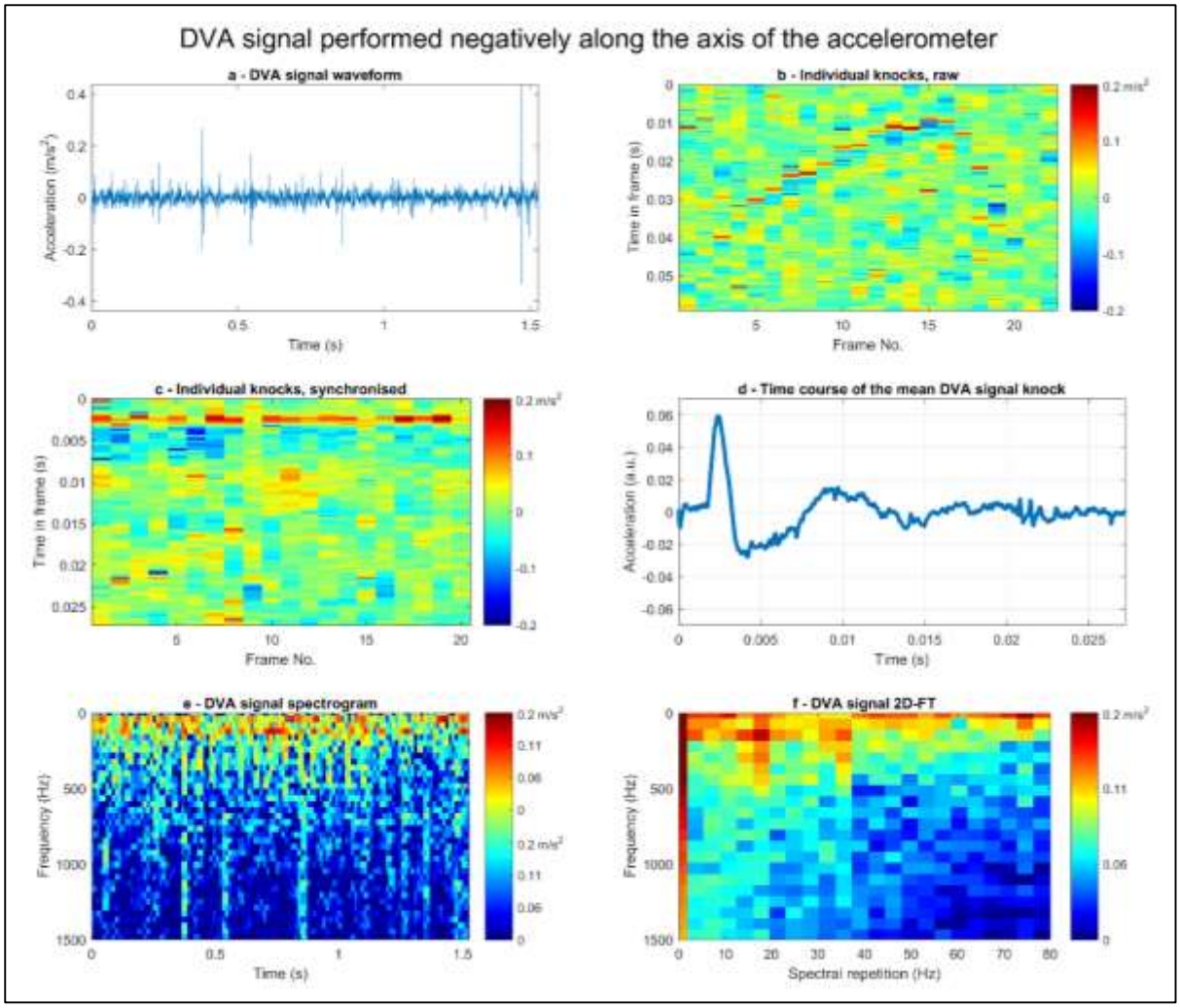

Figure D8. Vibrational properties of a DVA signal delivered onto the other side of the frame to the one seen in Figure D6.

The figure is presented in parts identical to that in Figures D4 and D6.

In Figure D8a, the complex waveform of the DVA signal in D2 Video that occurred on the opposite side of the frame to the protruding accelerometers can be seen. As in Figure D4 and D6, the signal can be observed to last around one second and contains seventeen individual knocks (Figure D8b) that end abruptly as the signaller falls from the honeycomb (Video D2). Upon averaging of the individual abdominal knocks, it can be seen that the sharp bursts of acceleration associated with DVA signals occurs in a positive direction as opposed to a negative direction as in Figure D6 for the DVA signal that occurred on the opposite side of the frame. The signal in Figure D8 and Video D2 has a much lower amplitude than that of the DVA signal that occurred directly on top of the sensor on the other side due to the accelerometer not being wedged directly in the centre (see Figure D7). Oscillations similar

to the signal in Figure D6 can be seen as the honeycomb relaxes, however this is much weaker due to the lateral distance between the sensor and the signaller (see Figure D7). As with previous DVA signals in Figures D4e and D6e, the spectrogram of the DVA signal waveform (Figure D8e) reveals little information regarding this pulse. The 2D-FT (Figure D8f), however, shows that this signal has a frequency of around 18Hz with upper harmonics at 34 and 52 Hz. This analysis shows that DVA signals can be detected on both sides of the frame and that the polarity of the acceleration reveals the side of the frame where the signaller resides.

4.3.1.iii. Extensive characterisation of multiple high-quality DVA signals

Analysis of the DVA signal physical parameters

Simple statistics were undertaken on the accelerometer trace of 27 high-SNR DVA signals that underwent physical characterisation. All descriptive statistics are given in Table D1 for the frequency, the duration, the number of abdominal knocks and the time difference between two consecutive knocks to give the reader insight into the distribution of data for each. It is seen that the mean frequency of the DVA signals is 18.21Hz with minima and maxima at 13.1 and 22.75Hz respectively. The distribution of data is approximately symmetrical. Table D1 shows that the DVA signals have a mean duration of 1.01 seconds with a range of 0.49 to 1.68 seconds, a mode of 0.92s and a median value of 0.97, again with an approximately symmetric distribution as seen by the skew and kurtosis values for each. The potential brevity and longevity of the DVA signal can be seen further by way of the number of knocks that are delivered in each signal ranging from 8 to 27, with a mean and median of 17.92. I show the average time difference between each DVA abdominal knock (0.056s), which dictated the value of the window length of the chopped time course. Full characterisation of these signals along with the corresponding accelerometer audio has been made available in Video D3.

	Mean	Mode	Median	Min	Max	Skew	Kurtosis
Frequency (Hz)	18.21	16.11	17.89	13.1	22.75	0.065	2.67
Duration (s)	1.01	0.92	0.99	0.49	1.68	0.46	2.54
Number of knocks	17.92	17.92	18	8	27	-0.12	2.27
Time between two knocks (s)	0.0056	0.0054	0.05	0.044	0.065	0.84	4.2

Table D1. Simple statistics of the vibration properties of 27 audible DVA signals extracted by our software.

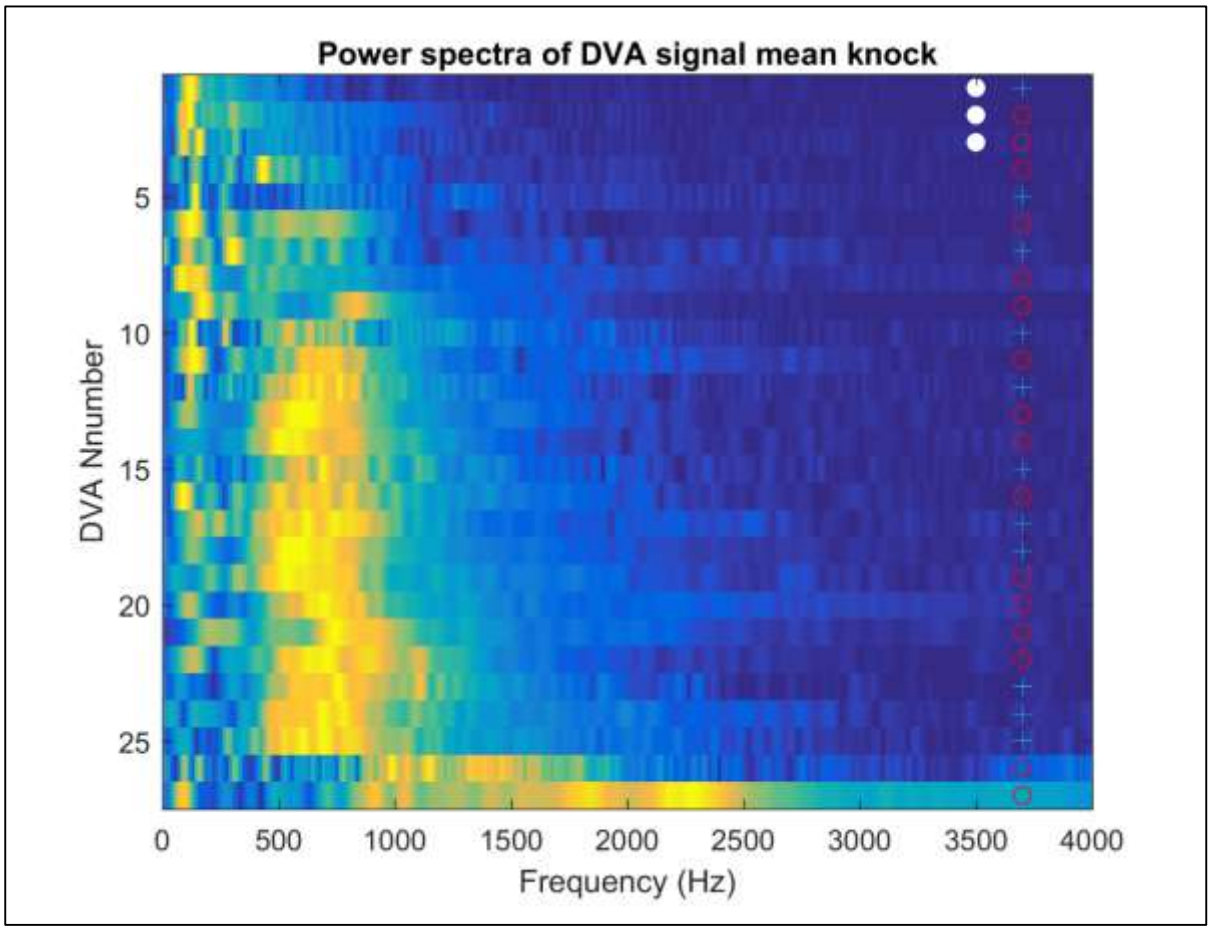

Figure D9. The power spectra of each averaged knock of the twenty-seven high SNR pulses used in the initial quantitation of DVA signals (see Video D3). These pulses have been ordered by their increasing similarity to the population mean. Pixel intensity denotes the amplitude of each frequency. White filled dots show DVA signals extracted from the Clifton Observation hive recordings. The remaining pulses come from a recording that took place before the primary swarm in the French 2015 dataset. The cyan + symbol and the red O respectively mark a pulse with knocks that are of positive and negative polarity.

In Figure D9 the power spectra of each averaged knock of the twenty-seven high SNR pulses used in the initial quantitation of DVA signals is shown in each horizontal line of the image. Principal component analysis was used to order the pulses by decreasing distance to the population mean. It can be seen that the majority of pulses have a sharp peak at around 60Hz, characteristic of a slow long-lived oscillation, and a secondary broadband peak, that is characteristic of a short-lived ultra-fast oscillation, between 500 and 1000 Hz. There appears to be little relevant information above 1500 Hz for the majority of DVA signals. The polarity of the pulses, caused by the side of the frame upon which the signal was delivered, appears to have no effect on the spectra of the pulse's mean knock, as they seem to alternate randomly within the ranking of similarity. Figure D9 also shows that the DVA signals that come from other hives to that of the majority are outliers to the rest of the population. This further supports the concept that the current status of the honeycomb influences the frequency response of its relaxation that immediately follows the individual abdominal–honeycomb collisions within the DVA signal.

Spectral comparison with other one-second-long honeybee signals

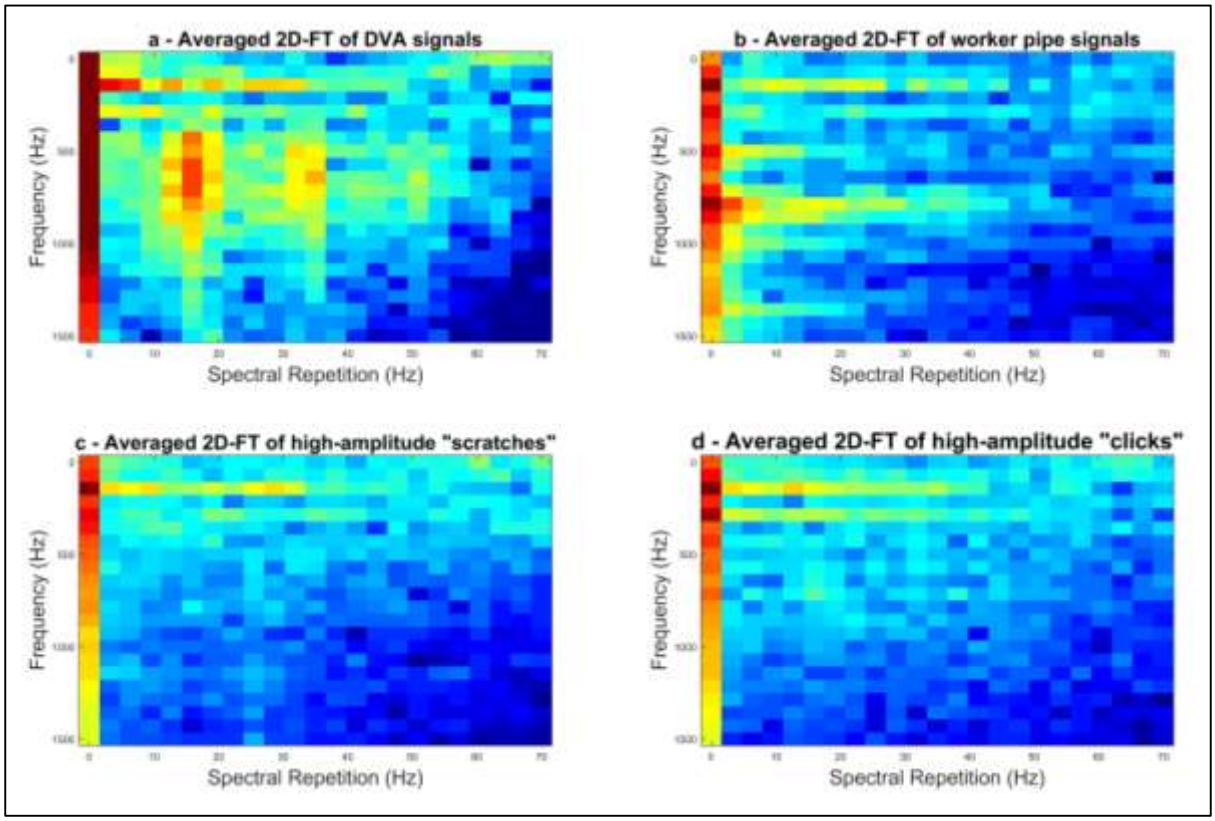

Figure D10. The averaged 2D-FT calculated on 150 examples of the signal waveform of commonly encountered pulsed vibrations (a) DVA signals, (b) worker pipes, (c) wax scratching, and (d) high-amplitude "click" vibrations. The pixel intensity of each image is acceleration shown in a linear scale.

To demonstrate the strength of the method that utilises the 2D-FT, Figure D10 shows a comparison of the 2D-FT of DVA signals with other common one-second-long signals that can be found within the long-term accelerometer datasets. It is seen in Figure D10a that the averaged 2D-FT of 150 examples of extracted high-quality audible DVA signal waveforms exhibits broadband vertical peaks at around 18Hz, 32Hz and 45Hz (second and third harmonics). For comparison, in Figure D10b, c, and d, an averaged 2D-FT of worker pipes, wax scratching and high-amplitude 'clicks' that are also averaged over 150 examples for each are also displayed. From this analysis it is apparent that well-defined narrow band vertical bands are unique to DVA signals at these frequencies, supporting its use within the detection software. The 2DFT works so well for the DVA signal over the other signals owing to the

regularity of the sharp individual knocks over a one-second time course. It is seen that all 2DFT images exhibit horizontal broadband peaks at 125Hz and 250Hz that can be attributed to the background sound of wing buzzing by members of the colony (e.g. Ramsey et al., 2017). The worker pipes (Figure D10b) exhibit enhanced horizontal peaks at 500Hz and 800Hz. No definitive information can be seen for the high-amplitude “scratching” in Figure D10c or the high-amplitude “clicks” presented in Figure D10d, probably due to the averaging of images that do not exhibit repeatable features.

4.3.2. The spatial distribution of DVA signals

A total of 26 videos that represent an overall time duration of 8 hours of recording were visually examined to detect the actual number and location of DVA signals that occurred on both sides of the focal frame (see methods). As all assessments showed a similar spatial distribution, four specific examples are presented below to give a representation of the distribution over each season.

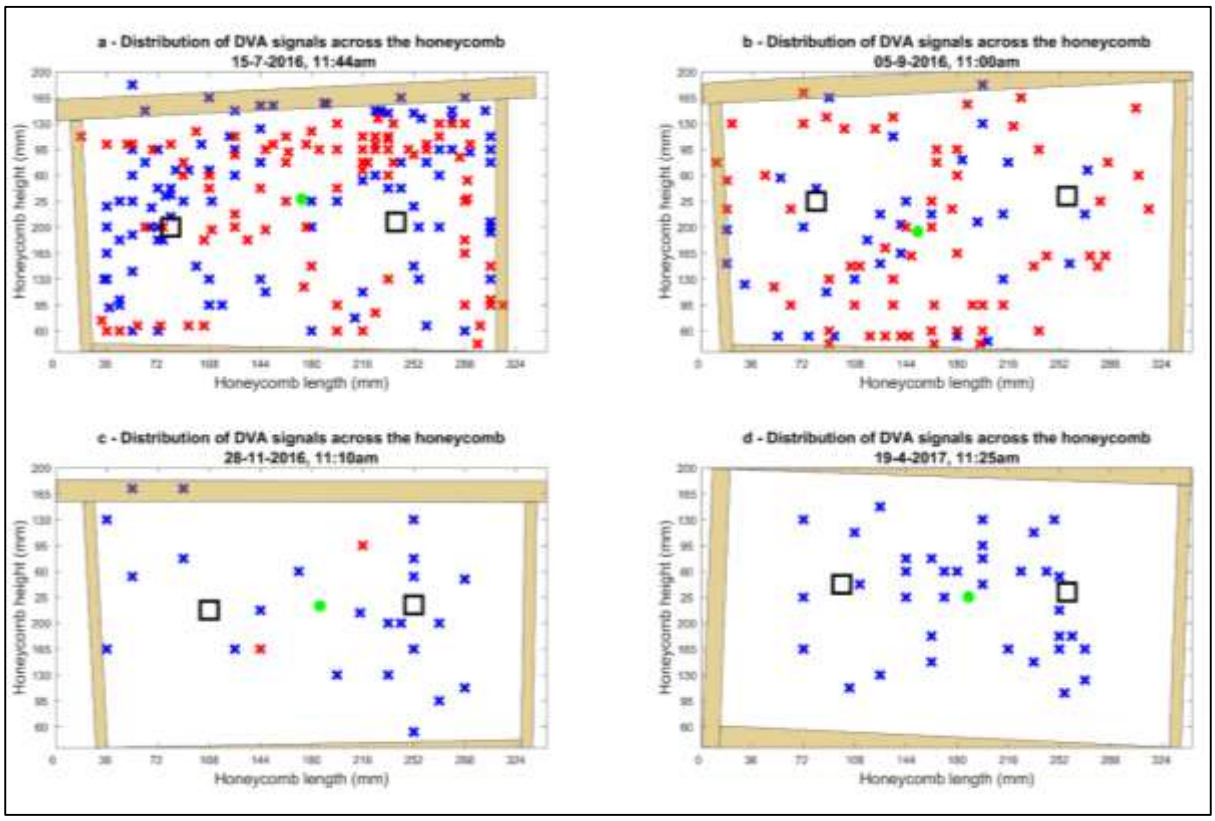

Figure D11. The spatial analysis of DVA signals occurring across the honeycomb recorded over a series of 10-minutes of videos recorded in (a) July 2016, (b) September 2016, (c) November 2016, and (d) April 2017. The large black squares indicate the location of the accelerometers. The blue and red X's respectively indicate the location of DVAs on the side of the honeycomb with visibly implanted accelerometers and on the other side, behind the accelerometers. Green dots signify the mean coordinates. The light brown shapes mark the location of the wooden frame surrounding the honeycomb as seen in the video footage.

In all 10-minute long videos sampled at various points throughout the year, an even distribution of DVA signals across the honeycomb can be observed (Figure D11), regardless of the total count captured on the film or the side they were recorded on. A full breakdown of the statistics corresponding to the plots in Figure D11 is given in Table D2.

Label	Figure D10a	Figure D10b	Figure D10c	Figure D10d
Date	15-07-2016	05-09-2016	28-11-2016	16-4-2017
Total DVA signals	204	95	25	37
Side A	107	61	23	37
Side B	97	34	2	0

Table D2. Tabulation of the spatial distribution results presented in Figure D11.

4.3.3. Extensive visual inspection

In Table D3 it can be seen that upon testing of the detection software with accelerometer data synchronous with video footage, the percentage of the overall detections that were genuine DVA signals was confirmed by visual analysis to be 89%. It can be seen from Table D3 that the overall number of detections relative to the number of actual DVA signals is around 2%. However, the percentage of detections overall appears to increase to 27% when the honeycomb appears visually to have lower frame content (19th April 2017 in Table D3). It can also be seen that videos captured around 2pm produced the fewest DVA signals and that DVA signals can be observed in the winter when temperatures precede 8°C (see Table D3). Observations within this analysis also suggests that the signaller makes full contact with the honeycomb in 33% of cases when performing a DVA signal, whether the direct recipient was a conspecific or not. At no point during this analysis was a DVA signal detected that was delivered whereby the abdomen of the sender made full contact with another bee rather than hitting the honeycomb. True detections always came from direct abdomen-honeycomb collisions.

Video Names	Date/Time of Video	Dur. (min)	No. of DVAs	Detection Number	Correct Detections	% Genuine	Notes
DSC0007 00006.MTS	11:44am 8th July 2016	10	205	13	10	77	Bees observed to completely cover the focal frame. No capped brood. **Hot (25°C) and sunny day.**
DSC0002 00007.MTS	14:00pm 21st July 2016	10	0	0	0	100	0 occurred. 0 were falsely detected. Capped brood. Waggle Dances. **Hot (25°C) and sunny day.**
DSC0011	12:05pm 29th July 2016	20	114	3	3	100	Fully capped brood at the centre with capped honey at the periphery. 0 occurred within around 7cm of the accelerometer. 10 in range of the accelerometer, 4 of which were on top of other bees. Audible DVA on 00010.MTS @ 34s. **Hot (25°C) and Sunny day.**
DSC0016 00017.MTS	13:58pm 19th Aug 2016	20	19	1	1	100	2 in range of Acc. Capped Brood. Waggle Dances. On 00017.MTS, between 30 and 90s a bee DVA signals until she receives a strange behaviour at the top of the frame and then does no more DVAs. **Rainy day (20°C).**
DSC0018 00019.MTS	14:31pm 22nd Aug 2016	20	0	0	0	100	0 detections, 0 seen visually. **Rainy day (20°C).**
DSC0021 00005.MTS	16:00pm 30th Aug 2016	20	0	1	0	-	0 occurred. 1 was falsely detected. **Hot (25°C) and sunny day.**
DSC0024 00007.MTS	11:20am 5th Sep 2016	20	95	1	1	100	Honeycomb almost empty. Some capped brood. Waggle dances occurring on both sides. No DVAs occurred within the vicinity of the accelerometers other than 9:28 acc. 1. **Hot (25°C) and sunny day.**
DSC0005 00011.MTS	11:00am 7th Sep 2016	20	30	0	0	100	Honeycomb almost empty. Some capped brood. All DVAs transitioned into Waggle dances occurring on both sides. No DVAs occurred within the vicinity of the accelerometers. **Warm (19°C) and overcast day.**
DSC0010 00024.MTS	13:01pm 15th Sep 2016	20	20	0	0	100	Empty comb. 1 DVA on the left accelerometer but it did not make contact with the comb. **Light rain and overcast. (18°C).**
DSC0012 00026.MTS	10:00am 16th Sep 2016	20	11	0	0	100	Empty comb. 0 in range of accelerometer. **Heavy Rain and Fog. (18°C).**
DSC0013 00008.MTS	15:10pm 28th Nov 2016	20	21	0	0	100	Very densely packed honey on comb. No waggle dances due to winter. 0 near the accelerometer. **Sunny day (18°C).**
DSC0015 00032.MTS	16:21pm 19th April 2017	20	37	11	10	91	Honeycomb empty and very few bees on the frame. The side of the frame without protruding accelerometers is completely empty of bees and any contents within the frame. **Warm (17°C) sunny day.**
DSC_0013 00036.MTS	14:00pm 9th Aug 2017	10	0	0	0	100	The frame was completely covered, on both sides, with capped brood. No DVA signals occurred in this video. **Rainy day (18°C).**

Table D3. The extensive visual analysis of DVA signals that occurred throughout videos recorded on both sides of the focal frame pertaining to the Clifton observation hive. The table features the number of actual DVA signals that occurred, how many were identified by the detection software and in how many instances could the bee's abdomen be seen making contact with the honeycomb.

4.3.4. Hourly occurrences of detected DVA signals

4.3.4.i. French 2015 hive

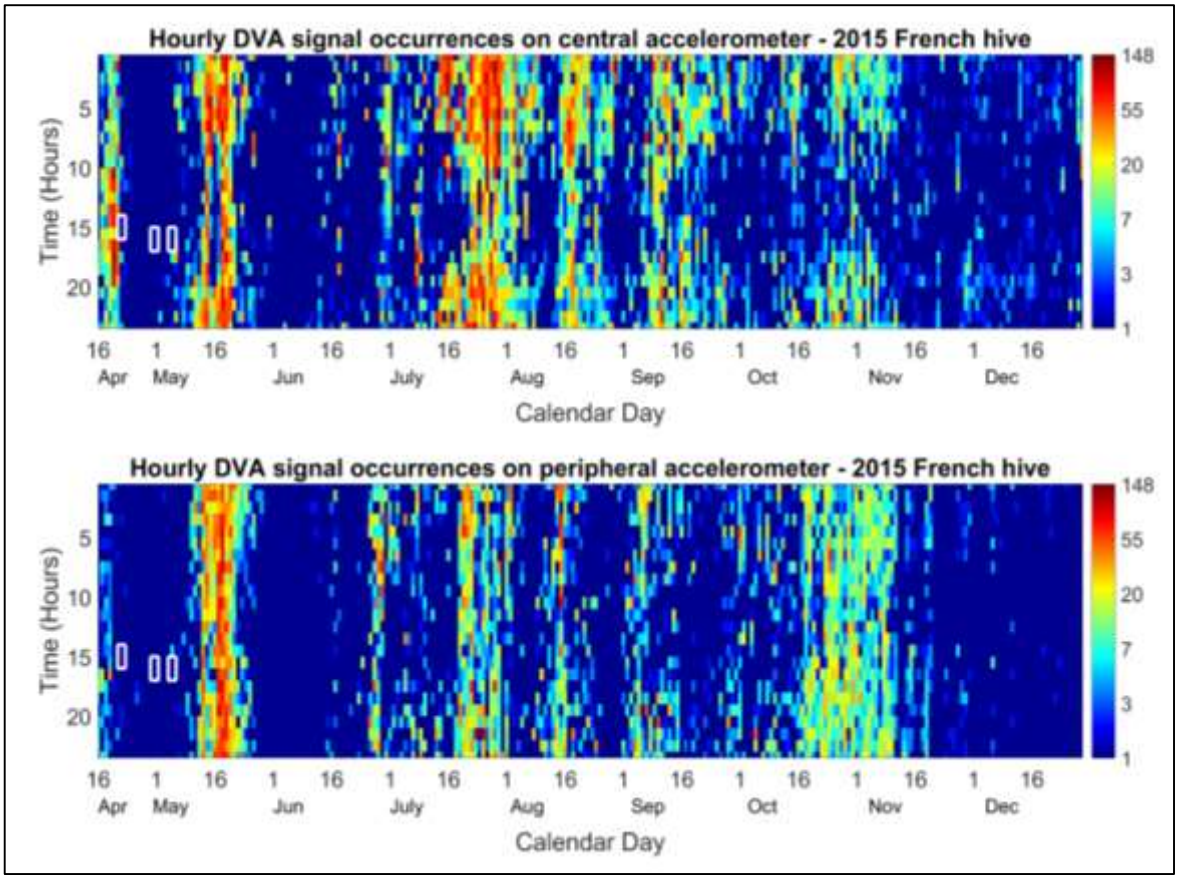

Figure D12. DVA signal hourly occurrences. Central (top) and peripheral (bottom) accelerometer logs of the French colony (2015 season). The colour codes the number of hourly occurrences from dark blue (1) to dark brown (403 signals) on a logarithmic scale. White boxes highlight the occurrences of the three swarms that occurred from this hive, with the first one being the primary swarm.

Figure D12 clearly demonstrates that the signal occurs relatively frequently within the immediate vicinity of the accelerometer, recorded at up to twice per minute with an average of nine per hour. There is also a pronounced and consistent decrease of occurrences of approximately 70% between 2pm and 4pm, further evident upon averaging DVA signal occurrences for every hour across each day of the recording for each accelerometer (Figures D13a and D13b). Figure D13c and D13d also show that this hourly trend holds stable across the entire dataset. This “lunchtime lull” is also apparent

within the French 2017 hive (Figure D24) as well as the Clifton Observation hive (Figure D29). It is seen that there is a large DVA signal occurrence increase in the days before and the hours immediately following the primary swarm, with a dramatic decrease thereafter. Upon critical listening to these detections' raw signal, audible DVA signals can only be heard on the central accelerometer, and at 55 audible pulses an hour, there is no other point within the recording that DVA signals can be heard in such high density.

There appears to be a positive correlation, over the entire season, between the numbers of DVA signals across the two accelerometers, a trend that was not observed within the detection of whooping signals in Ramsey et al. (2017). This dataset also reveals a high occurrence of night-time (between 8pm and 5am) DVA signals, never shown or investigated in any previous study. There is a significant positive correlation between the modal midnight amplitude (Bencsik, et al., 2015) of the entire dataset and the daily mean number of DVA signals recorded by the software on both the central (Figure D14) ($R_s = 0.2475, p < 0.001$) and peripheral (Figure D15) ($R_s = 0.3505, p < 0.001$) accelerometers, with peaks every 21 to 24 days. Interestingly, there is no correlation between the hourly number of DVA and whooping signals (from Chapter 3), recorded on either the central (Figure D14) ($R_s = 0.0735, p = 0.2461$) or the peripheral ($R_s = 0.256, p = 0.1002$) accelerometer (Figure D15). Finally, there appears to be a gradual reduction in overall signal production captured by the accelerometer as the year progresses into the winter with a sustained drop-off from early November. Amongst other signals, including worker pipes, wax scratching and high amplitude clicks, (that were successfully dismissed by the software), it is easy to check (through computation of the individual pulse's 2D-FT) the validity of the DVA signals highlighted by red hotspots. Through the visual inspection of the 2D-FT images computed for 600 detected signals chosen at random times throughout the year, the reliability for the detection software developed as part of this study was estimated. 83% of the pulses elicited vertical broad bands at horizontal frequencies previously demonstrated to be unique to the DVA signal. An audio file containing a collection of audible DVA signals concatenated using the timings around

midnight on the 18th April is provided in Audio D1 for the listener to appreciate the high degree of repeatability of this unique type of honeybee signal.

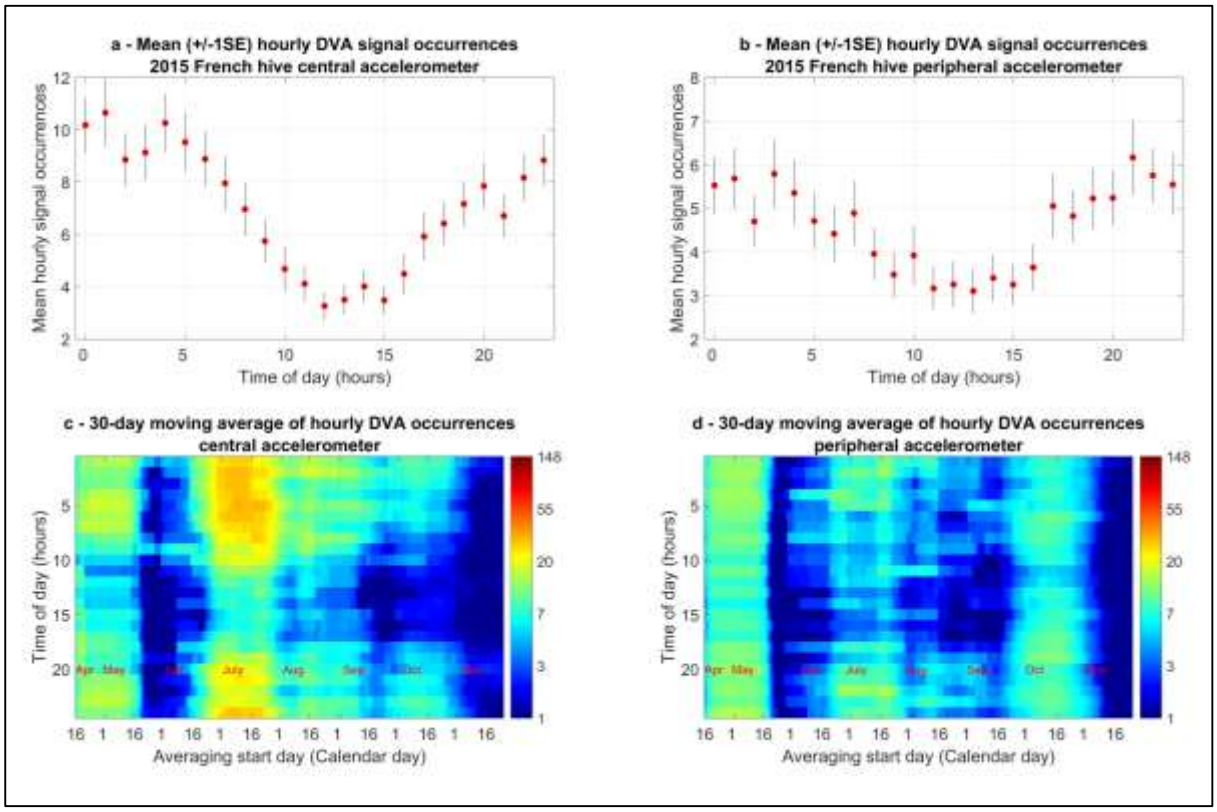

Figure D13. The mean hourly trend in DVA signals detected over 24 hours across the entire French 2015 dataset recorded by a) the central accelerometer; and b) the peripheral accelerometer; The mean hourly trend calculated over 30 dates and moved 1 day across for c) the central accelerometer dataset; and d) peripheral accelerometer dataset. This graph is obtained over the vibrational dataset shown in the previous figure. The vertical bars indicate +/- 1 standard error (SE).

In Figure D13a and D13b, the hourly number of DVA signals that have been detected by the software within the French 2015 dataset for each hour of the day was calculated and averaged over all days across the dataset for both accelerometers. It can be seen that there is a maximum between 11pm and 4am and a minimum between 11am and 4pm with smooth gradual increases and decreases in between. This trend is generic as it can also be observed across the French 2017 hive (Figure D14b) as

well as the Clifton Observation hive (Figures D16a and D16b) and is supported by video analysis in Table D3.

In Figure D13c and D13d, the average number of DVA signals for each hour of the day is only calculated over a 30-day period that is shifted along the time axis in one day increments ("moving average"). These show that the hourly trend seen in Figure D13a and D13b is stable and holds across the entire active season, even if it is not so clear on a day to day basis. The same trend is also observed within the French 2017 hive data (Figure D14c) as well as the Clifton Observation hive (Figures D16c and D16d).

4.3.4.ii. French 2017 hive

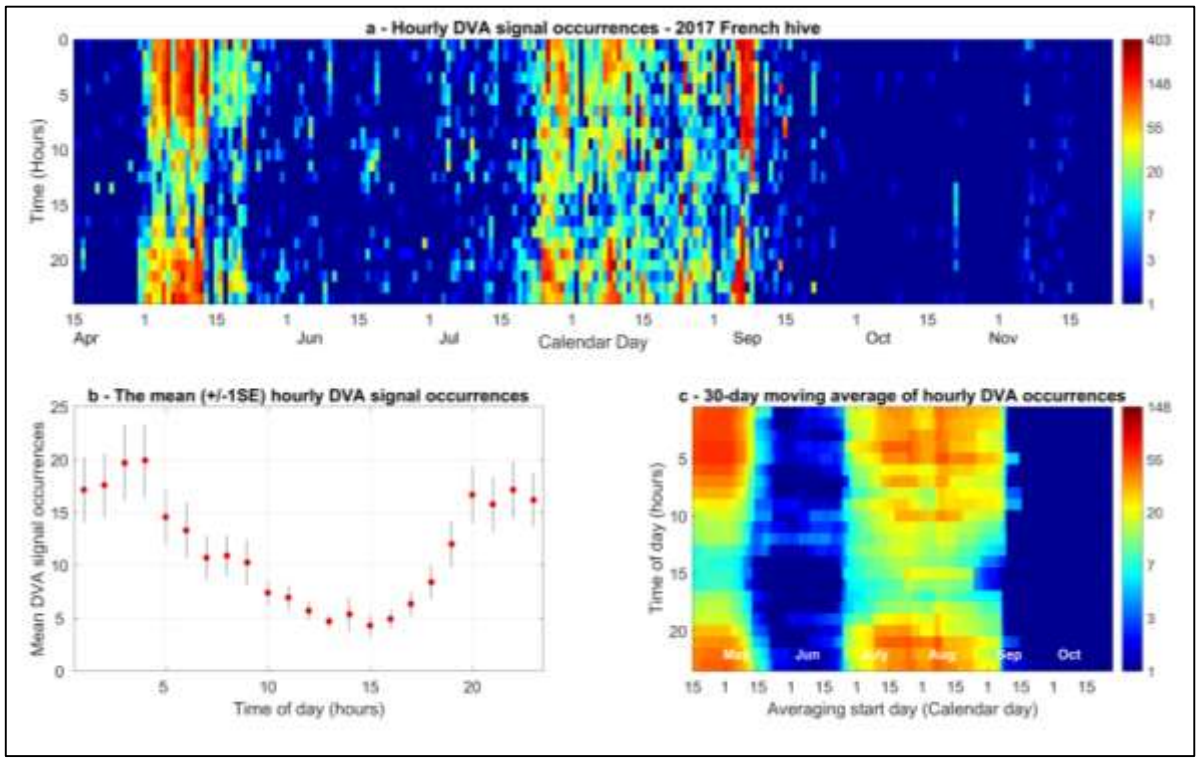

Figure D14. The hourly occurrence statistics for the 2017 French hive dataset showing: a) the histogram of the hourly occurrences of the DVA signal for each day of recording, b) the mean number of DVA signal detections for each hour of the day throughout the dataset, and c) the number of DVA signals that occurred for each hour of the day averaged over 30-days and shifted along the dataset by one day.

Presented in Figure D14a, is the hourly occurrence statistics for the French 2017 hive dataset, which spans the entire 2017 active season until the death of the colony was found on the 28th November 2017. This hive was monitored using one accelerometer only, placed directly into the centre of the central frame of honeycomb. From when the recording was launched on the 15th April 2017, there were very few DVA signals detected until the 29th April when a large increase in the number of DVA signals is seen that is also apparent on the French 2015 dataset. This was data ascertained from a hive where the colony did not swarm and perhaps as a result, there is no increase in DVA signals detected as seen for the 2015 French dataset in Figure D12 in April, which supports the DVA signal's association with pre and post swarming practices. As with all other datasets (Figure D12 and D15), there is

heightened signal detection in May and July, yet there is no 21-day brood cycle apparent within this dataset. However, there is a regular 12-day peak in DVA signal detection perhaps suggesting an asynchrony of laying and emergence between each side of the frame or could indicate the presence of drone-laying workers. The number of DVA signals averaged for each hour of the day across the entire 2017 French dataset (Figure D14b) shows the same 10am to 4pm minima and 10pm to 4am maxima as seen across all other datasets. This “lunchtime lull” is seen to hold steady across the dataset until the collapse of the colony (Figure D14c).

4.3.4.ii. Clifton Observation hive

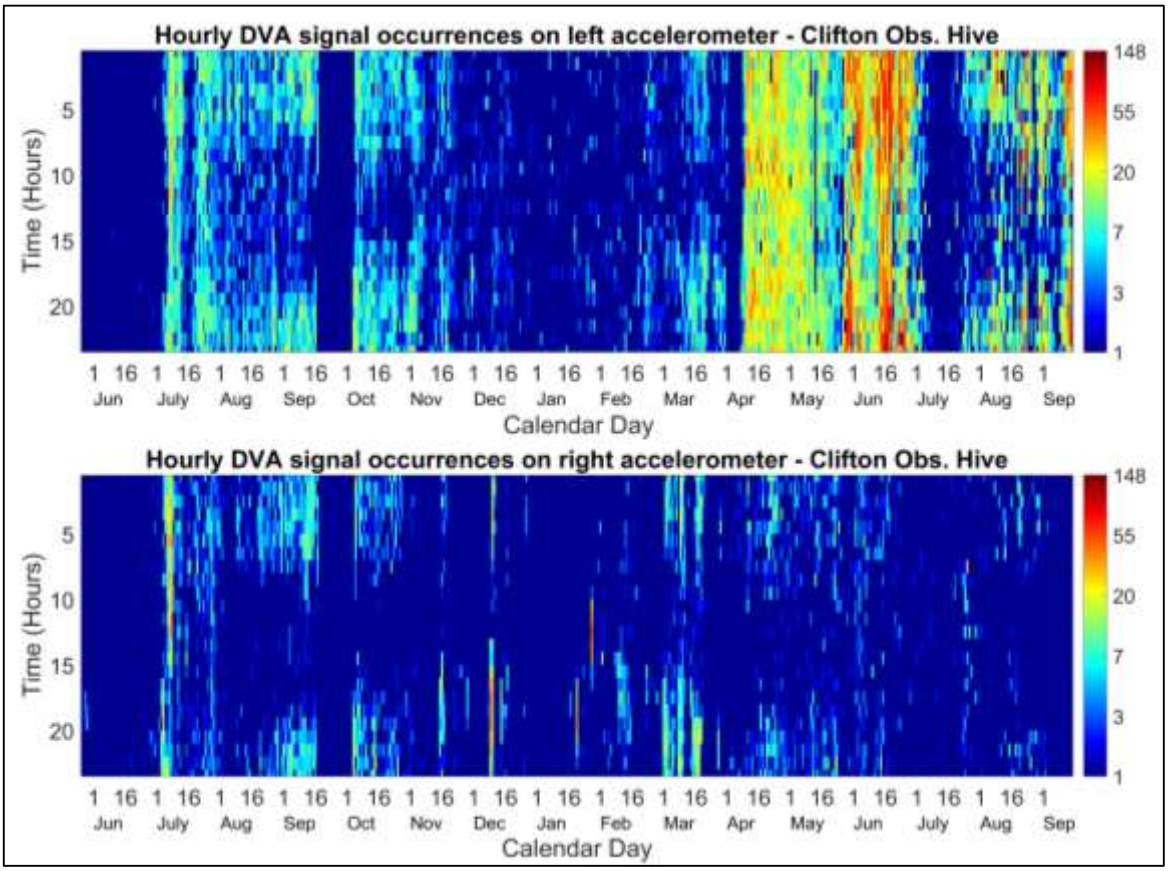

Figure D15. Hourly DVA signal occurrences. Left (top) and right (bottom) accelerometer logs of the Clifton observation colony (2016/17 season). The colour codes the number of hourly occurrences from dark blue (1) to dark brown (148 signals) on a logarithmic scale.

The dataset for the Clifton Observation hive, situated on the Clifton Campus of Nottingham Trent University, Nottingham, makes for an interesting comparison to that of the 2015 French dataset. This colony experienced many natural and human induced changes throughout its period under observation. The colony was introduced to its new observation hive on the 24th May 2016. It was placed into the box via a purpose cut hole on the left side. From there the colony developed across the box and began work on the observation frame on the 5th July 2016. But did not expand much beyond, making it a frame peripheral to the colony centre. On 16th September 2016, the colony was removed from campus for 3 weeks so that they could be brought back and relocated in another

building on the same campus. This caused the 3-week interruption to the measurement seen in September. The recordings then continued across the winter until 28th March 2017 when the hive was brought back to the lab for cleaning and replacement of the observation frame's honeycomb with fresh foundation wax, causing a weeklong interruption to the recording. The frames were rearranged so that the observation frame ended up at the centre of the colony, which causes the increase in the number of detections during this period. The right accelerometer was accidentally placed so that its axis faced parallel to the honeycomb, instead of perpendicular and thus the detection of the DVA signal is much less frequent on the right channel to the left. Additionally, identified through visual observations and on video recordings following the reintroduction of the observation stage in April 2017, once the bees had drawn out the frames foundation wax into full honeycomb, the left accelerometer, for the most part, appeared much more exposed and surrounded by empty cells after the bees had in contrast to the right accelerometer that was buried deep surrounded by capped honey stores.

This frame was at the periphery of the colony throughout the 2016 recordings and half of the recordings from 2017, making it an interesting comparison to the central frames of the 2015 and 2017 French datasets. The brood cycle is not regularly seen on this UK dataset because this frame only experienced one in August 2016 and one in July and August 2017. However, trends such as the signal reduction towards winter with the increase in May and drop off in July that can be seen on the French 2015 dataset can be observed again in this dataset.

The 2016 queen of this colony was an aging queen who became a very inefficient egg-layer, evident by the decreasing amount of capped brood throughout the brood cycle. On 16th June 2017, the old queen was found on surrounded by only 5 bees at the top of the observation unit. On inspection within the hive, queen cells were found within several frames of the colony. A few days later, the original queen was found outside the hive and a new queen was seen within. This dual-queen period could be the cause of the drop in DVA signal occurrences detected in July 2017.

On the 9th August 2017, a video was recorded of the observation frame for 10 minutes where no DVA signals occurred on a frame full of capped brood. However, the associated accelerometer track is full of high-amplitude clicks. In spite of this, there was no false detections recorded by the software in this period, giving further confidence in the reliability of the algorithm.

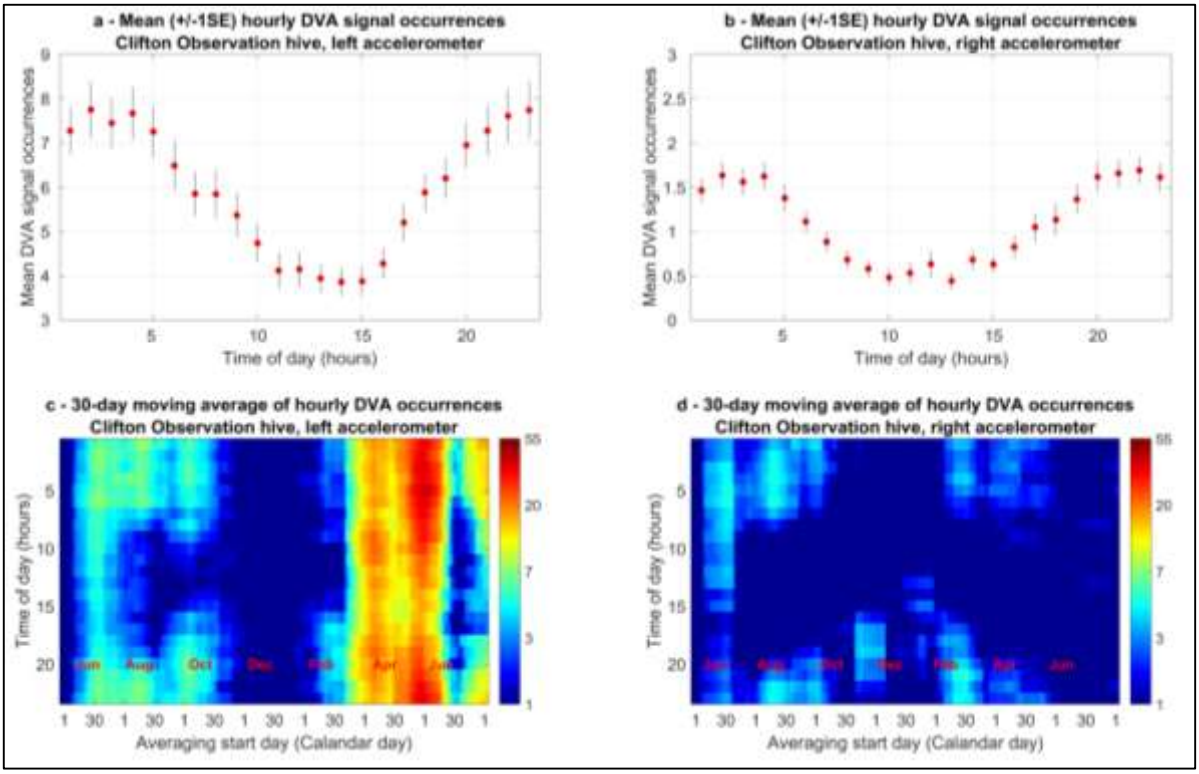

Figure D16. Average hourly occurrences within the Clifton Observation hive dataset. The mean hourly trend in DVA signals detected over 24 hours across the entire dataset, recorded by a) the central accelerometer; and b) the peripheral accelerometer. The mean hourly trend calculated over 30 dates and moved 1 day across the c) central accelerometer dataset; and d) the peripheral accelerometer dataset. This graph is obtained over the vibrational dataset shown in the previous figure. The vertical bars indicate +/- 1 standard error (SE).

The hourly statistics of the Clifton Observation hive (Figure D16) mirror that of the 2015 French dataset (Figure D12) and also that of the 2017 French dataset (Figure D14) with maxima in the evening and minima between the hours of 10am and 4pm (Figure D16a and D16b), which holds stable across the entirety of the recording (Figure D16c and D16d). Figure D16 further demonstrates the reduction in the number of detected DVA signals on this (mostly) peripheral frame compared to the central frame

of the other datasets. It suggests that the same trends in signal occurrence can be observed across the other frames of the hive and is not restricted to the one most central to the colony.

4.3.5. DVA signals and weather

4.3.5.i. French 2015 hive

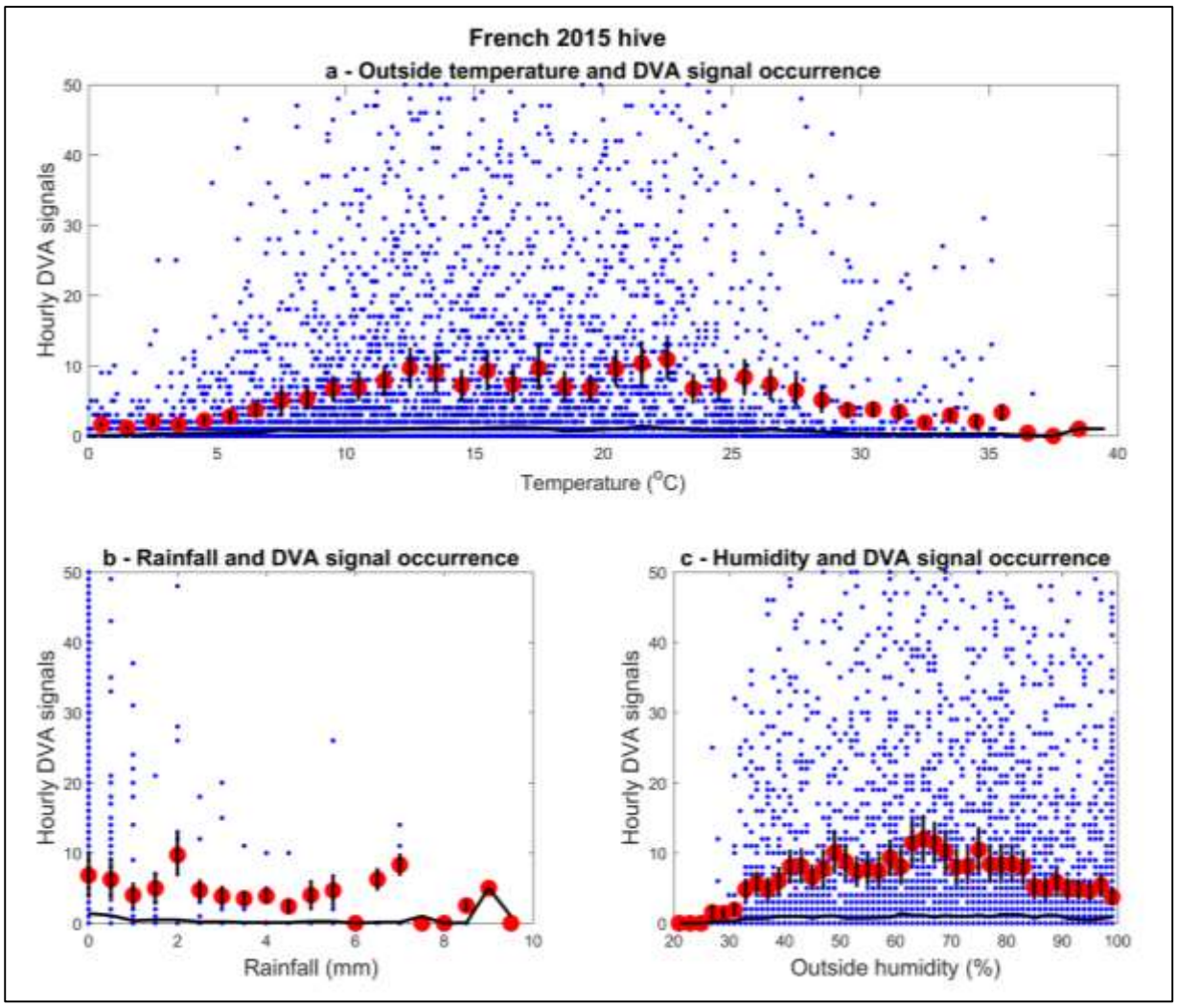

Figure D17. Hourly occurrences of DVA signals in relation to weather for the French dataset (2015 season) with corresponding: (a) average outside temperature, (b) cumulative rainfall, and (c) average outside humidity. Red dots indicate the average number of DVA signals with black bars displaying ± 1 SE.

The black curve on each graph shows the modal hourly DVA signals.

Plots of the complete hourly data for temperature, humidity and rainfall that co-inside with the French 2015 hive recordings can be found in Supplementary Figure 1 in Appendix 7. It can be seen in Figure D17a that in relation to temperature, the occurrence of honeybee DVA signals is at its lowest at the extremes, i.e. at 0 and 38°C, a trend that is mirrored for the 2017 French hive dataset in Figure D18a.

There is a steady increase in the occurrence of DVA signals from 0 to 12°C and then a plateau until 27°C when a steady decline can be seen thereafter. The same trend is displayed in the humidity plot in Figure D17c, where a steady increase in DVA signal occurrences can be seen until around 40%, with a steady decrease after 80%. As seen for the 2017 French hive dataset in Figure D17b, there is also no perceivable trend between rainfall and the number of DVA signals but it can also be seen that the majority of days saw very little precipitation. However, one day of prolonged heavy rain on the 28th October 2015 (Supplementary Figure 1 in Appendix 7) appears to correspond to a day clearly lacking of the late afternoon lull in the occurrences of DVA signals (Figure D12), in steep contrast with the rest of the data.

4.3.5.ii. French 2017 hive

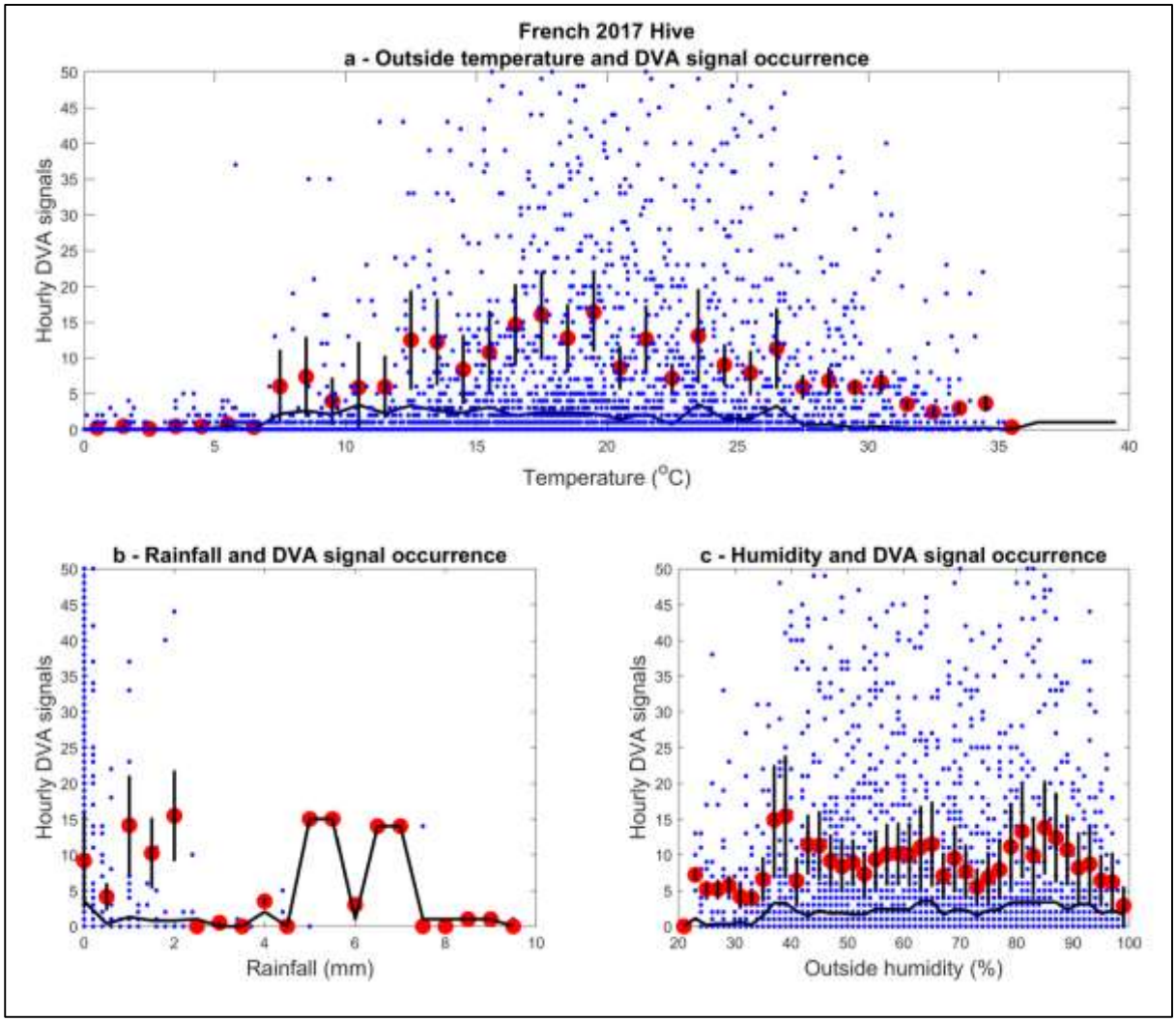

Figure D18. Hourly occurrences of DVA signals in relation to weather for the French dataset (2017 season) with corresponding: (a) average outside temperature, (b) cumulative rainfall, and (c) average outside humidity. Red dots indicate the average number of DVA signals with black bars displaying ± 1 SE. The black curve on each graph shows the modal hourly DVA signals.

Plots of the complete hourly data for temperature, humidity and rainfall that co-inside with the 2017 French data recordings can be found in Supplementary Figure 1 in Appendix 8. For all plots on this figure and Figure D17, there is a high degree of scatter within the data. It can be seen in Figure 18a that the occurrence of honeybee DVA signals within this dataset is at its lowest at the extremes, i.e. at below 7°C and above 35°C, a trend that is mirrored for the 2015 French hive dataset in Figure D17a.

There is a steady increase in the occurrence of DVA signals from 7 to 15°C and then a plateau until 24°C when a steady decline can be seen thereafter. No trend can be seen displayed in the humidity plot in Figure D18c meaning that while temperature and humidity appear to have an inverse correlation in Supplementary Figure 1 in Appendix 8, they act upon DVA signals independently. As seen for the 2015 French hive dataset in Figure D17b, there is no perceivable trend between rainfall and the number of DVA signals; however, Supplementary Figure 8 shows that the majority of days saw very little precipitation, with full days of prolonged heavy rain being rare after June 2017.

4.3.4.iii. DVA signal comparison with the daily trends of whooping signals and the brood cycle

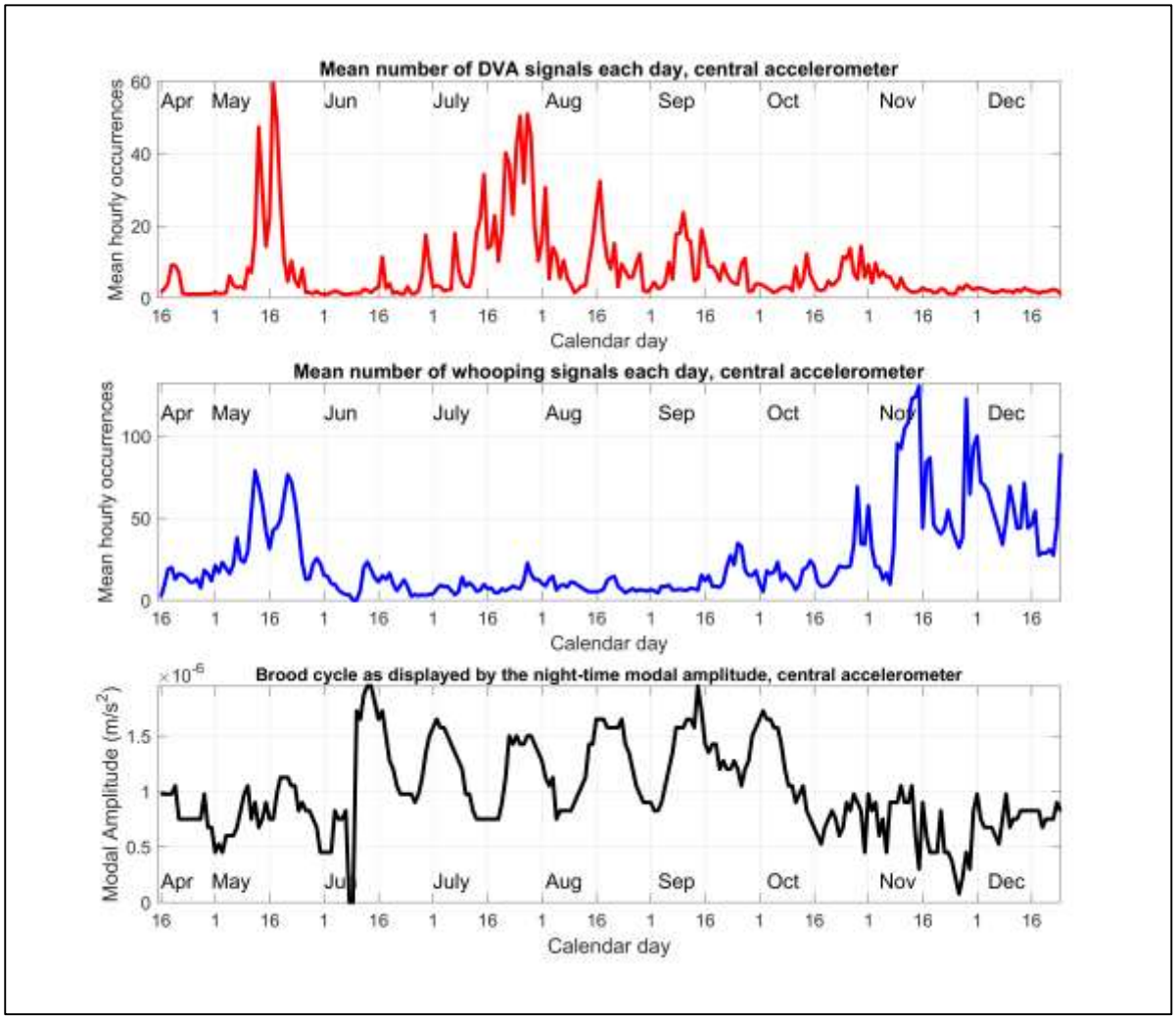

Figure D19. Comparison of the daily trend in the mean number of hourly DVA signals (red), whooping signals (blue), and the night-time modal amplitude (black), for the central accelerometer of the 2015 French dataset.

The comparison between the daily trends of DVA signals, whooping signals and the brood cycle data found in section (3.4.) for the French 2015 hive dataset is shown in Figure D19 for the central accelerometer and in Figure D20 for the peripheral. There is a significant positive correlation between the modal midnight amplitude (Bencsik, et al., 2015) of the entire dataset and the daily mean number of DVA signals recorded by the software on both the central (Figure D19) ($R_s = 0.2475$, $p < 0.001$) and peripheral (Figure D20) ($R_s = 0.3505$, $p < 0.001$) accelerometers, with peaks in both every 21 to 24 days.

When the modal amplitude peaks (after the hatching of brood) the number of detected DVA signals increases. This trend, however, starts with the second brood cycle and is not seen after the first hatching on the 7th June. There is a final DVA signal occurrence peak 21-days after the last hatching of brood on the 4th October, a feature seen on both accelerometers.

Interestingly, there is no correlation between the hourly number of DVA and whooping signals, recorded on the central (Figure D19) ($R_s = 0.0735, p = 0.2461$) or peripheral ($R_s = 0.256, p = 0.1002$) accelerometer (Figure D20). There are peaks in DVA and whooping signals, most evident in the peripheral accelerometer data, that are concordant, such as around the 17th May, however the peaks in DVA signals always occur around 3 days before that of the whopping signals. There is also an increase in the occurrence of whooping signals in November and December that is not seen for the DVA signals. The whooping signals also exhibit a peak in occurrence around the 11th June that is in line with the first brood cycle, a feature that is not evident within the occurrences of DVA signals.

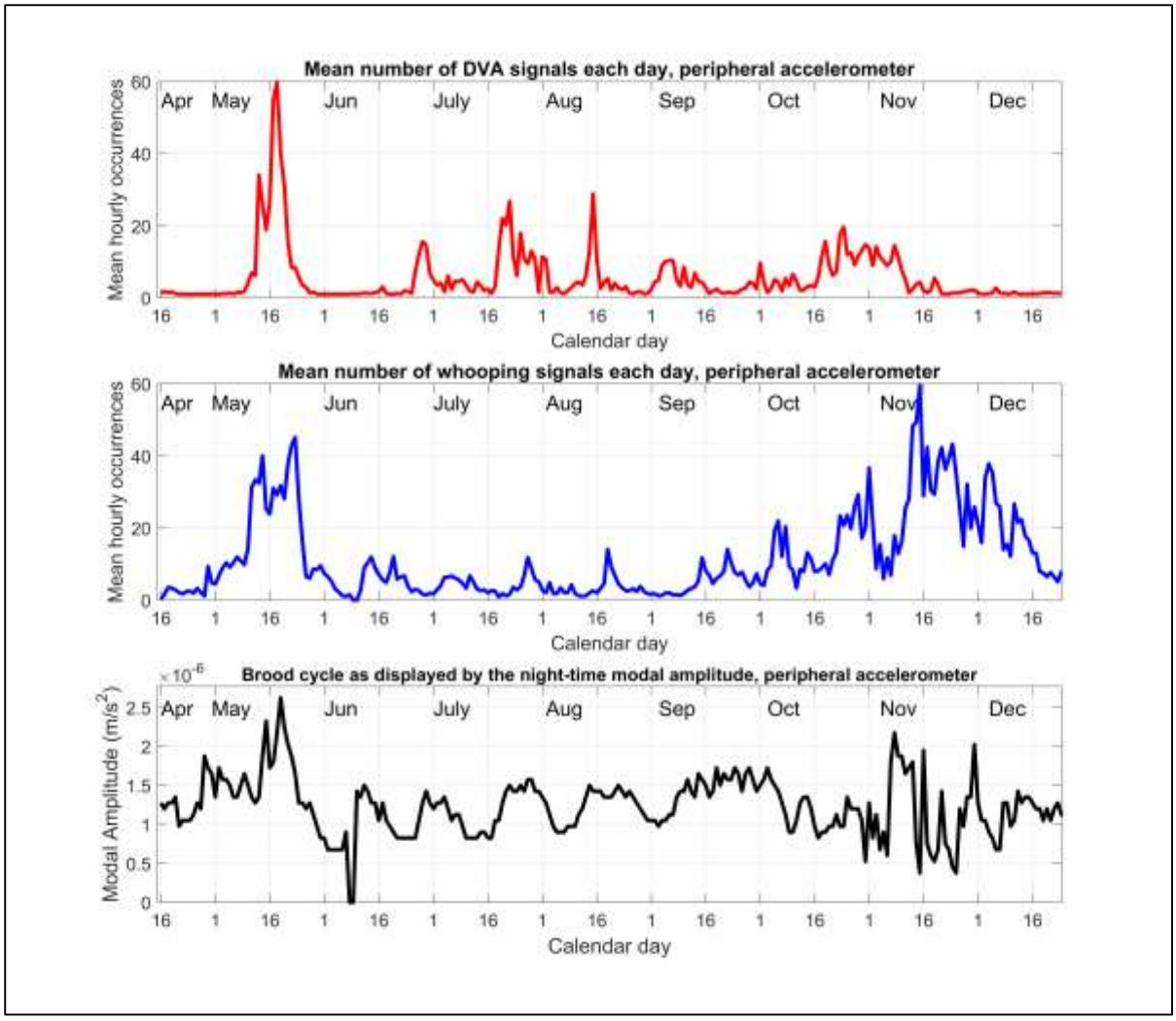

Figure D20. Comparison of the daily trend in the mean number of hourly DVA signals (red), whooping signals (blue), and the night-time modal amplitude (black), for the peripheral accelerometer of the 2015 French hive dataset.

4.3.5. Hourly two-dimensional Fourier analysis

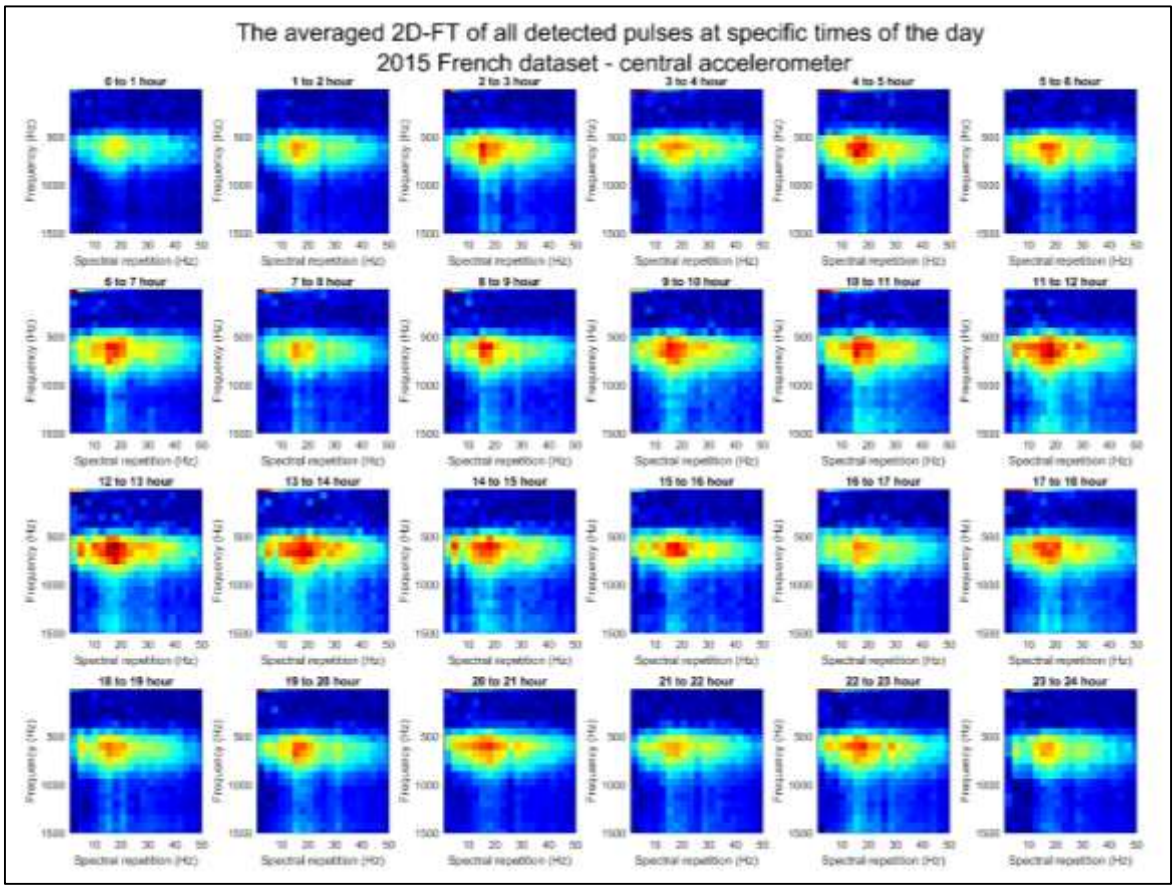

Figure D21. The mean 2D-FT of all DVA signals detected on the central accelerometer for each hour of the day throughout the full 2015 French dataset. Pixel intensity shows the acceleration amplitude from highest (deep red) to lowest (dark blue) in arbitrary units and logarithmic scale.

To investigate any possible general trend in the hourly change in DVA signal features, all DVA signals that were detected across the entire 2015 French dataset were categorised into one of twenty four groups depending on which hour of the day it was detected. The mean of the 2D-FTs over all pulses within each group was calculated and displayed in Figure D21 for detections pertaining to the central accelerometer and Figure D22 for those from the periphery. It must be noted that the signal to noise ratio of these DVA signals was so low that in order to display the 2D-FT image of the DVA signal, the background noise had to be removed from the pulsed vibration by subtraction of data immediately

following the pulsed vibration as for the whooping signals in the previous chapter. If this subtraction is not undertaken, the data is dominated by the features of the wing buzzing of the bees.

It can be seen that for both accelerometers there is no effect of the time of day on the spectral repetition of the broadband frequency spectrum associated with the DVA signal, with it stably centred around 14 to 25Hz across all hours of the day, a trend that is also seen for the 2017 French hive data (Figure D24) and the Clifton Observation Hive data (Figure D26, left, and D27, right). However, a pronounced trend can be seen in the amplitude of the signal, and this is further emphasised for both accelerometer locations in Figure D23. Plotted in Figure D23 is the mean amplitude of the 12 to 25Hz bandwidth component of each mean 2D-FT from Figure D21 and D22. Here it is seen that the amplitude of the mean 2D-FT for each hour increases steadily from midnight, then peaks at 2pm and decreases again until 11pm). Interestingly, the trend appears inverse to that of the hourly occurrence of DVA signals (Figure D13a and D13b), with higher amplitude DVA signals occurring at times when the overall number of detections exhibits a minimum. This can also be seen in the 2017 French hive data (Figure D25), and is most apparent in the Clifton Observation hive data (Figure D28a the left accelerometer and D28b for the right accelerometer. Spearman's rank correlation coefficient confirmed that there is a strong negative statistical dependence between the hourly number of DVA signals and the amplitude of the detected signals for the central accelerometer *(rho = -0.703, $p < 0.001$)* and for the peripheral accelerometer *(rho = -0.835, $p < 0.001$)* of the French 2015 dataset. This trend is also observed for the Clifton Observation hive left accelerometer *(rho = -0.896, $p < 0.001$)* and the right accelerometer *(rho = -0.668, $p = 0.0155$)* and the French 2017 hive dataset *(rho = -0.898, $p < 0.001$)*.

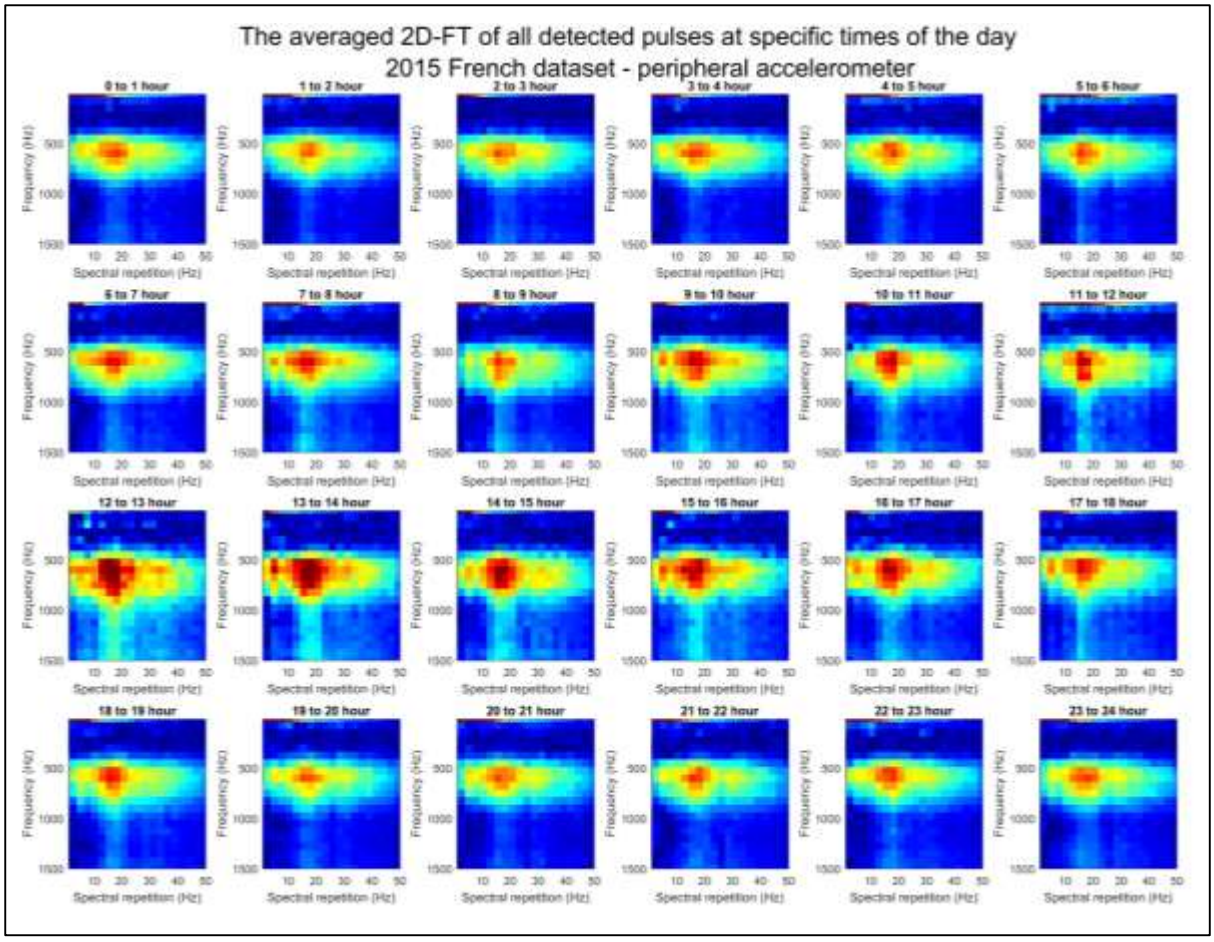

Figure D22. The mean 2D-FT of all DVA signals detected on the peripheral accelerometer for each hour of the day throughout the full 2015 French dataset. Pixel intensity shows the acceleration amplitude from highest (deep red) to lowest (dark blue) in arbitrary units and logarithmic scale.

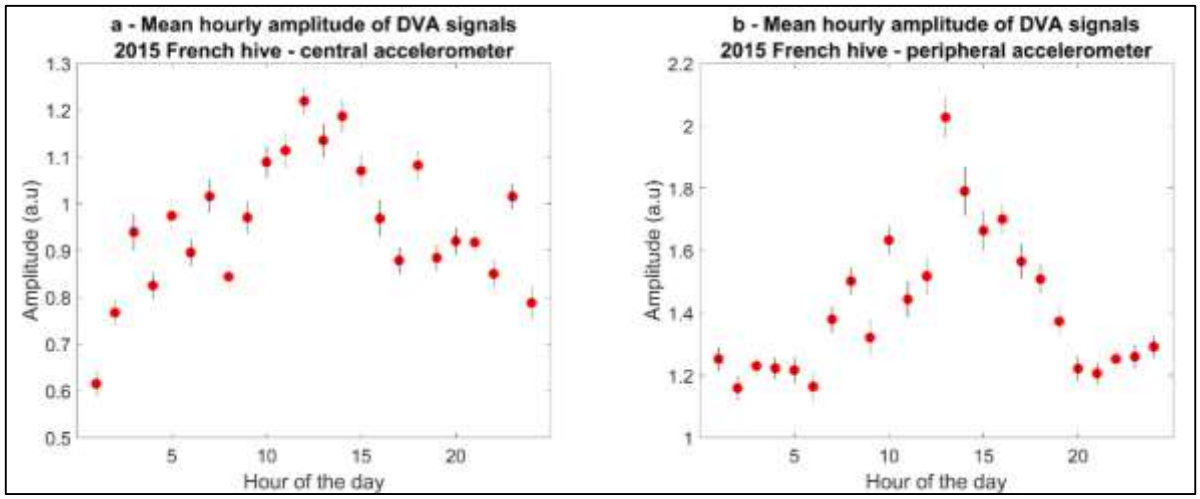

Figure D23. The mean (±1SE) hourly amplitude for the 14 to 25Hz horizontal spectral bandwidth of the DVA signals detected within the 2015 French hive dataset by a) the central and b) the peripheral accelerometer.

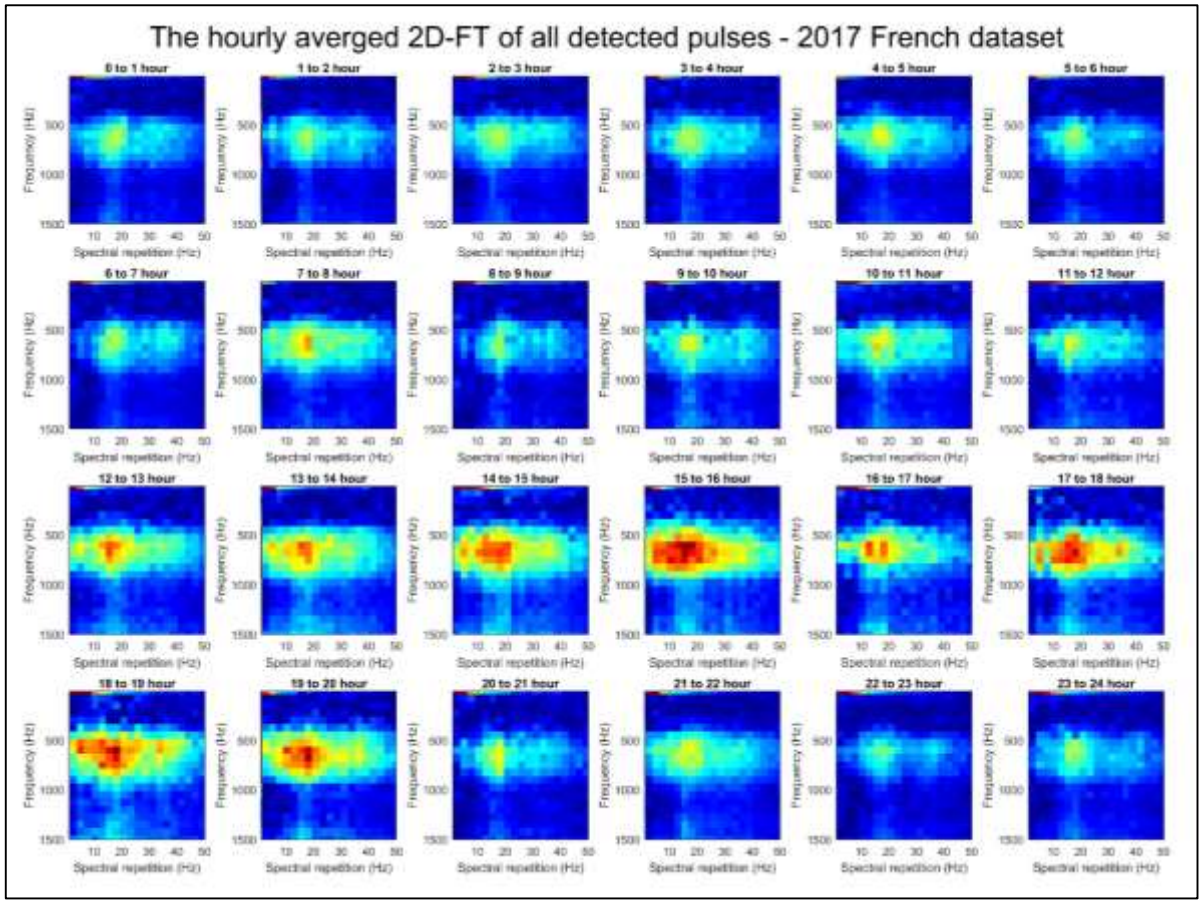

Figure D24. The mean 2D-FT of all DVA signals detected on the centrally placed accelerometer for each hour of the day throughout the full French 2017 hive dataset. Pixel intensity from dark blue (low) to dark red (high) denotes the amplitude in arbitrary units.

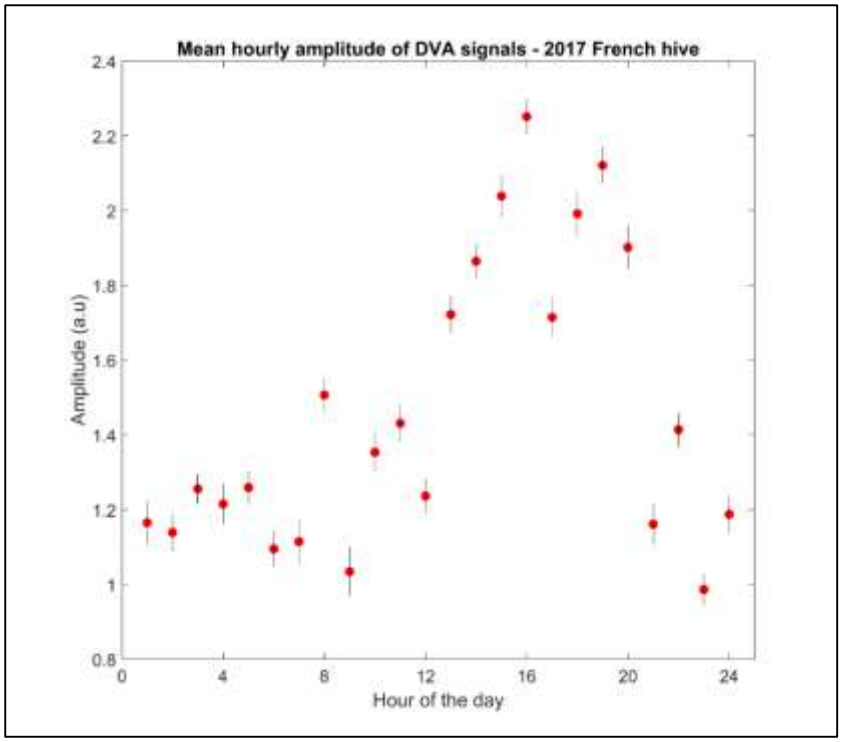

Figure D25. The mean (±1SE) hourly amplitude for the 14-25Hz horizontal spectral band of the DVA signals detected within the French 2017 hive dataset

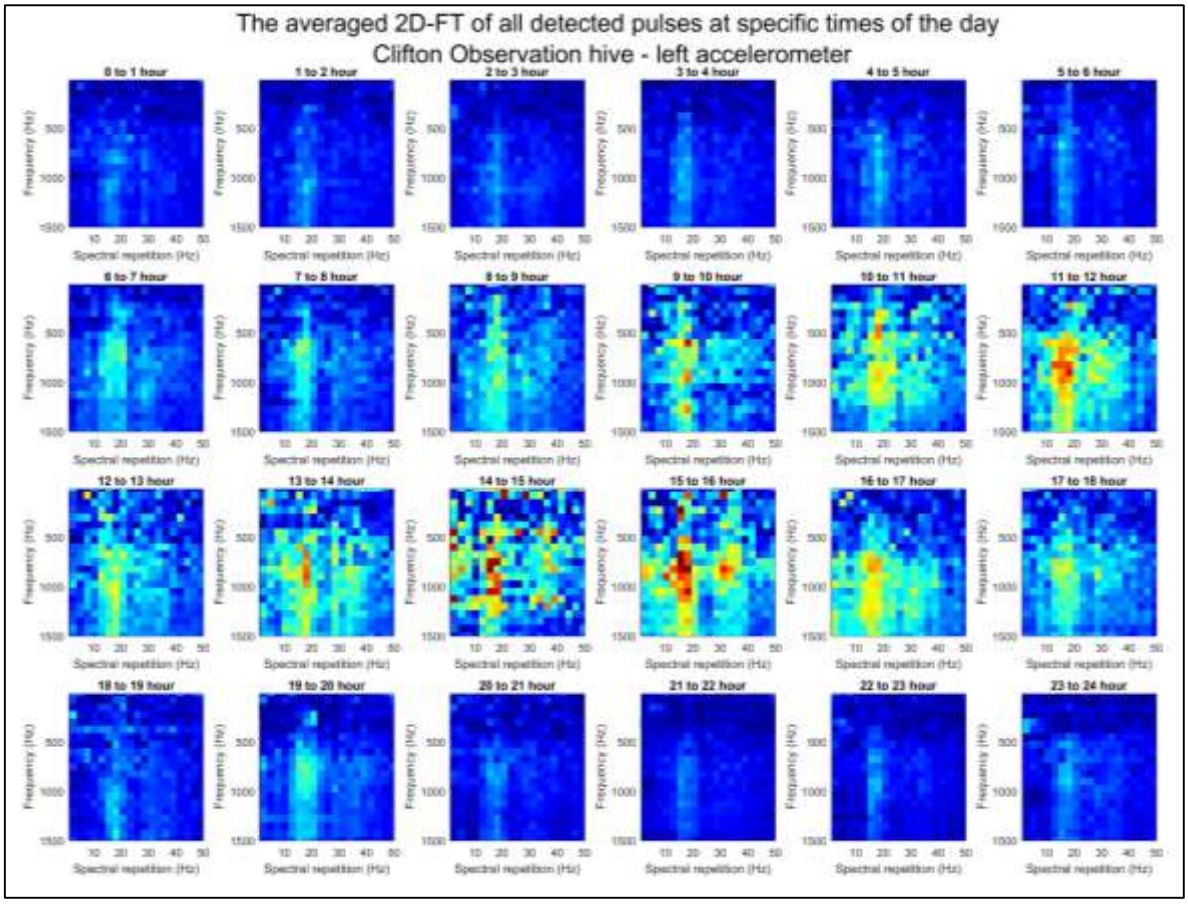

Figure D26. The mean 2D-FT of all DVA signals detected on the left accelerometer for each hour of the day throughout the full Clifton Observation hive dataset. Pixel intensity from dark blue (low) to dark red (high) denotes the amplitude in arbitrary units.

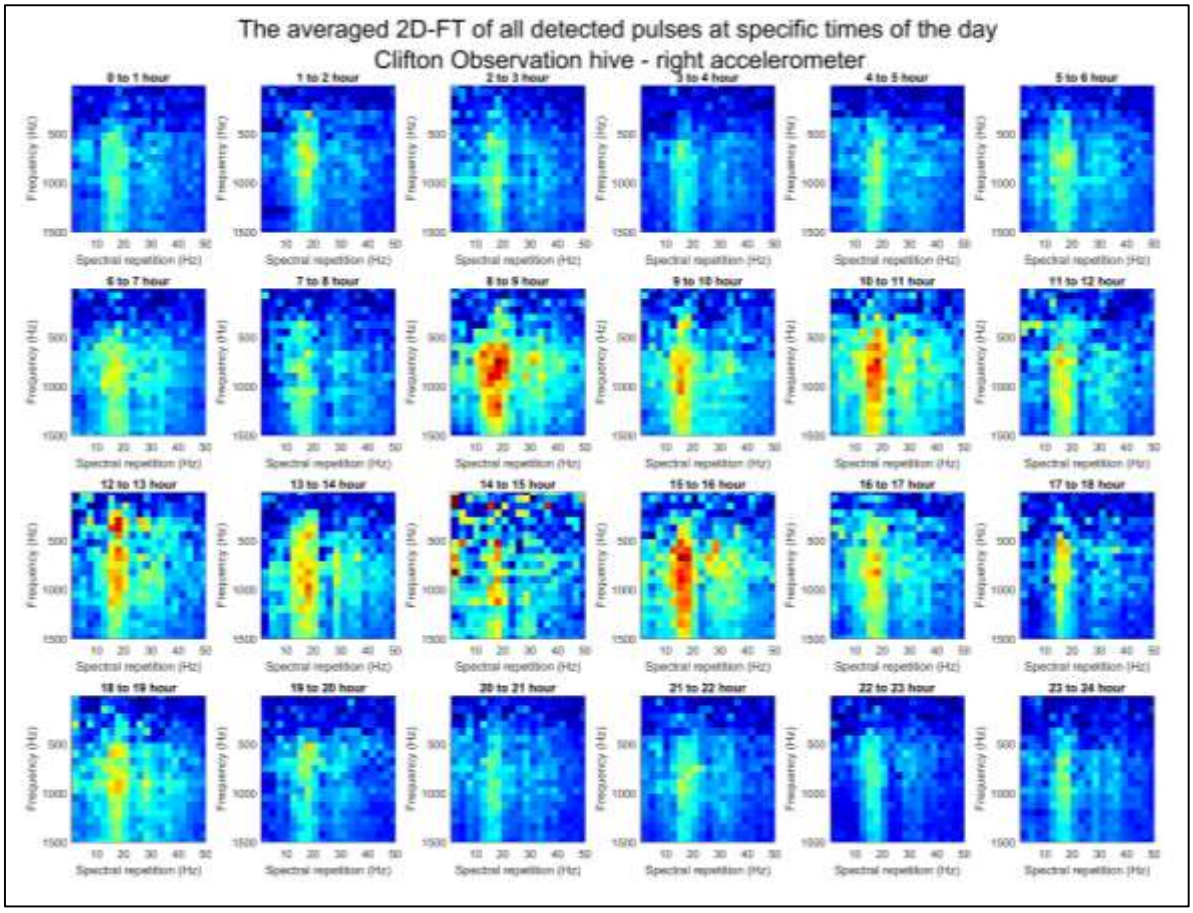

Figure D27. The mean 2DFT computed over all DVA signals detected on the right accelerometer between each hour of the day across the entire Clifton Observation hive dataset. Pixel intensity from dark blue (low) to dark red (high) denotes the amplitude in arbitrary units.

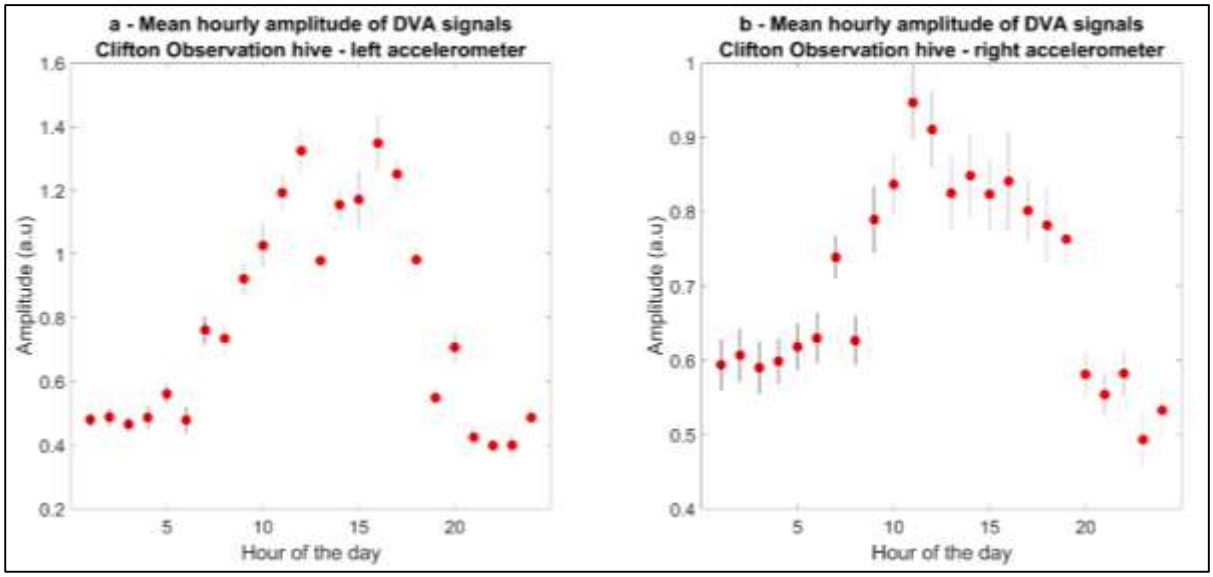

Figure D28. The mean (±1SE) hourly amplitude for the 14-25Hz horizontal spectral band of the DVA signals detected within the Clifton Observation hive dataset.

Interestingly, as seen for the French 2015 hive, the DVA signals that were detected at the periphery of the frame were observed to have a 50% higher amplitude overall to those found at the centre of the frame (*t = 8.308, p < 0.001*), with a mean amplitude of 1.453 ± 0.252 (a.u.) compared to 0.947 ± 0.146 (a.u.), respectively. There is no significant difference between the amplitudes of DVA signals detected by the left (mean = 0.7817 ± 0.136; Figure D31) or the right (mean = 0.7917 ± 0.321; Figure D32) accelerometers that made the Clifton observation hive dataset that were placed on the same horizontal axis equidistant from each other and the wooden frame *(t = -1.35, p = 0.893)*.

In order to investigate this hourly phenomena on a daily basis, the amplitude of DVA signals that occurred over each hour of recording was computed and is displayed over each day, in Figure D29 for the central accelerometer and Figure D30 for the peripheral, which allows us. However, as seen in Figures D29a and D30a, it is difficult to observe any trend over a single day. It is only upon averaging the data across enough days (e.g. 20, as shown in Figures D29b and D30b), that the trend in Figures D21 and D22 becomes more apparent. In other words, there are not enough DVA signals detected throughout an average day to show confidently that this trend definitely occurs throughout each day of the recording.

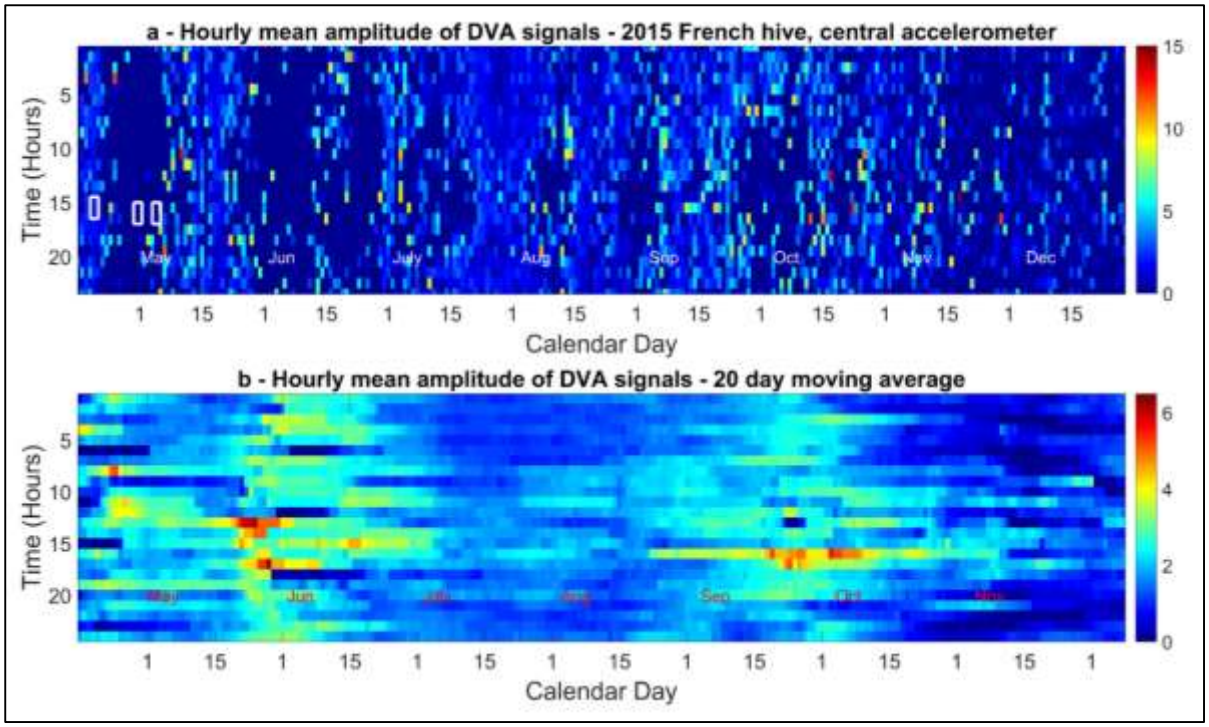

Figure D29. The mean amplitude of DVA signals (a) calculated for each hour of recording; and then (b) averaged horizontally over a 20-day window for the detections by the central accelerometer of the French 2015 hive dataset.

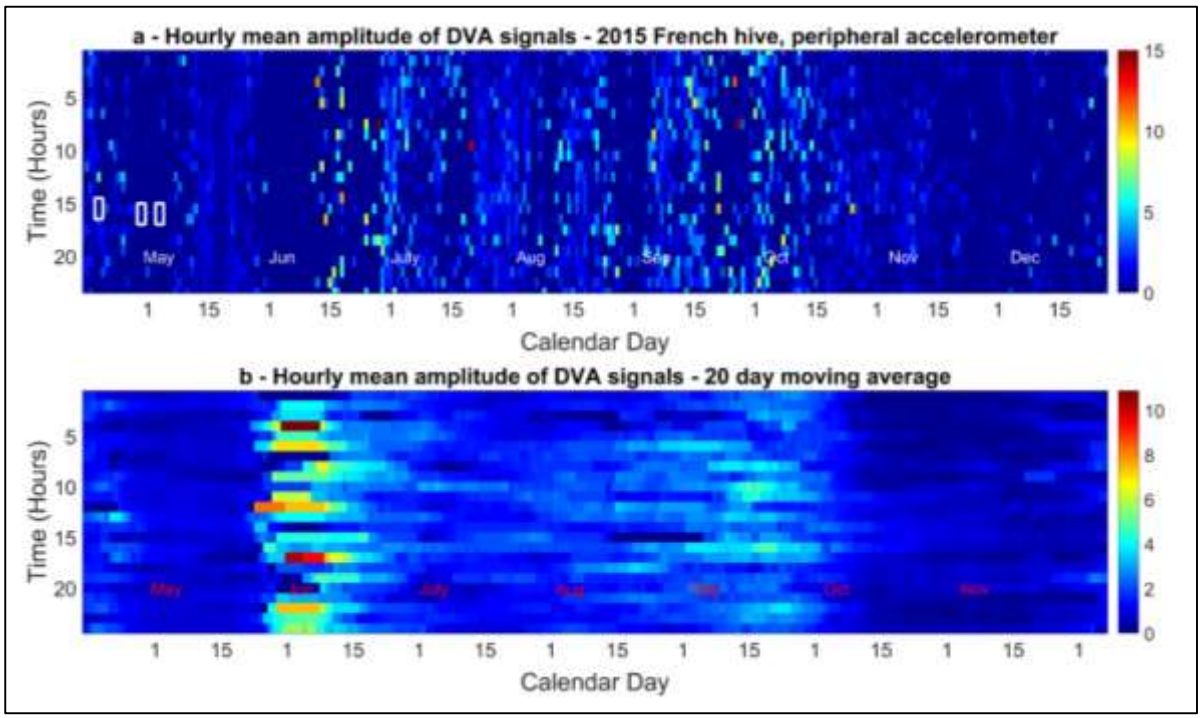

Figure D30. The mean amplitude of DVA signals (a) calculated for each hour of recording; and then (b) averaged horizontally over a 20-day window for the detections by the peripheral accelerometer of the French 2015 hive dataset.

Cumulating rather than averaging the amplitudes of the DVA signals detected for each hour (Figure D26a and D27a) allows for instances of DVA signals that are both numerous ***and*** strong to be highlighted. At 11am on the 20th April 2015, the highest sustained cumulative amplitude over the entire 2015 French hive recording can be observed, and this is sustained in the hours either side of the primary swarm, confirming that these sections of recording contain the highest density of high SNR DVA signals (>50 per hour). In the hour containing the primary swarm, no DVA signal is detected and thus the cumulative signal amplitude is zero. When summating the hourly amplitudes (Figure D26 and D27) of DVA signals, the opposite trend can be observed compared to the computation of the mean (Figure D24 and D25), due to (around three times) more DVA signals having been detected at night (around 3x), as compared to the middle of the day (Figure D13).

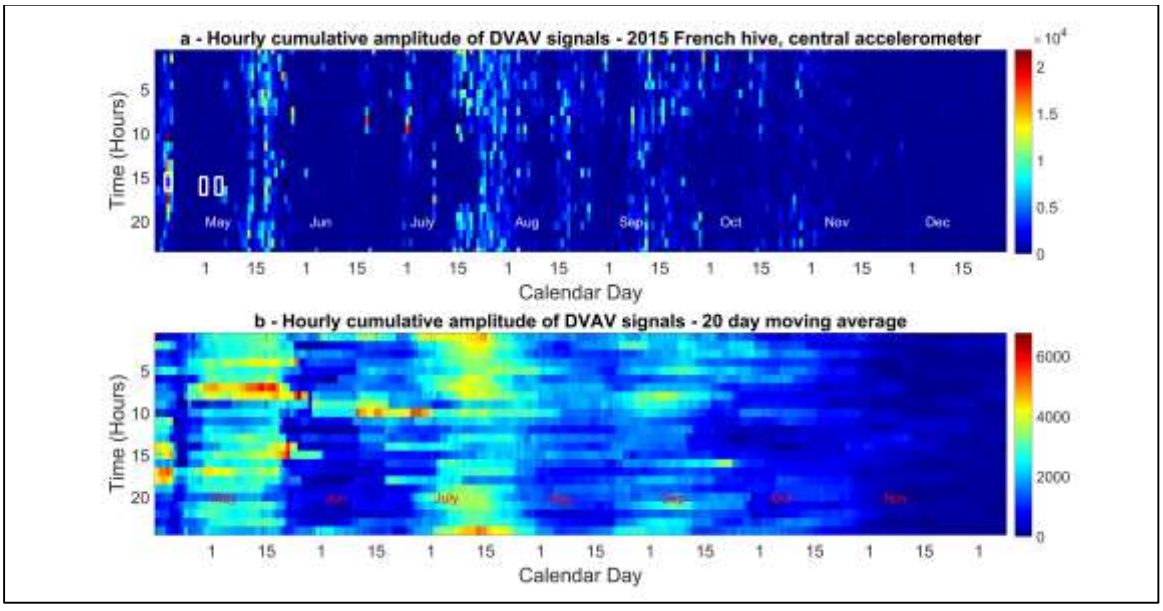

Figure D31. The amplitude of DVA signals that are (a) summated over each hour of recording; and then (b) averaged over a 20-day window for the detections by the central accelerometer of the French 2015 hive dataset.

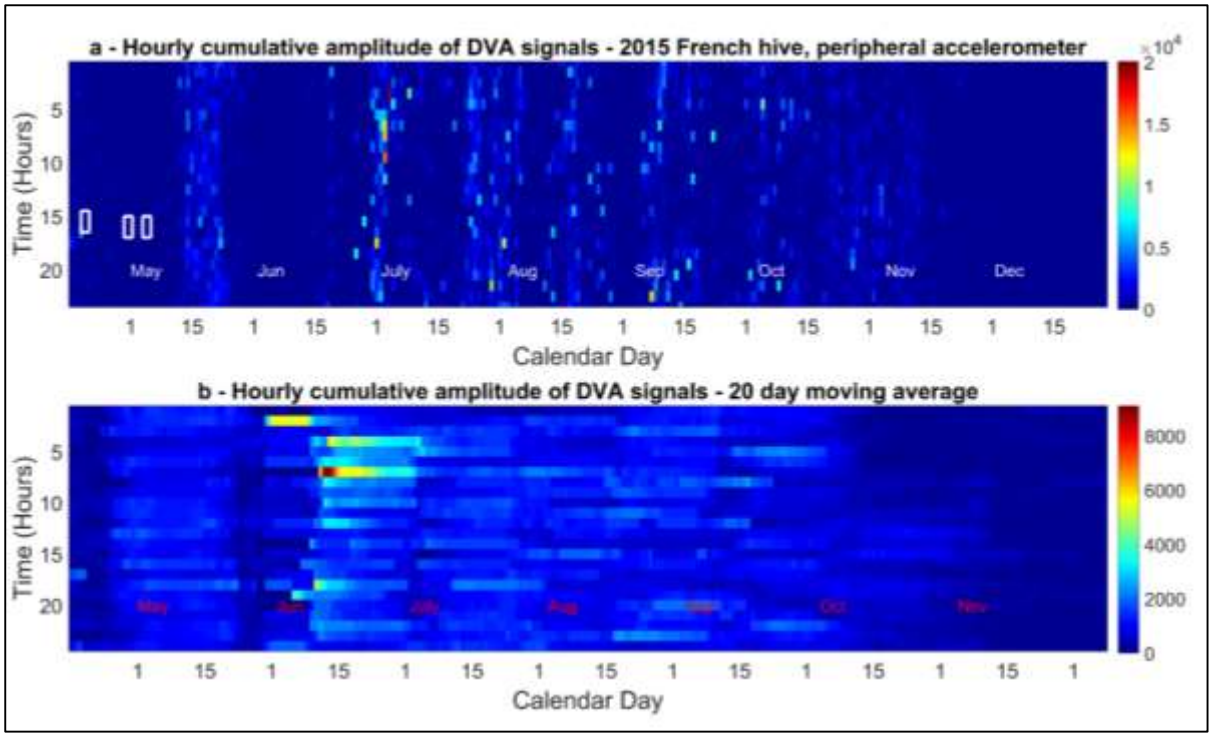

Figure D32. The amplitude of DVA signals that are (a) summated over each hour of recording; and then (b) averaged over a 20-day window for the detections by the peripheral accelerometer of the French 2015 hive dataset.

4.3.6. Daily two-dimensional Fourier analysis

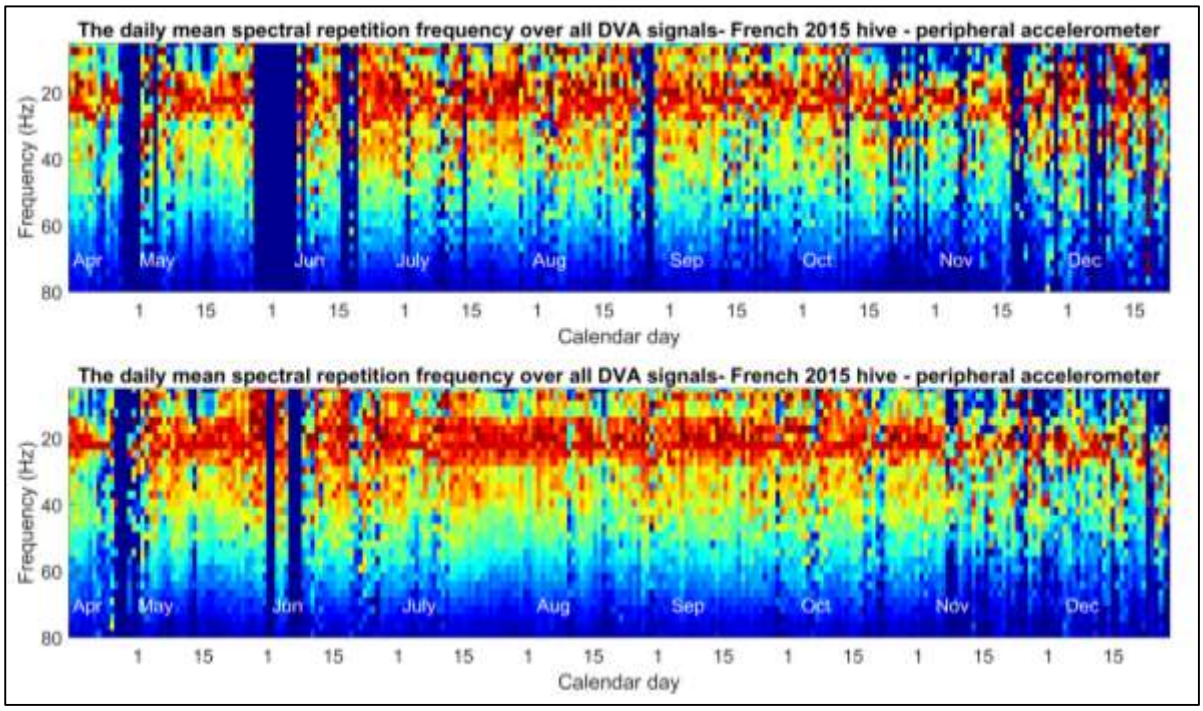

Figure D33. The daily mean spectral repetition frequencies of the DVA signals detected within the 2015 French hive dataset for the central (top) and the peripheral accelerometer (bottom). The x-axis shows the calendar day number over which the 2D-FT average was calculated, the y-axis is the spectral repetition frequency and the pixel intensity shows the mean acceleration amplitude at each frequency of the DVA signal in arbitrary units, scaled to its maximum every day.

In Figure D33 it is seen that the peak frequency (spectral repetition) of recorded DVA signals remains stable across the year at a fundamental frequency found between 14Hz and 25Hz at both the centre and periphery of the frame for the French 2015 dataset. There is a reoccurring strong peak at 7Hz that disappears in the winter time. Further, the mean peak frequency over the year is 20.3Hz ± 3, supporting the findings of Figure D10. This trend stability is confirmed by simple linear regression that deduced that the peak frequency of detected DVA signals cannot be predicted by the day number ($r = 0.0011$) with data showing statistical significance ($p < 0.001$). The same trend can be seen for the peripheral accelerometer, with no relationship occurring between frequency and time ($r = 0.024$, $p = 0.283$).

In Figure D33, the frequency of the mean daily spectral repetition of the DVA signals detected within the 2017 French hive dataset (Figure D34) also remains stable across the entirety of recording centred at a mean of 20.1Hz ± 3.2 until it was found to have collapsed in late November. This is confirmed by simple linear regression showing that the peak frequency of detected DVA signals cannot be predicted by the day number *(R =0.523, p =0.0306)*. There was no detection of DVA signals until the 16th May and therefore the image appears dark blue for this period. After mid-September, the plot becomes more scattered owing to the reduction in the number of detections as the colony gradually deteriorated as seen in Figure D14.

Again, the data pertaining to the mean daily 2D-FT of the Clifton Observation Hive (Figure D35) shows that the frequency of the DVA signals also remains stably centred at a mean of 19.679Hz ± 3.21, confirmed by simple linear regression for the left *(Frequency: r =0.054, p =0.0269)* and the right accelerometer *(Frequency: r =0.035, p = 0.149).* Due to the reduction in the number of detections during December through until March, the plot appears noisier for these months in Figure D34. However, the trend is retained during this period.

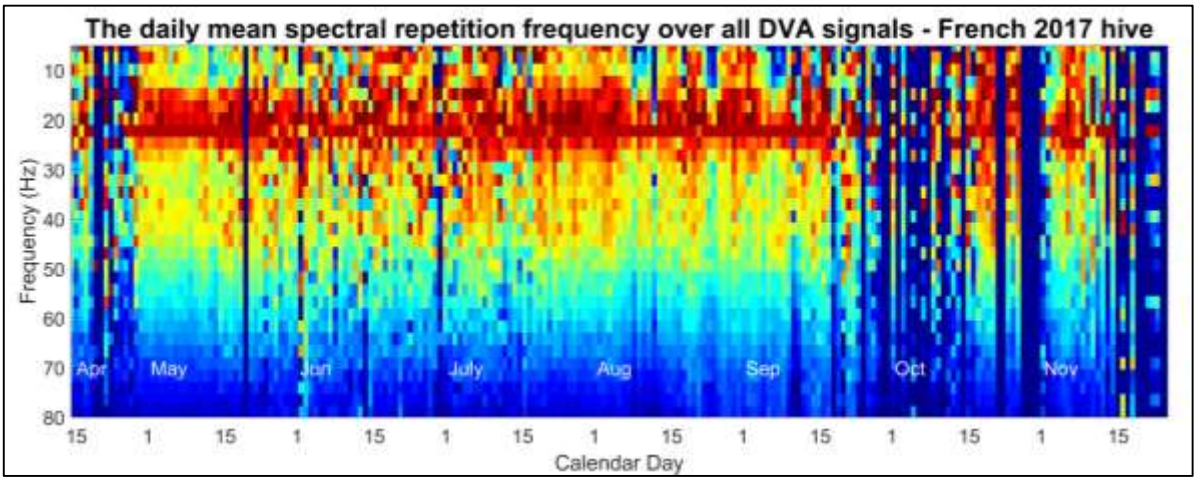

Figure D34. The spectral repetition of the mean 2D-FT (y-axis) computed for all DVA signals within each day of the recording. The x-axis shows the day over which the 2D-FT average was calculated, the y-axis is the mean over the spectral repetition (Hz) for the mean daily 2D-FT image and the pixel intensity shows the intensity of each frequency of the DVA signal in arbitrary units, scaled to its maximum each day.

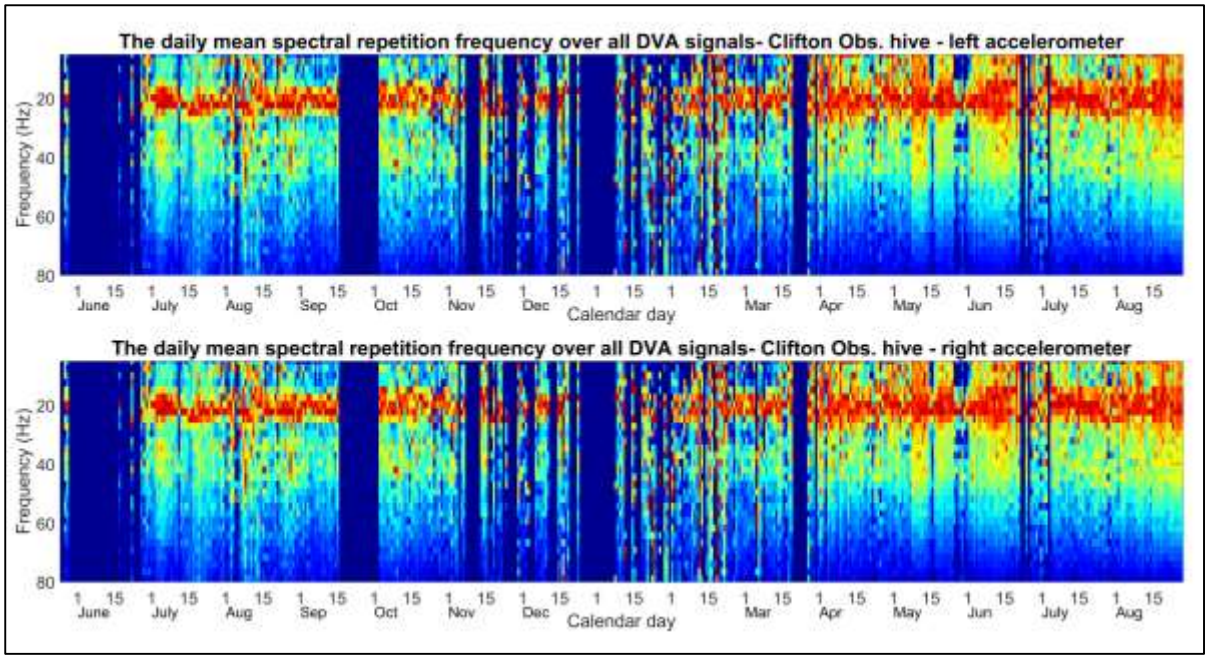

Figure D35. The daily mean spectral repetition of the DVA signals detected within the Clifton Observation hive dataset for (a) the central accelerometer (top) and (b) the peripheral accelerometer (bottom). The x-axis shows the day number over which the 2D-FT average was calculated, the y-axis is the mean over the spectral repetition (Hz) for the mean daily 2D-FT image and the pixel intensity shows the intensity of each frequency of the DVA signal in arbitrary units.

4.3.5. Supporting video evidence

All videos are comprised of a soundtrack, containing the raw data from the accelerometers embedded in the honeycomb under video analysis. The left channel always corresponds to the left accelerometer of the side with visible sensors.

A honeybee delivering a DVA signal directly onto one embedded accelerometer can be seen and heard in Video D1. For comparison, a honeybee delivering a DVA signal on the other face of the frame, near the same embedded accelerometer (not visible), can be found in Video D2. Both produce high SNR traces. In Video D2, following the first audible DVA signal, the signaller is seen to move slightly away (~5mm) from the accelerometer and produces a second, inaudible DVA signal. This demonstrates how local the DVA must be (to the accelerometer) in order to be audible and it also provides evidence that the software is able to detect DVA signals on both sides of the frame.

Both DVA signals display the characteristic Π-shape in the frame by frame image of the time course of acceleration, which is also shown in synchrony in Video D1 and D2. The major difference between the videos is that each knock for the DVA performed on top of the accelerometer (Video D1) results in a sharp negative burst of acceleration whereas in Video D2, it is positive. This provides evidence that the polarity of the individual knocks that make up a DVA signal is disclosing the side of the frame on which the signaller is residing.

In Video D1 and D2, I also show the instantaneous 2DFT computed in synchrony with each of the DVA signals that occurred on each side of the frame. On both videos, two vertical bands at around 17Hz and 34 Hz can be observed. Furthermore in Video D2, as the bee moves further away and produces an inaudible DVA signal, the vertical bands still appear on the 2DFT image showing how sensitive and useful the 2DFT is in the analysis of these pulsed vibrations that convey very weak audible signals.

Provided in Video D3 is the analysis of the collection of 27 high-SNR pulsed vibrations that were used in the initial vibrational quantitation of DVA signals. The time course of the acceleration, the image of the time course chopped into its individual knocks, the mean acceleration of a typical knock and the

2D-FT image are all provided, together with the raw accelerometer recording in the audio of the movie. It can be seen that each elicits the characteristic Π-shape in the knocks, as the signaller's rate of delivery increases, remains constant and finally decreases. These knocks can be seen to have either sharp positive or negative acceleration depending on the side of the accelerometer the DVA signal was performed. Analysis of the 2D-FT for each signal showed that each systematically elicited two vertical broad bands at a spectral repetition corresponding to that of the number of knocks (between 13 and 24Hz), and a second harmonic at twice higher frequency. These DVA signals have such high SNR that no background removal is necessary for their analysis.

To further demonstrate the sensitivity of 2D-FT analysis for DVA signal examination, in Video D5 I present an example of an inaudible DVA signal that was successfully identified by the detection software. The data shows that the vertical bands on the 2D-FT image that are associated with honeybee DVA signals are clearly visible even though no audible information can be perceived. This, in combination with other examples of inaudible true detections (Table D3), is strong evidence that the 2D-FT is a better assessment of the validity of the accelerometer trace that pertains to DVA signals than human hearing.

4.4.0. Discussion

4.4.1. Detection of DVA signals – New horizons

The DVA signal is well known from visual inspections of honeybee activities upon the comb, requiring an observation hive and necessarily resulting in relatively short-term measurements. However, this work discloses the first ever measurement of DVA signals that does not rely on any visual inspection. In this study, I showcase an intra-comb pulsed vibration that matches a DVA signal with strong video evidence of the one-to-one relationship between a DVA signal being produced and the resulting accelerometer waveform.

One of the most exciting outcomes of this work is that the characterisation of the physical properties of a DVA signal, the vibrational properties of which have never previously been explored, has provided an effective method to automatically detect pulsed vibrations that are inaudible without enhancing technology and not necessarily audible to human hearing even with the use of ultra-sensitive accelerometers; advancing the use of accelerometer technology for the in-situ non-invasive monitoring of honeybees and other social insects. This is validated by the extensive video analysis of true positives, false negatives and false positives where instances of DVA signals occurring on the honeycomb are shown without any perceptible trace in the raw waveform, but correctly detected by the software.

The initial analysis of the physical properties of DVA signals is in keeping with the results of past previous researchers, such as Gahl (1975) who determined that a DVA signal lasted for 1.2 ± 0.3 s and produced vibrations at 16.3 ± 5.8 Hz. Upon analysis of the twenty-seven extracted DVA signals with high signal to noise ratio, a mean DVA signal frequency of 18.21Hz and a duration of 1.01 seconds was obtained, well within the range described by Gahl (1975). Owing to the repeating pattern of individual knocks that make up the DVA signal, the existence of these features within a signal waveform can best be identified using 2D-FT analysis, even when the signal to noise ratio is exceptionally low. The 2D-FT

can therefore be considered as a tool more powerful than critical listening for detecting and assessing the validity of detected DVA signals, where strong vertical broad bands at narrow horizontal frequencies around 20 Hz and multiples, known to be associated with DVA signals, are clearly seen. In instances where a bee delivers a DVA on the honeycomb, the collisions between the honeybee's abdomen and the honeycomb does produce a detectable vibratory component within the immediate vicinity of the collision focus. It is sometimes possible to hear the signal due to the strength and resonances caused by the individual abdominal knock but this is modulated by the current state of the honeycomb or concealed within the ambient vibrational noise coming from other sources of bee activity. To my knowledge, the 2D-FT has never been a used as a method for the assessment of biological signals and as a result I am able to monitor the DVA signal continuously within long-term datasets with outstanding sensitivity. While not every DVA will result in the detection of the trace, further work could act to improve the efficiency of this detection method. Furthermore, DVA signals are often delivered by bees repeatedly during a shaking run (see Video I1) whilst they move around the honeycomb, resulting in meaningful statistics even when measured at a single location upon the frame. Finally, their very high occurrences and fairly high (33%) rate of delivery with abdomen-honeycomb collisions are also in favour of this method.

4.4.2. Quantitation of DVA signal properties

Through the analysis of the time course of the acceleration of DVA signals that were delivered directly on to the locus of the accelerometer, a characteristic Π-shape appears when the window length is appropriately adjusted. This shows that the individual abdominal knocks associated with this signal's production occur at regular intervals that decrease, plateau and then increase in duration towards the end. Through the alignment and averaging of these knocks, it is possible to determine an acceleration of approximately 0.16m/s^2 for each knock, another feature of strong DVA signals that has never been seen before for this signal. Owing to the fact that the accelerometer has been placed onto one side of

the foundation wax supplied to the young swarm, the sensor subsurface depths are different on each side, and the magnitude of the accelerometer signal that occurs on the side of the frame without the protruding accelerometers is much reduced to 0.07 m/s^2 as a result.

The spectrogram of the acceleration of the waveform does not provide generic-enough information specific to the accelerometer trace of the DVA signal, although it allowed us to successfully extract whooping signals in Chapter 3. Each abdomen-to-honeycomb knock produces a high amplitude ultra-sharp spike containing a broadband spectrum of frequencies. It is the regularity in time and in shape of these high amplitude spikes that makes the 2D-FT an effective tool in the extraction of features that are highly specific to the DVA signal. Whooping signals do not exhibit spectral repetition patterns that would be detected by the 2D-FT and thus software aimed at their detection would not benefit from using it. Through computation of the 2D-FT of other commonly occurring signals within a hive, it was possible to demonstrate the exclusivity of the two vertical bands at approximately 18 and 36Hz to DVA signals. The software that was written to automatically detect DVA signals was originally shown to confuse DVA signals and high amplitude clicks resulting in the necessity of an additional second pass to discriminate between them. Owing to the multiple vertical broad bands associated with the high amplitude "clicks" on the spectrogram in Figure D5e, resembling the broadband spectra originating from DVA knocks, it is easy to see how the software struggled to segregate the "DVAs" and the "clicks" categories in initial efforts of using a single-pass detection software. The initial analysis of the 27 high-SNR DVA signals along with the findings of Gahl (1975), suggested that the pulse takes place for an average duration of around one second, dictating the time duration that was used as the period over which the 2D-FT was calculated in the detection software. Through computation of the 2D-FT on the collection of DVA signals digitally extracted after the second pass, in addition to critical listening (for more information see Table D3 and Audio D1), signals were visually inspected and they all exhibited the two bands with a fundamental frequency between 13 and 25 Hz, which previously had been shown to be unique to DVA signals, although not over such a large range of values. It can be seen that the broad band between 13 and 25Hz is present in all analyses. Finally, extensive analysis of video software

was undertaken where the detection software scanned the raw accelerometer data associated with video footage of the Clifton observation hive. The results were then cross-checked using visual inspection of DVA signals occurring in the footage. This gave further confidence that the majority of what the detection software had been identifying was made up of true DVA signals. In the future, other honeybee vibrational pulses of interest my benefit from 2D-FT analysis, including queen tooting and quaking for example.

4.4.3. Long-term statistics – New insights into the function of the DVA signal

On an hourly basis, upon averaging the amplitude of DVA signals detected at specific hours of the day across the entirety of the dataset, it was found that at times of low occurrence the DVA signal amplitude is higher than during times of high occurrence. In other words, DVA signals at night were lower in amplitude but higher in occurrence and those detected during the "lunchtime lull" had a higher amplitude. This trend is found across all three datasets, even though there is statistically not enough DVA signals throughout an average day to show confidently that this definitively occurs throughout each day of the recording. Averaging over multiple days (e.g. 20) is required to highlight this trend. Nevertheless, one possible explanation for this inverse correlation between amplitude and occurrences is that those DVA signals that take place during the day may be associated with excited foragers returning from resource patches conveying urgent information. This could cause the foragers to DVA with more energy to alert the colony. In contrast, at night time the individuals are less frantic within the hive as the urgency of foraging has diminished. An important remaining question is why is there an activation signal occurring so commonly at night time. Perhaps there is a function beyond that of being solely a honeybee activator. If the purpose of the DVA signal differs at night time, then this would also suggest that the function of the DVA signal can be switched by the amplitude that the signal is delivered with.

It is also possible that more DVA signals are detected at night because of a shift in the ratio of DVA signals in favour towards those that are delivered directly onto the honeycomb. Observations throughout this study suggested that the abdomen of a honeybee performing a DVA signal made contact with the honeycomb around 30% of the time. It has also been shown that each knock of the DVA signal responds vibrationally in a different way depending on the load within the frame. As seen throughout videos that were acquired as part of this thesis, in addition to observations by numerous authors, honeybees will repeatedly produce a DVA signal even on the honeycomb where there is stored honey and on other features such as queen cups. It could therefore be that honeybees can make assessments into the local contents of the frame below them by producing this signal then sensing and analysing the vibrational response. At night, the probability of a honeybee delivering a DVA signal into the honeycomb might be much greater as they assess the honeycomb beneath for the storage of the days forage. There might even be a detectable difference in the honeycomb response between the areas of developing brood and that of honey storage.

4.4.4. DVA signal stability

It can be seen that there is no noticeable effect of time on the daily average of the peak signal frequency, which remains remarkably stable throughout all three datasets. These results showed that, on average, a honeybee administering a DVA signal within a colony will use a similar frequency regardless of the country, the current colony status, and even in this particular case of colony failure, as demonstrated by French 2017 hive, where the colony deteriorated until it died. Fewer DVA signals were detected during this time causing a more scattered image on the daily 2D-FT but this is perhaps a consequence of a decline in population size. It is also possible that the colony did produce weaker DVA signals that were dismissed due to the low SNR exhibited by any DVA signal waveform, and the DVA signals displayed are only those produced by the remaining healthy individuals of the colony. Video data for such failing colonies is the only way to determine the cause of lower detection numbers.

It is seen that DVA signals correlate positively with the brood cycle as seen with previously published data on the occurrences of honeybee whooping signal. It is therefore interesting that there is no relationship found between whooping signals and DVA signals. One explanation for this is the effect of frame load that attenuates whooping signals and probably DVA signals. The differences in the occurrence of these two pulsed signals strongly supports their major difference in function, with the whooping signal probably most often being an un-intentional startle response to a surprise stimulus within the hive and the DVA signal being an intentional modulatory signal likely produced by an individual in response to external stimuli.

4.4.5. Spatial analysis of DVA signals.

For accelerometer technology to be an effective method of sampling DVA signal occurrences, the signals must appear to be delivered homogenously across the honeycomb, even when the density of individuals is low and the percentage of DVAs delivered onto the honeycomb must be constant when compared to those delivered onto another honeybee. The fact that the number of detected DVA signals correlates positively between the two accelerometers in Figure D11, for the French 2015 hive, and Figure D29 for the Clifton Observation hive, is in keeping with the results of Figure D10, which suggests that regardless of the number of DVA signals that occur the distribution should be even across the honeycomb. This further supports the use of a single accelerometer placed in the centre of the honeycomb as being sufficient in capturing a meaningful and representative general view of the number of DVA signals occurring at that time on that frame, providing that the time duration of the accelerometer measurement is long enough (one hour to one day, depending on the occurrence rate).

In this study, through the cumulative analysis of the amplitude of DVA signals that occurred in each hour of recording, it is shown for the first time that there is an unprecedented increase in the cumulative amplitude of DVA signals in the hours preceding and following a primary swarm. These, however, can only be heard on one channel, but the occurrence plots (Figure D11) exhibit enhanced

DVA signals both on the peripheral and central accelerometers. As I have shown that the spatial distribution of DVA signals is even across the comb, this provides further evidence that the detection algorithm detects DVA signals that are not necessarily audible.

Albeit anecdotal, there does appear to be a decrease in the number of DVA signals recorded on each video footage used in the analysis of the spatial distribution as the 2016-year progresses with an increase in the April 2017 footage. This supports the long-term trends seen for the 2015 French hive (Figure D11) and the Clifton Observation hive (Figure D29) that suggests a peak in the occurrence of DVA signals in July with a steady decrease as the year progresses until a drop off in November. In addition, Figure D10a shows that in July 2016, 214 signals were recorded on film in only 10 minutes, which extrapolates to 1284 signals taking place on the honeycomb per hour. Thorough observations of video data for the corresponding hours suggest that an hourly average of 339 DVA signals occur on this particular frame. Therefore, this data showing that an average of nine per hour are captured on the accelerometer suggests that perhaps 1 to 2% of the DVA signals delivered on the frame are captured by this method. However this capture rate has shown to be as high as 30% at times of low frame-load. This is to be expected as this study was only focused on DVA signals that occur (i) directly on the honeycomb and (ii) on or in the immediate vicinity of one to the sensors, thus it would suggest that the technology was only sampling around 2% of the frame's total surface area. As hightlighted before, due to the homogeneity of DVA signal delivery across the honeycomb (Figure D10), sampling such a small surface area can be still be meaningful.

Our observations for the Clifton observation hive also showed that as the colony developed only to the left side of the hive, and the number of DVA signals reduced on the right face as it became the outer edge of the colony. Had the frame been at the centre of the colony, the number of DVA signals observed might have been much increased, suggesting that DVA signals tend to be focussed more towards the heart of the population.

The significant increase in the amplitude of DVA signals detected at the bottom periphery of the frame compared to those at the centre, as shown by the amplitude comparisons of the French 2015 hive dataset could result from the peripheral accelerometer being subjected to a lighter frame load than that of the centrally placed sensor. This is quite usual on any frame and is further supported by the lack of such a difference in the amplitudes of DVA signals detected by accelerometers placed along the same horizontal axis at the centre of the frame. Additional support for this can be found in Sandeman et al. (1996) where it was shown that combs that had been detached from the outer wooden frame facilitated the transmission of vibrational cues whereas attached combs had a dampening effect, and honeybees were shown to proactively free the comb from those attachments precisely in those areas of the nest used for recruiting other foragers, which is usually at the bottom of the frame (Sandeman et al., 1996). They also found that signals sent on empty cells were transmitted much better than on capped brood cells and had less attenuation (Sandeman et al., 1996). This further supports the suggestion that the peripheral accelerometer was placed near an area of free / less loaded comb that allowed for reduced dampening of the DVA signals.

4.4.6. DVA signals and weather

The data for the DVA signals recorded under different weather conditions was highly scattered. This is probably a result of honeybees being largely unaffected by external weather variations, as they produce their own microclimate within the hive. However, we do see that the detected DVA signals are most frequent between 13 and 28 °C. The fact that there appears to be an upper threshold for temperature, where honeybees start producing less DVA signals further supports it being a signal associated with foraging, as bees are known to restrict foraging above and below certain outside temperatures (between 7 and 43 °C, Abou-Shaara, 2014). In keeping with the results of this research, other studies have shown that outside temperatures around 20 °C result in the highest level of foraging from focal hives (Tan, et al., 2012), while temperatures exceeding 40 °C (Blazyte-Cereskiene,

et al., 2012) and preceding 10 °C (Joshi and Joshi, 2010) result in the lowest observation of foraging activity.

Shown in the hourly weather plots for both the 2015 and 2017 French hive datasets in Supplementary Figure 1 of Appendix 7 and 8, respectively, there is a negative relationship between outside humidity and outside temperature. Therefore, the relationship between outside humidity and DVA signals was expected to be inverse of that between DVA signals and temperature. Nevertheless, the same effect of outside temperature can be seen for outside humidity in the weather analysis of the French 2015 data. However, in the French 2017 weather analysis, whilst the same effect of temperature on DVA signals can be seen, there appears to be no trend associated with humidity. This suggests that humidity and temperature act upon DVA signals independently and the effect of humidity is perhaps driven by diurnal variations. As seen in Supplementary Figure 7 and 8, the humidity is highest during the night, when most DVA signals are detected. However, the reduction seen above 80% humidity can be attributed to the decrease in DVA signals detected in the winter time when humidity reached its peak in the 2015 season. It therefore seems unlikely that humidity has any great effect on the occurrences of DVA signals on its own, supporting the findings of Joshi and Joshi (2010).

As seen for the French 2015 and 2017 hive weather data (see Supplementary Figure 1 of Appendix 7 and 8, respectively), days of prolonged and heavy precipitation are actually quite rare, skewing the analysis. This could explain why, overall, rainfall had little effect on DVA signal occurrences. However, it can also be explained by the dual-functionality of DVA signals proposed by this research. It is widely known that honeybees do not forage in the rain returning to the hive to take shelter. It is therefore to be expected that a foraging signal would cease during these times. The overall lack of trend between rainfall the occurrence of DVA signals, the day of heavy rain experienced on the 28th October 2015 that resulted in a reversal in the daily trend seen in Figure D13 and the increased occurrences of DVA signals at night, are all evidence of DVA signals occuring outside the remit of foraging.

4.4.7. DVA signals and foragers.

In keeping with Painter-Kurt and Schneider (1998b), this study supports the hypothesis that DVA signals are a product of the foraging caste. Firstly, they tend to occur more at times when more foragers are more likely to be present in the hive (in the mornings, the evenings and during times of heavy rain). Secondly, the daily histograms of occurrences across all three datasets also fit with Nieh's (1998) findings that foragers tend to produce more DVA signals in the mornings prior to foraging flights and in the evenings when they return to the hive. It also agrees with the interpretation "prepare for greater activity" (Neih, 1998; Schneider, 1991; Seeley, et al., 1998) as in the evenings the foragers would be returning from a day's forage causing a sudden surge in nectar and pollen influx. The reduction of DVA signals during the winter months, a time when the amount of available resources for the bees will be minimal, is further suggestive that this signal is linked to the foraging caste.

On the daily histogram of the French 2015 hive dataset (Figure D11), an enhanced number of DVA signals is seen that are detected prior to the primary swarm (further supporting the "prepare for greater activity" hypothesis) that is followed by a sudden drop off in the subsequent hours, only returning in the hours after the final swarm takes place. It is possible that this is related to the average age and the number of foragers that are remaining within the hive. Until the swarming season is over, the average age of the colony's population is much lower as the majority of the older foragers left with the primary swarm (Winston, 1987). It may also be the case that the majority of DVA signals are localised to the cells of developing virgin queens during this period (Allen, 1959a; b; Schneider, 1991).

4.4.8. Further directions and final conclusions.

Future work will involve further assessment of the vibrational properties of the DVA signals extracted from vibrational datasets of honeybee colonies that are experiencing adverse conditions, such as intoxication from pesticides. It is possible that colonies experiencing specific health disorders do exhibit detectable variations in the characteristics of DVA signals and due to the remarkable stability

of the features that have been shown in this study, any deviations from normality should be easy to spot. One way to confidently make this assessment would be to monitor declining colonies in observation hives, linking the DVA signals that were produced to their exact accelerometer waveforms. If this could be achieved, it would provide an effective early warning sign for beekeepers. It would also be beneficial to assess this signal in relation to agricultural practices. For example, it would be interesting to examine the effect that the sudden harvesting of flowering crops such as oil seed rape (*Brassica napus*) has on the DVA signal production. This crop is planted in spring and harvested in the early summer. During this time, local honeybees have an abundant forage source and the colonies massively expand as a result (Williams, 2015). Upon mass harvesting in early summer it is expected that these large colonies will have lost their primary foraging resource at the peak of their active season. It is therefore to be expected that this signal would significantly reduce after the crop harvesting, as this greatly reduces the availability of forage. However, peaks in DVA signal production will occur as new foraging patches are found (Seeley, et al., 1998).

To conclude, presented here is a study that has made significant advancements in the use of accelerometer technology to study honeybee DVA signals without the severe limitations imposed by visual observations. Through use of analysis techniques that are novel to the science of animal communication I have successfully been able to quantitate the physical properties of the DVA signal that was thought to have no vibrational component, presenting strong evidence for the one-to-one relationship between it and an accelerometer trace, and this has led to a unique signature that has provided the capability to study this signal continuously within long term vibrational datasets. This long term analysis has highlighted that there is still much more work needed to decode the meaning of the DVA signal and to examine what extent it can be used as a proxy for colony health. The present results add another category of honeybee vibrational pulse, the DVA signal, to the collection of pulses that can already be successfully detected (whooping signals, worker pipes, queen toots and queen quacks, see Chapter 3), advancing the field closer to the long-term goal in which all categories will be

automatically logged, without the need to store the raw data, providing a sensitive tool for the non-invasive assessment of honeybee colony status.

4.5.0. Supporting information

Audio D1. Collection of DVAs from a hot spot

- This collection of signals was detected by our software half an hour either side of the primary swarm and is the occurrence hotspot between 2 and 3pm on the 21st April 2015 recorded on the central accelerometer in Figure D11.

Video D1. DVA signal performed on the left accelerometer

- A video excerpt of a honeybee delivering a DVA signal directly onto the accelerometer. The audible accelerometer data is also provided. A window containing a 2x zoom of the DVA signal is interpolated into the video. The synchronised image of the acceleration of each individual abdominal knock demonstrating the typical Π-shape is also shown alongside the synchronised 2D-FT image showing 18Hz broadband peaks in spectral repetition.

Video D2. DVA signal performed on the other side of the frame to that in Video D1 without protruding accelerometers

- In this video excerpt, the raw accelerometer data is provided as the soundtrack. A window containing a 2x zoom of the DVA signal is interpolated into the video. The synchronised 3D image of the acceleration of each individual abdominal knock demonstrating the typical Π-shape is also shown alongside the synchronised 2D-FT image showing 22Hz broadband peaks in spectral repetition. Two DVA signals occur, one is audible and the one that follows is not.

Video D3. Collection of DVA signals with full vibrational quantitation

- Provided in this video is the analysis of the 27 high-SNR pulsed vibrations that were used in the initial vibrational quantitation of DVA signals. The time course of the acceleration of the digital signal can be found in subplot (a), the image of the time course chopped into its individual knocks can be found in subplot (b), mean acceleration of a typical knock is provided provided in subplot (c) and the 2D-FT analysis can be found in subplot (d) throughout the video. For each signal, the audible trace from the raw accelerometer data is also provided. It can be seen that each elicits the characteristic C-shape in the knocks and vertical broad bands at a spectral repetition corresponding to that of the number of knocks in sublot (a). The abdominal knocks can be seen to have either sharp positive or negative acceleration depending on the side of the accelerometer the DVA signal was performed.

Video D4. Video with Grid.

- This is a short sample of video footage with a grid superimposed over the top. The videos used in the analysis of spatial distribution had an identical grid superimposed. Whilst watching the videos, the coordinates of the abdomen of each individual performing a DVA signal was recorded. All videos were in 1080p (full HD) definition at 50 frames per second. There is no audio in the video

Video D5. Inaudible DVA signal with 2D-FT analysis

- A video excerpt of a honeybee delivering a DVA signal directly onto the accelerometer. The accelerometer data is also provided but the signal has no audible trace. The synchronised 3D image 2D-FT showing the broadband peaks in spectral relation can be observed. A window containing a 2x zoom of the DVA signal is interpolated into the video.

Chapter 5: Conclusions and Recommendations

5.1.0. Thesis overview

Following a literature review detailing the background surrounding this work, this thesis is then comprised of three results chapters, each with three central themes at their core: (1) what the in-situ monitoring of specific honeybee pulsed vibrations can tell us about the status of a colony; (2) what long-term statistics be can identified to help to disentangle the function of two specific pulses of vibrations; and (3) how effective is accelerometer technology at assessing the ethology of honeybee colonies? In the first results chapter (chapter 2 of this thesis), the contributions of different sources of vibrational information detected by intra-comb accelerometer technology are shown with a particular focus on the contribution from larvae and pupae developing within the cells of the honeycomb. The next chapter is focussing on the in-situ monitoring of the honeybee whooping signal showing never before seen long-term statistics of this brief vibrational pulse. Finally, the third results chapter (chapter 4 of this thesis) is centred on the vibrational quantitation and long-term in-situ monitoring of honeybee dorso-ventral abdominal shaking signals, disclosing the first ever vibrational characterisation and exploration into the physical properties of this signal using novel methods that allows for its automated detection in long-term continuous datasets.

5.2.0. Contributions and main findings of my work

5.2.1. Data acquisition and processing

This work has pioneered the use of accelerometer technology for the study of honeybee pulsed vibrational messages; in particular, the whooping and DVA signal. No other published work was found to have ever used accelerometers to continuously monitor individual pulsed vibrational messages of honeybees and achieved the extensive data collection as detailed throughout this thesis. The method of using accelerometers placed directly into the centre of the honeycomb to continuously monitor honeybee pulsed vibrational messages has proven to be a completely non-invasive technique for the in-situ study of honeybee communication and behaviour, allowing their natural in-hive behaviour to remain intact whilst under observation. It has proven to be a stable and reliable technique to obtain constant information directly from the heart of the colony, providing advantages in revealing information that is unique to this method.

The machine-learning software that was developed to automatically detect and analyse the individual pulses that occurred in the large vibrational datasets required the use of analytical techniques that are common tools outside of biological sciences; however, their use within the study of biological systems is exceptional and certainly novel in the context of honeybee pulsed vibrations. The detection software can process a full year of continuous vibrational data in under a week and allows long-term statistics to be explored, that would otherwise be too time consuming to analyse manually and, especially in the case of the DVA signal, proved a more sensitive technique than critical listening for their identification. In particular, the methods allowed the continuous monitoring of two signals, the whooping and DVA signal, that have never been examined consecutively for more than a few hours, the statistics of which certainly challenged their most widely accepted definitions.

The observation hive designed as part of this thesis allowed extensive footage of natural in-hive behaviour to be captured from the central frame of the colony with little disturbance to its occupants. It allowed for full HD video recordings of both sides of the frame to be filmed in synchrony with

vibrational data obtained directly from the two accelerometers situated in the honeycomb. This meant that individual accelerometer signals could be paired with visible behaviours on a 1:1 ratio and was crucial in the validation of the software that was developed to automatically detect target pulses within the long-term datasets. Having a mechanised frame extractor, lighting system and through-wall tunnel system combined with the space and natural conditions of a double broodbox set up (see Appendix 1), there is no known laboratory based observation hive like it in the world.

5.2.2. Brood specific vibrational contributions

The first chapter of this thesis was centred on the vibrations associated with developing honeybee brood and aimed to establish the vibratory contribution of the un-emerged population and how it relates to other signals found within complex vibrational datasets that can be obtained using the accelerometer technology. It was found that very little vibratory information pertains to the brood within a honeybee hive than can be detected, suggesting that communication with the emerged worker population must rely on other methods. Whilst no direct vibratory communication signals were observed to emanate from the developing brood during this study, one vibratory cue was found that has the potential to indicate the presence of emerging bees. In some instances, immediately prior to the frame being placed in isolation, individuals that were seen to be emerging from the honeycomb were observed to use their mandibles to cut the wax capping that covered the entrance to their cell. This produced high amplitude clicks on the accelerometer recording that are similar in sound and magnitude to those clicks that were discovered to originate from and emerged adult worker bee captured on video operating upon the cells. However, upon close examination of the time course of the acceleration detected by the accelerometer technology, subtle differences could be observed between the waveforms of the two types of click. Further long-term statistics on the occurrence of the emerging bee clicks within long-term continuous accelerometer datasets reveal its power in determining the presence of emerging brood and, therefore, as a tool for monitoring the honeybee brood cycle.

This work then went on to show, for the first time, the comparative signal to noise ratio of different high quality pulses commonly found within the long-term vibrational datasets. This gave insight into the individual contributions of different vibratory sources within the complex waveform obtained from the heart of honeybee hives.

5.2.3. Whooping signals

The study into the whooping signal demonstrates the long term (over 9 months) automated in-situ non-invasive monitoring of a honeybee vibrational pulse with the same characteristics of what has previously been described as a “begging signal” or a “stop signal”. Statistics on a colony monitored in the UK and another in France show that the signal is very common and highly repeatable, occurring mainly at night with a distinct decrease in instances towards midday, appears correlated with the brood cycle, and that it can be elicited en masse by bees following the gentle shaking or knocking of their hive with distinct evidence of habituation. The results of this study suggest that this vibrational pulse is generated under many different circumstances, thereby unifying previous publication’s conflicting definitions, and I demonstrate that this pulse can also be generated in response to a unexpected stimulus, adding an additional function as a startle response. This work suggests that, using an artificial stimulus and monitoring the changes in the features of this signal would provide a sensitive tool to assess colony status.

5.2.3. DVA signals

In the study of DVA signals, this work discloses the first ever measurement of DVA signals that does not rely on any visual inspection, relying on the one-to-one relationship between a DVA signal being produced and the resulting accelerometer waveform. The vibrational characterisation of a DVA signal and assessments of its physical properties have been explored using novel techniques beyond the usual remit of biological sciences. From this, I propose a novel method, using machine learning and

advanced spectral analysis techniques, for the continuous in-situ non-invasive automated monitoring of a honeybee signal, previously thought to have no vibratory component, which is most often inaudible to human hearing. In this study, three hives were monitored, one in the UK and another two in France showing that the signal is very common and highly repeatable, occurring more frequently at night with a distinct decrease in instances towards mid-afternoon; a trend that is opposite to that of the amplitude of the signals for an average day. It was also shown that an unprecedented increase in the cumulative amplitude of DVA signals occurs in the hours preceding and following a primary swarm. The long-term statistics of this pulse suggests that this signal may have additional functions to that of solely an activation signal, as it appears to occur most commonly at night, and that the amplitude of the signal might be indicative of the switching of its dual, and potentially multiple functions.

5.3.0. Constraints and limitations

The major constraint of the use of accelerometers, or any remote sensing technique, is that they often require visual information to reliably validate the findings. This was overcome, somewhat, by the use of a custom build observation hive with mechanical frame extractor. However, the hive only allows the data to be sampled over limited observation windows before the frame has to be placed back into the hive. This means that constant visual information cannot be obtained resulting in some of the vibrational information remaining still unexplained. Thus far, there is no known non-invasive visual probe that can be placed inside a hive with a large enough field of view that is small enough to fit with the cavity of two adjacent frames.

Another limitation of the method is that it does not necessarily allow for the accurate monitoring of the vibrational pulses pertaining to specific individuals. In the case of the whooping signal, I tried to link the behaviours of the bees to the vibrational pulses based on the synchrony between an audible pulsed vibration and a specific behaviour. Since the vast majority of whooping signal pulses elicit no matching visual phenomena, it is visually impossible to pinpoint the signaller. This work focussed

mainly on monitoring the honeybees at the colony level and for the study of DVA signals there is an obvious visual component associated with them, so this was not an important limiting factor throughout this thesis. Additionally, the use of more accelerometers in an array may allow specific pulsed vibrations to be triangulated to their source, however as shown throughout this thesis, the properties of the honeycomb changes vastly from day to day due to permanent changes in the honeycomb content, honey and pollen storage, the brood cycle and wax aging. In addition to this, previous work has shown that areas of honeycomb have very different vibrational responses and are not even across its entirety. This will therefore provide a great challenge for attempts of vibrational source localisation.

Analysis of duplications in pulse detection between the two accelerometers in the whooping signal chapter shows that the placement of the accelerometers in the honeycomb allows for a detection range of up to 4cm radius when the honeycomb is empty of brood, and this is further reduced for the detection of the low SNR DVA signals. It is also shown that upon increasing the honeycomb mass density, the range of the detection is reduced significantly causing fluctuations in the number of pulses identified by the detection software. It is therefore difficult, in the analysis of long-term trends, to confidently distinguish between genuine pulse production increases and increases that are the result of a decreased frame load that allows for a greater detection radius. This can be overcome in future work by driving a standardised artificial vibration unto the honeycomb for detection by the accelerometer. The detected vibrational response will give an indication of the detection range and physical properties of the honeycomb, which can be used further in order to compensate for this artefact and access the time counts of bee pulses.

5.4.0. Recommendations for future research

An exciting extension of this research would be to comprehensively study the long term statistics of other honeybee pulsed vibrations that have been briefly described within this thesis, such as clicks,

queen pipes, worker pipes and purring signals. Further analysis of these signals and the interactions between them will provide a wider understanding and will shed further light on the function that they possess. It will also will make for a further comprehensive method of non-invasively monitoring the activities inside of a hive.

The method of data collection can be further improved so that it detects, analyses and saves only the information relevant to the pulse of interest. This would extensively reduce the need for the large storage space currently required to record all of the vibrational information that is collected. This would mean that the data collection could be completed by much less expensive technologies with less storage space, making the system more accessible to beekeepers and other scientists.

5.5.0. Concluding remarks

This was a large multidisciplinary project that combined aspects from the fields of behavioural ecology, physics and computer sciences. Through combining various techniques from within these different fields, the work in this thesis has pioneered the study of honeybee pulsed vibrations and has made a significant contribution to the field of biotremology.

The application of this technology extends far beyond the application of studying honeybees. The use of accelerometer technology provides an exciting avenue for the study of any biologically relevant vibration across the entire animal kingdom, further helping to advance the emerging field of biotremology. Extending this system's application to a broader range of animal taxa could unlock key information that enable species survival. As it stands, the study of animal vibrations remains a relatively understudied discipline, at least compared to bioacoustics, partly because most animal-produced signals are inconspicuous and undetectable to non-augmented human senses. Below I have detailed a far from extensive list of possible further applications for the technology explored in the context of honeybees for this thesis.

Studies into social wasps have shown vibrational signals are associated with adult-brood communication (Savoyard et al. 1998, Cummings et al. 1999) and gastral drumming (Taylor and Jeanne, 2018) appears to match closely with the honeybee DVAV signal in terms of its production, audio and function. Therefore, the technology and algorithms developed within this thesis would easily transfer into social wasp nests and similar long-term statistics could reveal exciting and novel insight, as it has for the honeybees, into the biology of this lesser studied Hymenopteran group.

Commercially, this technology also has potential for the monitoring pest species such as termites. The true cost of damage worldwide cannot be determined. However, the damage caused by termites in south-western USA alone costs approximately $1.5 billion each year in wood structure damage (Su and Scheffrahn, 2000; Flores, 2010). Termites will remain concealed within wood structures, which often results in their presence being undetected until the timbers are severely damaged. The detection of termites often will require destructive investigations to confirm their presence. The technology developed in this thesis could be developed as a device to monitor the presence of termites within the walls of houses and other wooden structures. Placing the sensors in areas of suspected infestation could detect the presence of this destructive pest species through the substrate-borne vibrations and/or comfort homeowners of eradication success.

Within the realms of companion animals, companies such as Mars Petcare ltd employ animal behavioural scientists to identify food preferences through observations of manipulative choice experiments (Mars Inc, 2018). Similarly to the work of Elliot et al. (2017), who automated the study of itching in mice using spectrograms of audio collected by acoustic technology, scientists in such companies could automate their observations of feeding performance and food preference by continuously and non-invasively monitoring the intra-bowl vibrations that occur during feeding and training a similar machine learning algorithm to discriminate between the unique vibrational waveforms of such behaviours as licking, chewing, sniffing and kibble nosing. Accelerometer

technology could therefore be used for the automated logging of behaviour from small audio files and remove the need for manually created ethograms based on the visual observations of large video files.

Within the confines of ecological consultancy, a similar device could be used to continuously detect and record the acoustics of bats roosting in buildings. Such a device could be left in the roof of a building in need of an ecological survey and left to monitor the surrounding area for an extended period of time to continuously record any vibro-acoustic information. A similar discrimination exercise as presented in this thesis optimised to the physical characteristics of bat calls, could easily be developed to reveal such information as bat presence, species, average colony age, abundance, and overall activity levels. This would reduce the requirements of ecologists to provide physical observations using handheld devices and visual detection, and provide more in depth information on the local bat population.

The further application of this system to monitor the biologically relevant sounds and vibrations of the animal kingdom will further open up a world that was previously inaccessible to us as humans. With the specific focus on the use of accelerometers for studying the European honeybee, what this study has shown is that often our interpretation of an organism's microcosm goes far beyond what we can observe with traditional methods, and with the advancements and application of similar cross-disciplinary techniques, scientists will further be able to create a more comprehensive understanding of the natural world.

Reference List

Abou-Shaara, H. F. (2014). The foraging behaviour of honey bees, Apis mellifera: a review. *Veterinarni Medicina.,* 59(1), 1–10.

Adams, J., Rothman. E. D., Kerr, W. E. and Paulino, Z. L. (1977). Estimation of the number of sex alleles and queen mating from diploid male frequencies in a population of *Apis mellifera*. *Genetics*, 86, 583-596.

Aizen, M. A. and Harder, L. D. (2009). The global stock of domesticated honeybees is growing slower than agricultural demand for pollination. *Curr. Biol.,* 19, 915-918.

Allen, M. D. (1956). The behaviour of honeybees preparing to swarm. *Anim. Behav.,* 4, 14-22.

Allen, M. D. (1958). Shaking of honeybee queens prior to flight. *Nature.* 181, 68.

Allen, M. D. (1959a). The occurrence and possible significance of the 'shaking' of honeybee queens by workers. *Anim. Behav.,* 7, 66–69.

Allen, M. D. (1959b). The 'shaking' of worker honeybees by other workers. *Anim. Behav.,* 7, 233–240.

Allen-Wardell G., Bernhardt P., Bitner R., Burquez A., Buchmann S., Cane J., Cox P.A., Dalton V., et al., (1998). The potential consequences of pollinator declines on the conservation of biodiversity and stability of food crop yields. *Conserv. Biol.,* 12(1), 8-17.

Altmann, J. (1974). Observational Study of Behavior: Sampling Methods. *Behaviour*. 49(3), 227-267.

Amiri, E., Strand, M. K., Rueppell, O. and Trapy, D. R. (2017). Queen Quality and the Impact of Honey Bee Diseases on Queen Health: Potential for Interactions between Two Major Threats to Colony Health. *Insects*, (8)88, 2-18.

Autrum H, Schneider, W. (1948) Vergleichende Untersuchungen über den Erschütterungssinn der *Insekten. Z. Vergl. Physiol.,* 31, 77–88.

Bailey, L., Gibbs, A. J. and Woods, R. D. (1964). Sacbrood virus of the larval honey bee (*Apis mellifera linnaeus*). *Virology*, 23(3), 425-429.

Bencsik, M., Bencsik, J., Baxter, M. and Millet, M. (2011). Identification of the honeybee swarming process by analysing the time course of hive vibrations. *Comput. Electron. Agric.,* 76(1) 44-50.

Bencsik, M., Le Conte, Y., Reyes, M., Pioz, M., Whittaker, D, Crauser D., et al. (2015). Honeybee Colony Vibrational Measurements to Highlight the Brood Cycle. *PLoS ONE,* 10(11), e0141926.

Bee Informed Partnership. (2017). Colony Loss Map [cited 2017 Nov 5]. Database [Internet]. Available from: https://bip2.beeinformed.org/geo/.

Bennet-Clark, H. C. (1998). Size and scale effects as constraints in insect sound communication. *Phil. Trans. Roy. Soc. London. B*., 353, 407-419.

Billen, J. (2006). Signal variety and communication in social insects. *Proc. Neth. Entomol. Soc. Meet*. *2006*.

Bisele, M., Bencsik, M., Lewis, M. G. C. and Barnett, C. T. (2017). Optimisation of a machine-learning algorithm in human locomotion using principal component and discriminant function analyses. *PLoS ONE*, 12(9), e0183990.

Blazyte-Cereskiene, L., Vaitkeviciene, G., Venskutonyte, S. and Buda, V. (2010). Honey bee foraging in spring oilseed rape crops under high ambient temperature conditions. *Zemdirbyste-Agriculture.* 97, 61-70.

Blum, M. S., Fales, H. M., Tucker, K. W. and Collins, A. M. (1978) Chemistry of the sting apparatus of the worker honey bee. *J. Apicult. Res.*, 17, 218-21.

Bodenheimer F. S. (1937). Studies in Animal Populations. II. Seasonal Population-Trends of the Honey-Bee. *Q. Rev. Biol.,* 12(4), 406-425.

Bortolotti, L. and Costa, C. (2014). Chemical Communication in the Honey Bee Society. In: *Neurobiology of Chemical Communication*. (Boca Raton, Florda, CRC Press/Taylor and Francis).

Boucher, N., Jinnaib, M. and Smolders, A. (2012). A fully automatic wildlife acoustic monitor and survey system. *Proc. Acoust. 2012 Nantes Conference*. 23-27.

Boucher, M. and Schneider, S. S. (2009). Communication signals used in worker–drone interactions in the honeybee, *Apis mellifera*. *Anim. Behav.,* 78, 247–254.

Brach, V. (1976). Subsocial Behavior in the Funnel-Web Wolf Spider *Sosippus Floridanus* (Araneae: Lycosidae). *Fl. Ent.,* 59(3), 225-229.

Breeze, T. D., Bailey, A. P., Balcombe, K. G. and Potts, S. G. (2011). Pollination services in the UK: How important are honeybees? *Agric. Ecosyst. Environ.,* 142(3), 137-143.

Brennan B. J. (2007). Abdominal wagging in the social paper wasp, *Polistes dominulus*: Behavior and substrate vibrations. *Ethology* 113: 692-702.

Bromenshenk et al. US 2007/0224914 A1, (2007).

Bromenshenk et al. US 7549907 B2, (2009).

Bruel, P. V. (1980).Lightweight piezoelectric accelerometer. US 1980/ 4189655 A

Camiletti, A. L., Percival-Smith, A. and Thompson, G. J. (2013), Honey bee queen mandibular pheromone inhibits ovary development and fecundity in a fruit fly. *Entomol. Exp. Appl.,* 147, 262-268.

Carreck N. and Williams I. (1998) The Economic Value of Bees in the UK; Bee World 79 (3), 115-123.

Clark, C. W., Marler, P., and Beeman, K. (1987). Quantitative analysis of animal vocal phonology: An application to swamp sparrow song. *Ethology,* 76, 101–115.

Chabot, D. (1988) A quantitative technique to compare and classify humpback whale *Megaptera novaeangliae* sounds, *Ethology*, 77, 89– 102.

Cocroft, R. B. (1999). Offspring-Parent Communication in a Subsocial Treehopper (*Hemiptera: Membracidae: Umbonia Crassicornis*). *Behaviour*, 136(1), 1–21.

Cummings, D. L. D., Gamboa, G. J. and Harding, B. J. (1999). Lateral Vibrations by Social Wasps Signal Larvae to Withhold Salivary Secretions (*Polistes fuscatus*, Hymenoptera: *Vespidae*). *Journal of Insect Behavior*, 12(4), 465-473.

Cuthill, I. (1991). Field experiments in animal behaviour: methods and ethics. *Anim. Behav*. 42, 1007–1014.

Czekońska, K., Chuda-Mickiewicz, B. and Chorbiński, P. (2013) The effect of brood incubation temperature on the reproductive value of honey bee (*Apis mellifera*) drones, *J. Apic. Res.,* 52(2), 96-105

de Miranda, J. R. and Genersch, E. (2010a). The Acute bee paralysis virus–Kashmir bee virus–Israeli acute paralysis virus complex. *J. Invert. Path*., 103(1), 30-47.

de Miranda, J. R. and Genersch, E. (2010b). Deformed wing virus. *J. Invert. Path*., 103(1), 48-61.

DeVries, P. J. (1990). Enhancement of symbioses between butterfly caterpillars and ants by vibrational communication. *Science*, 248(1), 1104 -1106.

Dreller, C. and Kirchner, W.H. (1993a). Hearing in honeybees: localization of the auditory sense organ. *J. Comp. Physiol. A.* 173, 275-279.

Dreller, C. and Kirchner, W. H. (1993b). How bees perceive the information in the dance language. *Naturwissenschaften,* 80, 319-321.

Dunteman, G. H. (1984). *Introduction to multivariate analysis*. (Thousand Oaks, USA, Sage Publications).

Ellis, J. D. and Munn, P. A. (2015). The worldwide health status of honey bees. *Bee World.* 86(4), 88-101.

Elliot, P., G'Sell. M., Snyder, L. M., Ross, S. E. and Ventura, V. (2017). Automated acoustic detection of mouse scratching. *PLoS ONE.* 12(7). e0179662.

Elobeid, A., Tokgoz, S., Hayes, D. J., Babcock, B. A. and Hart. C. E. (2007). The Long-Run Impact of Corn-Based Ethanol on the Grain, Oilseed and Livestock Sectors with Implications for Biotech Crops. *Ag. Bio. Forum.*, 10(1), 11-18.

Encyclopaedia Britannica (2006). The Honeybee. [Online] Available at: https://www.britannica.com/animal/honeybee. Accessed: 11/10/2017.

Encyclopaedia Britannica (2013). Life Cycle of the Honeybee. [Online] Available at: https://www.britannica.com/animal/honeybee. Accessed: 11/10/2017.

EPILOBEE. (2015). Study on honeybee colony mortality. Available from: https://ec.europa.eu/food/animals/live_animals/bees/study_on_mortality_en .

Esch, H. E. (1964). Beitrage zum Problem der Entfernungsweisung in den Schwanzeltanzen der Honigbiene. *Z. vergl. Physiol.,* 48, 534-546.

Etter, R., et al. CA 2 573 049, (2007).

Fletcher, D. J. C. (1975). Significance of dorsoventral abdominal vibration among honey-bees (*Apis mellifera L*). *Nature*. 256, 721–723.

Fletcher, D. J. C. (1978a). The influence of vibratory dances by worker honeybees on the activity of virgin queens. *J. Apic. Res.* 17, 3–13.

Fletcher, D. J. C. (1978b). Vibration of queen cells by worker honeybees and its relation to the issue of swarms with virgin queens. *J. Apic. Res.* 17, 14–26.

Flores, A. (2010). *New Assay Helps Track Termites, Other Insects*. (Agricultural Research Service, United States Department of Agriculture).

Free, J. B. (1987). *Pheromones of Social Bees*. (London, UK, Chapman and Hall).

Fristrup, K. M., and Watkins, W. A. (1994). *Marine animal sound classification.* Woods Hole Oceanographic Institution, Woods Hole, MA.

Forsgren. E. (2010). European foulbrood in honeybees. *J. Invert. Path*., 103, 5-9.

Gallai N., Salles, J. M., Settele, J. and Vaissiere, B. E. (2009). Economic Valuation of the Vulnerability of World Agriculture Confronted with Pollinator Decline. *Ecol. Econ.,* 68(3), 810-821.

Gahl, R. A. (1975). The shaking dance of honey bee workers: evidence for age discrimination. *Anim. Behav.* 23, 230-232.

Gary N. E. and Marston, J. (1971). Mating behavior of drone honey bees with queen models (*Apis mellifera L.*) *Anim. Behav*., 19, 299–304.

Gillespie, D. (2004) Detection and classification of right whale calls using an 'edge' detector operating on a smoothed spectrogram. *Can. Acoust.*, 32(2), 39-47.

Goodman, L. (2003). *Form and Function in the Honey Bee*. (Cardiff, UK, International Bee Research Association).

Hamilton W. D. (1964) Genetical evolution of social behaviour. *I. J. Theor. Biol*., 7, 1-16.

Hammann, E. (1957). Wer hat die Initiative bei den Ausflügen der Jungkönigin, die Königin oder die Arbeitsbienen? *Insectes Soc.* 4, 91–106.

Hansen, H. and Brødsgaard, C. J. (2015), American foulbrood: a review of its biology, diagnosis and control. *Bee World,* 80(1), 5-23.

Haydak, M. H. (1929). Some new observations of the bee life. *Cesky Vcilar*., 63, 133-135.

Heinrich, B. (1993). *The Hot-Blooded Insects, Strategies and Mechanisms of Thermoregulation*. (Berlin, Heidelberg, Springer Publishing).

Heinrich, B. and Esch, H. (1994). Thermoregulation in bees. *Am. Sci.,* 82, 164 -170.

Himmer, A. (1927a). A contribution to the knowledge of the heat balance in the nest building of social Hymenoptera. *Z. vergl. Physiol.,* 5, 375-389.

Holldobler, B. and Wilson, E. O. (1990). *The ants*. (Cambridge, Massachusetts, Belknap Press of Harvard University Press)

Hunt, J. H. and Richard, F. J. (2013). Intracolony vibroacoustic communication in social insects. *Insect. Soc*., 60, 403-409.

Ishay, J., Zaiman, A., Grundfeld, Y. and Gitter, L. S. (1974). Catecholamines in social wasps. *Comp. Biochem. Physiol*., 48(1), 369-373.

P. Jancovic and M. Kokuer, "Automatic detection and recognition of tonal bird sounds in noisy environments," *J. Ad. Sig. Proc.,* 2011, 1–10, (2011).

Jinnai, M., Tsuge, S., Kuroiwa, S., Ren, F. and Fukumi, M. (2012). A New Optimization Method of the Geometric Distance using Weighted Random Numbers. *IJAIP* . 4(1), 133-154.

Johnson, B. R. (2008a).Global information sampling in the honeybee. *Naturwissenschaften.* 95, 523–530.

Johnson, B. R. (2008b). Within-nest temporal polyethism in the honeybee. *Behav. Ecol. Sociobiol.,* 62, 777–784.

Johnson, B. R. (2010). Division of labour in honeybees: form, function, and proximate mechanisms. *Behav. Ecol. Sociobiol.* 64(3) 305–316.

Joshi, N. C. and Joshi, P. C. (2010). Foraging behaviour of *Apis Spp.* on Apple Flowers in a subtropical environment. *New York Science Journal.* 3, 71–76.

Mench, J. (1998). Why It Is Important to Understand Animal Behavior, *ILAR Journal*, 9(1), 20–26.

Judd, T. M. and Sherman, P. W. (1996). Naked mole-rats recruit colony mates to food sources. *Anim. Behav*., 52(5), 957-969.

Karlson, P. and Lüscher, M. (1959) 'Pheromones': a New Term for a Class of Biologically Active Substances. *Nature*, 183, 55-56.

Keller, L. and Nonacs, P. (1993). The role of queen pheromones in social insects: queen control or queen signal? *Anim. Behav.,* 45, 787-794.

Kietzman, P.M. and Visscher, P. K. (2015). The anti-waggle dance: use of the stop signal as negative feedback. *Front. Ecol. Evol.,* 3(14), 1-14.

Kilpinen, O. and Storm, J. (1997) Biophysics of the subgenual organ of the honeybee, *Apis mellifera*. *J. Comp. Physiol. A,* 181, 309-318.

Kirchner, W. H. (1993). Acoustical communication in honeybees. *Apidologie*. 24, 297–307.

Kirchner, W.H. (1994). Hearing in honeybees: The mechanical response of the bee's antenna to near field sound. *J. Comp. Physiol. A*, 175, 261-265.

Kirchner, W.H., C. Dreller and W.F. Towne (1991). Hearing in honeybees: Operant conditioning and spontaneous reactions to airborne sound. *J. Comp. Physiol. A*. 168, 85-89.

Klein, B. A., Klein, A., Wray, M. K., Mueller, U. G., and Seeley, T. D. (2010) Sleep deprivation impairs precision of waggle dance signaling in honey bees. *Proc. Natl. Acad. Sci. USA,* 107(52), 22705-22709.

Lau, C. W., and Nieh, J. C. (2009). Honey bee stop-signal production: temporal distribution and effect of feeder crowding. *Apidologie*, 41(1), 87-95.

Land, B. B. and Seeley, T. D. (2004). The grooming invitation dance of the Honey Bee. *Ethology*, 110, 1-10.

Le Conte, Y., Sreng, L., and Poitout, S. H. (1995). Brood pheromone can modulate the feeding behavior of *Apis mellifera* workers. *J. Econ. Ent.*, 88, 798-804.

Le Conte, Y., Mohammedi, A. and Robinson, G. E. (2001). Primer effects of a brood pheromone on honeybee behavioural development. *Proc. R. Soc. Lond. B.* 268, 163-168.

Le Conte, Y., Sreng, L., and Trouiller, J. (1994). The recognition of larvae by worker honeybees. *Naturwissenschaften,* 81, 462-465.

Lehner, P. N., (1998). *Handbook of Ethological Methods*. Cambridge University Press, Cambridge, UK.

Lemke, M. and Lamprecht, I. (1990). A model of heat production and thermoregulation in winter clusters of honeybees using differential heat conduction equations. *J. Theor. Biol*. 142, 261-273.

Lyons, R. (2004). *Understanding Digital Signal Processing*. (Prentice Hall, USA).

Malka, O., Shnieor, S., Hefetz, A. and Katzav-Gozansky, T. (2007). Reversible royalty in worker honey bees (Apis mellifera) under the queen influence. *Behav Ecol Sociobiol*., 61, 465-473.

Manning, A., and Dawkins, M. S. (2012). *An Introduction to Animal Behaviour*. (Cambridge University Press, Cambridge, UK).

Markl, H. (1983). Vibrational communication,. In Huber, F. and Markl, H. (eds.). *Neuroethology and behavioral physiology*., (Springer Verlag, Berlin, Heidelberg).

Markl, H. (1985). Manipulation, modulation, information, cognition: some of the riddles of communication. In: Hölldobler B., Lindauer M. (Eds.), *Experimental behavioral ecology and sociobiology*. (Fischer, Stuttgart).

Mars Inc. (2018). Cat Feeding Behaviour and Preference. [Online]. Available at: https://www.waltham.com/document/nutrition/cat/cat-feeding-behaviour-and-preference/272/. [Accessed on: 05/11/18].

McNeil, M.E.A. (2015). Sounds of the hive Part 1. *Am. Bee J.* 155(9), 985-989.

Medrzycki P., Sgolastra F., Bortolotti L., Bogo G., Tosi S., Padovani E., Porrini, C. and Sabatini A. G. (2010). Influence of brood rearing temperature on honey bee development and susceptibility to poisoning by pesticides. *J. Apic. Res.,* 49(1), 52-59.

Meikle, W. G. and Holst, N. (2015). Application of continuous monitoring of honeybee colonies. *Apidologie,* 46(1), 10-22.

Michelsen, A. (2014) *Mechanical signals in honeybee communication in Studying vibrational communication*. (Springer Verlag, Berlin, Heidelberg,).

Michelsen A., Kirchner W. H., Andersen B. B. and Lindauer M. (1986a). The tooting and quacking vibration signals of honey bee queens: a quantitative analysis. *J. Comp. Physiol. A,* 158, 605–611.

Michelsen, A., Kirchner, W. H. and Lindauer, M. (1986b). Sound and vibrational signals in the dance language of the honey bee, Apis mellifera. *Behav. Ecol. Sociobiol.,* 18, 207–212.

Michelsen, A. (1987). The acoustic near-field of a dancing honeybee. *J. Com. Physiol. A*, 161, 633-643.

Milum, U. (1955). Honeybee communication. *Am. Bee. J.* 95, 97-104.

Millor J, Pham-Delègue M, Deneubourg J.L, Camazine S. (1999). Self-organized defensive behavior in honey bees. *Proc. Natl. Acad. Sci. USA.,* 96, 12611–12615.

Moore, P. A., Wilson, M. E. and Skinner, J. A., (2015). Honey Bee Queens: Evaluating the Most Important Colony Member. *Bee Health*, 7, 10.

Moritz, R. F. A. and Fuchs, S. (1998). Organization of honeybee colonies: characteristics and consequences of a superorganism concept. *Apidologie.* 29(2), 7-21.

Mumford, J. and Knight, J. (2008). Honeybee health (risks) in England and Wales. National Audit Office. Available at: https://www.nao.org.uk/wpcontent/uploads/2009/03/0809288_honeybee_health.pdf

National Research Council, (2007). Status of pollinators in North America. (Washington, DC, The National Academies Press).

Nieh, J. C. (1993). The stop signal of honey bees: reconsidering its message. *Behavioral Ecology and Sociobiology*, 33(1), 51-56.

Nieh, J.(1998). The honeybee shaking signal: function and design of a modulatory communication signal. *Behav. Ecol. Sociobiol.,* 42, 23-30.

Nieh, J. C. (2010). A negative feedback signal that is triggered by peril curbs honey bee recruitment. *Curr. Biol.,* 20 310- 315.

Nieh, J. and Tautz, J. (2000). Behaviour-locked signal analysis reveals weak 200-300 Hz comb vibrations during the honeybee waggle dance. *J. Exp. Biol.*, 203, 1573-1579.

Nowak, M. A., Tarnita, C. E. and Wilson, E. O. (2010). The evolution of Eusociality. *Nature*, 466, 1057–1062.

Omholt, S. W. (1987). Thermoregulation in the winter cluster of the honeybee, Apis Mellifera. *J. Theor. Biol.* 128(2) 219-231.

Page. R. E, Robinson, G. E. (1991). The genetics of division of labor in honey bee colonies. *Adv. Insect. Physiol*. 23, 117–169.

Painter-Kurt, S. and Schneider, S. S. (1998a). Age and behavior of honey bees, *Apis mellifera (Hymenoptera: Apidae)*, that perform vibration signals on workers. *Ethology*. 104 457–473.

Painter-Kurt, S. and Schneider, S. S. (1998b). Age and behavior of honey bees, *Apis mellifera (Hymenoptera: Apidae)*, that perform vibration signals on queens and queen cells. *Ethology*. 104, 475-485.

Pankiw, T. (2004). Worker honeybee pheromone regulation of foraging ontogeny. *Naturwissenschaften.* 91, 178–181.

Pankiw, T., Huang, Z., Winston, M. L. and Robinson, G. E. (1998) Queen mandibular gland pheromone influences worker honey bee (Apis mellifera L.) foraging ontogeny and juvenile hormone titers. *J. Insect. Physiol.*, 44(7–8), 685–92.

Pastor, K. A. and Seeley, T. D. (2005).The brief piping signal of the honeybee: begging call or stop signal? *Ethology.* 111(8), 775-784

PEAK-HIVES. (2017). The National Observation Hive. Available at: http://www.peak-hives.co.uk. [Accessed on: 11/11/2017].

Peirce, A. L., Lewis, L. A. and Schneider, S. S. (2007). The use of the vibration signal and worker piping to influence queen behavior during swarming in honey bees, *Apis mellifera. Ethology*. 113, 267–275.

Peitsch D, Fietz A, Hertel H, de Souza J, Ventura DF, et al. (1992) The spectral input systems of hymenopteran insects and their receptor-based colour vision. *J. Comp. Physiol. A,* 170, 23-40.

Pickett, J. A, Williams, I. H, Martin, A. P, Smith, M. C. (1980). Nasonov pheromone of the honey bee Apis mellifera L. (Hymenoptera:Apidae). I. Chemical characterization. *J. Chem. Ecol.,* 6, 425-34.

POST. (2010). Insect Pollination POST Note 348; Parliamentary Office of Science and Technology; London.

Potts, S. G., Biesmeijer, J. C., Kremen, C., Neumann, P., Schweiger, O. and Kunin, W. E. (2010a). Global Pollinator Declines; Trends, Impacts and Drivers; Trends Ecol. Evol. 25, (6), 345-353.

Pratt, S.C., Kühnholz, S., Seeley, T.D. and Weidenmüller, A. (1996). Worker piping associated with foraging in undisturbed queenright colonies of honey bees. *Apidologie*, 27, 13–20.

Qhtani, T. and Kamada, T. (1980) . 'Worker piping': the piping sounds produced by laying and guarding worker honeybees. *J. Apic. Res.,* 19, 154-163.

Ramsey M, Bencsik M, Newton MI (2017) Long-term trends in the honeybee 'whooping signal' revealed by automated detection. *PLoS ONE*, 12(2): e0171162.

Ratnieks, F. and Anderson, C. (1999). Task partitioning in insect societies. *Insectes soc.,* 46(2), 95-108.

Reader, T. and Duce, I. R. (2009). Intraguild interactions promote assortative mating and affect sexual attractiveness in a phytophagous fly. *Biol. J. Linn. Soc.*, 98, 171-180.

Rigosi, E., Wiederman, S. D. and O'Carroll, D. C. (2017). Visual acuity of the honey bee retina and the limits for feature detection. *Sci. Rep.,* 7, e45972.

Ringnér, M. (2008). What is principal component analysis? *Nature Biotechnology* 26, 303–304.

Robinson G. E. (1992). Regulation of division of labour in insect societies. *Annu Rev. Entomol*., 37, 637–665.

Rosenkranz, P., Aumeier, P. and Ziegelmann, B. (2010). Biology and control of Varroa destructor. *J. Invert. Path*., 103, 96-119.

Roisin, Y. (2000) Diversity and Evolution of Caste Patterns. In *Evolution, Sociality, Symbioses, Ecology.* (Dordrecht, Netherlands, Springer).

Sandeman, D. C., Tautz, J. and Lindauer, M. (1996). Transmission of vibration across honeycombs and its detection by bee leg receptors. *J. Exp. Biol.,* 199, 2585-2594.

Sauer, S., Kinkelin, M., Herrmann, E. and Kaiser, W. (2003). The dynamics of sleep-like behaviour in honey bees. *J. Comp. Physiol. A,* 189, 599-607.

Savoyard, J. L., Gamboa, G. J., Cummings, D. L. D., and Foster, R. L. (1998). The communicative meaning of body oscillations in the social wasp, *Polistes fuscatus* (Hymenoptera: *Vespidae*). *Insectes Soc.* 45(1), 215-230.

Schneider, S. S. (1991). Modulation of queen activity by the vibration dance in swarming colonies of the African honey bee, Apis mellifera scutellata (Hymenoptera: Apidae), *J. Kans. Entomol. Soc*. 64, 269–278.

Schneider, S. S. and Lewis, L. L. (2004). The vibration signal, modulatory communication and the organisation of labour in honeybees, *Apis mellifera*. *Apidologie,* 35, 117-131.

Schneider, S. S. and McNally, L. C. (1991). The vibration dance behavior of queenless workers of the honey bee, *Apis mellifera* (Hymenoptera: Apidae). *J. Insect. Behav.,* 4, 319-332.

Schneider, S. S., Painter-Kurt, S. and Degrandi-Hoffman, G. (2001). The role of the vibration signal during queen competition in colonies of the honeybee, *Apis mellifera. Anim. Behav.,* 61, 1173–1180.

Schneider , S. S., Stamps, J. A. and Gary, N. E. (1986a). The vibration dance of the honey bee. I. Communication regulating foraging on two time scales. *Anim. Behav.,* 34, 377-385.

Schneider, S. S., Stamps, J. A. and Gary, N.E. (1986b). The vibration dance of the honey bee. II. The effects of foraging success on daily patterns of vibration activity. *Anim. Behav*., 34, 386–391.

Schnorbus, H. (1971) Die subgenualen Sinnesorgane von Periplaneta americana: Histologie und Vibrationsschwellen. *Z Vergl Physiol.,* 71, 14-48.

Seeley, T. D. (1982). Adaptive significance of the age polyethism schedule in honeybee colonies. *Behav. Ecol. Sociobiol*., 11, 287-294.

Seeley, T. D. (1985).The Annual Cycle of Colonies. In *Honeybee Ecology: A Study of Adaptation in Social Life*. (Princeton, New Jersey, Princeton University Press).

Seeley. T. D. (1989b). The honey bee colony as a superorganism. *Am Sci.,* 77, 546–553.

Seeley, T. D. (1992). The tremble dance of the honeybee: message and meanings. *Behav. Ecol. Sociobiol.,* 31, 375–383.

Seeley, T. D. (1995). *The Wisdom of the Hive.* (Cambridge, Massachusetts, Harvard University Press).

Seeley, T. D. (1998a). Thoughts on information and integration in honeybee colonies. *Apidologie.* 29, 67-80.

Seeley, T.D., Reich, A. M. and Tautz, J. (2005). Does plastic comb foundation hinder waggle dance communication? *Apidologie*, 36, 513-521.

Seeley, T. D. and Heinrich, B. (1981) Regulation of temperature in the nests of social insects. In *Insect thermoregulation* (New York, New York, Wiley).

Seeley, T. D. and Morse, R. A. (1976). The nest of the honey bee (*Apis mellifera L.*). *Insectes. Soc*., 23(4) 495-512.

Seeley, T. D. and Tautz, J. (2001). Worker piping in honey bee swarms and its role in preparing for lift-off. *J. Comp. Physiol. A.* 187, 667-676.

Seeley, T. D., Visscher, P. K., Schlegel, T., Hogan, P. M., Franks, N. R. and Marshall, J. A. R. (2012). Stop signals provide cross inhibition in collective decision making by honeybee swarms. *Science*, 335(6064) 108-111.

Seeley, T. D., Weidenmüller, A. and Kühnholz, S. (1998). The Shaking Signal of the Honey Bee Informs Workers to Prepare for Greater Activity. *Ethology*, 104, 10-26.

Seitz, N., Traynor, K.S., Steinhauer, N., Rennich, K., Wilson, M. E., Ellis, J. D., et al. (2015). A national survey of managed honey bee 2014–2015 annual colony losses in the USA. *J. Apic. Res.*, 54, 292–304.

Shearer D.A, Boch R. (1965). 2-Heptanone in the mandibular gland secretion of the honey bee. *Nature,* 206, 530-535.

Spangler, H. G. (1969). Suppression of honeybee flight activity with substrate vibration. *J. Econ. Ent.,* 62(5), 1185-1186.

Srinivasan, M. V. (2010) Honeybee communication: A signal for danger. *Curr. Biol.,* 20(8), 336-338.

Stabentheiner, A., Pressl, H., Papst, T., Hrassnigg, N. and Crailsheim, K. (2003). Endothermic heat production in honeybee winter clusters. *J. Exp. Biol.,* 206, 353-358.

Su, N. Y. and Scheffrahn, R. H. (2000). *Termites: Evolution, Sociality, Symbioses, Ecology.* (Springer, Netherlands) doi:10.1007/978-94-017-3223-9_20.

Taber, S. and Owens, C. D. (1970). Colony founding and intial nest design of honey bees, (*Apis mellifera L.*). *Anim. Behav.,* 18, 625-632.

Tarpy D. R., Nielsen, R. and Nielsen D. I. (2004). A scientific note on the revised estimates of effective paternity frequency in Apis. *Insectes Soc.,* 51, 203-204.

Tan, K., Dong, S., Li, X., Liu, X., Wang, C., Li, J., et al. (2016) Honey Bee Inhibitory Signaling Is Tuned to Threat Severity and Can Act as a Colony Alarm Signal. *PLoS Biol.,* 14(3), e1002423.

Tan, K., Yang, S., Wang, Z., Radloff, S. E. and Oldroyd, B. P. (2012). Differences in foraging and broodnest temperature in the honey bees *Apis cerana* and *A. mellifera. Apidologie*. 43, 618–623.

Tautz, J. (1996). Honey bee waggle dance: Recruitment success depends on the dance floor. *J. Exp. Biol.,* 199, 237-244.

Tautz, J., Casas, J. and Sandeman, D. (2001). Phase reversal of vibratory signals in honeycomb may assist dancing honeybees to attract their audience. *J. Exp. Biol.*, 204(15), 3737-3746.

Tautz, J., Maier, S., Groh, C., Rössler, W. and Brockmann, A. (2003). Behavioral performance in adult honey bees is influenced by the temperature experienced during their pupal development. *Proc. Natl. Acad. Sci. USA*. 100, 7343 -7347.

Thom, C. (2003). The tremble dance of honeybees can be caused by hive-external foraging experience. *J. Exp. Biol.*, 206(13), 2111-2116.

Thom, C., Gilley, D. C. and Tautz, J. (2003). Worker piping in honey bees (*Apis mellifera*): the behavior of piping nectar foragers. *Behav. Ecol. Sociobiol.,* 53, 199–205.

Tinbergen, N. (1963). On aims and methods of Ethology. *Ethology,* 20(4), 410–433.

Toates, F. (1998). The Interaction of Cognitive and Stimulus–Response Processes in the Control of Behaviour. *Neurosci. Biobehav. Rev.*, 22(1), 59–83.

THORNE. (2007a). National Mobile Nucleus Hive. [Online] Available at: https://www.thorne.co.uk/index.php?route=product/product&product_id=1678. [Accessed on: 11/11/2017].

THORNE. (2007b). The Bespoke Observation Hive. [Online] Available at: https://www.thorne.co.uk/index.php?route=product/product&product_id=6787. [Accessed on: 11/11/2017].

Towne, W. F. and W.H. Kirchner (1989). Hearing in honey bees: detection of air-particle oscillations. *Science*, 244, 686-688.

Towne, W. F. (1994). Frequency discrimination in the hearing of honeybees (Hymenoptera: Apidae). *J. Insect Behav*., 8, 281-286.

Towne, W. F., Ritrovato, A. E., Esposto, A. and Brown, D. F. (2017). Honeybees use the skyline in orientation. *J. Exp. Biol.,* 220(13), 2476-2485.

vanEngelsdorp D, Evans JD, Saegerman C, Mullin C, Haubruge E, Nguyen BK, et al. (2009) Colony Collapse Disorder: A Descriptive Study. *PLoS ONE*, 4(8), e6481.

vanEngelsdorp, D. and Meixner, M.D. (2010a) A Historical Review of Managed Honey Bee Populations in Europe and the United States and the Factors that May Affect them. *J. Invertebr. Pathol.,* 103(1), 80-95.

Von Frisch, K. (1914) Der Farbensinn und Formensinn der Biene. *Zool. Jahrb. Abt. Allg. Physiol.,* 35: 1-182

Von Frisch K. (1946). Die Tänze der Bienen. *Österr. Zool. Z*., 1, 1-48.

Von Frisch, K. (1967). The dance language and orientation of bees. (Cambridge, Massachusetts, The Belknap Press of Harvard University Press).

Von Hess, C., (1913). Experimentelle Untersuchungen über den angeblichen Farbensinn der Bienen. S. Fischer Verlag, Berlin, DE.

Watmough, J. and Camazine, S. (1995). Self-organized thermoregulation of honeybee clusters. *J. Theor. Biol.*, 176, 391-402.

West-Eberhard, M. J. (1983). Sexual selection, social competition, and speciation. *Q. Rev. Biol.*, 58, 155-183.

West-Eberhard, M. J. (1984). Sexual selection, competitive communication and species-specific signals in insects. In *Insect communication.* (New York, New York, Academic Press).

Williams, I. H. (2015). Oil-Seed Rape and Beekeeping, Particularly in Britain. *Bee World.* 61(4), 141-153.

Wilson, E. 0. (1985a). The sociogenesis of insect colonies. *Science*, 228(1), 1489-1495.

Winston, M. L. (1987*) The Biology of the Honey Bee* (Cambridge, Massachusetts, Harvard University press).

Winston, M. L., Slessor, K. N., Willis, L. G., Naumann, K., Higo, H. A., Wyborn, M. H. and Kaminski L. A. (1989). The influence of queen mandibular pheromones on worker attraction to swarm clusters and inhibition of queen rearing in the honey bee (*Apis mellifera L.*). *Insect Soc.*, 36, 15-27.

Yan, H., Simola, D. F., Bonasio, R., Liebig, J., Berger, S. L. and Reinberg, D. (2014). Eusocial insects as emerging models for behavioural epigenetics. *Nat. Rev. Gen.,* 15, 677-688.

The Appendices

This section contains all of the supplementary material relevant across all five chapters, appearing in the order that they are mentioned within the text. Each subsection contains a figure, its caption, followed by a written description.

Appendix 1: The Observation Hive

The original observation hive design

The initial hive for the study was a National Dual Use Observation hive (Figure 1). Such hives incorperate a brood box containing 5 standard national brood frames with the addition of a permedantly suspended obseravtion brood and super frame behind glass windows. For health and safety reasons the entrance hole has to be located above head-height. Therefore the beehive had to be kept high up in the laboritory as to reduce the gradient at which the members of the colony had to enter/exit the hive. This also required the hive to be kept parallel to the wall, owing t the location of the enterance hole. This presented a major issue with the design. As seen in Figure 1, the arrangment only allowed for the video observation of one side of the frame, leaving the source of many signals open for interrogation. It was soon made apparent that standard observation hives such as these are not a sustainable way of gaining long-term visual access to the activities of a honeybee colony. Once the bees had emptied the frame on the observation stage, they saw no reason to return to the singlely suspended frame. Honeybees self-regulate the temperature of their nests (Winston, 1987). They do this by living in tightly compacted space. Signal suspended frames are not desireable for honeybees as they are not able to affectly acheive thermoregulation. A normal healthy colony will be given an initial 10 – 12 frame broodbox with additional broodboxes and supers being added as the colony expands. The hive described in Figure 1 was only 5 frames wide with no ability to give additional space, thus giving the colony no room to expand. This can be detrimental to the health of the colony or even promote swarming (Winston, 1987). There was also an issue with condensation. An attempt was made to reduce the condensation by improving the insultion on the observation stage by double-glazing the window using perspex acrylic (Figure 2). However, the main issue with the condensation was due to the ventillation of the hive. Therefore, there became a need for a new design of observation hive.

Figure 1: The original obersvation hive used for visual datacollection. A National dual-use observation Hive.

Figure 2. Double glazing addition to the National Dual Use Observation Hive.

The new observation hive design

The requirements for designing a new type of observation hive were as follows: it had to be big enough to sustain a colony of honeybees throughout the active season, allow bees to traffic in and out of the hive without causing congestion or allowing bees to enter the lab, be suitable for them to regulate temperature effectively, retain the ability to be removed from the lab for beekeeping practices without allowing bees to escape, and finally, allow a frame to be lifted for visual observation of the accelerometers at the centre of the hive without letting bees escape into the laboritory.

The main hive body

The main body of the hive (Figure 3) is a standard national brood box (46cmx46cm). The floor is attched using eight 45mm nickel-plated toggle catches placed on each of the 4 sides of the box 10cm from the edge to the midpoint of the catch (Figure 4). The floor consists of a 46x46x5cm bottom board with vented flooring achieved using wire mesh (Figure 5). The entrance to the hive was restricted using two blocks of wood at either side, reducing the gap to a width of 9cm. This allowed me to create a restricted entryway where the bees could not escape into the lab (Figure 5).

Underneath the vented floor are runners, which support a 46cm x42cm x0.4cm yellow correx sheet. This, twinned with the mesh flooring, allows fallout to be collected from within the hive so that assessments can be made as to the colony's level of health, particularly with regards to Varroa (*Varroa destructor).*

Figure 3. The Body of the observation hive.

Figure 4. Toggle catch assembly.

Figure 5. The attached vented floor and restricted hive entrance.

Figure 6. The Varroa board.

The entrance to the hive

The entrance block was constructed using 3mm clear Perspex acrylic, which was later sprayed black to minimise confusion for the bees, as they are phototactic. The bottom of the entrance tube is flush with the bottom of the entrance box, which in turn is flush with the mesh floor of the hive (Figure 7). This allows the bees to remove the carcases of expired bees without obstruction and the plastic box helps to prevent congestion within the tube and the hive. The protruding attachment was inserted into a longer tube with a greater diameter that terminated on the other side of a purposely-drilled hole in the laboratory wall. This enabled the members of the colony to travel freely in and out of the hive without entering the laboratory. The diameter of the protruding tube was selected so that it could be removed from the outside leading pipe and be blocked using a rubber bung to stop traffic from leaving the hive (Figure 8). This is essential for effective hive maintenance as it means that the hive can be removed taken outside for beekeeping practices without bees entering the inside of the lab

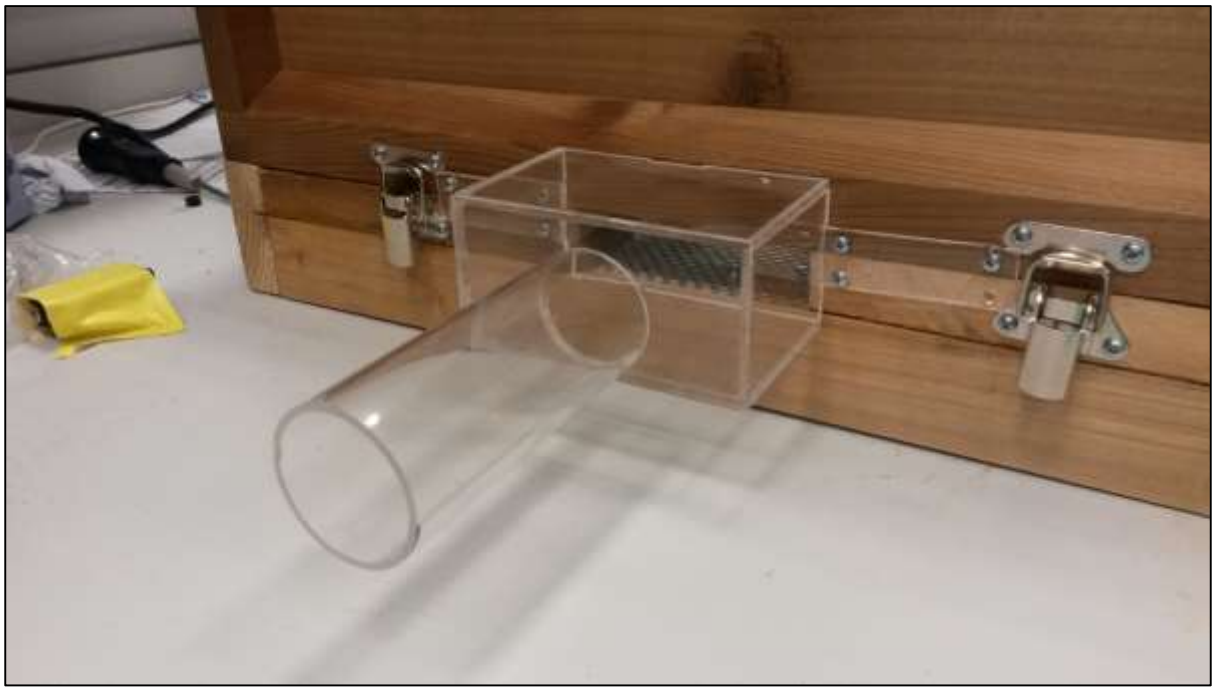

Figure 7. The entrance attachment.

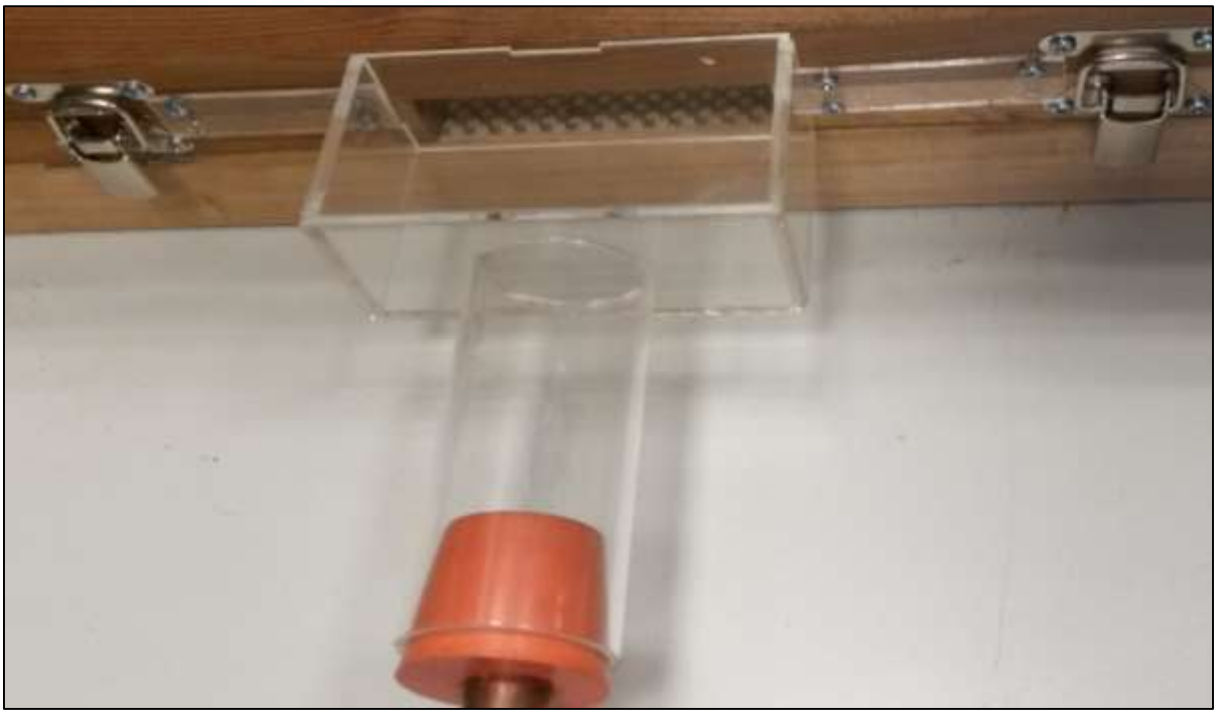

Figure 8. A rubber bung was used to block the entrance and stop forager traffic flow.

The roof of the hive

To cover the parts of the hive surrounding the observation stage, hinged roof hatches were attached to both sides of the brood box (see Figures 9 and 10). These were made out of 2.5cm thick plywood measuring 18cm x 46cm and 13.5cm x 46cm. They were attached to the box using 75mm black powder-coated iron butt hinges, one on each side of the wood 2cm in from edge to central hole. There was a 4mm gap allowed between the top of the brood box and the bottom of each roof lid for a clear Perspex acrylic sheet that protrudes from the observation unit. The hinged 'roof hatches' were secured to the top of the box using the same 45mm nickel toggle catches that were used to attached the brood box to the hive floor. As can be seen in Figure 10, it traps the acrylic protruding from the observation unit, locking the entire unit in place. The acrylic sheet also has the advantage of allowing the observer a bird's eye view into all frames without the bees escaping into the lab. The inside of the hive was also fitted with galvanised metal castellations with ten slots for spacing frames 2cm apart (Figure 11).

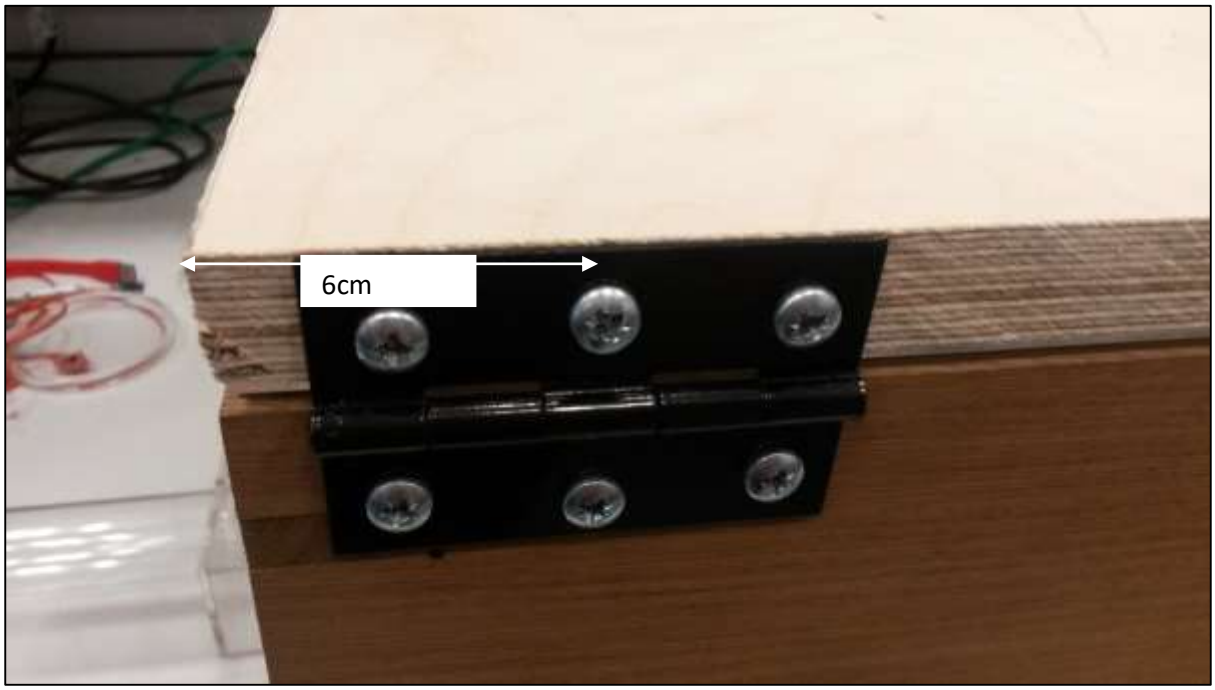

Figure 9. Distance between the hive's edge and the central screw of the hinge that secures the roof.

Figure 10. The hinged roof hatches were secured to the top of the box using 45mm nickel toggle catches, trapping the acrylic protruding from the observation unit and locking the unit in place.

Figure 11. Metal castellations were used seat each of the ten frames within the brood box spaced 2cm apart.

The hive's observation unit

The observation using was made from pieces of clear 2mm Perspex acrylic (Figure 12). Acrylic was chosen for its properties in heat transfer and light transmittance. At around 0.19 W/mK, the value of thermal conductivity is much higher for acrylic than for glass, which should result in reduced condensation. The entire box was also double-glazed to aid in the insulation. The front and rear faces (observation windows) were made of cuts 46cm x 30cm spaced 1cm apart. The sides were made of cuts 13.5cm x 30cm spaces 1cm apart and the roof was made of two cuts of 46cm x 13.5cm spaced 1cm apart. The box was glued together using RS 1-part extruded acrylic bonder. The observation unit was then fixed to the edge of two acrylic sheets, one 46cm x 19cm and the other 46cm x 15cm. This allowed the observation unit to be secured to the box when the roof hatches were closed and allowed birds-eye observation of other areas within the hive without releasing the bees. Holes (1cm in diameter) were drilled through the top of the observation unit to allow rods to protrude and extract the observation frame (Figure 13).

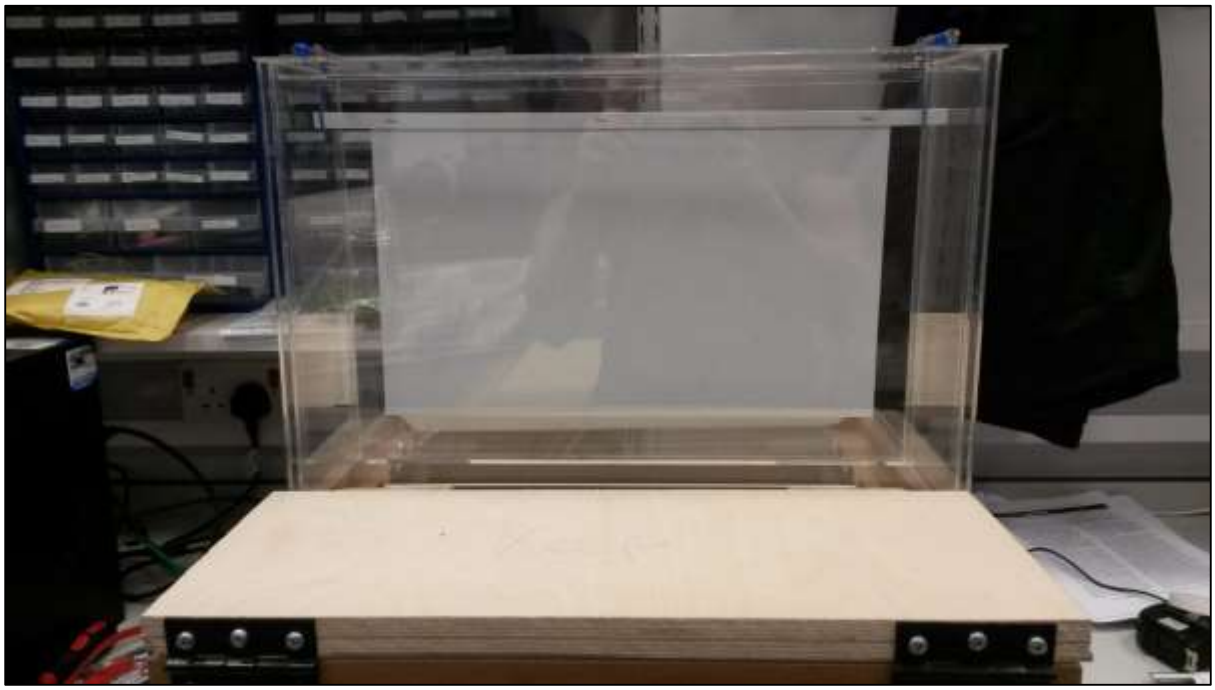

Figure 12. Lateral view of the observation stage with suspended white dummy frame.

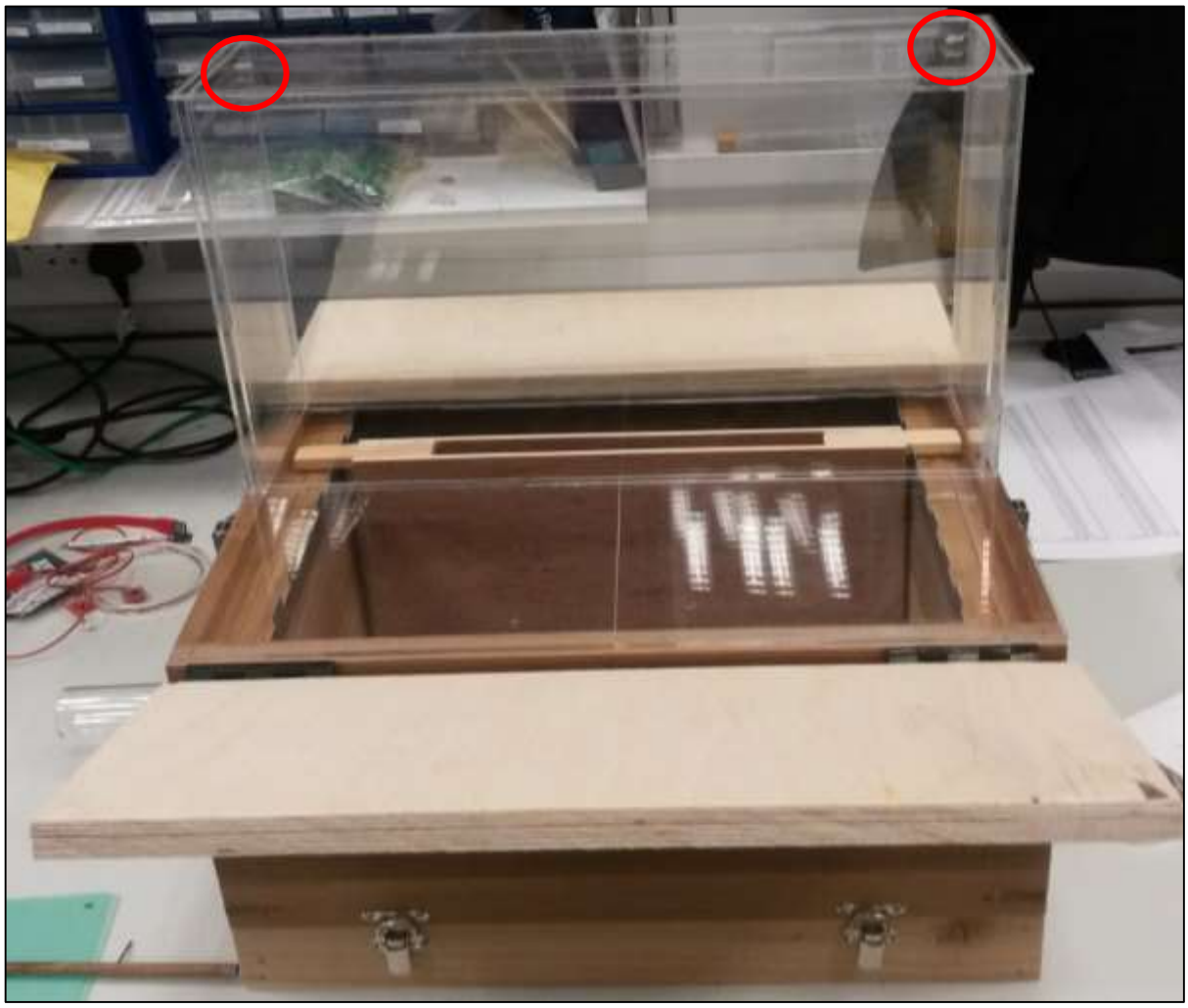

Figure 13. The observation unit from an elevated viewpoint. Red circles highlight the location of the holes drilled to accommodate the frame extraction rods.

The Observation Frame

The observation frame was equipped with two ultra-high performance accelerometers (Brüel and Kjær, 1000 mV/g) placed in the middle of the honeycomb along a horizontal line, located halfway down and equidistant from each other and the vertical sizes (see Figure 17). At the time of installation, small amounts of molten wax were dripped into the accelerometers to secure them onto the foundation comb and avoid the exposure of metal components. The accelerometers were polarised with individual ENDEVCO 4416B conditioners (MEGGITT, U.S.A.), the output of which was plugged into an i02 sound card (ALESIS, U.S.A.) for digitisation at 22kHz sampling rate. A hole was drilled at the top of the observation hive, in the centre, that fed through the able for the accelerometer.

On each side, at the top of the frame, a hole was drilled and then fitted with a tapped nut. Through this, two threaded rods were screwed to equal lengths. These were extended through the top of the observation unit and cogs attached. A chain was placed around the cogs with runners to guide it and prevent it from falling down (Figures 14 and 16). To drive the chain and lift the frame, one of the rods was fitted with a Pittman® 9V DC motor, attached to a Perspex stand above the observation unit (Figure 14). Switches were included at the top and the bottom of the rods that killed the power and stopped the frame from advancing further in that direction.

Figure 14. The frame extraction mechanism and additional brood box.

Cleaning, Varroa Treatment and Modifications

On the 12th April 2017, Apiguard® 25% Thymol Gel Varroa-treatment was administered via the hole in the Perspex lid (Figure 15). During annual cleaning, the box was disassembled, scraped out and a blowtorch was used to kill any remaining fungi or bacteria. The Perspex observation unit was repaired with Perspex glue in places where panels had detached. Ventilation holes were drilled in the top to help to avoid condensation and the resulting build-up of moisture (Figure 16). It was then cleaned thoroughly using ethanol. A second brood box was constructed filled with 12 additional standard frames containing foundation wax. This was placed under the existing brood box on top of the hive floor with a queen-excluder separating them to keep the queen (and the majority of the overall activity) around the observation frame (Figure 14). The second box was attached to the stack using the same toggle catches in the same locations previously used to attach the floor to the original brood box (Figure 14).

Figure 15. Apiguard® Thymol Gel Varroa-treatment administered through the hole in the Perspex crown-board.

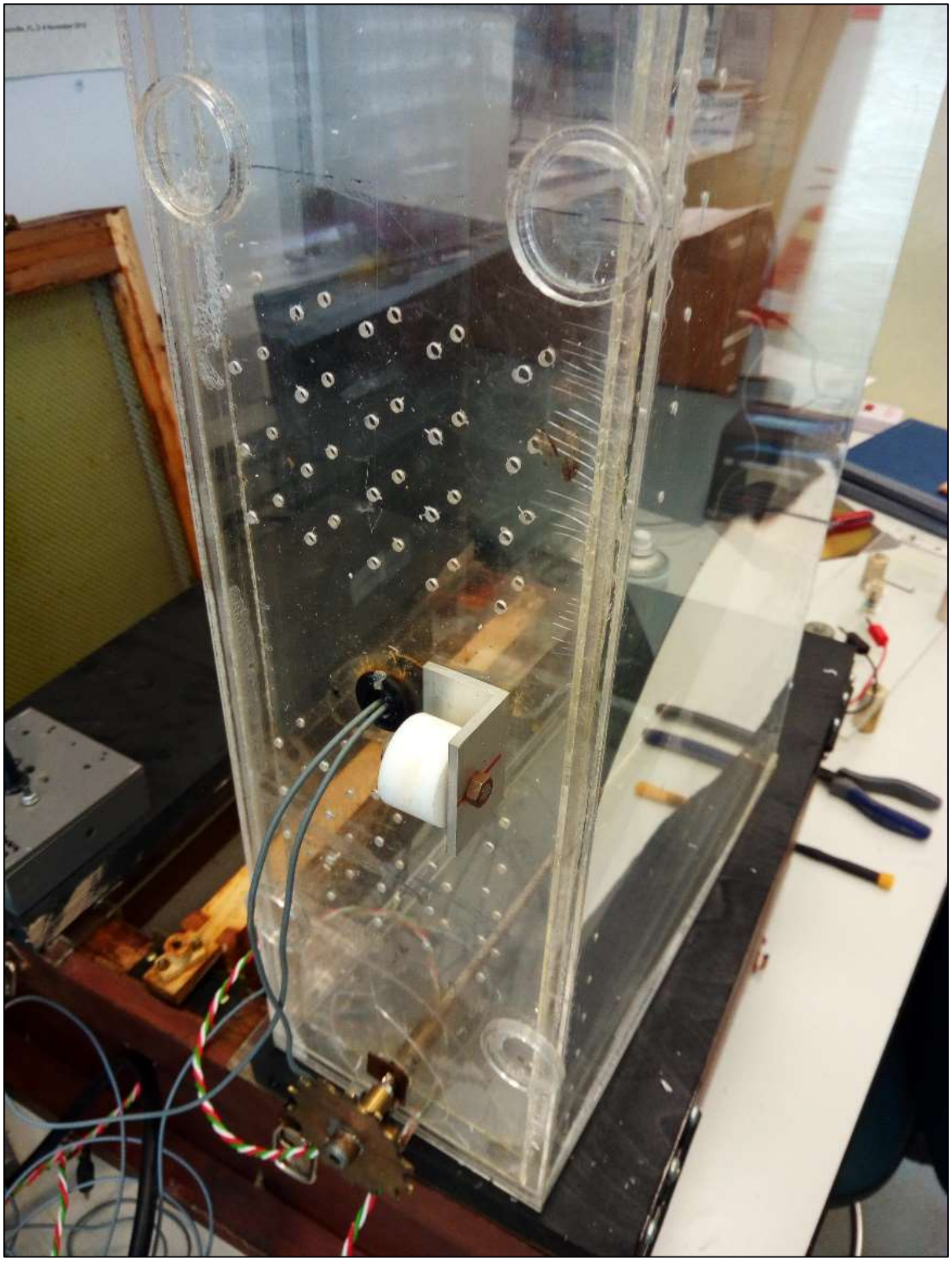

Figure 16. improved ventilation by drilling small holes at the top of the Perspex observation unit.

The Finished Product

Figure 17. The Finished Prototype

Appendix 2: Synopsis of Audio L1: a compilation of raw accelerometer data containing common signals discussed throughout this thesis.

We start the clip at 12:45pm on the 2nd May 2015; 1 week after the primary swarm of this colony had taken place. This colony has no mature laying queen at this time and the virgin queens are starting to emerge.

Immediately from the start, we hear the **125Hz hum** of the bees within the hive. This hum is the direct result of the bees buzzing their wings and is apparent throughout all of our recordings.

Throughout this recording, you will hear '**worker pipes'**. These are similar to the queen pipes you will hear later except they are much shorter in duration. These signals probably originate from extremely excited worker bees, preparing for another swarm lift off.

36 seconds into the recording and you will hear a series **of high amplitude picking** for about 20s. These vibrations are a direct result of the bees as they work on the wax surrounding the accelerometer. The bees are biting at the wax in order to remould it to their preference.

56 seconds into the recording and we hear the first emerged virgin queen as she walks all over the honeycomb generating a type of pipe known as "**queen tooting**". Listen carefully and you will hear the response of the un-emerged virgin queens still within their cells. They respond with a series of pipes knows as "**queen quacking**" named because of its likening to the sound that a duck makes. You will hear as the queen gets closer to the accelerometer the tooting gets louder. The best example of this call and response happens between 1min 48s and 2min 3s. We were lucky in that a queen cell was constructed directly on top of the accelerometer. Within this window of time, you can hear the emerged virgin queen as she toots on top of the queen cell to which she is replied to by the inhabitant quacking back at her. It is believed that the tooting and quacking is a form of quality assessment, or "sizing each other up" between the queens. The emerged queen will decide if she will stay and fight or leave the colony with an "afterswarm". This process also allows the workers to gauge how many

virgin queens there are within the colony so that they can time their release and also do not accidently end up queenless if a couple of afterswarms ensue.

Immediately after the tooting and the quacking (2min 6s and 2mins 11s), we hear the **honeybee DVA signal**. It a very fast (20/s) thumping sound that lasts for around 1 second. In the production of this signal, the honeybee will vigorously shake its body up and down whilst gripping the comb with its back legs and the receiver with its front legs. The receiver is static, non-resistant, and motions in response to the body of the shaker. Occasionally, a bee will simultaneously shake multiple bees or even just the honeycomb by holding on with all six legs producing the vibrational trace you just heard. This signal is a non-specific signal that is used on other honeybees as a way of telling them to increase their activity levels or on their favourite queen cells to facilitate their growth and development. This signal occurs very frequently during the day, with an individual bee producing these signals at a rate of 20 or more per min.

For the time immediately after the second DVA, we hear distant queen toots coming from the emerged virgin queen. At 2min 24s, we hear a very common signal we call the "**honeybee purr**", as it resembles the purring sound of a household cat. Beekeepers will have heard this signal especially whilst carrying swarms in cardboard boxes, which act as a low-level amplifier. It is believed that this signal is produced using the wings or the wing muscles but we are still unsure of its true function.

Between 2min 59s and 3min 1s you will hear 3 **whooping signals**. The first has a very high amplitude so probably occurred very close to the accelerometer the next two are slightly harder to hear. These take place throughout the recording and are very common throughout the entire data set we have. Originally, this was thought to be an inhibitory signal that stopped other bees from advertising dangerous or unprofitable food locations. We now believe this signal to be a startle response to the head butting used as part of many physical signals, such as food requests, as well as surprising events that may occur within the hive, such as a falling nest-mate or a knock to the hive.

We hear various queen pipes throughout the 5 minutes, with the tooting of the emerged queen as she walks around the comb and the quacking of virgins still in their cells. Another high quality example of queen tooting occurs at 4mins 14s and 4mins 47s.

Appendix 3: Spectrograms of the 10th and 15th August 2017 brood isolated datasets

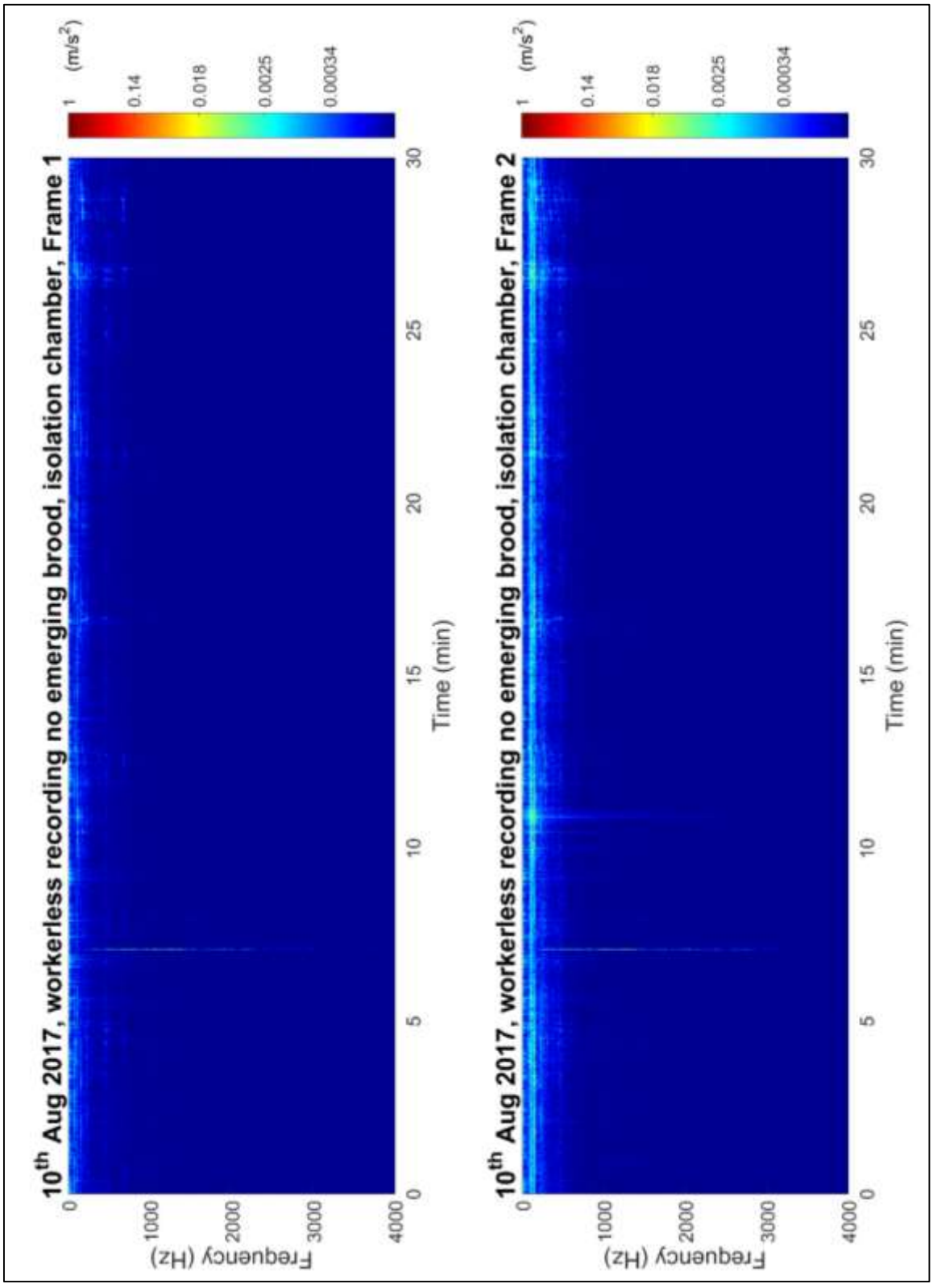

Supplementary Figure 1. Spectrogram of a 30 minute excerpt of a brood-isolated recording from 10th Aug 2017 when the incubation box was placed in a noise-isolated chamber. The figure shows the spectrum of frequencies from 0 to 4000Hz for both frames that were placed in isolation. Pixel intensity is in logarithmic scale denoting the acceleration in m/s^2.

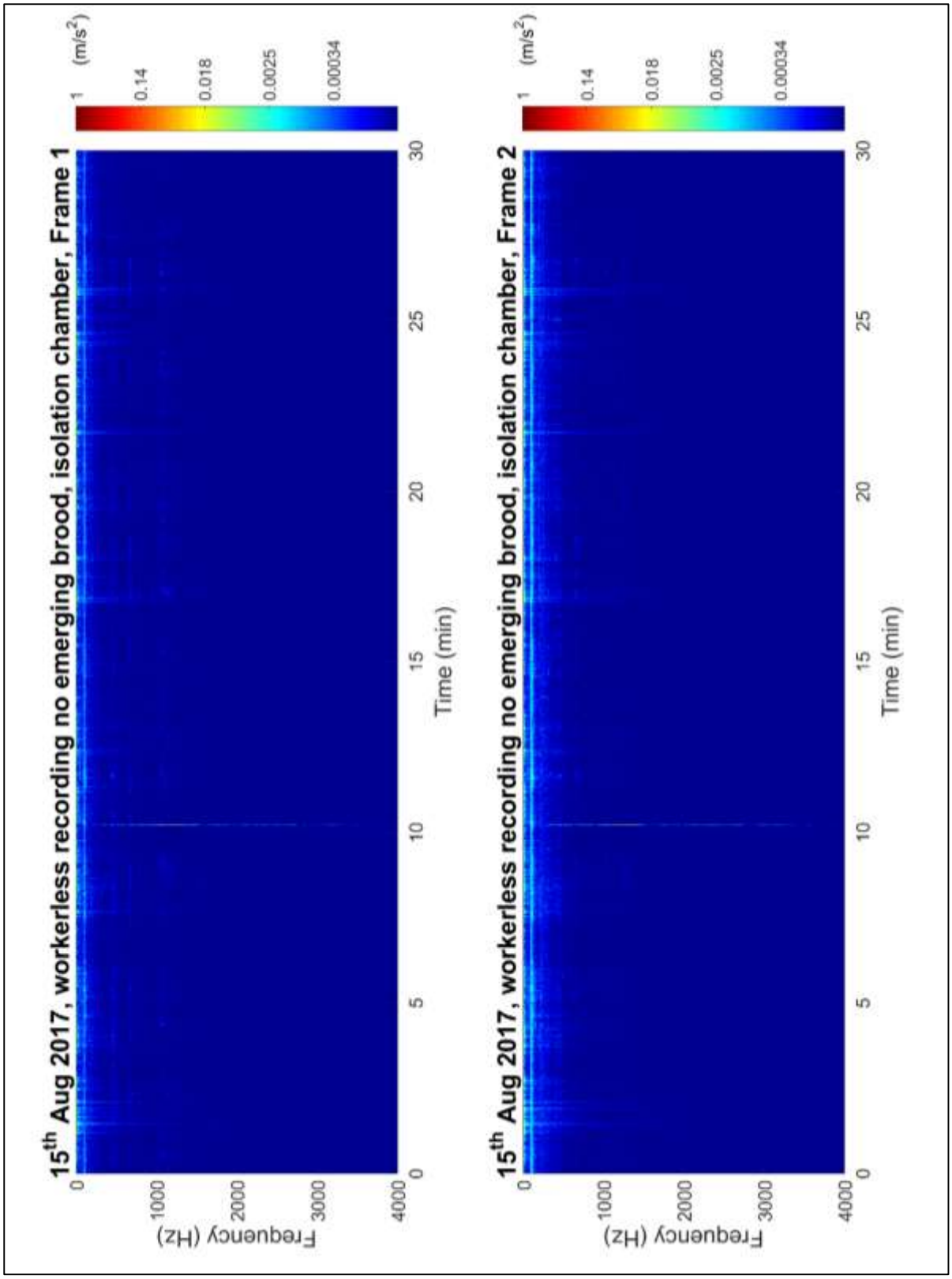

Supplementary Figure 2. Spectrogram of a 30 minute excerpt of a brood-isolated recording from 15th Aug 2017 when the incubation box was placed in a noise-isolated chamber. The figure shows the spectrum of frequencies from 0 to 4000Hz for both frames that were placed in isolation. Pixel intensity is in logarithmic scale denoting the acceleration in m/s^2.

The spectrogram of the data obtained from the 10th and 15th August 2017 experiments resembles that of the 1st September. Various faint broadband clouds can be seen throughout Supplementary Figures 1 and 2 that are the result of nearby traffic and ground work that , in comparison to the data obtained in Experiment 1 on the 28th July 2017, further shows that the use of the acoustic isolation chamber was sufficient in reducing the contribution pf external noise. This is evident by the reduction in the magnitude of the broadband clouds and the 300 Hz band from around 0.0025m/s^2 to around 0.0008m/s^2, as seen in Figure B6 and in Supplementary Figures 1 and 2, respectively. Broadband spikes can be seen on both Supplementary Figures 1 and 2 that can be attributed to the thermostat turning on / off the heating system. As no clicks could be heard within the raw audio for either dataset represented in Supplementary Figures 1 and 2, in addition to the visual observation that no bees emerged from their cells, no broadband traces above 2000 Hz can be seen on the spectrogram that are apparent in Figure B8 for the 18th August 2017 dataset.

Appendix 4 – The lasting effect of colony disturbance

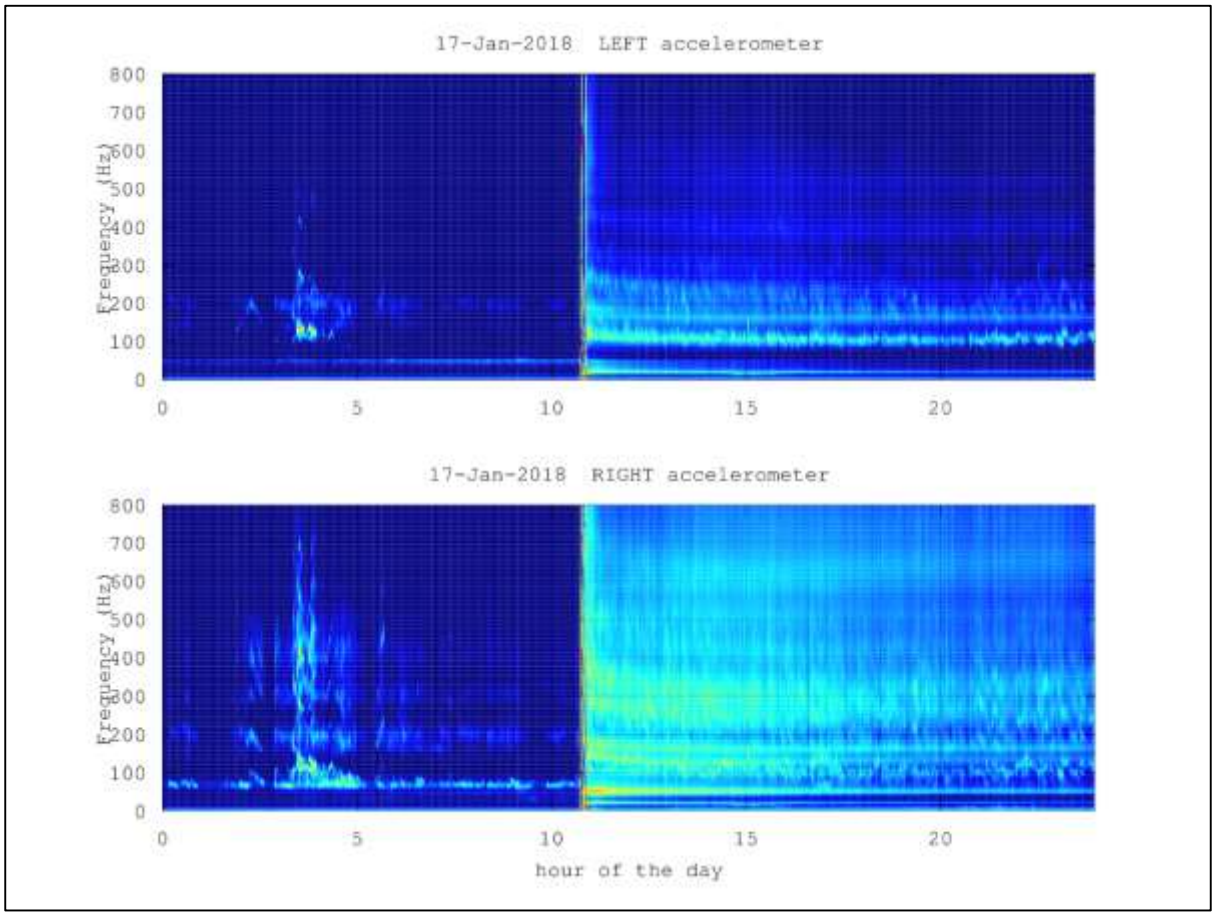

Supplementary Figure 1. The spectrogram of a full day's recorded vibrational spectra automatically generated by octave software and sent via email on a daily basis. This particular image was generated for the vibrations that took place within the Clifton Observation hive on 17th January 2018. Amplitude is denoted by the pixel intensity on a logarithmic scale from high (red) to low dark blue)

Both day's recordings, for which the spectrograms are shown in Supplementary Figures 1 and 2, were obtained during the 2017/2018 winter in January 2018 from the Clifton Observation hive featured regularly throughout this thesis. No bees were found to be foraging at this time and auditory inspection of information directly from the accelerometers suggested very little activity within the hive. In addition, the spectrogram in Supplementary Figure 1 shows very little vibrational signal (and therefore activity) upon the focal frame of the hive. At 10:30am, the observation frame was lifted causing the event on the spectrogram displayed by the broad band of high amplitude spectra. It was

then retuned 5 minutes later causing the second broadband peak on the spectrogram image. As you can see, this roused the honeybees residing on the frame from their dormancy and the effect can be seen lasting predominantly for the next 10 hours with the signal weakening after around 8pm until around 3pm the following day (Supplementary Figure 2).

This work shows the lasting effect that a disturbance can have on a honeybee colony. However, this is an extreme example of waking them from a winter dormancy. This also displays further the advantage of monitoring honeybees using this accelerometer technology, in that this information could only be obtained via these non-invasive *in-situ* methods.

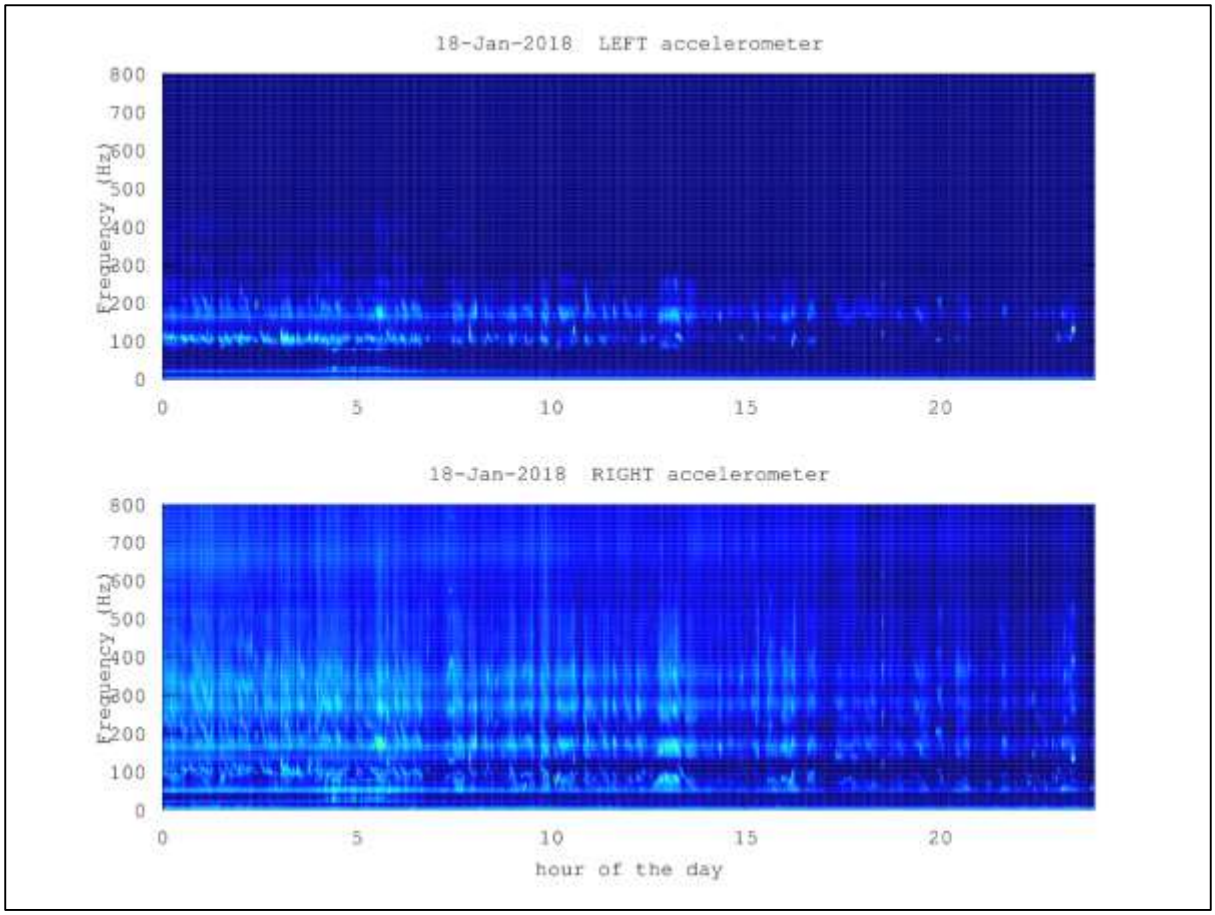

Supplementary Figure 1. The spectrogram of a full day's recorded vibrational spectra automatically generated by octave software and sent via email on a daily basis. This particular image was generated for the vibrations that took place within the Clifton Observation hive on 17th January 2018. Amplitude is denoted on a logarithmic scale by the pixel intensity from high (red) to low dark blue)

Appendix 5: Clicks detected during whooping signal discrimination

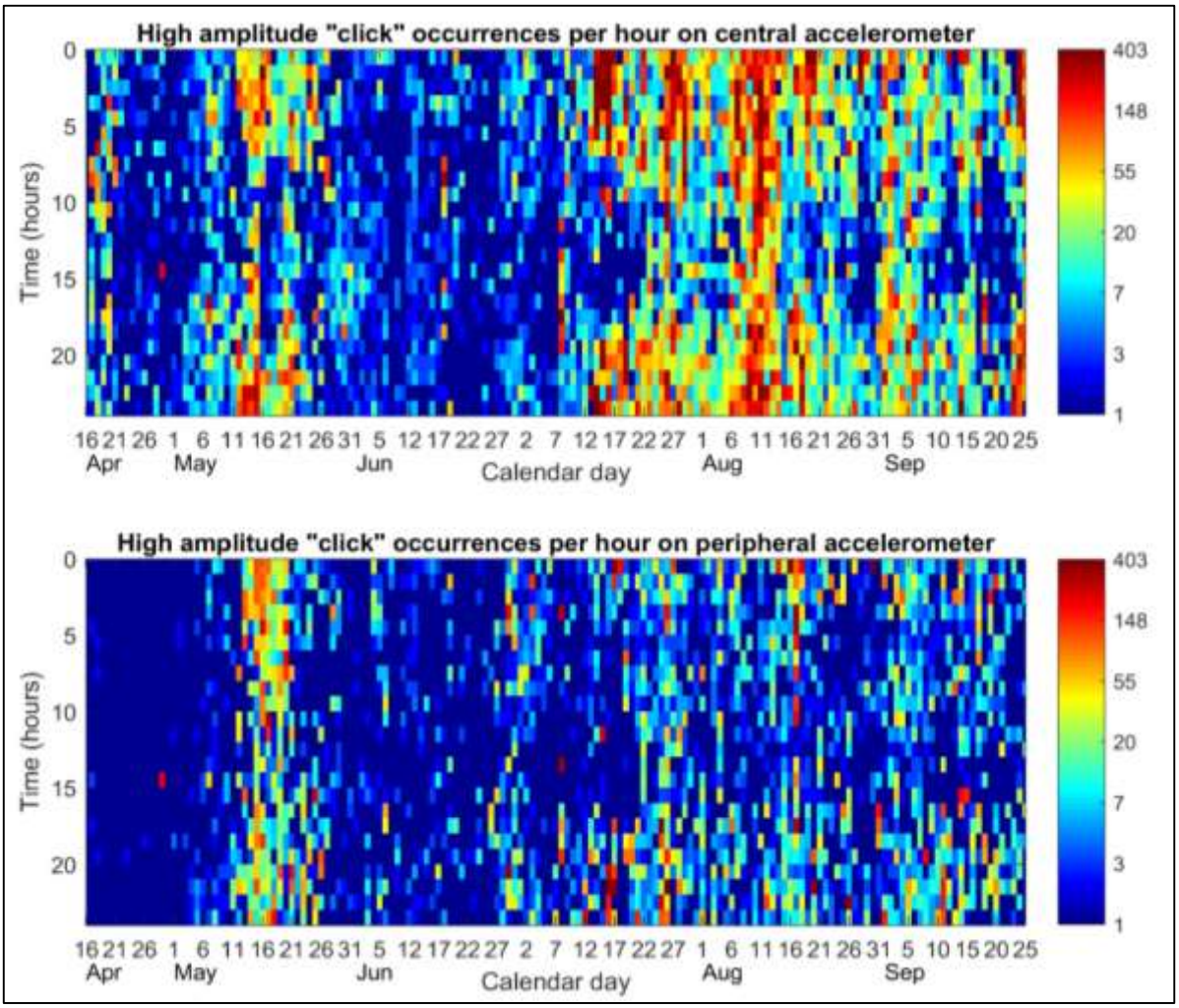

Supplementary Figure 1. The hourly histogram of high amplitude "clicks" that were detected within the first pass, and subsequently filtered out, of the whooping signal detection software. Central (top) and peripheral (bottom) accelerometer logs of the French 2015 season are shown. The pixel intensity reveals the number of hourly occurrences from dark blue (1) to dark brown (403 signals) on a logarithmic scale.

Supplementary Figure 1 shows the hourly occurrences of high amplitude clicks that were filtered out by the whooping signal detection software. The software is tailored towards the detection of whooping signals and thus what is shown is a collection of clicks that were mistaken for whooping signals and possibly not true representation of the actual statistics for this vibration.

Appendix 6: Queen / worker pipes detected during whooping signal discrimination

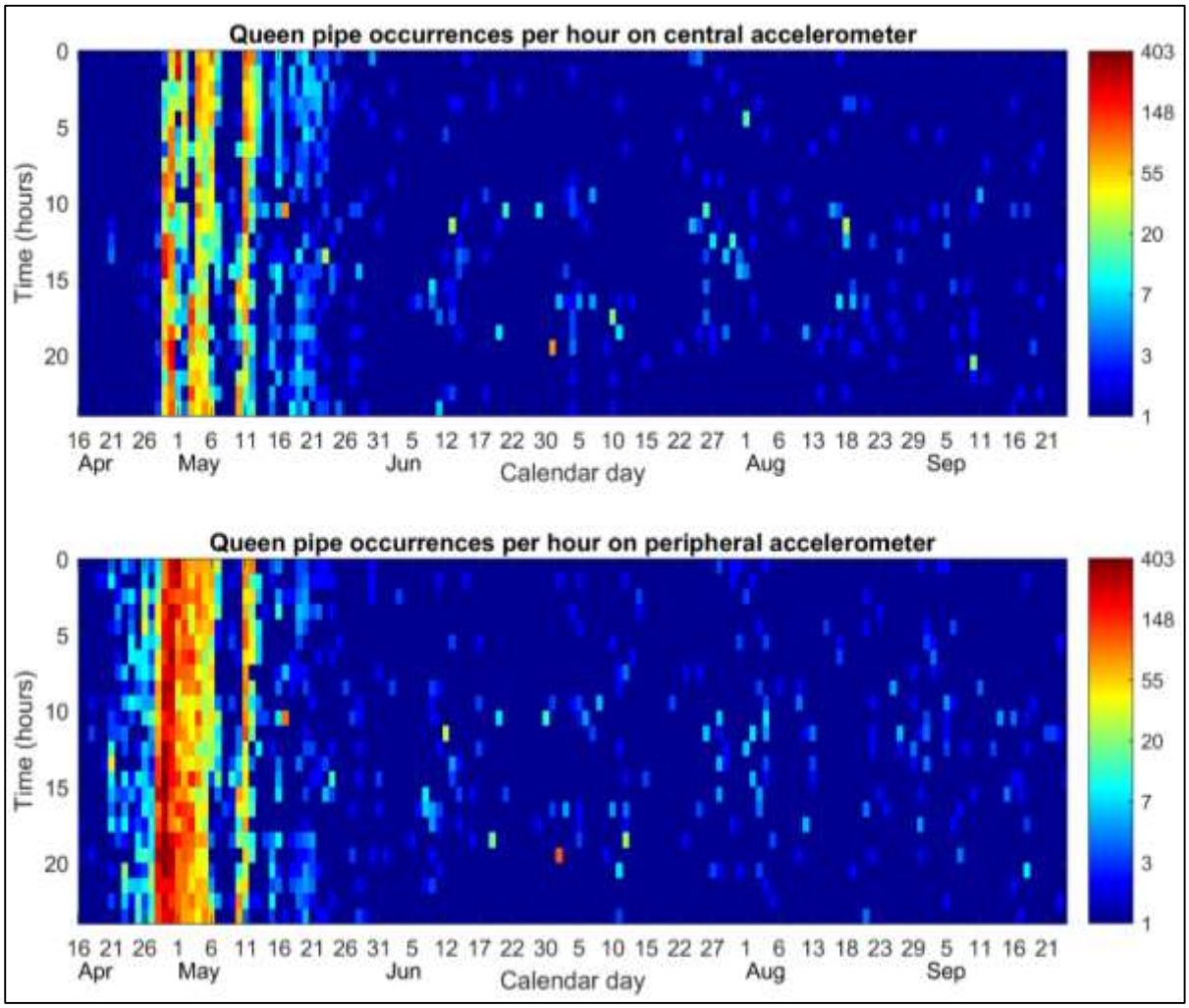

Supplementary Figure 1. The hourly histogram of queen / worker pipes that were detected within the first pass, and subsequently filtered out, of the whooping signal detection software. Central (top) and peripheral (bottom) accelerometer logs of the French 2015 season are shown. The pixel intensity reveals the number of hourly occurrences from dark blue (1) to dark brown (403 signals) on a logarithmic scale.

Supplementary Figure 1 shows the hourly occurrences of queen / worker pipes that were filtered out by the whooping signal detection software. The software is tailored towards the detection of whooping signals and thus what is shown is a collection of pulses that were mistaken for whooping signals and thus may not represent the complete collection of queen / worker pipes that occurred within the raw dataset. upon comparison with the long-term trends in Figure D12 for the DVA signal,

it is interesting to see that there is a DVA signal hiatus during the period of intense queen piping, returning two to three days after the third swarm had occurred on May 6th, lasting for 2-3 days. This data shows that the most intense bout of queen piping occurred in the four to five days leading up to the second swarm on the 1st May.

Appendix 7 – Hourly weather data corresponding to the 2015 active season in Jarnioux, France.

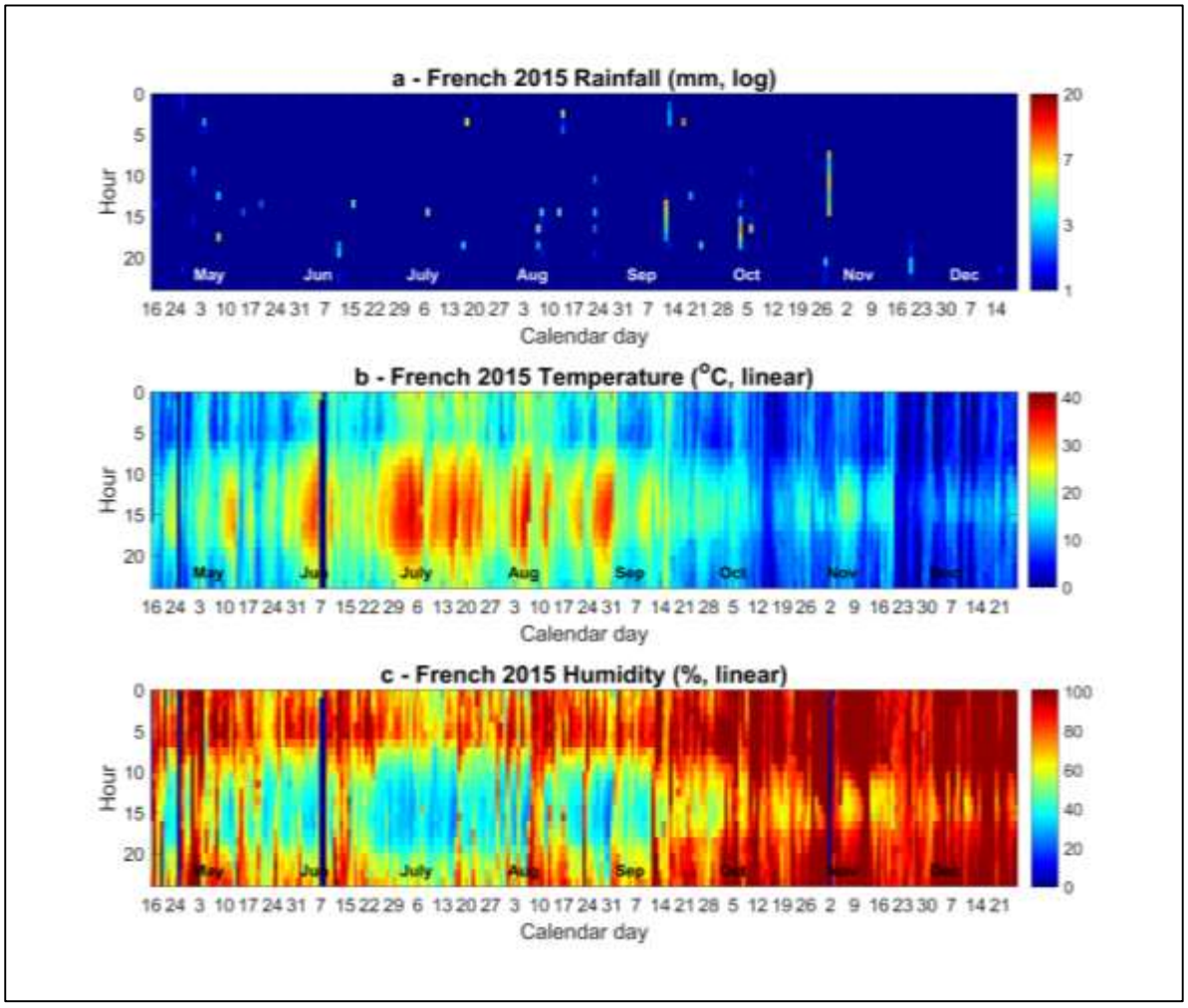

Supplementary Figure 1. The hourly histograms of rainfall (mm), outside temperature (°C) and humidity (%) plotted for each day that corresponds to and has been formatted to match our histograms of DVA signal occurrences in Figure D12.

Appendix 8 – Hourly weather data corresponding to the 2017 active season in Jarnioux, France.

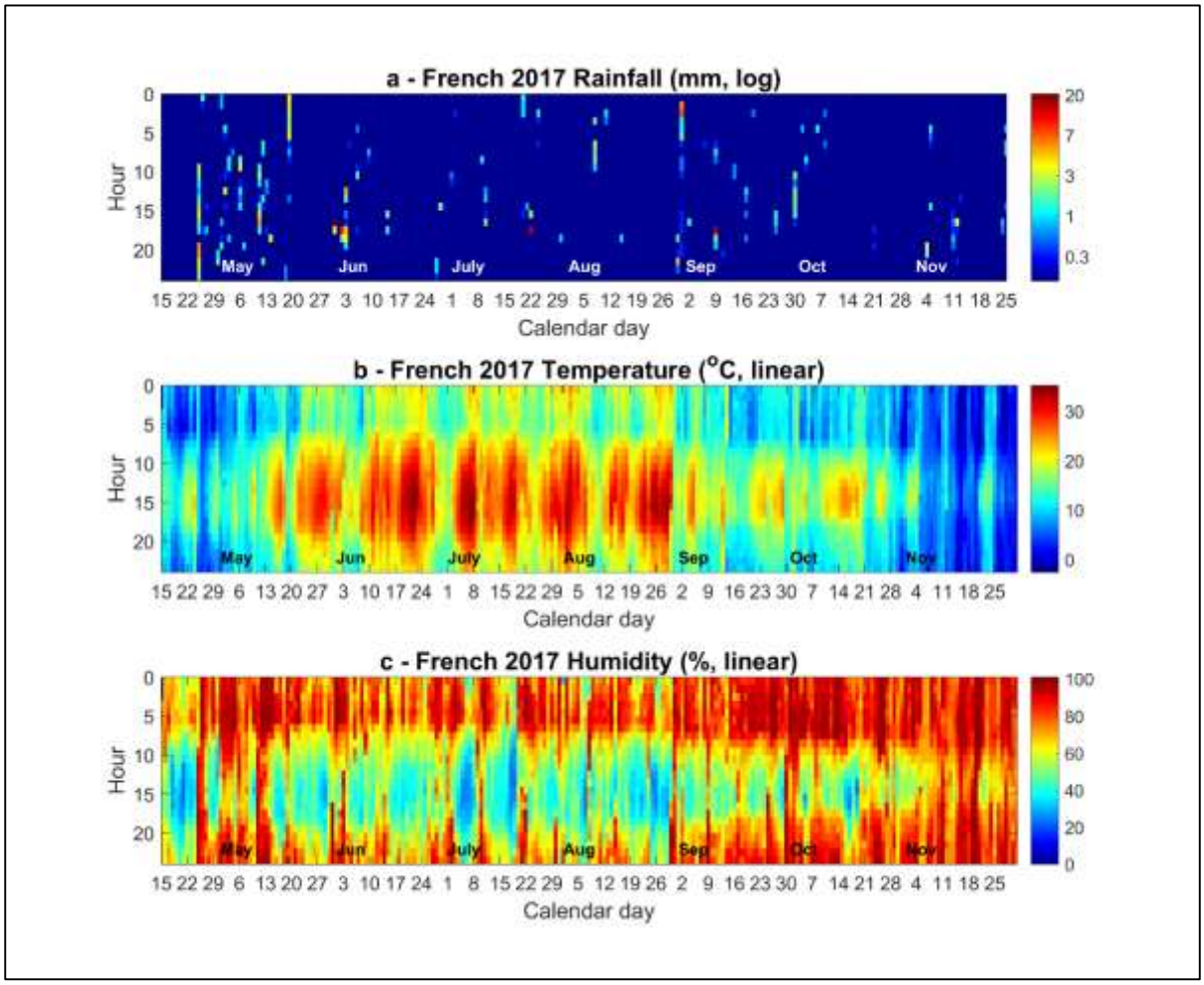

Supplementary Figure 1. The hourly histograms of rainfall (mm), outside temperature (°C) and humidity (%) plotted for each day that corresponds to corresponds to, and has been formatted to match our histograms of DVA signal occurrences for the French 2017 hive in Figure D14.